Role of Hyperhomocysteinemia in Liver Injury and Abnormal Lipid Metabolism

(Protective Effect of Folic Acid Supplementation)

by

Wai Hong Connie Woo
B. Sc Pharm (The Ohio State University, USA)
M. Phil (The University of Hong Kong, Hong Kong SAR)

A Thesis submitted to the Faculty of Graduate Studies of

The University of Manitoba

in partial fulfilment of the requirements of the degree of

Doctor of Philosophy

Department of Physiology

Faculty of Medicine

University of Manitoba

Winnipeg

Abstract

Hyperhomocysteinemia, a condition of elevated blood homocysteine level, is an independent risk factor for cardiovascular diseases. Folic acid can effectively reduce blood homocysteine levels. Recent studies have shown that hyperhomocysteinemia is also associated with liver disorders. However, the underlying mechanisms remain unclear. The general objective of my study was to investigate the biochemical and molecular mechanisms of homocysteine-induced liver injury and abnormal lipid metabolism.

Hyperhomocysteinemia was induced in Sprague-Dawley rats by feeding a high-methionine diet for 4 weeks. An elevation of serum aminotransferases activities (indicator for liver injury) and an increase in hepatic lipid peroxidation were observed in hyperhomocysteinemic rats. Hyperhomocysteinemia-induced superoxide anion production led to oxidative stress in the liver. Reduction of oxidative stress by inhibiting superoxide anion production ameliorated hyperhomocysteinemia-induced liver injury. A significant elevation of hepatic and serum cholesterol concentrations in hyperhomocysteinemic rats was observed, exclusively due to increased expression of HMG-CoA reductase in hepatocytes. The molecular mechanisms of homocysteine-induced adverse effects were further investigated in isolated rat hepatocytes and in human hepatoma cells (HepG2). Hcy stimulated HMG-CoA reductase expression in hepatocytes via activation of transcription factors, namely, sterol regulatory element-binding protein-2 (SREBP-2), cAMP response element binding protein (CREB) and nuclear factor Y (NF-Y). Activation of these 3 transcription factors was detected in hyperhomocysteinemic rat liver and in homocysteine-treated hepatocytes. Pretreatment of hepatocytes with inhibitors for individual transcription factors effectively attenuated Hcy-

induced HMG-CoA reductase mRNA expression. Supplementation of folic acid in diet significantly reduced serum homocysteine level and effectively inhibited hyperhomocysteinemia-induced superoxide anion production, resulting in amelioration of oxidative stress-mediated liver injury in hyperhomocysteinemic rats. These results reflected a protective role of folic acid in hyperhomocysteinemia-induced liver injury.

In conclusion, the present study demonstrates that (1) hyperhomocysteinemia can cause oxidative stress and liver injury; (2) homocysteine stimulates cholesterol biosynthesis in hepatocytes via transcriptional regulation of HMG-CoA reductase expression; (3) supplementation of folic acid offers a hepatoprotective effect during hyperhomocysteinemia. Oxidative stress and accumulation of cholesterol in the liver contribute to liver injury associated with hyperhomocysteinemia. The role of folic acid in maintaining good health may extend beyond the cardiovascular system to encompass hyperhomocysteinemia-associated liver disorders.

Acknowledgement

I would like to express my sincere gratitude to my supervisor, Dr. Karmin O for her valuable guidance throughout my Master and Ph.D studies. I deeply appreciate that she has given me a lot of opportunites and great support during my graduate studies. She is not merely a supervisor of my graduate studies but a mentor of my research career. I am very thankful that I met her in 2001 and became one of her students.

Also, I would like to thank Dr. Yaw L. Siow and my advisor committee members, Dr. Grant Pierce, Dr. Grant Hatch and Dr. Ian Dixon. Dr. Siow has offered me great helps and advices. Dr. Pierce, Dr. Hatch and Dr. Dixon have provided me with valuable suggestions for improvement in my Ph.D candidature.

I am glad that I met a lot of friends and colleagues in St. Boniface Hospital Research Centre. I very appreciate for their assistance, especially for the help from my labmates, Gamika Prathapasinghe and Vathsala Edirimanne. I am also pleased that I had a chance to work with two undergraduate students, Lucy Yan and Stephanie Armstrong.

My families are always the central support for me during my graduate studies, especially my parents. My older brother and sister were the ones encouraging me to continue my graduate studies in the first place. I would like to express my sincere gratitude to my families. In addition, I am glad that I met the families of Winnipeg Chinese Alliance Church who share with me warmth and support, especially Pastor Tran, Irene Tran and the members in my fellowship group. Praise God!

To

My beloved parents,

Woo, Kwok Leung

Yeung, Lai Sheung

Publications

FULL LENGTH PAPERS:

[1] **Woo CW**, Siow YL, O K: Homocysteine Activates cAMP-response Element Binding Protein in HepG2 through cAMP/PKA Signaling Pathway. Arterioscler Thromb Vasc Biol. 26: 1043-1050, 2006.

[2] **Woo CW**, Prathapasinghe GA, Siow YL, O K: Hyperhomocysteinemia Induces liver Injury in rat: Protective effect of folic acid supplementation. Biochim Biophys Acta. 1762: 656-665, 2006.

[3] Siow YL, Au-Yeung KK, **Woo CW**, O K: Homocysteine stimulates phosphorylation of NADPH oxidase p47 phox and p67 phox subunits in monocytes via protein kinase C-β activation. Biochem J. 398: 73-82, 2006.

[4] **Woo CW**, Siow YL, Pierce GN, Choy PC, Minuk GY, Mymin D, O K: Hyperhomocysteinemia Induces Hepatic Cholesterol Biosynthesis and Lipid Accumulation via Activation of Transcription Factors. Am J Physiol Endocrinol Metab. 288: E1002-E1010, 2005.

[5] **Woo CW**, Man RY, Siow YL, Choy PC, Wan EW, Lau CS, O K: Ganoderma *lucidum* inhibits Inducible Nitric Oxide Synthase Expression in Macrophages. Mol Cell Biochem. 275: 165-171, 2005.

[6] Siow YL, Gong Y, Au-Yeung KK, **Woo CW**, Choy PC, O K: Emerging issues in traditional Chinese medicine. Can J Physiol Pharmacol. 83: 321-334, 2005.

[7] Au-Yeung KK, **Woo CW**, Sung FL, Yip JC, Siow YL, O K: Hyperhomocysteinemia activates Nuclear Factor -κB in endothelial cells via Oxidative Stress. Circ Res. 94: 28-36, 2004.

[8] **Woo CW**, Cheung F, Chan VW, Siow YL, O K: Homocysteine stimulates inducible nitric oxide synthase expression in macrophages: antagonizing effect of ginkgolides and bilobalide. Mol Cell Biochem. 243: 37-47, 2003.

[9] Wang G, **Woo CW**, Sung FL, Siow YL, O K: Increased monocyte adhesion to the aortic endothelium in rats with hyperhomocysteinemia: Role of chemokine and adhesion molecules. Arterioscler Thromb Vasc Biol. 22:1777-1783, 2002.

ABSTRACTS:

[1] **Woo CW**, Siow YL, O K: Activation of cAMP response element binding protein (CREB) during hyperhomocysteinemia. Atherosclerosis Suppl. 7(3): 276: Tu-P10-418, 2006.

[2] O K, Au-Yeung KW, **Woo CW**, Edirimanne ERV: Regulation of homocysteine-induced superoxide anion generation and nuclear factor kappa B activation by folic acid. Atherosclerosis Suppl. 7(3): 274: Tu-P10:410, 2006.

[3] **Woo CW**, Siow YL, O K: Oxidative stress and liver injury in hyperhomocysteinemia. FASEB J. 20(5) Part II: A1268: 771.1, 2006.

[4] **Woo CW**, Siow YL, O K: Inhibitory effect on Medicinal Mushroom on Nitric Oxide Synthase Expression in Macrophages. Exp Clin Cardiol. 10(1): 68: 156, 2005.

[5] **Woo CW**, Siow YL, O K: Hyperhomocysteinemia stimulates cholesterol biosynthesis in liver. Atherosclerosis Suppl. 4(2): 121: 2P-0376, 2003.

[6] **Woo CW**, Chan WH, Cheung F, Siow YL, O K: Inhibitory effect of Ginkgo biloba on nitric oxide production in macrophages. The Pharmacologist. 44 suppl 1: A130: 77.16, 2002.

Table of Content

List of Tables

List of Figures

Abbreviations

AEBSF, 4- benzenesulfonyl fluoride

ALT, Alanine aminotransferase

AST, Aspartate aminotransferase

CAD, Coronary artery disease

cAMP, cyclic adenosine monophosphate

CBS, Cystathionine-β-synthase

CREB, cAMP response element-binding protein

DMEM, Dulbecco's modified Eagle's medium

DNA, Deoxyribonucleic acid

EMSA, Electrophoretic mobility shift assay

ERK, Extracellular signal-regulated kinase

FBS, Fetal bovine serum

GADPH, Glyceraldehyde 3-phosphate dehydrogenase

GPx, Glutathione peroxidase

GSH, Glutathione

GSSG, Glutathione (oxidized form)

Hcy, Homocysteine

HHcy, Hyperhomocysteinemia/hyperhomocysteinemic

HMG-CoA, 3-hydroxy-3methylglutaryl coenzyme A

IgG, Immunoglobin G

LDL, Low-density lipoprotein

MAP, Mitogen activating protein

MDA, Malondialdehyde

mRNA, messenger ribonucleic acid

MTHF, 5-Methyltetrahydrofolate

MTHFR, Methylenetetrahydrofolate reductase

NF-Y, Nuclear factor-Y

PBS, Phosphate buffered saline

PKA, Protein kinase A or cAMP-dependent protein kinase

RNA, Ribonucleic acid

RNS, Reactive nitrogen species

ROS, Reactive oxidative species

SD, Standard deviation

SDS-PAGE, Sodium dodecyl sulfate polyacrylamide gel electrophoresis

SEM, Standard error of mean

SOD, Superoxide dismutase

SREBP, Sterol regulatory element-binding protein

tHcy, Total homocysteine

VLDL, Very low-density lipoprotein

I. Introduction

1.1 Hyperhomocysteinemia

Homocysteine (Hcy) is an intermediate amino acid produced in cells during methionine metabolism. Hcy in the body is primarily derived from the metabolism of methionine. Foods contain only trace amount of Hcy (Jacobsen, 2000). The serum or plasma Hcy level in the body is maintained at a minimal level, less than 15 μM, in a healthy individual. In contrast, the circulating methionine level in the body varies widely and is highly dependent on food intake. A study demonstrated that plasma Hcy and methionine concentrations were related to food intake in healthy individuals (Guttormsen *et al.*, 1994). A high protein meal (50g proteins) (e.g. 100g portion of beef contains 30g proteins) can significantly increase both methionine and Hcy levels in blood (Guttormsen *et al.*, 1994). When the metabolic pathways of methionine are interrupted due to malnutrition or inherited gene error, Hcy level in the circulation will be elevated. It has been suggested that elevation of Hcy level in blood above normal physiological concentration is pathogenic (Gulsen *et al.*, 2005; Seshadri *et al.*, 2002; van Meurs *et al.*, 2004; Welch & Loscalzo, 1998). Hyperhomocysteinemia (HHcy) is defined as a plasma or serum total Hcy (tHcy) level higher than 15 μM (Welch & Loscalzo, 1998). In the circulation, 70% to 80% of Hcy is bound to serum proteins, mainly serum albumin (Jacobsen, 2000). Approximately 20% of Hcy is in a disulfide moiety (-S-S-) with another Hcy molecule or cysteine, and about 2% of Hcy is in the reduced sulfhydryl (-SH) form (Figure 1.1). On the contrary, intracellular Hcy is predominantly in reduced sulfhydryl form due to the presence of reducing agents and enzymes in cells (Mudd *et al.*, 1995).

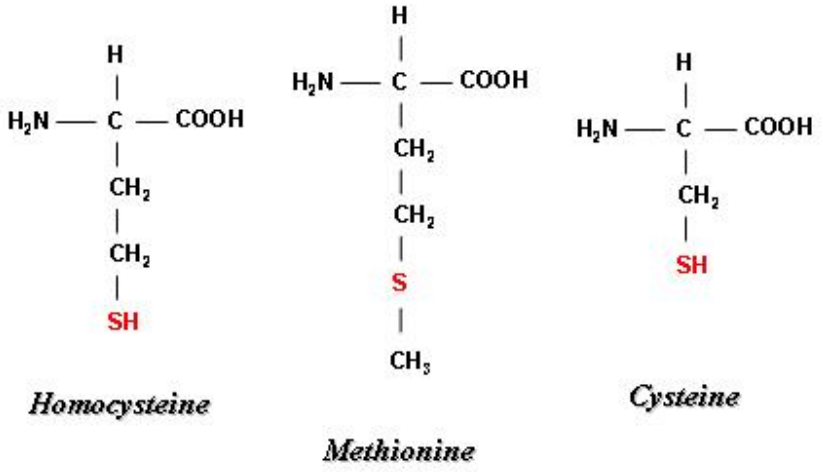

Figure 1.1 Structures of Sulfur-containing Amino Acid.

Methionine, Hcy and cysteine are the sulfur-containing amino acids. Hcy and cysteine contain a sulfhydryl (-SH) group where disulfide bond can be formed. Methionine is one of the essential amino acids which cannot be synthesized in the body. Cysteine is considered as "semi-essential" amino acid because it can be generated via the metabolism of methionine. Hcy is an intermediate amino acid formed during the methionine metabolism. In normal physiology, Hcy is not accumulated in the body. It is eliminated via the remethylation pathway or the transsulfuration pathway (see Figure 1.2).

Physiological parameters, for example, age, gender, renal function and hormonal states can affect Hcy levels in blood (Schneede *et al.*, 2000). HHcy has been suggested as one of the risk factors for atherosclerosis, atherothrombosis, Alzheimer's disease, steatohepatitis and osteoporosis (Clarke *et al.*, 1991; Gulsen *et al.*, 2005; McLean *et al.*, 2004; Seshadri *et al.*, 2002). In this section, the metabolic pathways of Hcy and the roles of HHcy in different types of disorders were reviewed.

1.1.1 Homocysteine Metabolism

Hcy is a sulfhydryl group (-SH)-containing amino acid (Figure 1.1). It is formed during the metabolism of methionine (Figure 1.2). Methionine is converted to Hcy after the removal of a methyl ($-CH_3$) group via transmethylation (Figure 1.2). Hcy can be further catabolized to cysteine via the transsulfuration pathway (Figure 1.2). The metabolic pathway of methionine supplies a methyl group to the body through the formation of S-adenosyl-homocysteine (SAH) from S-adenosyl-methionine (SAM) (Reaction B, Figure 1.2). Methylation, an attachment or substitution of a methyl group on various substrates, is a very important chemical reaction in the biological system. Methylation contributes to epigenetic inheritance via protein and DNA methylation. Protein methylation is the major post-translational modification of protein whereas DNA methylation is important for gene regulation. To prevent accumulation of Hcy in the body, there are two major pathways in the body to eliminate the Hcy: remethylation pathway and transsulfuration pathway. Hcy is either converted back to methionine via remethylation (Reaction D and E, Figure 1.2) or catabolized through transsulfuration to form cysteine (Reaction F, Figure 1.2).

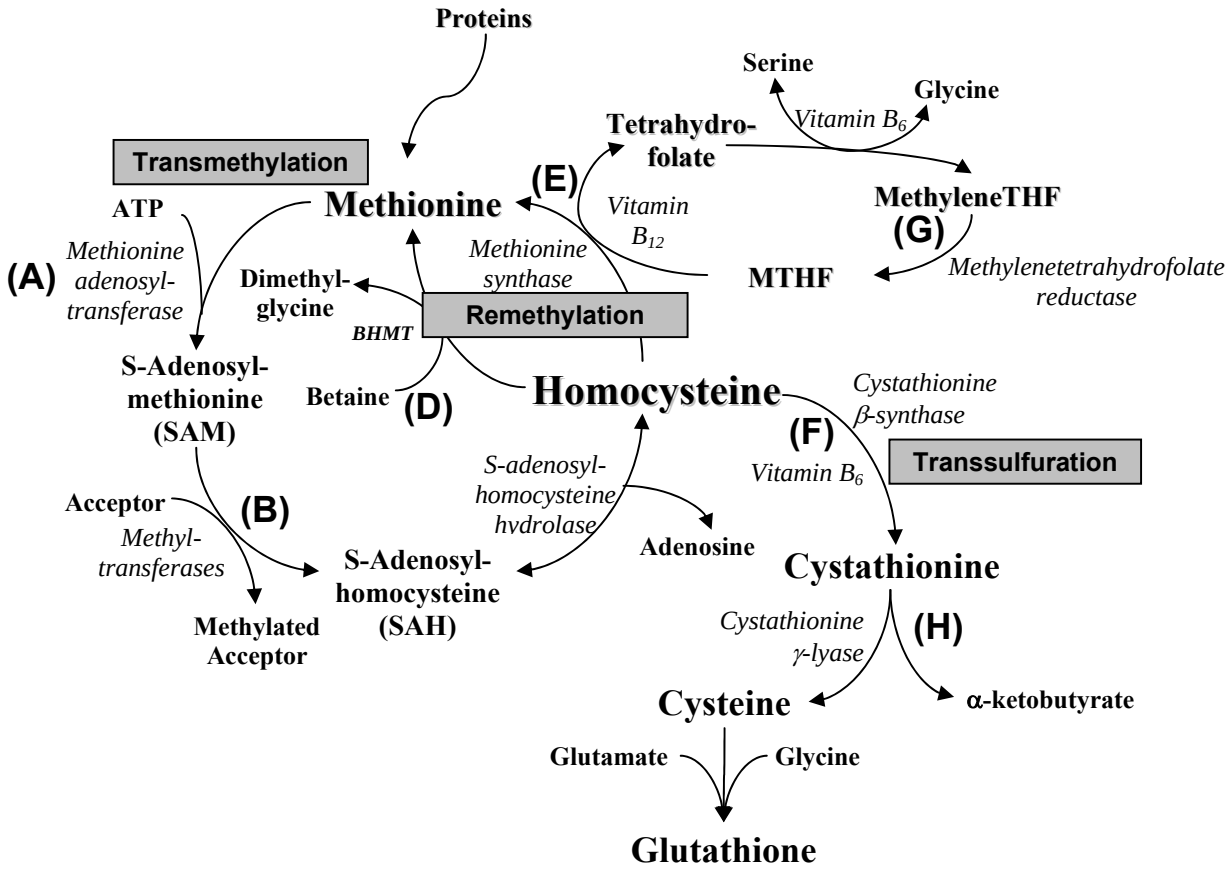

Figure 1.2 Metabolic Pathways of Homocysteine.

Hcy and methionine form a metabolic cycle via several pathways. Methionine is converted to S-adenosylmethionine (SAM) by the enzyme, methionine adenosyltransferase (Reaction A). SAM is the major methyl donor in the body. After the transmethylation, SAM is converted to S-adenosylhomocysteine (SAH) (Reaction B). SAH is further hydrolyzed to Hcy and adenosine (Reaction C). To prevent the accumulation of Hcy in the body, Hcy is removed via the action of methionine synthase (Reaction E), betaine-homocysteine methyltransferase (BHMT) (Reaction D) or cystathionine β-synthase (CBS) (Reaction F). The methionine synthase requires vitamin B_{12} as a co-factor and methyltetrahydrofolate (MTHF) as a methyl donor. On the other hand, CBS requires vitamin B_6 as a co-factor. The enzyme methylenetetrahydrofolate reductase assists the recovery of the supply of MTHF (Reaction G). The product cystathione from the action of CBS is further metabolized to cysteine or α-ketobutyrate (Reaction H).

1.1.1.1 Transmethylation Pathway

The formation of Hcy from methionine is mediated via the SAM and SAH pathway (Reaction A and B, Figure 1.2). Methionine is converted to SAM via the action of methionine adenosyltransferase which transfers the adenosyl group from ATP to methionine (Reaction A, Figure 1.2). SAM is the major methyl donor in the body. The transfer of the methyl group from SAM to a methyl-group acceptor is catalyzed by methyltransferases (Reaction B, Figure 1.2). For example, norepinephrine accepts a methyl group from SAM to form epinephrine. Macromolecules such as proteins, phospholipids and DNA can also accept a methyl group via catalysis of various methyltransferases. Methylation is an important biological process during gene expression, signal transduction and protein modification. After transferring the methyl group to an acceptor, SAM is converted to SAH (Reaction B, Figure 1.2). SAH is further hydrolyzed to Hcy and adenosine via the action of S-adenosylhomocysteine hydrolase (Reaction C, Figure 1.2). The conversion of SAH to Hcy is a reversible process (Reaction C, Figure 1.2). However, the back reaction (from Hcy to SAH) is favoured thermodynamically (Reaction C, Figure 1.2) (Jacobsen, 2000; Richards *et al.*, 1978). Therefore, only the removal of the products, Hcy or adenosine, would drive the reaction in the forward direction (Richards *et al.*, 1978). Adenosine is removed by the action of adenosine deaminase or other salvage pathways (Jacobsen, 2000). Hcy, on the other hand is removed by either the remethylation pathway or the transsulfuration pathway (Figure 1.2).

1.1.1.2 Remethylation Pathway

During remethylation, Hcy is converted to methionine through the transfer of a methyl group from a substrate onto Hcy by methionine synthase or betaine-Hcy methyltransferase (BHMT) (Reaction D and E, Figure 1.2). Methionine synthase requires vitamin B_{12} as a cofactor and a methyl group is donated by 5-methyltetrahydrofolate, a bioactive form of folate (Reaction E, Figure 1.2). Folic acid is a synthetic form of folate. Food folates predominantly exist as 5-methyltetrahydrofolate (Lucock, 2000; Steinberg, 1984). Dietary folates are absorbed via enterocytes in small intestine. During the remethylation via methionine synthase, 5-methyltetrahydrofolate is converted to tetrahydrofolate and the methyl group is transferred to Hcy to form methionine (Reaction E, Figure 1.2) (Lucock, 2000). 5-methyltetrahydrofolate can be recycled through the action methylenetetrahydrofolate reductase (MTHFR) (Reaction G, Figure 1.2). This methionine synthase-methyltetrahydrofolate reaction is present in all tissues. On the other hand, Hcy can also be converted to methionine through the action of BHMT. BHMT is a zinc metalloenzyme which is expressed in kidney and liver in human. It catalyzes the transfer of a methyl group from betaine onto Hcy to form methionine (Reaction D, Figure 1.2). Betaine is the metabolite of choline. Because of its role in the remethylation pathway, betaine has been studied as an Hcy-lowering agent (Reaction D, Figure 1.2) (Ji & Kaplowitz, 2003; Schwab *et al.*, 2002). Inhibition or a defect of enzymes catalyzing these pathways such as MTHFR and BHMT can lead to elevation of Hcy level in blood (Collinsova *et al.*, 2006; Kang *et al.*, 1988). Deficiency of vitamin B_{12} can also cause an elevation of Hcy in the circulation due to its role as a co-factor for MTHFR (Selhub *et al.*, 1993).

1.1.1.3 Transsulfuration Pathway

In the transsulfuration pathway, Hcy is irreversibly converted to cystathionine by cystathionine β-synthase (CBS) with vitamin B_6 as a co-factor (Reaction F, Figure 1.2). Cystathionine is further catabolized to cysteine and α-ketobutyrate (Reaction H, Figure 1.2). When the supply of methionine is normal, Hcy is recycled to methionine through the remethylation pathway twice before it is catabolized through the transsulfuration pathway (Selhub, 1999). The cycle of remethylation can be increased to adapt the dietary supply of methionine (Selhub, 1999).

Genetic deficiency of CBS can cause severe elevation of Hcy level in blood due to impairment of transsulfuration pathway (Carson *et al.*, 1965; McCully, 1969). The estimated prevalence of heterozygous CBS-deficiency in the general population is 1:100 to 1:290 (Mudd *et al.*, 1995). The homozygous and heterozygous CBS-deficient murine model has been developed to study the pathology of HHcy (Watanabe *et al.*, 1995). The action of CBS requires vitamin B_6 as a co-factor. Deficiency of vitamin B_6 can cause an elevation of Hcy level in the circulation (Selhub *et al.*, 1993). Based on their roles in the metabolic pathways of Hcy, folic acid, vitamin B_6 and vitamin B_{12} have been used to lower Hcy levels. These B vitamins can effectively lower Hcy levels in blood; however, the beneficial effects against Hcy-associated dysfunctions are varied (Bonaa *et al.*, 2006; Schnyder *et al.*, 2002; Stott *et al.*, 2005; Willems *et al.*, 2002).

1.1.2 Hyperhomocysteinemia (HHcy) as a Risk factor for Diseases

Hcy is one of the independent risk factors for atherosclerosis and atherothrombosis (Clarke *et al.*, 1991; Lawrence de Koning *et al.*, 2003). McCully first discovered that the vascular pathology of HHcy was associated with arteriosclerosis (McCully, 1969). Earlier

studies had illustrated the diagnoses of other organ disorders in the HHcy patients as well (Carson *et al.*, 1965). Mental retardation, ectopia lentis, skeletal deformities and fatty changes in the liver were found in HHcy patients (Carson *et al.*, 1965). Recent studies have demonstrated that HHcy is also linked to schizophrenia, Alzheimer's disease, hepatic steatosis, and osteoporosis (Gulsen *et al.*, 2005; Muntjewerff *et al.*, 2006; Seshadri *et al.*, 2002; van Meurs *et al.*, 2004). The underlying mechanisms of such associations are currently under investigation.

1.1.2.1 HHcy as a Risk Factor for Cardiovascular Disorders

Several studies have suggested that Hcy is one of the independent risk factors for cardiovascular diseases (Wald *et al.*, 2002; Welch & Loscalzo, 1998; Wu *et al.*, 1994). Every 5 μM increment of tHcy in blood elevates coronary artery disease (CAD) risk in a degree similar to a 20 mg/dL increment of plasma cholesterol, which is interpretated as 1.6- to 1.8- fold increased risk (Boushey *et al.*, 1995). Several lines of evidence have indicated the correlation between plasma Hcy level and atherosclerosis. For example, HHcy was observed in 28% of patients with peripheral vascular diseases and in 30% of patients with coronary vascular diseases (Clarke *et al.*, 1991). In another study, a 3 μM reduction of serum Hcy levels by folic acid intake would reduce the risk of ischemic heart disease by 16%, deep vein thrombosis by 25% and stroke by 24% (Wald *et al.*, 2002). Studies using the apo E knock-out animal model showed that HHcy was able to accelerate the lesion formation in mice that developed spontaneous atherosclerotic lesions (Hofmann *et al.*, 2001; Wang *et al.*, 2003). Many large clinical trials and molecular studies have shown the association of Hcy with cardiovascular diseases. However, some studies have stated the absence of beneficial effect by lowering Hcy levels (Bonaa *et al.*,

2006; Lange *et al.*, 2004; Stott *et al.*, 2005). These studies have involved a relatively small number of patients and the patients were predisposed to severe cardiovascular diseases such as myocardial infarction.

Several mechanisms of Hcy-associated atherosclerosis have been proposed. These include endothelial dysfunction, an increase in vascular smooth muscle cell proliferation, stimulation of chemokines expression, oxidative stress, endoplasmic reticulum stress and disruption of lipid metabolism (Au-Yeung *et al.*, 2004; O *et al.*, 1998; Tsai *et al.*, 1996; Wang *et al.*, 2000; Wang *et al.*, 2002; Werstuck *et al.*, 2001; Woo *et al.*, 2005). Harker *et al.* first demonstrated that Hcy induced loss of endothelium and platelet-mediated smooth muscle cell proliferation in a HHcy primate model (Harker *et al.*, 1976). It was the first mechanism of Hcy-associated atherosclerosis in a continuous HHcy model (Harker *et al.*, 1976). Previous studies of HHcy were investigated in transient HHcy models. The mechanism of endothelial dysfunction is one of the main focuses of studying Hcy-associated atherosclerosis. Endothelial dysfunction is characterized by a shift of the actions of the endothelium toward reduced vasodilation, a proinflammatory state, and prothrombic properties (Endemann & Schiffrin, 2004). It was suggested that Hcy-induced oxidative stress resulting in decreased nitric oxide bioavailability contributed to endothelial dysfunction (Weiss *et al.*, 2003). Our previous study using a diet-induced HHcy model demonstrated an increase in chemokines and adhesion molecules in the aortic endothelium (Wang *et al.*, 2002). Chemokines and adhesion molecules can trigger the migration of inflammatory cells into vascular beds, which promotes the formation of atherosclerotic lesions (Glass & Witztum, 2001). The *in vitro* study showed that Hcy could induce proliferation of vascular smooth muscle cells (Tsai *et al.*, 1996). It has been

suggested that Hcy-stimulated inflammatory response may be one of the mechanisms of atherosclerotic lesion formation (Wang & O, 2001; Wang *et al.*, 2001). Other than the vascular pathology, Hcy has been shown to affect lipid metabolism, which in turn contributes to the development of atherosclerosis. Our laboratory previously showed that Hcy could increase the production and secretion of cholesterol in human hepatocytes (O *et al.*, 1998). Subsequently, we also observed an increase in serum cholesterol levels in the diet-induced HHcy rat model (Woo *et al.*, 2005). A negative correlation of plasma Hcy level and HDL level was observed in patients with coronary artery disease (Liao *et al.*, 2006). It was suggested that Hcy inhibited the reverse transport of cholesterol, which might contribute to Hcy-induced atherosclerosis (Liao *et al.*, 2006).

1.1.2.2 HHcy as a Risk factor for Liver Disorders

Other than the association of Hcy with cardiovascular diseases, it has been reported that Hcy, at elevated levels, exerts detrimental effects to other organs such as liver (O *et al.*, 1998; Robert *et al.*, 2005; Werstuck *et al.*, 2001). In the early studies, fatty liver and liver hypertrophy were commonly found in HHcy patients (Carson *et al.*, 1965; Gaull *et al.*, 1974). However, it was merely a part of diagnoses of cystathionine β-synthase (CBS) deficiency. There was no evidence yet stating that lipid accumulation in the liver was caused by the elevation of Hcy levels. In 1995, a CBS-deficient mouse model was bred (Watanabe *et al*., 1995). Enlarged and multi-nucleated hepatocytes with lipid droplets were observed in the homozygous CBS-/- mutants (Watanabe *et al.*, 1995). Such an observation was made in 21-days old mice and the majority of these CBS-/- mice died before 4 weeks of age (Watanabe *et al.*, 1995). The heterozygous CBS+/- mutants which had half of the CBS activity did not show any sign of abnormal morphology in the liver

(Watanabe *et al.*, 1995). Many investigations have been conducted in this CBS-deficient model to study the pathophysiology of HHcy. Austin's group conducted a study using the CBS-deficient model in combination with dietary modification (Werstuck *et al.*, 2001). They treated the heterozygous mutants CBS+/- and homozygous CBS+/+ with a high-methionine and low-folic acid diet (Werstuck *et al.*, 2001). Similar hepatic morphology including micro- and macrovesicular lipid disposition and multi-nucleated hepatocytes was found in these two mutants with dietary modification (Werstuck *et al.*, 2001). Their finding demonstrated that the hepatic abnormality seen in CBS-deficient mice was due to the elevation of Hcy levels rather than a non-specific adverse effect of genetic intervention (Werstuck *et al.*, 2001).

Several studies have been conducted to investigate the mechanisms of hepatic lipid accumulation during HHcy (Mikael *et al.*, 2006; Robert *et al.*, 2005; Werstuck *et al.*, 2001). The proposed mechanisms include endoplasmic reticulum stress-mediated activation of lipogenic enzymes and activation of biosynthetic enzyme for cholesterol production (O *et al.*, 1998; Werstuck *et al.*, 2001). A recent study revealed alterations of several genes for hepatic lipid homeostasis including scavenger receptor-BI, ATP binding cassettes transporters and nuclear hormone receptors in CBS-deficient mice (Hamelet *et al.*, 2007).

Apart from the simple steatosis (characterized by the presence of abnormally large quantities of fat within a cell) diagnosed in HHcy, Hcy has been shown to promote the development of liver fibrosis (Adinolfi *et al.*, 2005; Garcia-Tevijano *et al.*, 2001). Liver fibrosis can develop into steatohepatitis and eventually into cirrhosis, leading to progressive loss of liver function. Oxidative stress, lipotoxicity and proinflammatory

stimulation all play roles in the transition of steatosis to steatohepatitis (Farrell & Larter, 2006). HHcy was found to promote the development of steatosis and fibrosis in chronic hepatitis C patients (Adinolfi *et al.*, 2005). An *in vitro* study demonstrated that Hcy was able to stimulate expression of fibrotic factors including tissue inhibitor of metalloproteinases (TIMP) and procollagen expressions in hepatic cells (Torres *et al.*, 1999). It was suggested that an alteration in extracellular matrix homeostasis was one of the mechanisms for Hcy-promoting liver fibrosis (Torres *et al.*, 1999). The same study also demonstrated that Hcy stimulated TIMP expression in vascular smooth muscle cells (Torres *et al.*, 1999). It was speculated that Hcy might promote net collagen deposition in atherosclerotic lesions (Torres *et al.*, 1999). However, it is still uncertain whether HHcy alone, without other predisposed factors, can lead to liver fibrosis or cirrhosis.

1.1.2.3 HHcy as a Risk factor for Other Diseases

Skeletal deformities, mental retardation and ectopia lentis were observed in HHcy patients (Carson *et al.*, 1965). Recent studies have found that Hcy is an independent risk factor for osteoporosis, cognitive deterioration and schizophrenia (Muntjewerff *et al.*, 2006; Seshadri *et al.*, 2002; van Meurs *et al.*, 2004). It was shown that Hcy-induced oxidative stress could increase bone resorption by stimulation of osteoclast formation and activity (Koh *et al.*, 2006). Another study showed that Hcy enhanced apoptosis of bone marrow stromal cells leading to decreased bone formation (Kim *et al.*, 2006). Alternatively, a neurological study suggested that an increase in brain amyloid beta peptide levels might be one of the mechanisms of HHcy as a risk factor for Alzheimer's disease (Pacheco-Quinto *et al.*, 2006). It was shown that Hcy could induce neurotoxicity by increasing the production of reactive oxygen species (White *et al.*, 2001). Many

studies on the mechanisms of Hcy-associated disorders have suggested that Hcy-induced oxidative stress plays a major role in the pathology (Kim *et al.*, 2006; Koh *et al.*, 2006; White *et al.*, 2001). The mechanisms by which Hcy induces oxidative stress are still ambiguous.

1.1.3 Beneficial effects of Folic acid on Hyperhomocysteinemia

Folate is a generic term for a B-vitamin containing the basic chemical structure composed of a pteridine residue and a p-aminobenzoylglutamate residue (Lucock, 2000). Folic acid is the stable synthetic analog of the parent structure of the folate family. Humans cannot synthesize folate and must rely on dietary sources. Folates in the diet are absorbed via enterocytes in the small intestine and subsequently converted to formyltetrahydrofolate or methyltetrahydrofolate (predominant) monoglutamates in enterocytes (Steinberg, 1984). Once absorbed, folate in the form of formyltetrahydrofolate or methyltetrahydrofolate monoglutamates can be distributed to liver or peripheral tissues via the transport by serum proteins (e.g. albumin and α-2-macroglobulin) or folic acid binding proteins (FABP) (Steinberg, 1984).

Folic acid supplementation is used to prevent fetal neural defects during pregnancy (Hillman, 2001; Smithells *et al.*, 1980). Folate deficiency can lead to megalobastic anaemia (Hillman, 2001). Due to its ability to lower plasma Hcy levels during HHcy, its role in cardiovascular diseases has been increasingly studied. Folate deficiency due to a genetic defect or malnutrition is associated with HHcy. The active metabolite of folic acid, 5-methyltetrahydrofolate, facilitates remethylation of Hcy to methionine by donating a methyl group to Hcy (Reaction E, Figure 1.2). This reaction is catalyzed by methionine synthase with vitamin B_{12} as a co-factor (Reaction E, Figure 1.2). Studies in

animal models and clinical trials show that folic acid depletion can cause HHcy (Faurschou *et al.*, 2000; Lentz *et al.*, 2000; Symons *et al.*, 2002). Supplementation of folic acid to HHcy patients can effectively lower plasma Hcy levels (1998; Boushey *et al.*, 1995; Venn *et al.*, 2003).

It has been postulated that the beneficial effect of folic acid on cardiovascular diseases is mediated by its Hcy-lowering effect. However, more and more studies have demonstrated that the benefits of folic acid supplementation are independent of Hcy lowering (Doshi *et al.*, 2002; Stroes *et al.*, 2000). Intake of 5mg folic acid per day for 6 weeks was able to improve flow-mediated dilatation (FMD) of the brachial artery and such an improvement was not correlated with a reduction of plasma Hcy levels (Doshi *et al.*, 2001). However, in this randomized crossover study, 88% of the subjects were taking statins (HMG-CoA reductase inhibitors) simultaneously (Doshi *et al.*, 2001). One of the statins, atorvastatin was found to improve endothelial function (Feron *et al.*, 2001). The same group of scientists did another randomized, placebo controlled study in 2002 and confirmed the Hcy-independent effect of folic acid in improving endothelial function (Doshi *et al.*, 2002). Folic acid may improve endothelial function through an endothelial nitric oxide pathway (Hyndman *et al.*, 2002; Stroes *et al.*, 2000). Conversely, one study conducted in South Wales, United Kingdom showed that folic acid supplementation could lower plasma Hcy levels but did not improve endothelial function in healthy individuals (Pullin *et al.*, 2001). A recent study analyzing the data from 16,958 participants in 12 randomized controlled trials also showed no reduction of cardiovascular risk by folic acid administration in patients with a history of end-stage renal disease or vascular diseases including stroke, myocardial infarction, cononary heart disease, intermittent claudication,

etc (Bazzano *et al.*, 2006). The severity of the pre-existing cardiovascular diseases or renal diseases might contribute to the negative result of folic acid. The controversy may be clarified by more well-designed studies with a larger sample size and a longer monitoring period.

Beside studies on endothelial function, the effect of folic acid was also examined in liver. Depletion of folic acid in the diet increased plasma Hcy levels and eventually promoted oxidative stress in rat liver (Huang *et al.*, 2001). Another study showed that supplementation of folic acid for 4 weeks improved liver morphology in aged rats (18 months old) (Roncales *et al.*, 2004). Even though several studies have confirmed the beneficial effect of folic acid in disease states, the exact mechanisms by which folic acid improves organ functions are largely unknown.

1.2 Oxidative Stress and Liver Injury

Previous studies have suggested that the pathophysiological effects of Hcy are mediated via oxidative stress (Au-Yeung *et al.*, 2004; Wang & O, 2001). Several studies have demonstrated liver abnormalities during HHcy (Carson *et al.*, 1965; Robert *et al.*, 2005; Werstuck *et al.*, 2001; Woo *et al.*, 2005). Oxidative stress plays an important role in different types of liver injuries (Choi & Ou, 2006; Chowdhury *et al.*, 2006; Wheeler *et al.*, 2001b). Oxidative stress contributed to the transition of non-fatal hepatic steatosis to steatohepatitis with progressive fibrosis (Starkel *et al.*, 2003). The review in this section will focus on the role of oxidative stress in liver injury.

1.2.1 Role of Oxidative Stress in Liver Injury

Reactive oxygen species (ROS) or reactive nitrogen species (RNS) are molecules produced in cells under normal physiology, which elicit immunological responses as well as control signal transduction. However, ROS or RNS can cause cell/tissue damages under pathophysiological conditions (Figure 1.3) (Kaplowitz & Tsukamoto, 1996). Superoxide anion (O_2^-), hydroxyl radical ($^{\bullet}OH$), hydroperoxyl radical ($^{\bullet}OOH$), nitrosoperoxy carbonate ($ONO_2CO_2^-$) and peroxynitrite ($ONOO^-$) are the major injury-causing ROS or RNS (Klaunig & Kamendulis, 2004). They can cause liver injury via different mechanisms (Jaeschke *et al.*, 2003). As shown in Figure 1.3, there are several sources generating oxidative stress, including mitochondrial respiration, oxidases, iron overload and phagocytic cells such as macrophages (Kaplowitz & Tsukamoto, 1996). The free radicals produced can activate transcription factors leading to gene regulation or

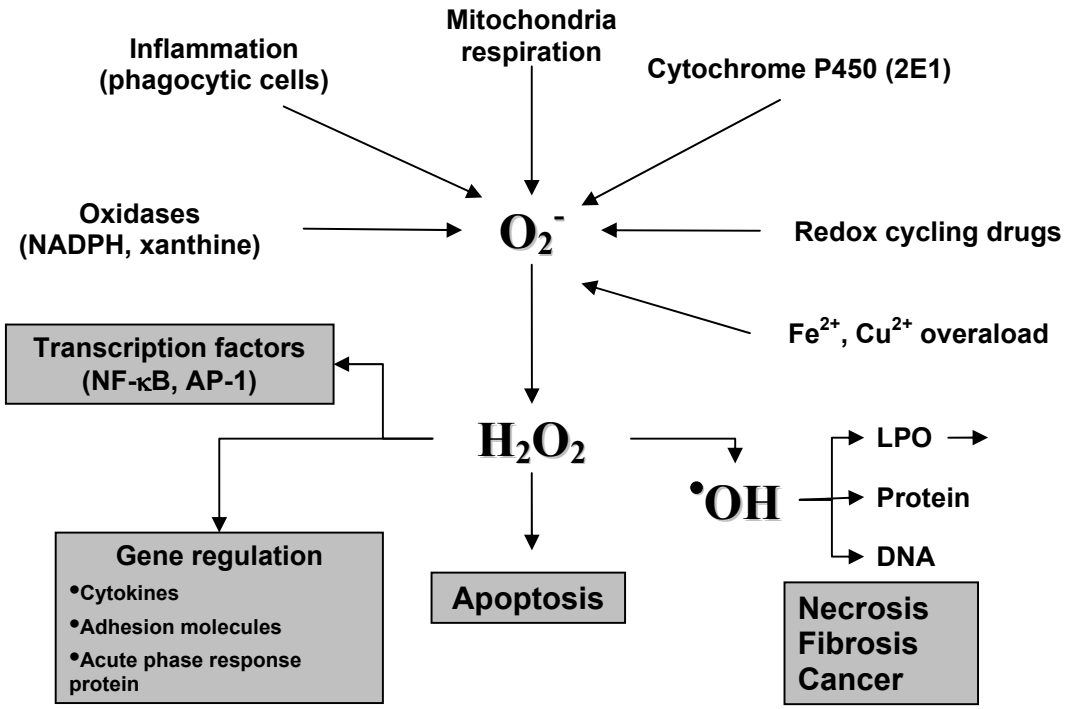

(Based on ideas from Kaplowitz *et al*., Progress in Liver Diseases 14: 131-159, 1996)

Figure 1.3 Sources and Consequences of Oxidative Stress.

Superoxide anion (O_2^-) is a reactive free radical produced naturally in the body. It is the key molecule initiating the propagation of other reactive oxygen species production. Several systems can generate superoxide anion including mitochondria respiration, cytochrome P450 2E1, redox cycling drugs, iron overload, oxidases, and inflammatory factors. The produced superoxide anion is rapidly converted into other kinds of free radicals e.g. hydrogen peroxide (H_2O_2) and hydroxyl radical ($^{\bullet}OH$). These radicals can trigger activation of transcription factors leading to gene regulation. They can also initiate oxidation of macromolecules, apoptosis or necrosis. Abbreviation: NF-κB, nuclear factor-kappaB; AP-1, activator protein-1.

initiate apoptosis (Figure 1.3). Free radicals may also cause modification of lipids, proteins or DNA. The modified lipids, proteins or DNA cannot function normally, which may lead to necrosis, fibrosis or cancer (Figure 1.3) (Kaplowitz & Tsukamoto, 1996). Oxidative stress manifested as elevated free radical levels, for example, lipid peroxides can initiate an inflammatory response during liver injury (Mottaran *et al.*, 2002). Overproduction of superoxide anion was part of the causes for alcohol-induced liver injury (Kono *et al.*, 2001; Kono *et al.*, 2000). Increased mitochondrial oxidative stress contributed to anti-tuberculosis drug-induced liver toxicity (Chowdhury *et al.*, 2006). Other than superoxide, peroxynitrite is also a potent pro-oxidant playing major role in liver injury. Peroxynitrite is the product from the reaction between nitric oxide and superoxide anion, which can cause nitration, oxidation as well as nitrosation of proteins (Jourd'heuil *et al.*, 2001). An elevation of peroxynitrite displayed as an increase in nitrotyrosine protein adducts was found in acetaminophen-induced liver injury (Ito *et al.*, 2004). Depletion of the non-enzymatic antioxidant, glutathione, also contributed to the liver injury caused by acetaminophen toxicity (Ito *et al.*, 2004).

1.2.2 Mechanism of Hepatic Oxidative Stress

Oxidative stress is the result of an elevated oxidative burden and/or a decrease in antioxidant defence. Several enzymes in liver contribute to the production of oxidative free radicals, including NADPH oxidase, xanthine oxidase, fatty acid oxidase and myeloperoxidase (Table 1.1) (Kaplowitz & Tsukamoto, 1996). Mitochondrial respiration and the cytochrome P450 system are also the major sources of free radical production (Table 1.1). The oxidative free radical producing enzymes or cascades respond to different stimuli, and their abundance also varies among different types of cells.

Table 1.1 Sources of ROS, RNS and Antioxidants in the Liver

Cellular oxidants	***Source***	***Oxidative species***	***Example***
Endogenous	Mitochondria	O_2^-, H_2O_2, $^{\bullet}OH$	Ischemia/reperfusion
	Cytochrome P450 2E1	O_2^-, H_2O_2	Ethanol induction
	Macrophage/inflammatory cells	O_2^-, $NO^{\bullet}$, H_2O_2,OCl^-	Inflammation
	NADPH oxidase	O_2^-	
	Myeloperoxidase	OCl^-	
	Xanthine oxidase	O_2^-	Alcohol and fatty liver, reperfusion injury
	NO synthase	$NO^{\bullet}$	Endotoxemia
	iNOS (hepatocytes, macrophages)		
	eNOS (endothelial cells)		
Exogenous	Redox cycling compounds	O_2^-	Drug toxicity
	Metals (Fenton reaction)	$^{\bullet}OH$	Hemochromatosis, Wilson's disease
	Radiation	$^{\bullet}OH$	

Cellular antioxidants	***Enzymatic***	***Nonenzymatic***
	Superoxide dismutase	Vitamin E
	Catalase	Glutathione
	Glutathione peroxidase	
	GSSG reductase	

(Based on ideas from Klaunig *et al.*, Annual Review of Pharmacology and Toxicology, 44: 239-267, 2004)

Reactive oxygen species (ROS) including superoxide anions can be generated from mitochondrial electron transport (mitochondrial respiration), cytochrome P450 2E1, NADPH oxidase, xanthine oxidase. Myeloperoxidase can produce hypochlorous radical (OCl^-). Reactive nitrogen species (RNS), on the other hand, are produced through the nitric oxide (NO) synthase system. Different stimuli would trigger the generation of different types of free radicals. For example, alcoholic liver injury can convert xanthine dehydrogenase into xanthine oxidase resulting in superoxide anion production. Endotoxemia (e.g. lipopolysaccharide) can induce production of ROS as well as RNS. Numerous antioxidant systems are present in liver including enzymatic and non-enzymatic antioxidants. Antioxidant enzymes present in liver include superoxide dismutases (SOD), catalase, glutathione peroxidase, and glutathione reductase (GSSG reductase). The most abundant non-enzymatic antioxidants in liver are glutathione and vitamin E. Abbreviation: iNOS, inducible nitric oxide synthase; eNOS, endothelial nitric oxide synthase.

Studies found that NADPH oxidase-derived free radicals from Kupffer cells (macrophages residing in the liver) was the main cause of liver impairment in alcoholic liver injury (Kono *et al.*, 2001; Kono *et al.*, 2000). NADPH oxidase is expressed in both hepatocytes and Kupffer cells (Mizukami *et al.*, 1983; Wang *et al.*, 1992). Genetic deletion and pharmacological inhibition of NADPH oxidase were shown to protect the liver against alcohol-induced injury (Kono *et al.*, 2001; Kono *et al.*, 2000).

Peroxynitrite is a potent free radical causing liver injury (Ito *et al.*, 2004). High concentrations of NO can compete with superoxide dismutase to react with superoxide anion resulting in the formation of peroxynitrite (Estevez & Jordan, 2002). The reaction rate of superoxide anion with NO is three times faster than the scavenging rate of superoxide dismutase (Km = 7×10^{-9} $mol^{-1}Ls^{-1}$ vs. 2×10^{-9} $mol^{-1}Ls^{-1}$) (Estevez & Jordan, 2002). Inducible nitric oxide synthase (iNOS) can produce a high concentration of NO (in nanomolar to millimolar range). iNOS is expressed in many types of cells in the liver including Kupffer cells and hepatocytes. These cells also possess several systems to generate superoxide anion including NADPH oxidase, mitochondrial respiration, cytochrome P450 2E1, etc. Therefore, both NO and superoxide can be generated in the same cellular compartment in the liver to form peroxynitrite without the limitation of diffusion rate. Superoxide anion has a very short half-life and a short migration distance. The co-existence of superoxide anion and NO in the same cellular compartment is a very important criterion for peroxynitrite formation.

Lipid peroxides are also important oxidants formed during liver injury and can be generated in the presence of pro-oxidants along with unsaturated fatty acids or other reactive lipids such as phospholipids or free cholesterol (Marnett, 2002; Tribble *et al.*,

1987). Aldehydes such as 4-hydroxy-2-nonenal (HNE) and malondialdehyde (MDA) are examples of lipid peroxidation products. The half-life of lipid peroxides is much longer than other reactive oxygen species. Lipid peroxides can diffuse to a distal cellular or extracellular compartment (Browning & Horton, 2004). Lipid peroxidation is a chain reaction of oxidations. For example, the initial oxidation of a fatty acid by ROS can generate another fatty acid radical as the product. This fatty acid radical is unstable and it can elicit the second oxidation resulting in the generation of another unstable free radical. This kind of chain reaction mechanism is referred as the propagation of lipid peroxidation. This special feature may contribute to the wide-spread damage caused by lipid peroxidation (Tribble *et al.*, 1987).

A decrease in antioxidant defences can also cause oxidative stress. Many antioxidant enzymes are present in the liver including superoxide dismutase (SOD), catalase, glutathione peroxidase, and glutathione reductase (GSSG reductase) (Table 1.1) (Kaplowitz & Tsukamoto, 1996). A study on chronic alcoholism showed an decrease in glutathione peroxidase activity in rat livers upon ethanol administration (Bailey *et al.*, 2001). However, chronic ethanol administration was shown to increase the expression of mitochondrial manganese superoxide dismutase in rat livers (Koch *et al.*, 1994). This might represent one of the self-protecting systems arised upon liver injury (Koch *et al.*, 1994). Other than enzymatic antioxidants, non-enzymatic antioxidants also play a major role in defending against oxidative injury. Glutathione is the major non-enzymatic antioxidant in the liver (Table 1.1) (Lu, 1999). During acetominophen toxicity, depletion of glutathione is the key mechanism in liver injury (James *et al.*, 2003). Several studies have demonstrated that the responses of free radical production and antioxidant defence

upon liver injury are different between acute and chronic conditions (Navasumrit *et al.*, 2000). In acute liver injury, an increase in the oxidative burden plays a major role in deterioration of liver function. CYP2E1 and xanthine oxidase activities are increased, resulting in elevated superoxide anion production in acute alcoholic liver disease (Navasumrit *et al.*, 2000; Sultatos, 1988). Production of peroxynitrite is also increased due to the stimulation of iNOS in the liver upon ethanol adminstration (Baraona *et al.*, 2002). On the other hand, chronic alcohol administration can decrease antioxidant enzymes such as glutathione peroxidase and superoxide dismutase in the liver (Bailey *et al.*, 2001; Chen *et al.*, 1995; Misra *et al.*, 1992).

1.2.3 Hepatic Oxidative Stress in Hyperhomocysteinemia

Several studies have proposed that Hcy-induced oxidative stress is one of the mechanisms for HHcy-associated cardiovascular disease (Au-Yeung *et al.*, 2004; Dayal *et al.*, 2006; Wang & O, 2001). Recent studies have demonstrated that oxidative stress also occurs in the liver of HHcy animal models. Rats fed a folate-depleted diet showed an elevation of plasma Hcy levels, and such an elevation was correlated with increased hepatic lipid peroxidation (Huang *et al.*, 2001). CBS-deficient mice also showed an increase in oxidative stress in liver (Robert *et al.*, 2005; Vitvitsky *et al.*, 2004).

Glutathione (GSH) is one of the downstream products in the transsulfuration pathway during Hcy metabolism (Reaction H, Figure 1.2). It has been proposed that increased hepatic oxidative stress in CBS-deficient mice might be due to decreased production of glutathione. A study demonstrated a significant reduction in the hepatic GSH content in homozygous CBS-deficient mice (Vitvitsky *et al.*, 2004). However, in heterozygous CBS deficient mice, no change in the hepatic GSH content was observed but there was a

significant decrease in the GSH/GSSG ratio (GSH, reduced form of glutathione and GSSG, oxidized from of glutathione) (Vitvitsky *et al.*, 2004). The decrease in GSH/GSSG ratio indicated a sign of oxidative stress (Vitvitsky *et al.*, 2004). It is speculated that Hcy-induced oxidative stress in the liver may be mediated by mechanisms other than GSH depletion. However, the molecular mechanisms by which HHcy induces oxidative stress remain to be clarified.

1.3 Cholesterol Metabolism in Liver

Cholesterol is a very important biological molecule. It plays essential roles in biological membrane structure, the endocrine system as well as the digestive system (precursor of steroid hormones and bile acid). High levels of lipids (triacylglycerol and cholesterol) in blood are associated with increased risk of cardiovascular disease (1994; Gotto, 1992). Hypercholesterolemia is a form of hyperlipidemia, which indicates an abnormally high level of cholesterol in blood. A genetic defect is one of the factors causing hypercholesterolemia (Brown & Goldstein, 1976; Goldstein & Brown, 1973). Studies have found that obesity and diabetes can contribute to hypercholesterolemia (Morabia & Costanza, 2005; Tershakovec *et al.*, 2002). High plasma LDL cholesterol is conclusively linked to coronary heart disease (1984; Manninen *et al.*, 1988; Sacks *et al.*, 1996). According to the guidelines of the National Cholesterol Education Program, the concentration of total cholesterol in the plasma in a healthy individual is between 150 to 200 mg/dL (1994). Total cholesterol in the plasma above 200mg/dL will increase the risk for heart diseases.

Accumulation of lipids in the circulation can lead to cardiovascular disease due to atherosclerosis whereas in other organs can lead to dysfunction as well. Hepatic steatosis is characterized as an abnormal fatty change in the liver. Obesity and alcoholism are the known factors causing hepatic steatosis. With the presence of inflammatory triggers, steatosis can progress to cirrhosis and eventually loss of liver function (Farrell & Larter, 2006). In this section, lipoprotein and cholsterol metabolism, and the role of liver in hypercholesterolemia are reviewed.

1.3.1 Transport of Cholesterol in Lipoprotein

Cholesterol and triacylglycerol form the core of a lipoprotein complex. Lipids are transported in a form of lipoprotein complex. A lipoprotein complex includes a lipid core that is composed of triacylglycerol and cholesterol ester and a hydrophilic surface that consists of free cholesterol, phospholipids and apolipoproteins. The plasma lipoproteins are classified according to their particle densities, including chylomicrons (0.93 g/mL), very-low-density lipoproteins (VLDL, 0.93 – 1.006 g/mL), low-density lipoproteins (LDL, 1.019 – 1.063 g/mL) and high-density lipoproteins (HDL, above 1.063 g/mL). The density of lipoprotein is proportional to the protein content of the particle. Chylomicrons and VLDL are triacylglycerol-rich lipoproteins and the protein proportions are lower compared to that in LDL and HDL, which result in lower particle densities. LDL and HDL are the two major circulating lipoproteins.

VLDL is a lipoprotein synthesized in the liver and is rich in triacylglycerol. It is composed of 2% protein and 98% lipids. Triacylglycerol and peptides (except apolipoprotein B) in VLDL are removed by the action of lipoprotein lipase in the extrahepatic capillary beds (Figure 1.4) (Kwiterovich, 2000). Lipoprotein lipase hydrolyzes fatty acid from triacylglycerol. After the hydrolysis of triacylglycerol by lipoprotein lipase, the ratio of cholesterol to triacylglycerol in VLDL is increased (Reardon *et al.*, 1982). This modified VLDL becomes LDL which is a lipoprotein relatively rich in cholesterol (Reardon *et al.*, 1982). LDL contains 25% protein and 75% lipid in which 60% is cholesterol (Havel *et al.*, 1980). The size of LDL is smaller than VLDL due to the removal of the core lipid, triacylglycerol (Jackson *et al.*, 1976). Cholesterol ester inside a LDL particle is taken up and utilized by peripheral tissues

(From Brown *et al.,* Science 212: 628-635, 1981)

Figure 1.4 Lipoprotein metabolism

Lipids from the diet are packaged in intestine into a chylomicron particle. Chylomicron is a triacylglycerol-rich lipoprotein. The triacylglycerol in the chylomicron particle is hydrolyzed by lipoprotein lipase (LPL) at the endothelium of the vessel. The chylomicron remnant is taken up by the liver via low density lipoprotein receptor-related protein (LRP). HDL can be derived from chylomicron remnant. Very-low-density lipoprotein (VLDL) is synthesized by liver. VLDL is also a triacylglycerol-rich lipoprotein. LPL on the extrahepatic capillary beds hydrolyses fatty acids from triacylglycerol in VLDL. VLDL is then converted to low-density lipoprotein (LDL) which is removed by LDL receptor in liver and extrahepatic tissues. Nascent HDL secreted from liver or intestine can take up cholesterol from cell membranes or other lipoproteins. Nascent HDL becomes mature by increasing the proportion of cholesterol in HDL particle. With the action of lecithin-cholesterol acyltransferase (LCAT), free cholesterol is converted into cholesteryl esters, a storage form of cholesterol. On the other hand, the cholesterol esters in HDL can be transferred to VLDL or chylomicron remnants via the catalysis of cholesteryl ester transfer protein (CETP).

after internalization of LDL by the LDL receptor on the cell membrane.

HDL is a lipoprotein derived in extracellular space. HDL in a nascent form consists of phospholipids and apolipoprotein A1 (apo-A1). Hepatocytes and enterocytes can synthesize apo-A1 which is secreted in a lipid-poor form (Jackson *et al.*, 1976; Rader, 2006). The lipid-poor apo-A1 then recruits more phospholipids and free cholesterol, forming a nascent HDL particle (Rader, 2006). Nascent HDL particle can acquire more lipids from peripheral cells or other lipoproteins, and becomes a mature HDL particle (Figure 1.4) (Kwiterovich, 2000; Rader, 2006). The protein to lipid ratio in a mature HDL particle is about 50/50. The lipid component of a mature HDL particle consists of 30% phospholipid, 20% cholesterol and 5% triacylglycerol (Havel *et al.*, 1980). HDL particles are crucial in transferring lipid components between other lipoprotein particles and between cells. The proteins on the surface of HDL particle such as apo-A1 and apo-C2 activate the metabolic enzymes of lipoproteins including lecithin-cholesterol acyltransferase (LCAT) and lipoprotein lipase (LPL) (Smith *et al.*, 1978). The apo-A1 present on a nascent HDL particle activates LCAT which facilitates the formation of cholesterol ester, a storage form of cholesterol (Figure 1.4) (Smith *et al.*, 1978). LCAT hydrolyzes a fatty acid group from phospholipid and transfers it to free cholesterol to form cholesterol ester (Kwiterovich, 2000; Rader, 2002; Smith *et al.*, 1978). HDL cholesterol is taken up by the liver via scavenger receptor class-BI (SR-BI) (Rader, 2006). Cholesterol ester in HDL can also be exchanged with triacylglycerol in triacylglycerol-rich lipoproteins via the action of cholesteryl ester transfer protein (CETP). The apo-A1 on HDL (remnant) is eventually metabolized by liver or kidney (Rader, 2006).

1.3.2 Role of Liver in Hypercholesterolemia

Cholesterol can be derived from the diet or synthesized *de novo* in cells. Only the cholesterol synthesized in hepatocytes can be supplied to peripheral tissues. Non-hepatic cells can synthesize a minimal amount of cholesterol for local use. In normal physiology, when there is an excess of intracellular cholesterol, hepatocytes can maintain a homeostasis by decreasing the uptake of cholesterol by down-regulating LDL receptor density as well as decreasing cholesterol production (Havel *et al.*, 1980).

The liver produces and recycles endogenous and exogenous cholesterol. It can eliminate excess cholesterol from the periphery by taking up lipoproteins through the LDL receptor (Figure 1.4). Dysfunction of the LDL receptor can cause accumulation of LDL in the circulation (Brown & Goldstein, 1976). The most common type of hypercholesterolemia, familial hypercholesterolemia (FH) is a metabolic disorder with genetic defects in LDL receptor function leading to abnormal accumulation of circulating LDL (Brown & Goldstein, 1976). The estimated occurrence of heterozygous FH is 1 in 1000 to 1 in 500 in general population (Goldstein *et al.*, 1973). Several types of mutations causing LDL receptor dysfunction in FH have been discovered (Brown & Goldstein, 1986; Goldstein & Brown, 1984). As shown in Figure 1.5, mutations of LDL receptor can happen during (1) the synthesis in endoplasmic reticulum (null alleles), (2) the transport of encoded protein from endoplasmic to Golgi apparatus (transport-deficient alleles), (3) the binding of substrate (binding-deficient alleles) and (4) the engulfment of substrate in the coated pit (internalization-defective alleles) (Goldstein & Brown, 1989). One or more of these mutations would lead to a malfunction of the LDL receptor. Failure to take up LDL from the circulation causes its accumulation in the blood resulting in

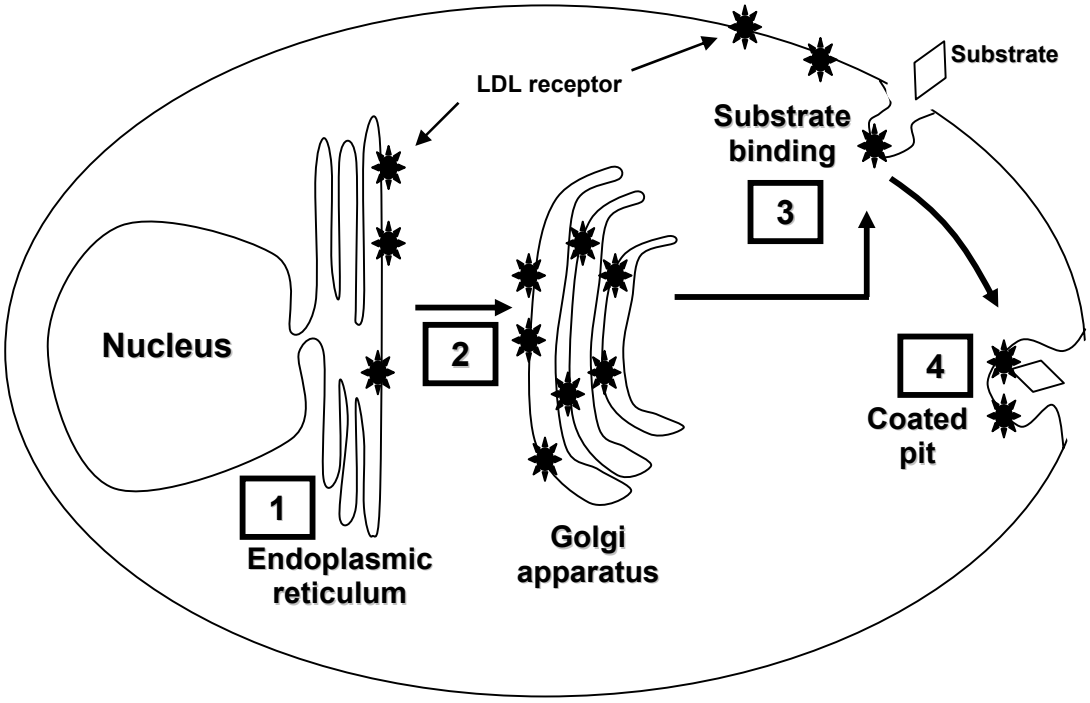

Figure 1.5 Systhesis and Mutations of LDL Receptor

LDL receptor is synthesized in endoplasmic reticulum as a precursor form. The precursor form of LDL receptor is modified into a mature form in Golgi complex. The mature LDL receptor is then secreted onto the cell surface. The substrate, LDL binds to the receptor and a coated pit is formed to internalize the LDL particle. The mutation of LDL receptor can happen during (1) the synthesis in endoplasmic reticulum, (2) the transport from endoplasmic reticulum to Golgi apparatus, (3) the binding of substrate and (4) the clustering in the coated pits.

hypercholesterolemia.

Another common type of inherited hypercholesterolemia is due to an abnormal elevation of cholesterol synthesis mediated by 3-hydroxymethylglutaryl-coenzyme A reductase (HMG-CoA reductase) (Goldstein & Brown, 1973). HMG-CoA reductase is the enzyme controlling the rate-limiting step in cholesterol biosynthesis (Qureshi *et al.*, 1976). It catalyzes the reduction of HMG-CoA to mevalonate (Figure 1.6). Mevalonate then undergoes a series of complex reactions to form cholesterol (Figure 1.6). Mevalonate is a natural inhibitor of HMG-CoA reductase. HMG-CoA reductase is located in endoplasmic reticulum with its catalytic site protruding out into the cytosol (Liscum, 2002). HMG-CoA reductase is strictly regulated by the supply of cholesterol (Liscum, 2002). Both endogenous and exogenous cholesterol can inhibit HMG-CoA reductase expression through the feedback mechanism (Chambers & Ness, 1997; Straka & Panini, 1995). Absence of normal feedback suppression of HMG-CoA reductase due to the presence of LDL can lead to overproduction of cholesterol (Goldstein & Brown, 1973). This type of inherited hypercholesterolemia is not due to a defect in the gene structure of HMG-CoA reductase but an impairment in the feedback control of the reductase (Goldstein & Brown, 1973). Because approximately half of the cholesterol in the body is derived from *de novo* biosynthesis in the liver, inhibition of hepatic cholesterol biosynthesis becomes one of the targets for lipid lowering therapy. A group of HMG-CoA reductase inhibitors refered to "statins" has been developed. Statins are the most commonly used drugs for treating hypercholesterolemia today, and they can effectively lower cholesterol in different types of hypercholesterolemia. Atorvastatin (Lipitor), pravastatin (Pravachol), and simvastatin (Zocor) are the most popularly used lipid lowering drugs.

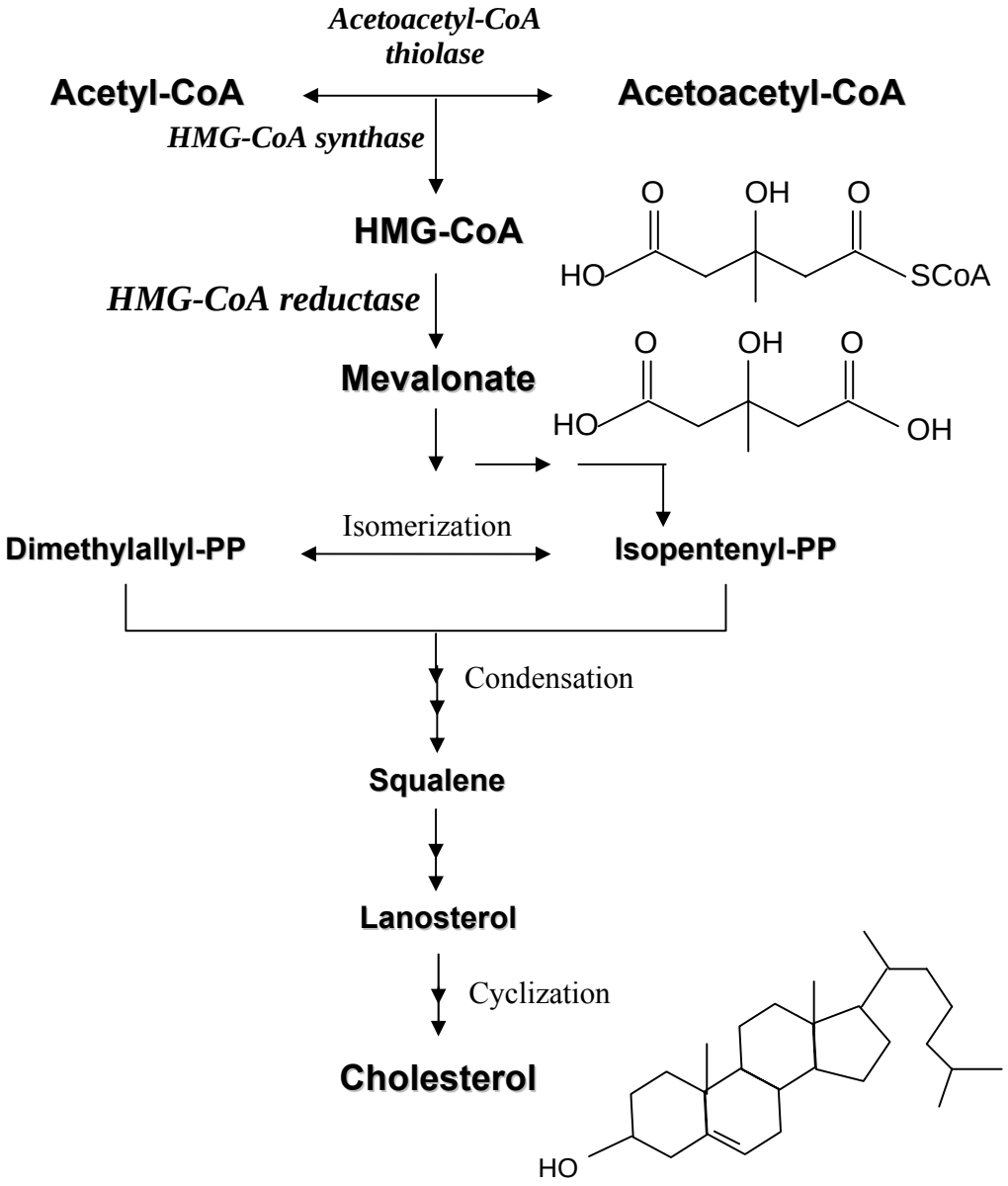

Figure 1.6 Biosynthesis of Cholesterol

Cholesterol biosynthesis is orginated by the supply of acetyl-CoA. Two acetyl-CoA molecules form acetoacetyl-CoA. Another acetyl-CoA is added onto acetoacetyl-CoA to form HMG-CoA by the catalysis of HMG-CoA synthase. HMG-CoA is reduced by HMG-CoA reductase to form mevalonate with NADPH as a reductant. Mevalonate is converted into isopentenyl pyrophosphate (PP) via the actions of kinases and decarboxylase. Squalene is formed after the isomerization and condensation of isopentenyl-PP. Squalene is a 30-carbon compound and is converted to squalene epoxide. Squalene epoxide then undergoes a complex cyclization to form lanosterol which is eventually converted into cholesterol.

1.3.3 Regulation of HMG-CoA Reductase

HMG-CoA reductase can be regulated by various biological pathways. Several kinases are involved in the post-translational regulation of HMG-CoA reductase, such as protein kinase C and AMP-activated protein kinase (Beg *et al.*, 1985; Clarke & Hardie, 1990). Insulin and thyroid hormone can regulate HMG-CoA reductase transcriptionally by up-regulating HMG-CoA reductase mRNA expression (Ness *et al.*, 1994; Simonet & Ness, 1988). All of these pathways together maintain the homeostasis of cholesterol in biological compartments.

1.3.3.1 Post-Translational Regulation of HMG-CoA Reductase Activity

HMG-CoA reductase activity can be regulated by phosphorylation and dephosphorylation (Figure 1.7) (Beg *et al.*, 1979). The phosphorylation of HMG-CoA reductase can be catalyzed by protein kinase C and AMP-activated protein kinase (which is also called reductase kinase) (Beg *et al.*, 1985; Clarke & Hardie, 1990). AMP-activated protein kinase can phosphorylate the serine-872 site of HMG-CoA reductase (Clarke & Hardie, 1990). The phosphorylated form of HMG-CoA reductase is inactive (Figure 1.7). The phosphorylated reductase can be re-activated by removal of the phosphate group by reductase phosphatase (Figure 1.7) (Beg *et al.*, 1979). However, the phosphorylation-dephosphorylation system may not account for long term control of HMG-CoA reductase activity (Brown *et al.*, 1979). Regulations of HMG-CoA reductase during diurnal cycle, cholesterol intake from diet and fasting conditions are not mediated by this post-translational modification but rather by protein synthesis (Brown *et al.*, 1979). When cellular adenosine triphophate (ATP) levels are depleted (energy deficit state), adenosine monophate (AMP) levels are

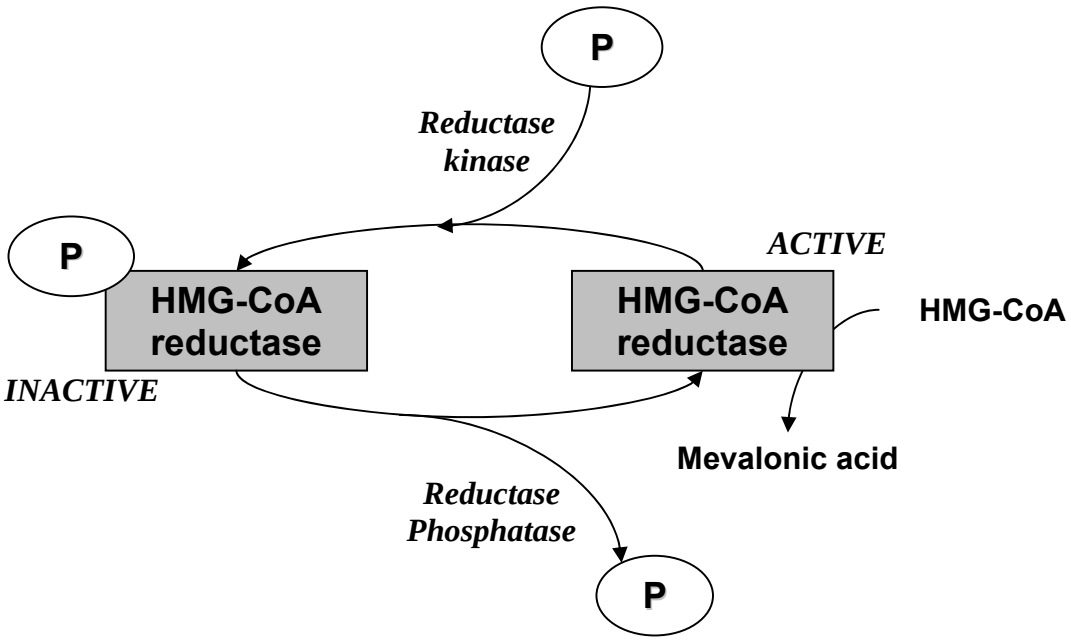

Figure 1.7 Phosphorylation of HMG-CoA Reductase

HMG-CoA reductase can be inactivated by phosphoryation. AMP-activated protein kinase (also called reductase kinase) controls the phosphorylation of HMG-CoA reductase. To re-activate HMG-CoA reductase or reductase kinase, the phosphate group is removed via the action of reductase phosphatase. (P: phosphate group).

increased due to the utilization of ATP to generate energy. The increased AMP levels can lead to an activation of AMP-activated protein kinase resulting in an inhibition of HMG-CoA reductase and cholesterol synthesis. This phosphorylation control of the reductase activity may provide a short-term preservation of energy by preventing cholesterol synthesis (Hardie, 1992). This pathway plays an important role in cell survival during unfavourable conditions.

1.3.3.2 Transcriptional Regulation of HMG-CoA Reductase Expression

In the recent decade, several transcription factors that regulate HMG-CoA reductase gene expression have been identified (Bennett & Osborne, 2000; Ngo *et al.*, 2002; Vallett *et al.*, 1996). Sterol regulatory element-binding proteins (SREBPs), a subfamily of basic helix-loop-helix zipper proteins, are important transcription factors regulating lipid homeostasis (Brown & Goldstein, 1997; Horton *et al.*, 2002). Two genes, SREBP-1 and -2 encode three SREBP proteins: SREBP-1a, -1c and –2 (Brown & Goldstein, 1997; Horton *et al.*, 2002). SREBP-1a is a potent activator for genes mediating synthesis of cholesterol, fatty acids and triacylglycerol (Horton *et al.*, 2002). SREBP-1c dominantly activates genes for fatty acid synthesis; however, it is a much weaker activator compared with SREBP-1a and SREBP-2 (Brown & Goldstein, 1997; Horton *et al.*, 2002). SREBP-2 preferentially activates transcription of enzymes for cholesterol production such as HMG-CoA reductase rather than those for fatty acid biosynthesis (Botolin & Jump, 2003; Horton *et al.*, 1998). SREBP is bound to endoplasmic reticulum in an inactive precursor form (Figure 1.8). Upon stimulation or when the cell is depleted of sterol, a sterol sensor protein, SREBP-activating protein (SCAP) transports SREBP from endoplasmic

(Modified from Horton, Biochemical Society Transactions, 30: 1091-1095, 2002)

Figure 1.8 Activation of SREBP

Upon stimulation or depletion of sterol, SREBP-activating protein (SCAP) anchors the precursor form of SREBP from endoplasmic reticulum to Golgi apparatus. In the Golgi apparatus, the precursor form of SREBP (125 kDa) is cleaved by site-1 protease (S1P) and site-2 protease (S2P) and converted to the active form (68 kDa). The active form of SREBP then enters the nucleus and bind to the sterol regulatory element (SRE) of the promoter region of DNA.

reticulum to theGolgi apparatus (Figure 1.8) (Horton *et al.*, 2002). The full-length SREBP (125kDa) is cleaved in Golgi apparatus to a truncated form (68kDa). The cleavage of SREBP is facilitated via two proteases, Site-1 protease (S1P) and Site-2 protease (S1P) (Figure 1.8) (Horton *et al.*, 2002). The truncated form of SREBP enters the nucleus and activates the transcription of target genes such as HMG-CoA reductase (Figure 1.8).

SREBP is a weak transcription factor which requires the presence of co-regulators to elicit maximal transcription activation. In order to efficiently activate the transcription of HMG-CoA reductase, concurrent activations of other transcription factors (co-regulators) along with SREBP-2 are essential. The two known co-regulators for HMG-CoA reductase are cAMP response element binding protein (CREB) and nuclear factor (NF-Y) (Bennett & Osborne, 2000; Ngo *et al.*, 2002). CREB and NF-Y were recruited to the promoter region of HMG-CoA reductase when cells were depleted with cholesterol (Bennett & Osborne, 2000; Ngo *et al.*, 2002).

CREB is a basic domain leucine zipper (bZip) transcription factor (Figure 1.9). Its ability to activate gene transcription requires phosphorylation at the site of serine (Ser)-133 (Figure 1.9) (Gonzalez & Montminy, 1989). Insulin, a known activator of HMG-CoA reductase, was reported to stimulate CREB activity in HepG2 cells by inducing CREB phosphorylation (Klemm *et al.*, 1998). The structure of CREB includes an activation domain and a DNA binding domain (Figure 1.9) (Servillo *et al.*, 2002). The site of Ser-133 is located at the P-box (KID, kinase inducible domain) in the activation domain (Figure 1.9) (Servillo *et al.*, 2002). Several kinases are able to phosphorylate CREB, including cAMP-dependent kinase (protein kinase A, PKA), p38 mitogen-activating

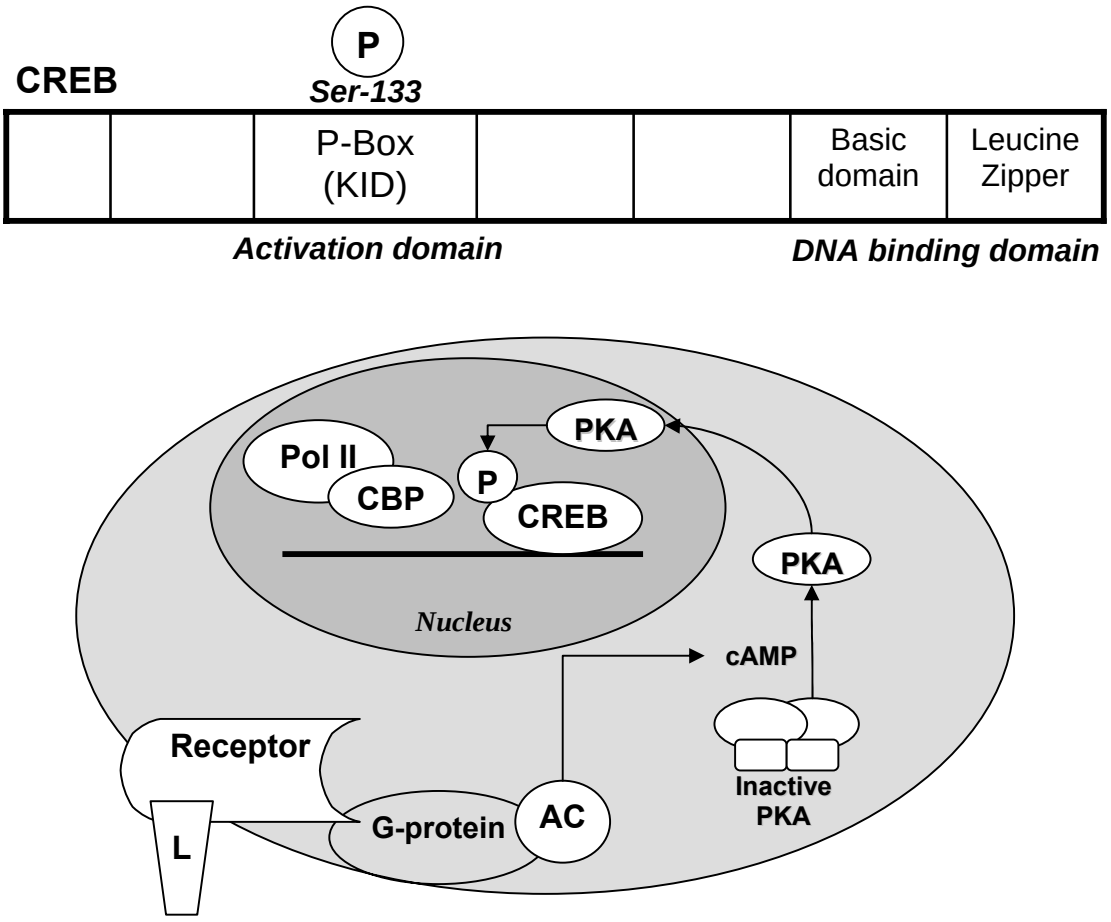

Figure 1.9 Structure and Activation of CREB

CREB is a basic domain leucine zipper (bZip) protein including an activation domain and DNA binding domain. Upon stimulation, CREB is phosphorylated at Ser-133 in the kinase inducible domain (KID or P-box). Several kinases can phosphorylate CREB, including PKA, p38 MAP kinase and ERK-1/2. For example, the binding of ligand (L) to a receptor leads to the activation of G-protein and adenylyl cyclase (AC). Activation of AC causes an elevation of cAMP level which, in turn, activates PKA. The catalytic unit of PKA then translocates into nucleus and phosphorylates CREB. The phosphorylated CREB binds to CREB-binding protein (CBP). Such interaction facilitates the binding of CBP to RNA polymerase-linked transcription factor IIB (Pol II) resulting in gene transcription. Abbreviation: P, phosphate group.

protein kinase (p38 MAPK), extracellular signal-regulated kinase-1/2 (ERK-1/2) and calmodulin kinases (CaMK) (Shaywitz & Greenberg, 1999). Upon phosphorylation, CREB binds toCREB-binding protein (CBP) (Figure 1.9) (Chrivia *et al.*, 1993). Such interaction facilitates the binding of CBP to RNA polymerase-linked transcription factor IIB (TFIIB) resulting in the initiation of gene transcription (Figure 1.9) (Servillo *et al.*, 2002).

NF-Y (also called CCAAT-binding factor, CBF) is a heterotrimeric complex consisting of NF-YA, NF-YB and NF-YC (Figure 1.10) (Sinha *et al.*, 1995). It frequently acts as a synergistical transcription factor for others (Romier *et al.*, 2003). NF-Y can increase the affinity of the neighbouring transcription factor(s) binding to DNA. The interaction of NF-Y with SREBP-1 is one of the examples of such synergism (Jackson *et al.*, 1998). All the subunits of NF-Y are constitutively present in the nucleus. In order to activate transcription, NF-YB and NF-YC first interact with each other to form a heterodimer (Figure 1.10) (Mantovani, 1999). NF-YA then binds to the heterodimer to form a heterotrimer which binds DNA with high specificity and affinity (Figure 1.10) (Bi *et al.*, 1997; Kim & Sheffery, 1990).

1.3.4 Homocysteine and Cholesterol Metabolism

Both HHcy and hypercholesterolemia are independent risk factors for cardiovascular disease. Researchers have attempted to determine the possible association between these two risk factors. Several studies using animal models have shown abnormal lipid metabolism in liver during HHcy (Hamelet *et al.*, 2007; Namekata *et al.*, 2004; Werstuck *et al.*, 2001; Woo *et al.*, 2005). The underlying mechanisms have been investigated in

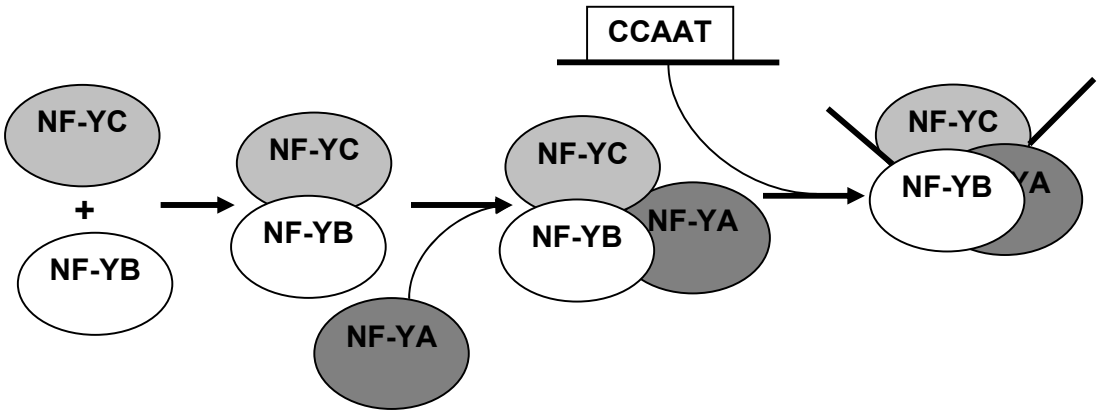

(Based on ideas from Mantovani, Gene, 239: 15-27, 1999)

Figure 1.10 Binding of NF-Y Subunits

NF-Y (also called CCAAT-binding factor, CBF) is a heterotrimeric complex consisting of NF-YA, NF-YB and NF-YC. All the subunits of NF-Y are constitutively present in the nucleus. In order to activate transcription, NF-YB and NF-YC first interact with each other to form a heterodimer. NF-YA then binds to the heterodimer to form a heterotrimer. The heterotrimer binds the CCAAT site of DNA with high specificity and affinity.

cultured hepatocytes (O *et al.*, 1998; Werstuck *et al.*, 2001; Woo *et al.*, 2006b; Woo *et al.*, 2005). Despite the *in vivo* and *in vitro* studies have shown a positive correlation of Hcy and cholesterol synthesis, whether such a correlation happens in humans remains to be investigated.

1.3.4.1 *In vitro* and *In vivo* Studies

Our laboratory previously investigated the relationship between Hcy and cholesterol biosynthesis in HepG2 cells (a human hepatoma cell line) (O *et al.*, 1998). Hcy can stimulate biosynthesis and secretion of cholesterol in HepG2 cells (O *et al.*, 1998). Hcy increased HMG-CoA reductase activity, which was not due to the direct interaction between the enzyme and Hcy (O *et al.*, 1998). It was suggested that Hcy caused an up-regulation of HMG-CoA reductase synthesis at the transcription or translation level (O *et al.*, 1998). The same study also demonstrated that addition of Hcy into the cell culture medium would abolish the normal feedback inhibitory mechanism of LDL on HMG-CoA reductase (O *et al.*, 1998). Other than hepatic cells, HMG-CoA reductase expression in vascular cells was also studied. Li *et al*. investigated the effect of Hcy on HMG-CoA reductase in vascular endothelial cells and showed that Hcy increased the stability of HMG-CoA reductase mRNA (Li *et al.*, 2002).

Werstuck *et al*. studied the effect of Hcy on cholesterol metabolism using the heterozygous CBS-deficient HHcy model (Werstuck *et al.*, 2001). They revealed that dysfunction of cholesterol and triacylglycerol biosynthetic pathways in HHcy mouse liver was mediated by increased endoplasmic reticulum stress (Werstuck *et al.*, 2001). In the same study, they also demonstrated an increase in HMG-CoA reductase mRNA level in Hcy-treated HepG2 cells (Werstuck *et al.*, 2001). Namekata *et al*. showed an increase in

serum apo B-100 and VLDL levels in homozygous CBS-deficient mice (Namekata *et al.*, 2004). However, an increase in triacylglycerol but not cholesterol in the liver and serum was found in this CBS-deficient model (Namekata *et al.*, 2004). Nevertheless, the authors suggested that these mice were still prone to atherosclerosis because of hypertriglyceridemia and decreased HDL levels (Namekata *et al.*, 2004). Hcy was also able to reduce apolipoprotein-A1 expression in HHcy mouse liver and in HHcy human plasma (Mikael *et al.*, 2006). Another study demonstrated a reduction of circulating HDL and an increase in HDL cholesterol clearance in CBS-deficient HHcy mice with spontaneous atherosclerosis (Liao *et al.*, 2006). These studies suggested several mechanisms for the decrease in plasma HDL levels during HHcy (Liao *et al.*, 2006; Mikael *et al.*, 2006). The mechanisms by which Hcy affects lipid metabolism are increasingly studied.

1.3.4.2 Clinical Trials

Although several *in vivo* and *in vitro* studies have proven that Hcy is able to interfere with lipid metabolism, the association of Hcy with elevated plasma cholesterol or lipid levels is still controversial due to the discrepancies in clinical studies. One epidemiological study, the Hordaland Homocysteine Study (7591 men and 8585 women), stated that plasma total Hcy level was positively related to total cholesterol level, blood pressure and heart rate, and inversely related to physical activity (Nygard *et al.*, 1995). A relatively small sample size study conducted in Utah, United States (n=266) also showed that plasma LDL cholesterol concentration was positively correlated with plasma Hcy levels (Wu *et al.*, 1994). Another study (n=60) showed a negative correlation between Hcy levels and apolipoprotein-A1 protein expression in the plasma of coronary artery

disease patients (Mikael *et al.*, 2006). The same study also showed a negative correlation between plasma Hcy levels and HDL cholesterol levels (Mikael *et al.*, 2006). In contrast, in the study done by Dalery *et al*. in Quebec, Canada (n=734), no significant correlation was found between Hcy and lipids or lipoprotein cholesterol levels (Dalery *et al.*, 1995). Even though some studies have showed a positive correlation between plasma Hcy and cholesterol levels, there is no conclusion on the causality between these two parameters.

II. Hypothesis and Objectives

2.1 Rationale and Hypothesis

Previous studies investigating liver abnormalities in HHcy were conducted in genetically modified animal model, heterozygous or homozygous cystathionine β-synthase (CBS)-deficient mice (Hamelet *et al.*, 2007; Namekata *et al.*, 2004; Robert *et al.*, 2005; Werstuck *et al.*, 2001). CBS is a crucial enzyme in the transsulfuration pathway (Reaction F, Figure 1.2). Elimination of CBS activity may result in decreased production of biologically important downstream products such as cysteine and glutathione (Figure 1.2). In this situation, it is difficult to evaluate the specific effects elicited by HHcy alone. In the present study, a diet-induced HHcy model was developed to examine the abnormalities and the underlying mechanisms in liver. Along with the results of other studies, the present study may provide more comprehensive mechanisms of Hcy-associated liver disorders.

Our laboratory has established a diet-induced HHcy model which yielded a moderately high blood Hcy level in order to study the effect of Hcy on endothelial function and its underlying mechanisms (Au-Yeung *et al.*, 2004; Wang *et al.*, 2002). It was shown that Hcy increased superoxide anion levels in aortic endothelium and also in vascular cells (Au-Yeung *et al.*, 2004; Wang & O, 2001; Woo *et al.*, 2003). Hcy-induced oxidative stress might contribute to an inflammatory response in vascular cells resulting in endothelial dysfunction (Au-Yeung *et al.*, 2004; Wang & O, 2001; Wang *et al.*, 2002). Several studies using CBS-deficient mice and folate-deficient rats showed that there was an increase in hepatic oxidative stress during HHcy (Huang *et al.*, 2001; Robert *et al.*, 2005). Hepatic oxidative stress has been shown to contribute to liver injury (Jaeschke *et al.*, 2003; Kono *et al.*, 2001; Kono *et al.*, 2000).

On the other hand, several studies have found hepatic steatosis in HHcy patients and animal models (Carson *et al.*, 1965; Namekata *et al.*, 2004; Werstuck *et al.*, 2001). Hcy induced endoplasmic reticulum stress led to dysregulation of cholesterol and triacylglycerol biosynthetic pathways (Werstuck *et al.*, 2001). Another recent study demonstrated that several genes involved in hepatic lipid homeostasis including ATP-binding cassette transporters and nuclear hormone receptors were altered in CBS-deficient mice (Hamelet *et al.*, 2007). It was previously found that Hcy was able to increase HMG-CoA reductase activity in human hepatocytes leading to an increase in cholesterol synthesis (O *et al.*, 1998). In this *in vitro* study, it was suggested that the effect of Hcy on HMG-CoA reductase was not due to the direct interaction between Hcy and the enzyme (O *et al.*, 1998).

We hypothesized that (1) diet-induced HHcy will result in liver injury via oxidative stress; (2) the effect of Hcy on hepatic HMG-CoA reductase will be mediated by transcriptional regulation; and (3) folic acid supplementation will offer a hepatoprotective effect during HHcy.

2.2 Objectives

The general objective of the study was to investigate the biochemical and molecular mechanisms of Hcy-induced liver injury and abnormal lipid metabolism.

The specific aims were:

(1) to examine the morphological changes in the liver of diet-induced HHcy rats;

(2) to examine the role of oxidative stress in Hcy-induced liver injury;

(3) to investigate the effect of HHcy on cholesterol biosynthesis in the liver and the molecular mechanism of Hcy-induced HMG-CoA reductase expression via transcriptional regulation in cultured hepatocytes; and

(4) to examine whether folic acid was effective in protecting the liver during HHcy.

III. Methods

3.1 Materials

3.1.1 Chemicals and Reagents

See Appendix I

3.1.2 Buffers

See Appendix II

3.1.3 Equipment

See Appendix III

3.2 Animal Model

Male Sprague-Dawley rats (Charles River Laboratories, Wilmington, MA, USA) aged 8 weeks were divided into three groups and maintained for 4 weeks on the following diets: (1) control diet (regular diet) consisting of Lab Diet Rodent Diet 5001 (PMI Nutrition International, St Louis, MO, USA); (2) high-methionine diet consisting of regular diet plus 1.7% (w/w) methionine; and (3) high-methionine plus folic acid diet, consisting of regular diet plus 1.7% (w/w) methionine and 0.025% (w/w) folic acid (Au-Yeung *et al.*, 2004; Wang *et al.*, 2002; Woo *et al.*, 2006b; Woo *et al.*, 2005). Each group consisted of 12 to 16 rats. Results from our previous studies demonstrated that HHcy could be induced in rats after 4 weeks of high-methionine diet (Au-Yeung *et al.*, 2004; Wang *et al.*, 2002; Woo *et al.*, 2006b; Woo *et al.*, 2005). After 4 weeks dietary treatment, rats were anesthetized with pentobarbital followed by euthanasia. Blood was collected and centrifuged at 3000 × *g* for 20 minutes at 4°C to collect serum. Hcy and folate concentrations in serum were measured with the IMx assays (Abbott Diagnostics, Abbott

Park, IL, USA) and DELFIA® Folate kit (PerkinElmer, Boston, MA, USA), respectively according to manufacturer's instructions (Au-Yeung *et al.*, 2004; Wang *et al.*, 2002; Woo *et al.*, 2006b; Woo *et al.*, 2005). All procedures were performed in accordance with the Guide to the Care and Use of Experimental Animals published by Canadian Council on Animal Care and approved by University of Manitoba Protocol Management and Review Committee.

Diet	**Methionine (%)**	**Folic acid (%)**
Control	0.43	0.00059
High-methionine	17.43	0.00059
High-methionine plus folic acid	17.43	0.02559

3.3 Cell Culture

3.3.1 Rat Hepatocytes

Hepatocytes were isolated from rat liver as previously described (Page & Garvey, 1979). Briefly, a Sprague-Dawley rat (250 - 300g) fed a regular diet was anesthetized using pentobarbital followed by euthanasia. Liver was perfused via portal vein with PBS at 3 mL/min for 15 minutes to flush out blood cells, followed by perfusion with 0.5 mM EGTA in PBS for another 10 minutes. The perfusion with EGTA was to chelate multivalent cations including calcium, magnesium and iron. Hepatic cells were no longer adherent after perfusion with a chelating agent (Coman, 1954). Liver was then perfused with Hank's buffered salt solution (HBSS) containing 0.05% type I collagenase (Sigma-Aldrich, St Louis, MO, USA) for another 15 minutes. Collagenase digestion requires the

presence of calcium. Calcium was replenished by HBSS after perfusion with EGTA. The perfused liver was cut into small pieces and further digested with 0.05% type I collagenase in HBSS at 37°C for 20 minutes. The digested tissue was then minced and filtered. Cells in the filtrate were collected after centrifugation at 100 × g for 5 min at 25°C. The isolated cells were washed 4 times with PBS and 1 time with HBSS. Trypan blue test showed a typical higher than 95% viability of the isolated hepatocytes. Hepatocytes were cultured in Dulbecco's modified Eagle's medium (DMEM) containing 10% fetal bovine serum (Invitrogen, Carlsbad, CA, USA) in the Thermo Forma Direct Heat CO_2 incubator with 5% CO_2 and 95% O_2 at 37°C. Medium was replaced with fresh one after 2 hours post-isolation incubation for hepatocyte attachment. Hepatocytes were incubated for 24 hours post-isolation prior to experiments (Woo *et al.*, 2005).

3.3.2 HepG2 Cells

HepG2 cells (American Type Culture Collection, Manassas, VA, USA) were cultured in DMEM supplemented with 10% fetal bovine serum. Cells were maintained at 70% to 80% confluence for experiments. Trypsin-EDTA buffer (see Appendix II) was used for cell detachment during subcultivation. HepG2, a cell line derived from human hepatoblastoma, is commonly used as a human hepatocyte model to study regulation of lipid metabolism (Gibbons, 1994; Javitt, 1990).

3.3.3 Preparation of L-Homocysteine

L-Hcy was prepared from L-Hcy thiolactone by a method described previously (Duerre & Miller, 1966; Hatch *et al.*, 1961; Sengupta *et al.*, 2001). In brief, L-Hcy thiolactone was dissolved and hydrolyzed in sodium hydroxide (5 M) to remove the thiolactone

group (Duerre & Miller, 1966; Hatch *et al.*, 1961; Sengupta *et al.*, 2001). The preparation was then neutralized with HCl. The concentration of L-Hcy was quantified with the IMx Hcy assay. Freshly prepared L-Hcy was used in all of the experiments (Woo *et al.*, 2006b; Woo *et al.*, 2005).

3.4 Western Immunoblot

Cellular levels of specific proteins were determined by Western immunoblot analysis in cells and liver tissue (Laemmli, 1970). After incubation, cells were lysed with the lysis buffer (20 mM Tris, 150 mM NaCl, 1 mM EDTA, 1 mM EGTA, 2.5 mM sodium pyrophosphate, 1 mM β-glycerophosphate, 1 mM sodium orthovanadate, 2.1 μM leupeptin, 1 mM PMSF, 1% Triton-X 100). For preparing tissue samples, a portion of liver was homogenized in the lysis buffer in 1:4 (w/v) ratio. The homogenate was sonicated at 60 Amp for 5 seconds for cells or at 120 Amp for 20 seconds for tissue at 4°C followed by centrifugation at 3000 × *g* for 10 minutes to remove cell or tissue debris. Supernatant was collected and subjected to protein measurement. Sample with equal amount of cellular protein were denatured and prepared in 1× SDS sample buffer. The denatured protein sample was separated by SDS-PAGE, and then transferred to a nitrocellulose membrane. The membrane with protein attached was blocked with 5% non-fat milk in Tris-buffered saline (TBS) with 0.05% Tween-20 (TBST) for 1 hour at room temperature. Next, after washing 3 times for 10 minutes with TBST, the membrane was probed with specific primary antibodies overnight at 4°C. Finally, the membrane was incubated with peroxidase-conjugated secondary antibody for 60 minutes at room temperature. Bands corresponding to target proteins were visualized with enhanced

chemiluminescence (ECL) reagents using hydrogen peroxide as a substrate. ECL signal was detected by X-OMAT blue film (KODAK). The film was scanned and converted to a TIFF file, and bands were analyzed with a gel documentation system (Bio-Rad Gel Doc & Quantity One version 4.2.1).

3.5 Electrophoretic Mobility Shift Assay (EMSA)

EMSA was performed to investigate the DNA binding activity of transcription factors including CREB and NF-Y.

3.5.1 Probe Labeling

CREB or NF-Y consensus oligonucleotide (3 pmol) was incubated with a labeling mixture containing 20μCi γ-^{32}P ATP (PerkinElmer, Wellesley, MA, USA), 5 units T4 polynucleotide kinase and 1× T4 polynucleotide kinase buffer (Promega, Madison, WI, USA) in sterile water as total volume of 10 μL at 37°C for 10 minutes. A 1 μL aliquot of 0.5 M EDTA was added to stop the reaction. The radioactive probe was further diluted with 39 μL Tris-EDTA (TE) buffer and passed through Microspin^{TM} S-300 HR columns twice for purification. The radiolabeled probe was stored at -20°C prior to the EMSA assay.

3.5.2 Isolation of Nuclear protein

Nuclear protein was isolated from hepatocytes and liver tissue as previously described (Dignam *et al.*, 1983; Sitrin *et al.*, 1998). In brief, after incubation, cells were washed with TBS and the cell pellet was collected. For preparing the liver sample, a portion of

tissue was homogenized in TBS in 1:4 (w/v) ratio and tissue pellet was collected after centrifugation at 3000 × *g* for 10 minutes. The cell pellet or tissue pellet was lysed with buffer A (10 mM HEPES, 10 mM KCl, 0.1 mM EDTA, 0.1 mM EGTA, pH 7.9, 0.5 mM PMSF, 1 mM DTT, 2.5 μg/mL leupeptin, 0.8μg/mL pepstatin and 0.1% Nonidet-P). The nuclear portion of cells was collected after centrifugation at 15,000 × *g* for 15 minutes at 4°C. The pellet was further lysed with buffer C (20 mM HEPES, 0.4 M NaCl, 1 mM EDTA, 1 mM EGTA, pH 7.9, 1 mM PMSF, 1 mM DTT, 5 μg/mL leupeptin and 1.6 μg/mL pepstatin) to release the nuclear contents. The supernatant, nuclear content was collected after centrifuging at 15,000 × *g* for 15 minutes at 4°C. Protein concentration of the nuclear content was determined and samples were equalized to 10 μg of protein.

3.5.3 EMSA

The transcription factor and DNA binding activity was determined by EMSA (Sitrin *et al.*, 1998). 10 μg of nuclear protein was incubated with 10 μL of a reaction buffer containing 100 mM Tris, 1 M NaCl, 50 mM DTT, 10 mM EDTA, 40% glycerol, 1 mg/ml BSA, 50 ng/ml double-stranded poly (dI.dC) for 15 minutes at 25°C (Sitrin *et al.*, 1998). To the reaction mixture was then added 2 μL of specific ^{32}P end-labeled oligonucleotide probe and the reaction was carried out at 25°C for 20 minutes. After the reaction, 2 μL of 0.1% bromophenol blue was added to the final radioactive mixture. The radioactive samples were separated by a 6% non-denaturing polyacrylamide gel. The gel was dried on a piece of filter paper at 80°C for 90 minuties using a gel dryer, followed by autoradiography with KODAK™ X-OMAT blue film. The film was scanned and bands were analyzed with a gel documentation system (Bio-Rad Gel Doc & Quantity One version 4.2.1).

For supershift experiments, nuclear protein samples were pre-incubated with antibodies specifically bound to the transcription factor for 30 minutes at 25°C prior to the addition of ^{32}P end-labeled oligonucleotide probe. Experiment was carried out as the same way mentioned in previous paragraph.

To confirm the specificity of the binding of ^{32}P end-labeled consensus oligonucleotide probe to transcription factor (protein), a 100-fold excessive unlabeled oligonucleotide was added to the reaction mixture. For both CREB and NF-Y, the unlabeled oligonucleotides prevented the binding of ^{32}P end-labeled oligonucleotide probes to transcription factor and no signal was observed in the autoradiography.

3.6 Enzyme Activity

3.6.1 Aminotransferases

Liver injury was assessed by measuring the activity of aspartate aminotransferase (AST) and alanine aminotransferase (ALT) in serum. During liver injury, AST and ALT are released from the liver and secreted into the circulation. The activity of AST and ALT in serum can be measured and their elevations indicate liver damage. The serum AST and ALT activities in rats were measured with enzymatic kits following the instructions provided by the manufacturer (Wako Chemicals, Richmond, VA, USA).

3.6.2 HMG-CoA Reductase

HMG-CoA reductase activity was measured by a radiochemical method using [3-^{14}C]-HMG-CoA as a substrate (Wilce & Kroon, 1992). In brief, a portion of liver was homogenized (1:4, w/v) or cells were lysed in a buffer containing 50 mM Tris and 150

mM NaCl at pH 7.4. The resulting pellet was collected after centrifugation at 3000 × *g* for tissue or at 900 × *g* for cells. The tissue or cell pellet was resuspended in a phosphate buffer containing 50 mM K_2HPO_4, 5 mM DTT and 1 mM EDTA (pH 7.4 using H_3PO_4) and protein concentration was determined. An aliquot of the resuspension (1 mg protein for tissue or 100 μg protein for cells) in a volume of 200 μL was used for the enzyme assay. Sample was incubated with a enzyme assay mixture (100 μL) containing 80 mM K_2HPO_4 (pH 7.4 using H_3PO_4), 4 mM DTT, 0.8 mM EDTA 20 mM glucose 6-phosphate, 2.5 mM NADP, 1 unit of glucose-6-phosphate dehydrogenase, 50 μM HMG-CoA and 0.04 μCi [3-^{14}C]-HMG-CoA (PerkinElmer). The reaction was carried out at 37°C for 60 minutes. The assay tubes were then placed on ice, and mevalonolactone (1 mg) and 5 M HCl were added to stop the reaction. The [3-^{14}C]-mevalonate produced underwent lactonization with HCl as a catalyst to form mevalonolactone. The reaction mixture was loaded on a thin-layer chromatography (TLC) plate. Radiolabeled HMG-CoA (substrate) and mevalonolactone (product) were separated by TLC using a solvent system of chloroform-acetone (2:1 v/v). TLC plate was air-dried, and the location of mevalonolactone was visualized after staining with iodine vapor. The area containing mevalonolactone was scraped from the plate, and the radioactivity was measured using a scintillation counter. HMG-CoA reductase activity was calculated and expressed as pmol of mevalonate produced per mg of protein per minute.

3.6.3 Superoxide Dismutase

The activity of superoxide dismustase in liver tissue was determined by a method previously described (Crapo *et al.*, 1978). A portion of liver tissue was homogenized in a

50 mM potassium phosphate buffer (pH 7.8) containing 0.1 mM EDTA in a ratio of 1:8 (w/v) followed by centrifugation at 15,000 × *g* for 10 minutes at 4°C. Supernatant was collected and protein concentration was equalized to 5 μg/μL for all samples. Prior to the initiation of reaction, 0.15 mL of 100 μM cytochrome *c*, 0.15 mL of 2 mM xanthine, 20 μL of sample and 580 μL of 50mM potassium phosphate buffer (pH 7.8) were added into a 3-mL cuvette. The reaction was initiated by adding 90 mU of xanthine oxidase to generate superoxide anion. The generated superoxide anion would oxidize cytochrome *c* and the rate of change in absorbance at λ = 550nm (oxidized form of cytochrome *c*) was recorded every 15 seconds for 4 minutes. The superoxide dismutase in the sample would scavenge xanthine oxidase-generated superoxide anion and decrease the rate of oxidization of cytochrome *c*. Superoxide dismutase activity in the sample can be determined by calculating the percentage decrease in the rate of oxidation of cytochrome *c*. One unit of superoxide dismutase activity was defined as the ability to decrease 50% in change of the absorbance per minute of that yielded by xanthine oxidase alone. A commercially available superoxide dismutase (Sigma-Aldrich) was used as a standard.

3.6.4 Glutathione Peroxidase

Glutathione peroxidase activity was determined as previously described (Everson *et al.*, 2005; Takahashi, 2000). In brief, a portion of liver tissue was homogenized in a 75mM potassium phosphate buffer (pH 7.0) containing 300 mM sucrose and 2 mM DTT (1:10 w/v) followed by centrifugation at 15,000 × *g* for 25 minutes at 4°C. Supernatant was collected and protein concentration was equalized to 1.5 μg/μL. A 15 μL of sample was added to a 985 μL reaction mixture containing 2.8 mM Na azide, 0.7 mM EDTA, 1.25

mM glutathione and 1.25 U/mL glutathione reductase, and 0.125 mM NADPH in 75 mM potassium phosphate buffer (pH 7.0) followed by 2 minutes equilibrium at 37°C in a glass cuvette. After equilibration, 10 μL of 7.8 mM tert-butyl hydroperoxide was added to the mixture to initiate the reaction, and the absorbance at λ = 340nm (to measure utilization of NADPH) was recorded every 15 seconds for 5 minutes. The activity was calculated using the absorption coefficient of NADPH as 6.22 $mM^{-1}cm^{-1}$ (Everson *et al.*, 2005; Takahashi, 2000).

3.6.5 Glutathione Reductase

Glutathione reductase activity was determined as previously described (Everson *et al.*, 2005; Takahashi, 2000). In brief, a portion of liver tissue was homogenized in a 100 mM potassium phosphate buffer (pH 7.5) containing 300 mM sucrose and 2 mM DTT (1:10 w/v) followed by centrifugation at 15,000 × *g* for 20 minutes at 4°C. Supernatant was collected and protein concentration was equalized to 3 μg/μL. A 50 μL of sample was added to a glass cuvette containing 440 μL reaction buffer (100mM potassium phosphate buffer (pH 7.5) with 1mM EDTA). The reaction was initiated by adding 500 μL of 2 mM oxidized glutathione (GSSG) and 10 μL of 10mM NADPH. The absorbance at λ = 340nm was recorded every 10 seconds for 2 minutes, which monitored the utilization of NADPH. The activity of glutathione reductase was calculated using the absorption coefficient of NADPH as 6.22 $mM^{-1}cm^{-1}$ (Everson *et al.*, 2005; Takahashi, 2000).

3.6.6 Catalase

Catalase activity in liver tissue was measured as previously described (Aebi, 1984; Everson *et al.*, 2005). A piece of liver tissue was homogenized in a 50 mM potassium

phosphate buffer (pH 7.4) with 0.1% Triton-X. Supernatant was collected and protein concentration was equalized to 1.5 μg/μL. In a glass cuvette, 5 μL of sample and 595 μL of 50 mM phosphate buffer (pH 7.4) were added and incubated at room temperature for 2 minutes. The reaction was initiated by adding 300 μL of 30 mM H_2O_2 solution into the cuvette, and the change of absorbance at λ = 240 nm (to measure the degradation of H_2O_2) was measured every 15 seconds for 45 seconds. The activity was calculated using the degradation coefficient of H_2O_2 as 0.00394 $mM^{-1}mm^{-1}$ (Aebi, 1984; Everson *et al.*, 2005).

3.6.7 NADPH Oxidase

NADPH oxidase activity was measured by the lucigenin chemiluminescence assay (Kashiwagi *et al.*, 1999; Li *et al.*, 1998). A portion of liver was homogenized in a 50 mM phosphate buffer (pH 7.0, 1:8 w/v) containing 1 mM EDTA and 1 mM PMSF. After centrifugation at 3000 × g for 10 minutes at 4°C, supernatant was collected and protein concentration was measured. An aliquot of supernatant (100 μg proteins in a volume of 25μL) was incubated with lucigenin (5 μM) in a phosphate buffer (50 mM, pH 7.0) for 2 minutes followed by adding the substrate, 100 μM NADPH (Kashiwagi *et al.*, 1999). Chemiluminescent signal (photon emission) was measured every 15 seconds for 3 minutes using a luminometer (Lumet LB9507, Berthold Technologies GmbH & Co. KG, Bad Wildbad, Germany). In principle, the reaction of lucigenin with superoxide anion leads to the formation of lucigenin dioxetane that decomposes to produce two molecules of N-methylacridone (Li *et al.*, 1998). One of these two N-methylacridone molecules is in an electronically excited state and emits a photon. The photon emission that reflects the amount of superoxide anion in the sample can be detected using a luminometer (Li *et al.*,

1998). To verify that the photon signal in the liver during HHcy was mainly generated from NADPH oxidase, the same experiments were performed using sodium succinate, arginine or xanthine as a substrate in the lucigenin chemiluminescene assay, and a negligible chemiluminescent signal was detected. A standard curve was prepared by using xanthine (100 μM) and known serial concentrations of xanthine oxidase (Sigma-Aldrich) to generate a defined amount of superoxide anion. NADPH oxidase activity was calculated based on the amount of superoxide anion produced in the reaction mixture.

3.6.8 Nitric Oxide Synthase

Total NOS activity in liver was measured using the L-citrulline assay (Shah *et al.*, 1999). In brief, a portion of liver was homogenized in a lysis buffer (1:4 w/v) containing 50 mM Tris, 0.1 mM EGTA, 0.1 mM EDTA, 2 μM leupeptin, 1 mM PMSF, 1% (v/v) Nonidet P-40, 0.1% SDS, 0.1% sodium deoxycholate, pH 7.5 followed by centrifugation at 3000 × g for 10 minutes (Shah *et al.*, 1999). Supernatant was collected and protein concentration was determined. An aliquot of supernatant (500 μL) was incubated in a reaction mixture (200 μL) containing 50 mM Tris, 1 mM NADPH, 3 μM tetrahydrobiopterin, 100 mM calmodulin, 2.5 mM $CaCl_2$, 50 mM L-valine, 10 μM L-arginine and 0.2 μCi L-[^{3}H]-arginine as a substrate at 37°C for 1 hour. The reaction was stopped by adding 1 mL of cold stopping buffer composed of 20 mM HEPES, 2 mM EDTA and 2 mM EGTA, pH 5.5. The radiolabeled reaction product, L-citrulline was purified by anion exchange chromatography with a Dowex AG 50WX-8 resin column (Bio-Rad, Hercules, CA, USA). At pH 5.5, L-citrulline is neutral charge and is not retained by the resin. The eluent

was collected and the radioactivity associated with L-citrulline was measured with a scintillation counter and NOS activity was calculated (Shah *et al.*, 1999).

3.6.9 cAMP-dependent Kinase/Protein Kinase A

PKA activity was determined using a synthetic substrate, kemptide (Sigma-Aldrich) (Siow *et al.*, 1992). In brief, cells were lysed in the lysis buffer described in section 3.4. For tissue samples, a portion of liver was homogenized in a buffer containing 10 mM imidazole acetate, 4 mM $MgCl_2$, 0.5 mM PMSF, 5 mM 2-mercaptoethanol, pH 7.4, and 0.32 M sucrose (1:4, w/v). The cell lysate or tissue homogenate was sonicated and centrifuged at 15,000 × *g* for 10 minutes at 4°C. Supernatant was collected and protein concentration was determined. Sample (100 μg tissue protein or 20 μg cell protein) was incubated with a reaction mixture containing 0.5 M HEPES pH 7.4, 100 mM $MgCl_2$, 10 mM EGTA, 10 mM 2-mercaptoethanol, 170 μM kemptide, and an ATP solution including 0.12 μM [γ-^{32}P]-ATP (10 μCi/mL, 3000 Ci/mmol, PerkinElmer) and 0.1 μM ATP (Cell Signaling Technology) in a total volume of 25 μL for 15 minutes at 30°C (Siow *et al.*, 1992). After the reaction, sample was spotted onto a piece of P-81 filter paper and washed 4 times with 0.4% phosphoric acid and once in 95% ethanol. Radioactivity of samples was measured by a scintillation counter and PKA activity was calculated (Siow *et al.*, 1992).

3.6.10 Cystathione β-synthase

Cystathione β-synthase (CBS) activity in liver was determined as previously described (Taoka *et al.*, 1998). Briefly, a portion of liver was homogenized in 50 mM potassium phosphate buffer (pH 6.9) (1.4, w/v) followed by centrifugation at 18,000 × *g* for 30

minutes at 4°C to remove debris. Supernatant was collected and samples with equal concentration of proteins were prepared to carry on the assay. The reaction mixture contained 187.5 mM Tris (pH 8.3), 3.125 mM EDTA, 0.219 mM L-cystathionine, 62.5 mM DL-Hcy, 0.475 mM S-adenosylmethionine, 3.125 mM propargylglycine, 0.625 mM pyridoxal phosphate (in the volume of 400 μL) and 150 μL supernatant. The reaction was initiated by adding 50 μL of a serine mixture composed of 300 μM of L-serine and 0.1 μCi [^{14}C]-L-serine followed by 1 hour incubation at 37°C. The reaction was terminated by adding 300 μL of 15% ice-cold trichloroacetic acid. The final product was centrifuged at 6000 × *g* for 5 minutes to remove precipitants. The clear supernatant was loaded onto a 1.5 × 12-cm column (Bio-Rad Econo-Pac polypropylene columns) containing AG-50W-X8 resin (Bio-Rad) to bind the product, cystathionine. The column was washed 2 times with 4 mL water, 6 times with 4 mL 0.6 N HCl followed by 4 times with 4 mL water. The bound cystathionine was then eluted with 5 mL 3 N ammonium hydroxide. The radioactivity of [^{14}C]-cystathionine was determined by a scintillation counter (Taoka *et al.*, 1998). CBS activity was calculated and expressed as nmol of cystathionine produced per mg of protein per minute.

3.7 Reverse Transcriptase – Polymerase Chain Reaction (RT-PCR)

3.7.1 Isolation of Total RNA

Total RNAs were isolated from cells and liver tissue with TriZol reagent (Invitrogen) as per the manufacturer's instructions. In brief, cells were washed with PBS three times and

collected in TriZol reagent. For tissue preparation, a portion of liver was homogenized in TriZol reagent (1:4 w/v) and tissue debris was removed by centrifugation at 12,000 × g for 10 minutes at 4°C. Supernatant of homogenized tissue or Trizol-dissolved cell pellet was added 200 μL chloroform followed by gentle mixing. The aqueous layer was collected after centrifugation at 12,000 × g for 15 minutes at 4°C and RNA was precipitated by adding 500 μL isopropanol. RNA pellet was collected and washed with 75% ethanol in sterile DEPC-treated water after centrifuged at 12,000 × g for 10 minutes at 4°C. The RNA pellet was then dissolved in sterile DEPC-treated water and the RNA concentration was measured.

3.7.2 Reverse Transcription from RNA to DNA

In the RT reaction, 2 μg of total RNA was incubated with a RT mixture containing 1st strand buffer (50 mM Tris pH 8.3, 75 mM KCl and 3 mM $MgCl_2$), 10 mM DTT, 0.5 mM dNTPs, 10 ng/μL oligo$(dT)_{12\text{-}18}$ primer (Invitrogen), 1 U/μL RNase inhibitor (Promega) and 1 U/μL MMLV reverse transcriptase (Invitrogen) in a total volume of 20 μL for 1 hour at 37°C. The reaction was stopped by heating the mixture at 95°C for 2 minutes to denature the reverse transcriptase.

3.7.3 Polymerase Chain Reaction

HMG-CoA reductase mRNA expression was examined by semi-quantitative reverse transcriptase-polymerase chain reaction (RT-PCR) analysis. The primers used for specifically detecting HMG-CoA reductase expression (Forward primer: 5'-CCTGCT-GCCATAAACTGGAT-3' and reverse primer: 5'-GGGCACATGCAATGTAGATG-3'; Genbank accession no. NM_013134) were synthesized by Invitrogen Corp. The reaction

mixture of PCR contained 0.2 mM dNTP (Invitrogen), 0.4 μM forward and reverse primer, 2 units Taq-DNA polymerase (Cell Signaling) and 2 μL cDNA product from RT reaction in a total volume of 50 μL. The number of cycles for PCR amplification was 28 with the annealing temperature at 60°C (94°C for 30 seconds, 60°C for 30 seconds, 72°C for 1 minute) and additional 10 minutes extension was carried out at 72°C. The PCR products were separated by 1.8% agarose gel (in 0.5× TE buffer containing 0.5 μg/mL ethidium bromide) electrophoresis and visualized under UV light with a gel documentation system (Bio-Rad Gel Doc, Quantity One). The band intensity was analyzed with Quantity One software (Bio-Rad). Glyceraldehyde 3-phosphate dehydrogenase (GAPDH) (Forward primer: 5'-ATTGCATCCTGCACCACCAA-3' and reverse primer: 5'-GTAGCCATA-TTCATTGTCATA-3'; Genbank accession no. NM_017008) was used as an internal standard to verify equal PCR product loading for each experiment. Values were expressed as a ratio of HMG-CoA reductase to GAPDH.

3.8 Histological Analysis

3.8.1 Histochemical Staining

3.8.1.1 Hematoxylin and Eosin Staining

In brief, liver was excised and a portion of it was immersion-fixed in 10% neutral-buffered formalin (10% formalin, 25 mM NaH_2PO4, 45 mM Na_2HPO_4) overnight followed by dehydration with ethanol and xylene, and was embedded in paraffin. Sequential 5 μm paraffin-embedded cross sections were prepared. Sections were subjected to hematoxylin and eosin (H&E) staining in order to examine the morphology.

After deparaffinization, sections were washed with tap water, and first stained with Harris hematoxylin solution then with 0.05% eosin solution. Sections were then dehydrated with ethanol and xylene, and mounted with Permount® (Fisher scientific, Fairlawn, NJ, USA) and cover-slip.

3.8.1.2 Oil Red O Staining

Liver was excised and a portion of it was frozen immediately in liquid nitrogen. Sections were stained with Oil Red O to visualize neutral lipids including cholesterol ester and triacylglycerol in tissue. In brief, cryosections of liver tissue (10 μm) were prepared and fixed with 40% formalin calcium solution (40% formalin and 10% $CaCl_2$). Sections were washed with 100% propylene glycol for 5 minutes twice and then stained with 0.5% Oil Red O solution in propylene glycol for 10 minutes with agitation. The stained sections were then washed with 85% propylene glycol for 3 minutes and rinsed with distilled water. Nuclei were visualized by staining the sections with Harris hematoxylin solution followed by rinsing with running tap water. Slides were mounted with 80% glycerol, and images were captured and analyzed by using an Axioskop2 MOT microscope (Carl Zeiss Microimaging, Thornwood, NY), an Axiocam camera, and Photoshop 6.0 (Adobe, San Jose, CA) (Lehr *et al.*, 1999).

3.8.2 Immunohistochemical Staining

Immunohistochemical staining was performed to examine the distribution of nitrotyrosine protein adducts in liver tissue. Sequential 5 μm paraffin-embedded cross sections were prepared. After deparaffination, sections were incubated with 2% BSA blocking agent following permeablization. Mouse anti- nitrotyrosine antibodies (1:100)

(Zymed Laboratories, South San Francisco, CA) were used as primary antibody. Sections were incubated with primary antibodies overnight at 4°C, followed by treatment with 0.3% hydrogen peroxide (H_2O_2) for 20 minutes at room temperature to inhibit endogenous peroxidase. Sections were then incubated with biotin-conjugated anti-mouse immunoglobulins (1:200, DakoCytomation, Carpinteria, CA) as secondary antibodies for 1 hour followed by peroxidase conjugated-streptavidin for 30 minutes (Zymed). To visualize nitrotyrosine product adducts in tissue, sections were then treated with 3,3-diaminobenzidine (DAB)-H_2O_2 colorimetric substrate solution. The attached peroxidase catalyzed the H_2O_2-mediated oxidation of DAB to yield an insoluble brown precipitate. The area displaying as brownish color indicated nitrotyrosine protein adducts. Images were captured and examined using an Axioskop2 MOT microscope (Carl Zeiss Microimaging, Thornwood, NY), an Axiocam camera, and Photoshop 6.0 (Adobe, San Jose, CA). For a negative control, normal IgG was used as a primary antibody.

3.8.3 Immunofluorescent Staining

For detecting activated transcription factors and examining their distributions, isolated hepatocytes (2×10^5 cells) were cultured on collagen-coated chamber slides in DMEM in the absence or presence of Hcy. After incubation for 15 minutes, cells were preserved with a fixative containing 4% paraformaldehyde in PBS and permeabilized with ice-cold methanol. The fixed cells were blocked with 2% BSA for 30 minutes and then incubated with primary antibodies against SREBP-2, phosphorylated-CREB (Ser133), and/or NF-YA/CBF-B (Bennett & Osborne, 2000) (Santa Cruz Biotechnology, Santa Cruz, CA, USA) at 4°C overnight. After washing with PBS, cells were incubated with FITC-conjugated goat anti-rabbit IgG, Cy3-conjugated rabbit anti-goat IgG (Zymed

Laboratories) and Alexa Fluor 405 goat anti-mouse IgG (Molecular Probes) as secondary antibodies at 25°C for 45 minutes. Slides were mounted with anti-fade buffer containing 4% n-propyl gallate and 80% glycerol in PBS. Sections were viewed under Zeiss fluorescence microscopy (Axioskop2 MOT) and images were captured and examined using an Axiocam camera and Photoshop 6.0 (Adobe).

3.9 Detection of Reactive Oxygen Species

3.9.1 Lipid Peroxides

Lipid peroxidation in liver tissue was determined by measuring the thiobarbituric acid reactive substances (TBARS), malondialdehyde (MDA) (Bjorkegren *et al.*, 2002; Ohkawa *et al.*, 1979). Briefly, a portion of liver was homogenized in 1.14% KCl solution containing 50 mM desferroxamine in 1:10 w/v ratio followed by centrifugation at 3000 × g for 10 minutes at 4°C. The protein concentration of the supernatant was determined. An aliquot of supernatant (0.1 mL) was added to the reaction mixture containing 0.05 mL 8.1 % SDS, 0.375 mL 20% acetic acid, 0.375 mL 0.8% thiobarbituric acid and 0.1 mL distilled water. After incubation at 95°C for 1 hour, the amount of MDA formed in the reaction mixture was measured by a spectrophotometer at an absorbance of λ = 532 nm. A known concentration of MDA (Sigma-Aldrich) was used as the standard. Results were expressed as nmol MDA produced per mg protein. The amount of MDA correlated to the level of lipid peroxides in liver (Woo *et al.*, 2006a).

3.9.2 Superoxide Anion

The level of superoxide anion in liver was determined as previously described with minor modification (Au-Yeung *et al.*, 2004; Zou *et al.*, 2001). A portion of liver was homogenized in a buffer (1:4, w/v) containing 20 mM HEPES, 1 mM EDTA and 0.1 mM PMSF. After centrifugation at 6000 × *g* for 10 min, an aliquot of supernatant was incubated in a reaction mixture containing 10 μM dihydroethidium and 0.5 mg/mL salmon testes DNA for 30 min at 37°C. The superoxide anion in liver homogenate caused the oxidation of dihydroethidium leading to the formation of ethidium which was detected at an excitation of 475 nm and an emission of 610 nm using a fluorometer (Spectra Max Gemini, Molecular Devices, Sunnyvale, CA, USA). The fluorescent signal produced by ethidium was proportional to the level of superoxide anion present in liver (Woo *et al.*, 2006a).

3.9.3 Nitric Oxide

The measurement of nitrite and nitrate was used to assess the NO levels in liver tissue (Schmidt & Kelm, 1996). In brief, a portion of liver was homogenized in a buffer containing 20 mM Tris, 2 mM EDTA, pH 7.4. After centrifugation at 400 × *g* for 10 minutes at 4°C, 400 μL of distilled water and 300 μL of 0.3M NaOH were added to 100 μL of supernatant. Protein was denatured after 5 minutes at room temperature incubation and 300 μL of 5% $ZnSO_4$ was then added to the mixture to precipitate the denatured protein. Supernatant was collected after centrifugation at 10,000 × *g* for 20 minutes at 4°C. The amount of nitrite and nitrate was determined in supernatant with Griess reaction method based on the azo coupling reaction (Schmidt & Kelm, 1996).

In brief, supernatant was treated with nitrate reductase and the co-factors, FAD and NADPH at 37°C for 25 minutes to reduce nitrate to nitrite (Schmidt & Kelm, 1996). The reductase reaction was stopped by adding 14.5 units of lactate dehydrogenase and 1 mM Na pyruvate to oxidize the NADPH. 12.5 mM sulfanilamide in 6 M HCl and 12.5 mM N-(1-naphthyl)ethylenediamine in methanol were then added to the reaction to complete the azo coupling reaction. The diazoamino benzene formed in the reaction mixture was measured by a spectrophotometer at absorbance of λ = 520nm. The $NaNO_2$ at different concentrations was used as standards (Woo *et al.*, 2006a).

3.10 Detection of Biological Molecules

3.10.1 Homocysteine

The unbound Hcy in liver tissue was extracted as previously described (Ueland *et al.*, 1984). A portion of liver was homogenized in a buffer containing 0.8 N perchloric acid and 10 mM EDTA in a 1:2 (w/v) ratio. The precipitated protein was removed by centrifugation at 3000 × *g* for 10 minutes at 4°C. Supernatant was collected and adjusted the pH to 7.0 with 5 N NaOH. Perchloric acid was precipitated by adding 1M KCl followed by centrifugation at 5000 × *g* for 10 minutes at 4°C. The neutral solution was subjected to Hcy measurement by IMx (Au-Yeung *et al.*, 2004; Wang *et al.*, 2002; Woo *et al.*, 2005).

To determine the intracellular Hcy levels in hepatocytes, cells were lysed by three freeze/thaw cycles and sonication (Werstuck *et al.*, 2001). Supernatant was collected after

centrifugation at 3000 × *g* for 10 minutes at 4°C and subjected to Hcy measurement by IMx (Werstuck *et al.*, 2001).

3.10.2 Cholesterol and Triacylglycerol

Cholesterol and triacylglycerol content in liver tissue, hepatocytes or medium was extracted and measured by commercially available kits (Wako Chemicals) (Folch *et al.*, 1957). In brief, a portion of liver (1:20 w/v) or hepatocytes pellet was homogenized in chloroform and methanol (1:1) mixture. After homogenization, a portion of chloroform and distilled water were added to create an extraction system as 4:2:3 chloroform:methanol:water (Folch *et al.*, 1957). Lipid content was extracted to the chloroform phase after vortex. Following centrifugation at 300 × *g* for 3 minutes at room temperature, the aqueous layer and tissue debris were removed. The chloroform phase was dried under stream of nitrogen gas. The lipid pellet was collected and resuspended in 100% ethanol, and subjected to the measurement using the kits. For lipid extraction in medium, the extraction system of 4:2:3 (chloroform:methanol:medium) was used.

3.10.3 Glutathione

The concentration of reduced glutathione (GSH) and oxidized glutathione (GSSG) in liver was measured using 5,5'-dithiobis-2-nitrobenzoic acid (DTNB) (Anderson, 1985). In brief, a portion of liver was homogenized in 5% sulphosalicylic acid (1:5 w/v) followed by centrifugation at 3000 × g for 10 minutes to remove denatured proteins. An aliquot of supernatant (20μL) was incubated with 10μL 0.01 M DTNB in a phosphate buffer (0.2M Na_2HPO_4/NaH_2PO_4, pH 7.8). Another aliquot of supernatant was pretreated with 2-vinylpyridine to bind the reduced form GSH. Samples were then treated with

glutathione reductase to reduce the unbound oxidized glutathione (GSSG) to GSH prior to the addition of DTNB in order to measure the amount of GSSG. The color product, 5-thio-2-nitrobenzoic acid (TNB) in the reaction mixture was measured by a spectrophotometer at absorbance λ = 412nm. The GSH or GSSG (Sigma-Aldrich) at different concentrations was used as a standard.

3.10.4 Cyclic Adenosine Monophosphate (cAMP)

The cAMP levels in liver or HepG2 cells were measured using DELFIA® cAMP kit (PerkinElmer). The procedures were carried out according to the instruction provided by the manufacturer. Prior to the assay, cAMP in liver tissue was extracted with diluted HCl (Leffler *et al.*, 1999). In brief, a portion of liver tissue was homogenized in 0.1 M HCl (1:2 w/v). Protein concentration of the homogenate was determined. An equal amount of 0.1 M NaOH was added to the homogenate to neutralize the acid followed by centrifugation at 15,000 × *g* for 15 minutes. Supernatant was collected and subjected to the cAMP assay. To measure cellular levels of cAMP, cultured hepatocytes were lysed in a buffer provided by the manufacturer prior to the assay (Woo *et al.*, 2006b).

3.11 Statistical Analysis

Statistical analysis was performed using the unpaired Student's t-test, ANOVA or Pearson correlation analysis where appropriate (GraphPad Prism 3, GraphPad, San Diego, CA). Data are represented as mean ± standard error of mean (SEM), where n represents the number of animals, or as mean ± standard deviation (SD) with n indicating the number of sets of cells. A value of $P<0.05$ was considered statistically significant.

IV Results

4.1 Liver Function and Morphology in Hyperhomocysteinemic Model

Objective

In the early studies, fatty liver and liver hypertrophy were found in HHcy patients (Carson *et al.*, 1965; Gaull *et al.*, 1974). In addition, several recent studies demonstrated lipid accumulation or hepatic steatosis in the CBS-deficient HHcy murine model (Namekata *et al.*, 2004; Robert *et al.*, 2005; Werstuck *et al.*, 2001). These studies were performed on either a genetically modified murine model alone or in combination with dietary modification (Namekata *et al.*, 2004; Robert *et al.*, 2005; Werstuck *et al.*, 2001). It was known that a high protein meal can siginificantly increase both methionine and Hcy levels in the blood (Guttormsen *et al.*, 1994). Intake of excess methionine can increase Hcy levels in circulation (Bostom *et al.*, 1995). In the present study, a diet-induced HHcy model was developed and used to study hepatic abnomalities (Au-Yeung *et al.*, 2004; Wang *et al.*, 2002; Woo *et al.*, 2005). The **first objective** of my study was to investigate the functional and morphological changes in the liver of the diet-induced HHcy rat.

Results

4.1.1 Induction of HHcy in Sprague-Dawley Rats

HHcy rats were induced by feeding 8-week old Sprague-Dawley rats a high-methionine diet for 4 weeks (Au-Yeung *et al.*, 2004; Wang *et al.*, 2002; Woo *et al.*, 2006a; Woo *et al.*, 2005). After 4-weeks dietary treatment, rats were sacrificed. Blood was collected and centrifuged at 3000 × *g* for 20 minutes at 4°C to prepare the serum samples. Livers were excised and collected for experiments.

4.1.1.1 Increase in Serum and Hepatic Hcy levels

The body weight and liver wet weight of rats fed with different diets did not show any significant differences (Table 4.1). The group of rats fed a high-methionine diet showed more than a 6-fold increase in the serum Hcy concentrations compared with that of the rats fed a regular diet (Table 4.1). This group of rats fed a high-methonine would be referred as hyperhomocysteinemic (HHcy) rats in the following sections. Livers of different groups of rats were homogenized and hepatic Hcy concentrations were measured. The hepatic unbound (non protein-bound) Hcy level of HHcy rats was 3 to 4 times higher than that of the control group (Table 4.1). A 4-weeks high-methionine diet treatment successfully induced HHcy in Sprague-Dawley rats.

4.1.2 Impaired Liver Function

Liver injury was assessed by measuring the activities of aspartate aminotransferase (AST) and alanine aminotransferase (ALT) in serum samples. The measurements of aminotransferases activities in serum or plasma are included in a liver function test in a clinical setting. During liver injury, the liver produces a large amount of AST and ALT which are secreted to the circulation. The elevated activities of AST and ALT in the serum indicate the possible occurrence of liver injury. The ratio of AST and ALT activity can also help to differentiate the types of liver injury. Higher ALT activity than AST indicates the possibility of viral hepatitis, drug-induced toxicity or non-alcoholic fatty liver disease. The opposite situation is usually observed in alcoholic fatty liver disease. As shown in Table 4.2, the serum AST and ALT activities were significantly elevated in HHcy rat, indicating liver injury (Table 4.2). A higher level of the serum ALT activity suggested an occurrence non-alcoholic fatty liver disease.

Table 4.1 Hcy Concentrations in Livers and Serum

	Control	High-methionine (HHcy)
Body weight (g)	458.46±7.09	433.26±8.62
Liver wet weight (g)	17.36±0.96	18.46±0.66
Serum total Hcy (μM)	3.96±0.19	25.99±2.49*
Liver unbound Hcy (nmol/g)	3.74±0.21	12.12±0.97*

Rats were divided into 2 groups (n = 12 for each group) fed with different diets: regular (Control) or high methionine (HHcy). Body weight and liver wet weight of rats were measured. Hcy concentrations in serum and livers were determined by fluorescence polarization immunoassay (IMx). Values are expressed as means ± SEM. *$P < 0.05$ compared with control values.

Table 4.2 Indicators of Liver Injury and Oxidative Stress

	Control	HHcy
Serum		
AST (IU/L)	26.62±3.82	42.89±7.60*
ALT (IU/L)	36.28±6.06	60.62±9.54*
Liver		
Lipid peroxides/MDA (nmol/g)	298.94±33.53	403.42±33.89*

Rats were fed with following diets for 4 weeks: a regular diet (Control) and a high methionine diet (HHcy). The serum AST and ALT activities were measured. Lipid peroxides was determined by measuring the amount of MDA in liver tissue. Results were expressed as mean ± SEM (n = 12). *P < 0.05 compared with control values.

4.1.3 Increased Oxidative Stress in Livers

Although serum AST and ALT activities are used as indicators for liver injury, the elevations of these enzymes in the serum are not specific to liver damage. For example, elevated serum AST activity has also been observed during myocardium damage (Nekrassova, 1963). An additional parameter is required to confirm the presence of liver injury. Several studies have demonstrated or suggested that the pathological effects of Hcy are mediated by induction of oxidative stress (Au-Yeung *et al.*, 2004; Robert *et al.*, 2005; Upchurch *et al.*, 1997; Wang & O, 2001). In different types of liver injuries, for example, alcoholic liver disease and hepatitis C, oxidative stress is the common underlying mechanism (Choi & Ou, 2006; Kono *et al.*, 2001). In general, reactive oxygen species are molecules with a relatively short half-life (Browning & Horton, 2004). They can react with reactive lipids including cholesterol, unsaturated fatty acids, and glycolipids, leading to lipid peroxidation (Girotti, 1998). Lipid peroxides are commonly found in oxidative stress-mediated liver injury (Jayatilleke & Shaw, 1998; Sadrzadeh *et al.*, 1994). To examine the presence of oxidative stress in HHcy rat livers, lipid peroxidation in the liver tissue was examined by measuring the levels of malondialdehyde (MDA), an indicator of lipid peroxidation. The MDA level was significantly elevated in the livers of HHcy rats, reflecting an increased lipid peroxidation (Table 4.2). Taken together, these results suggested a possible occurrence of oxidative stress-mediated liver injury in HHcy rats. In the next section (Section 4.2), the mechanism of Hcy-induced liver injury would be investigated.

4.1.4 Lipid accumulaton in Livers

Fatty liver is one of the diagnoses in CBS-deficient HHcy patients as well as in HHcy animal models (Carson *et al.*, 1965; Watanabe *et al.*, 1995). To investigate the hepatic fatty changes in diet-induced HHcy rats, histological stainings were performed. Hematoxylin & eosin (H&E) staining was performed to investigate the fatty changes in livers. The H&E staining revealed microvesicular structure (lipid vacuoles) in HHcy rat livers (Figure 4.1). Oil-Red-O staining was performed to visualize neutral lipid (triacylglycerol and cholesterol ester) accumulation in livers. As is shown in Figure 4.1 shown, the area stained with red in HHcy rat livers was more intense than that in the control. Taken together, HHcy rats showed signs of hepatic steatosis, characterized by the presence of abnormal accumulation of lipids within cells.

4.1.4.1 Quantitative Analysis of Hepatic Lipids

In order to examine the amount and the type of lipids accumulated in HHcy rat livers, the lipid content in livers was extracted with a chloroform and methanol solvent system. The extracted lipids were quantified by using the commercial kits. Compared with the controls, HHcy rats demonstrated a significant increase in total cholesterol content in the livers (Table 4.3). The increased total cholesterol content also reflected the elevations of free cholesterol and cholesterol ester content in HHcy rat livers (Table 4.3). However, there was no significant increase in the triacylglycerol content in the livers of HHcy rats compared with that in the controls (Table 4.3). These results suggested the increased Oil-Red-O stained lipid in HHcy rat livers was mainly cholesterol ester.

The serum triacylglycerol and cholesterol levels were also measured. The serum total cholesterol and cholesterol ester were significantly elevated in HHcy rats

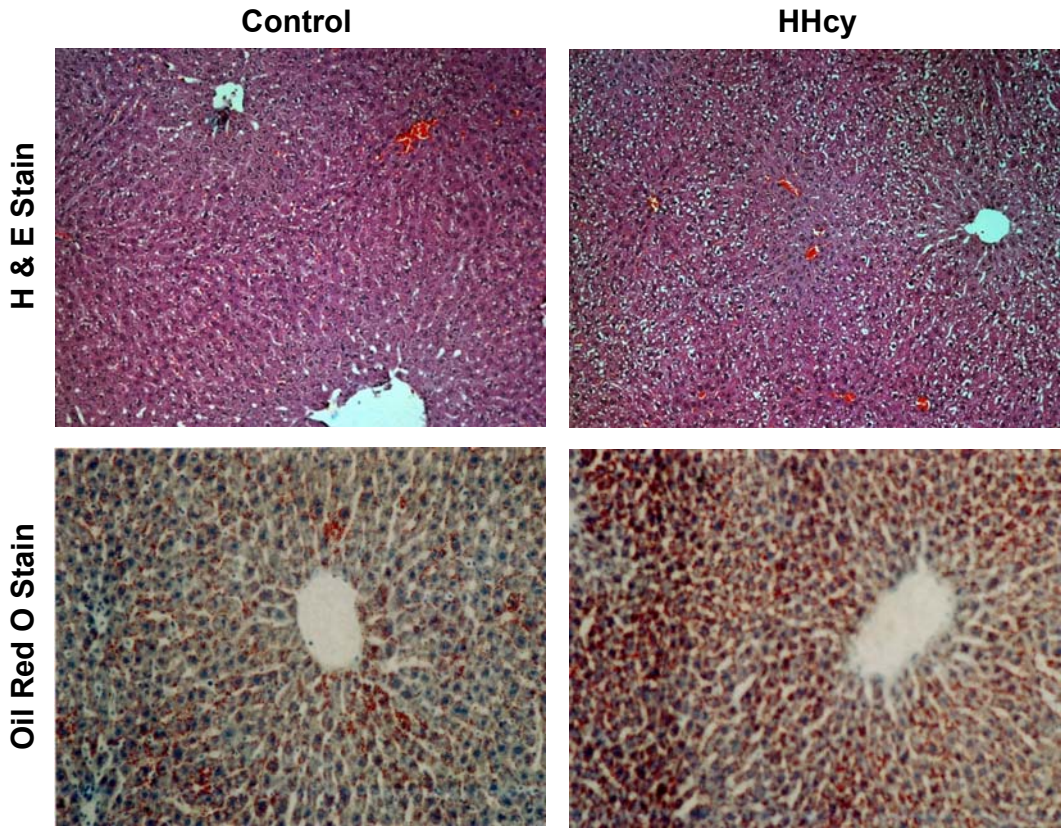

Figure 4.1 H&E and Oil Red O Staining of Livers

Formalin-fixed livers from rats fed with regular (Control) or high-methionine (HHcy) were examined with H&E staining for morphological changes. Cryosections of livers from these two groups of rats were stained with Oil Red O to visualize lipid droplets (in red). All staining analyses were performed in livers isolated from 12 rats per treatment group, and 5 sections were prepared for each liver. Representative photos are shown here.

Table 4.3 Lipid Parameters in Livers and Serum

	Control	HHcy
Liver		
Total cholesterol (mg/g)	1.75±0.06	2.29±0.15*
Free cholesterol (mg/g)	1.62±0.09	2.04±0.16*
Cholesteryl ester (mg/g)	0.17±0.13	0.27±0.06*
Triacyglycerol (mg/g)	8.13±0.61	8.85±1.00
Serum		
Total cholesterol (mg/dL)	55.82±3.62	69.25±3.33*
Free cholesterol (mg/dL)	22.13±5.02	23.85±2.80
Cholesteryl ester (mg/dL)	33.69±3.59	45.41±2.88*
Triacylglycerol (mg/dL)	67.70±3.91	73.30±6.81

Rats were divided into 2 groups (n = 12 for each group) fed with different diet: regular (Control) or high methionine (HHcy). Serum and liver levels of cholesterol and triacylglycerol were measured using a commercial kit. Results are expressed means ± SEM. *$P < 0.05$ compared with control values.

(Table 4.3). No significant increase in triacylglycerol in the serum of HHcy rats (Table 4.3). These results suggested that the elevation of hepatic cholesterol might contribute to the increased serum cholesterol level in HHcy rats. In the section 4.3 and 4.4, the underlying mechanism of Hcy-induced hepatic cholesterol content was investigated.

4.1.2 Liver Injury and Oxidative Stress

HHcy was successfully induced in Sprague-Dawley rats by dietary manipulation. The serum Hcy level in rats fed a high-methionine diet (referred as HHcy rats) was more than 6-fold higher than that of the control. The hepatic Hcy level, conversely, was 3 to 4 times higher in HHcy rats than that in control rats. The activity of aspartate aminotransferase and alanine aminotransferase in the serum was increased, indicating a sign of liver injury in HHcy rats. The ratio of AST and ALT activity can be an indicator for differentiating the types of liver injury. Higher ALT activity than AST indicates the possibility of viral hepatitis, drug-induced toxicity or non-alcoholic fatty liver disease. Interestingly, in the present HHcy model, a higher activity of ALT than of AST in the serum was observed. Elevated ALT activity in serum is regarded as an independent marker for systemic inflammation and oxidative stress (Yamada *et al.*, 2006). Lipid peroxidation is a common indication of oxidative damage in the liver (Mottaran *et al.*, 2002). A previous study demonstrated an elevation of lipid peroxidation in folate depletion-induced HHcy rat livers (Huang *et al.*, 2001). In the diet-induced HHcy rat used in the present study, there was an elevation of lipid peroxidation detected in the liver. These results suggested that Hcy might induce oxidative stress leading to liver injury in rats.

4.1.3 Hepatic Steatosis

Liver injury and increased oxidative stress were observed in the HHcy rats. Lipid accumulation was also found in the liver. The quantitative analysis of lipids extracted from HHcy rat livers revealed that the increased cholesteryl ester level contributed to

hepatic steatosis. However, different experimental models of HHcy have shown different results. In methylenetetrahydrofolate reductase-deficient mouse model and homozygous CBS-deficient with apoE knock-out mouse model, a decrease in plasma HDL levels was observed (Liao *et al.*, 2006; Mikael *et al.*, 2006). Increases in both cholesterol and triacylglycerol levels were found in the livers of heterozygous CBS-deficient mice (CBS+/-) fed a high-methionine and low folic acid diet (Werstuck *et al.*, 2001), whereas in our model only an increase in hepatic and serum cholesterol levels were observed. In addition, even though there was an observation in elevated hepatic triacylglycerol in CBS+/- mutant plus dietary modification model, no increase in plasma triacylglycerol levels was found (Werstuck *et al.*, 2001). An increase in the serum triacylglycerol level was found only in homozygous CBS knock-out (CBS-/-) mice (Namekata *et al.*, 2004). It is not known whether the discrepancies are due to the different plasma Hcy levels (severity) in these HHcy models or other characteristics of the types of models. It is also possible that different thresholds of plasma or serum Hcy levels are required to trigger distinct molecular or cellular pathways of lipid metabolism. Futher investigations are required to resolve the discrepancies.

A recent study suggested that oxidative stress (indicated as lipid peroxidation products) was involved in the progression of simple steatosis to fibrosis (Albano *et al.*, 2005). Hcy was shown to increase the transition of steatosis to fibrosis by altering extracellular matrix homeostasis (Torres *et al.*, 1999). The HHcy model used in the present study was induced by 4-weeks treatment of high-methionine diet, and did not show any sign of necrosis. Hepatic steatosis but not steatohepatitis or fibrosis was observed in diet-induced

HHcy rats. It is unknown whether hepatic steatosis will develop into fibrosis in rats under a longer exposure to HHcy.

4.2 Oxidative Stress-mediated Liver Injury in Hyperhomocysteinemia

Objective

Several studies have proposed that Hcy-induced oxidative stress is one of the mechanisms for HHcy-associated cardiovascular risk (Au-Yeung *et al.*, 2004; Dayal *et al.*, 2006; Wang & O, 2001). Oxidative stress plays a very important role in different types of liver injuries (Choi & Ou, 2006; Chowdhury *et al.*, 2006; Wheeler *et al.*, 2001b). A study showed that oxidative stress contributed to the transition of non-fatal hepatic steatosis to steatohepatitis with progressive fibrosis (Starkel *et al.*, 2003). The **second objective** of my study was to investigate the role of oxidative stress in HHcy-induced liver injury.

Results

4.2.1 Type(s) of ROS Leading to Lipid Peroxidation

In the previous section, the results showed increased lipid peroxidation in the livers of HHcy rats. In eukaryotic cells, several pathways can lead to lipid peroxidation (Figure 4.2) (Girotti, 1998). Superoxide anion (O_2^-) is the ROS initiating the formation of other free radicals (Figure 4.2). Superoxide anion has a very short half-life, and it is rapidly converted to hydrogen peroxide (Reaction B, Figure 4.2). Hydrogen peroxide (H_2O_2) can lead to the formation of hydroperoxide radical ($^{\bullet}OH$). Hydroperoxide radical can attack reactive lipids (e.g. unsaturated fatty acids, cholesterol and glycolipids) and lipid hydroperoxide is formed (LOOH). Lipid hydroperoxide can be further oxidized to form lipid peroxide radical ($OLOO^{\bullet}$) in the presence of iron and oxygen (Reaction C, Figure 4.2).

(From Girotti, Journal of Lipid Research, 39: 1529-1542, 1998.)

Figure 4.2 Pathways of Lipid Peroxide Formation

Reactive oxygen derivatives can be generated by photochemical pathway (A) or Fenton reaction (B). Lipids such as unsaturated phospholipid, cholesterol, and glycolipids (LH) can be oxidized, resulting in the formation of lipid hydroperoxides (LOOH) (Girotti, 1998). LOOH would undergo 1-electron pathway or 2-electrons pathway. (C) In the presence of metal ion (e.g. Fe^{2+}), LOOH is oxidized to lipid peroxide radical ($OLOO^{\bullet}$). On the other hand, (D) in the presence of glutathione and selenoperoxidase (SePX), LOOH is reduced to redox-inert alcohol and water (Girotti, 1998).

4.2.1.1 Increased Superoxide Anion Production

To investigate whether the increased lipid peroxidation in HHcy rat liver was due to the elevated production of superoxide anion, the level of superoxide anion in the liver was measured. A significant elevation of superoxide anion levels in the livers of HHcy rats was observed (Table 4.4).

There are several pathways in the liver to produce superoxide anion. Mitochondrial electron transport, NADPH oxidase and microsomal cytochrome P450 (CYP2E1) are the major pathways producing superoxide anion in the liver (Kaplowitz & Tsukamoto, 1996). During mitochondrial electron transport (mitochondrial respiration), superoxide anion is formed by auto-oxidation of ubisemiquinone radical. Ubisemiquinone is the intermediate transferring electron from complex I and II to complex III during mitochondrial respiration (Kaplowitz & Tsukamoto, 1996). NADPH oxidase is a superoxide anion-producing enzyme present in phagocytes as well as in hepatocytes (Bellavite, 1988; Reinehr *et al.*, 2005b). CYP2E1 behaves as NADPH oxidase in the absence of drug substrates (Kaplowitz & Tsukamoto, 1996). NADPH is the necessary molecule for these three superoxide anion-producing pathways. To examine which pathway(s) might contribute to increased superoxide production in HHcy rat liver, lucigenin chemiluminescene assay was performed. Upon addition of the substrate, NADPH, there was a significant elevation of chemilunminescent signal derived from the liver homogenates of HHcy rats compared with that of the controls (data not shown). To determine whether the increased chemiluminescent signal was derived from mitochondrial electron transport, rotenone (an inhibitor of mitochondrial respiration) was

Table 4.4 Superoxide Production in Livers

	Control	HHcy
Liver		
O_2^- content (% of control)	100.00±4.78	131.61±14.93*
NADPH oxidase (μmol/mg/min)	303.83±23.09	398.87±30.09*

Rats were fed with following diets for 4 weeks: a regular diet (Control) or a high methionine diet (HHcy). Superoxide anion content and NADPH oxidase activity were determined in livers. Results were expressed as mean ± SEM (n = 12). *P < 0.05 compared with control values.

added to liver homogenates prior to lucigenin chemiluminescene assay. The presence of rotenone did not affect the elevated signal from HHcy liver homogenates (Figure 4.3). This result showed that the superoxide anion which elicited the chemilunminescent signal was derived from NADPH oxidase. The activity of NADPH oxidase was calculated as previously described (Kashiwagi *et al.*, 1999). As shown in Table 4.4, there was a significant increase in NADPH oxidase in HHcy rat livers.

4.2.1.2 Increase in Nitrotyrosine Protein Adducts

Superoxide anion does not exist in a cellular compartment for an extensive period of time. It is rapidly scavenged by superoxide dismutase (SOD) and converted to hydrogen peroxide (H_2O_2) (Reaction A, Figure 4.4). However, in the presence of nitric oxide (NO), superoxide anion can be converted to peroxynitrite ($ONOO^-$) (Reaction B, Figure 4.4). The reaction rate of superoxide anion with NO is approximately three times faster than the scavenging rate by SOD (Km = 7 x $10^{-9}mol^{-1}$ Ls^{-1} vs Km = 2 x $10^{-9}mol^{-1}Ls^{-1}$). Peroxynitrite is a potent oxidant which can lead to the detrimental effects of DNA damage, lipid peroxidation and protein oxidation. To determine whether there was an increase in peroxynitrite formation in HHcy rat livers, immunohistochemical analysis was performed to detect nitrotyrosine protein adduct, a biomarker for peroxynitrite (Ischiropoulos *et al.*, 1992). Little nitrotyrosine protein adducts were detected in the livers isolated from control rats (Figure 4.5A). In contrast to the control, a significant increase in the intensity of nitrotyrosine protein adduct staining was found in the livers of HHcy rats (Figure 4.5B), indicating an increased peroxynitrite formation. Acetaminophen toxicity was known to cause elevation of peroxynitrite production resulting in

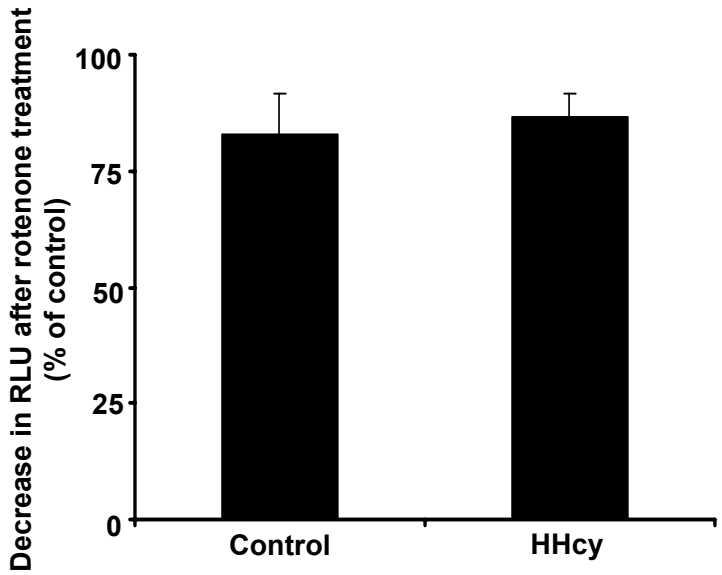

Figure 4.3 Chemiluminescence Signal Elicited by Liver Homogenates

Rats were fed with following diets for 4 weeks: a regular diet (Control) or a high methionine diet (HHcy). Liver homogenates were treated in the presence or absence of rotenone and chemiluminescene signals (RLU) were recorded. Percentage of decrease in the signal compared to that of the homogenate alone was calculated. Results were expressed as mean ± SEM (n = 4).

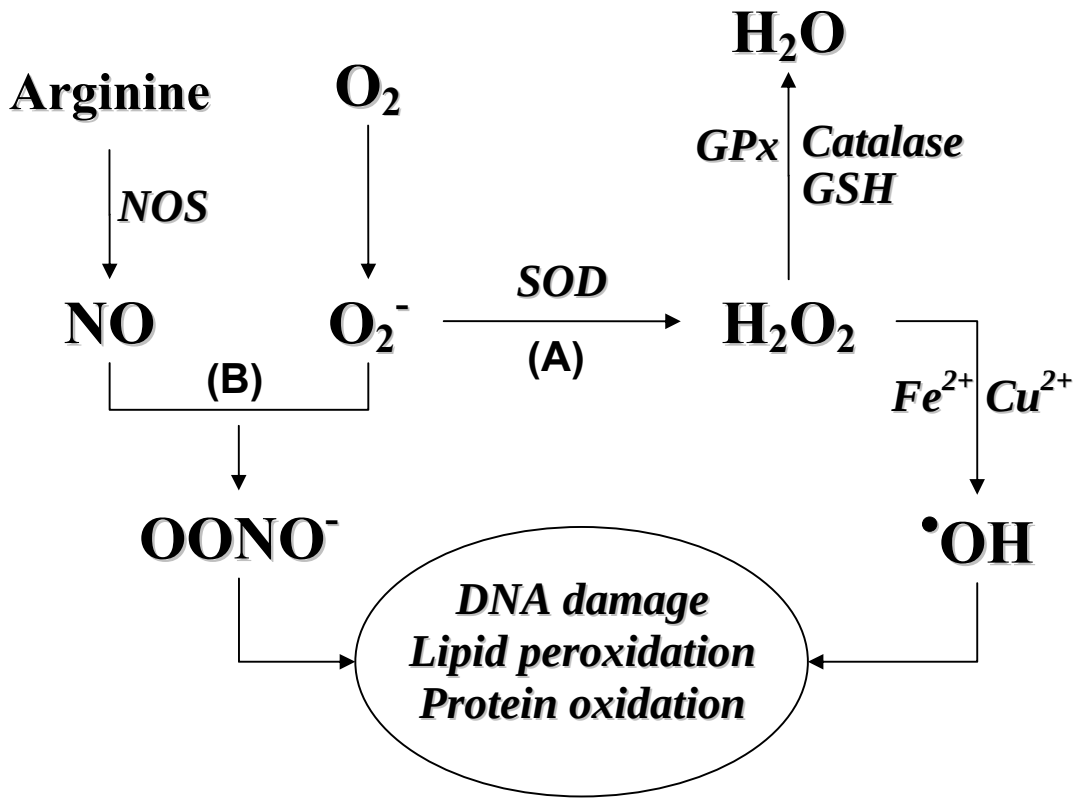

Figure 4.4 Fates of Superoxide Anion

The half-life of superoxide anion (O_2^-) is short. It is rapidly scavenged by superoxide dismutase (SOD) and converted to hydrogen peroxide (H_2O_2) (Reaction A). In the presence of high concentration of nitric oxide (NO), superoxide anion reacts with NO to form peroxynitrite ($ONOO^-$) (Reaction B). Peroxynitrite is a potent oxidant which can cause DNA damage, lipid peroxidation and protein oxidation (Based on ideas from Buetler *et al.*, 2004).

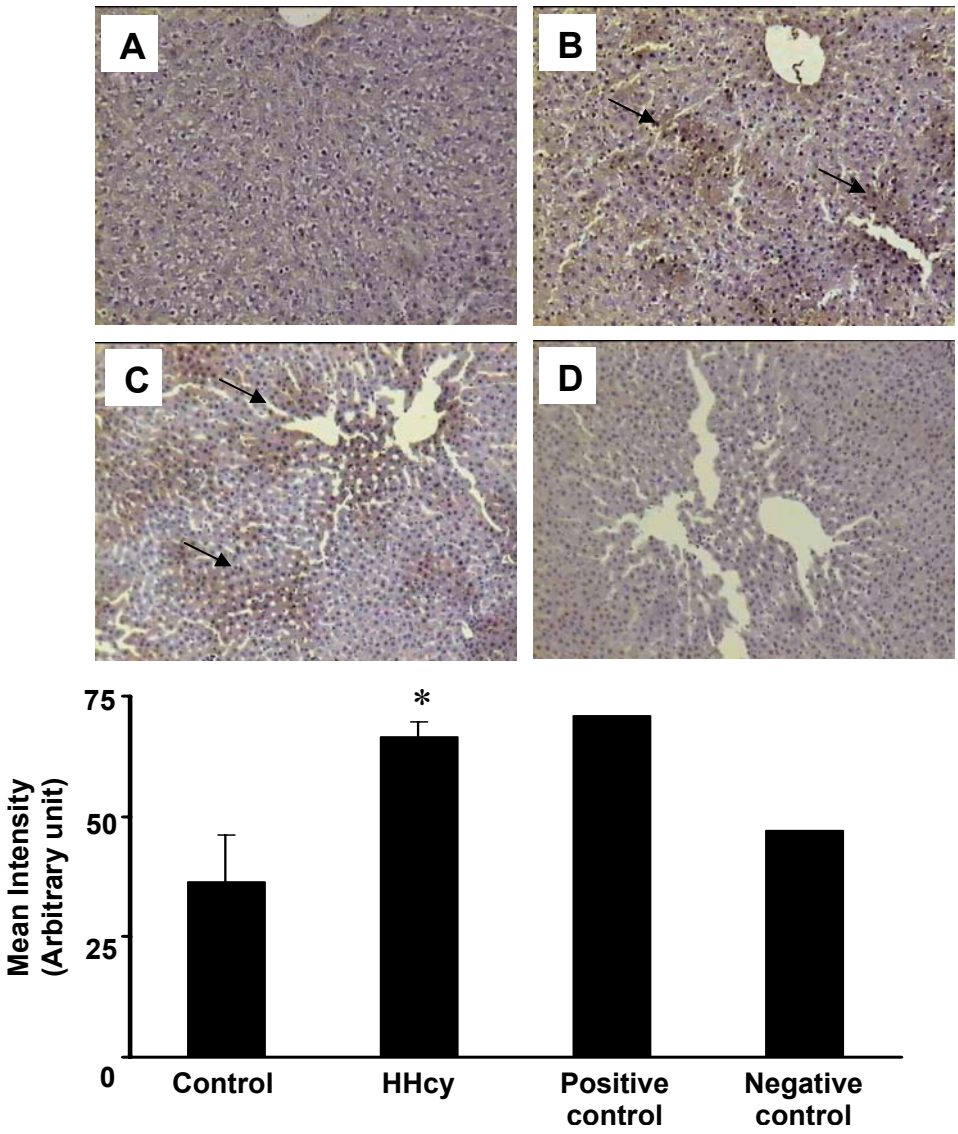

Figure 4.5 Immunohistochemical Staining of Nitrotyrosine in Livers

Livers were fixed in 10% neutral-buffered formalin overnight and then embedded in paraffin. Immunohistochemical staining for nitrotyrosine protein adducts was performed with anti-nitrotyrosine antibodies. After counterstaining with Harris hematoxylin, nitrotyrosine protein adducts were identified under light microscope with a magnification of 200×. Representative photos were obtained from rats fed (A) a regular diet and (B) high-methionine diet (HHcy). (C) A positive control was prepared from rats with IP injection of 300 mg/kg acetaminophen 6 hours prior to euthanasia. Arrows point to the areas positively stained with nitrotyrosine. (D) Section incubated with normal IgG as primary antibody was served as negative control. Staining analyses were performed in livers isolated from 8 rats per treatment group, and 4 sections were prepared for each liver. Representative images are shown. *$P < 0.05$ compared with the control values.

nitrotyrosine formation (Ito *et al.*, 2004). The liver of a rat injected with a toxic dose of acetaminophen served as a positive control in the experiment (Figure 4.5C).

4.2.1.3 No alteration in Nitric oxide Production

Other than superoxide anion, nitric oxide (NO) is another component for peroxynitrite formation. In liver, inducible nitric oxide synthase (iNOS) can produce a high concentration of NO and it is expressed in hepatocyte and Kupffer cell (liver-residing macrophage) (Reinehr *et al.*, 2005b; Teufelhofer *et al.*, 2005). To determine whether there was an elevation of NO production in the liver of HHcy rats, the level of NO metabolites (nitrite and nitrate) and total NOS activity were measured. There was no change in NO metabolite levels or total NOS activity in the livers of HHcy rats (Table 4.5). Taken together, these results suggested that the increase of peroxynitrite in HHcy rat livers was mainly due to the elevation of superoxide anion.

4.2.2 Hepatic Antioxidant Defence System

Oxidative stress may be resulted from an elevation of oxidative burden and/ or a decrease in antioxidant defence. In the present study, superoxide anion and peroxynitrite contents as well as NADPH oxidase activity were elevated in HHcy rat livers (Table 4.4 and Figure 4.5). Next, the enzymatic and non-enzymatic antioxidant systems in HHcy rat livers were examined.

4.2.2.1 Decrease in Enzymatic Antioxidant Defence

As shown in Figure 4.4, superoxide dismutase (SOD) is the major enzyme that removes superoxide anion from the cellular compartment, resulting in the production of H_2O_2. H_2O_2 is then converted to water by the enzymatic reaction of catalase or glutathione

Table 4.5 Nitric Oxide Production in Livers

	Control	HHcy
Liver		
NO metabolites (nmol/g)	393.88±29.18	381.79±22.18
NOS activity (pmol/mg/min)	4.44±0.66	4.71±0.66

Rats were fed with following diets for 4 weeks: a regular diet (Control) or a high methionine diet (HHcy). Nitric oxide metabolites and total nitric oxide synthase activity were determined in livers by Griess reaction and radiochemical assay, respectively. Results were expressed as mean ± SEM (n = 12).

Peroxidase (GPx) (Figure 4.4). The activities of the major hepatic antioxidant enzymes including superoxide dismutase (SOD), catalase and glutathione peroxidase (GPx) were measured in the control and HHcy rat livers. As shown in Table 4.6, the activities of hepatic SOD and catalase were significantly decreased in HHcy rats while GPx activity remained unchanged during HHcy.

4.2.2.2 Altered Equilibrium of Non-Enzymatic Antioxidant

Glutathione (GSH) is the major endogenous non-enzymatic antioxidant produced in the liver. The antioxidant activity of GSH is mediated by direct scavenging of free radicals (Reaction A, Figure 4.6) or being a substrate of glutathione peroxidase (GPx) (Reaction B, Figure 4.6). During the antioxidant reaction of GPx, GSH (reduced form of glutathione) is oxidized to GSSG (oxidized form of glutathione). GSSG can be converted back to GSH through the action of glutathione reductase (GRed) (Reaction C, Figure 4.6). The equilibrium between the reduced form (GSH) and the oxidized form (GSSG) of glutathione reflects the redox status of the tissue. There was no change in GSH levels in the livers of HHcy rats, but GSSG levels were more than 3 times higher than that in the control group (Table 4.7). The ratio of GSSG to GSH was significantly elevated in HHcy rat livers, suggesting the presence of oxidative stress (Table 4.7). The results from the previous section showed that there was no increase in glutathione peroxidase activity (Table 4.6). The elevated level of GSSG might be due to the decreased recovery pathway, glutathione reductase (GRed) activity (Reaction C, Figure 4.6). As shown in Table 4.7, there was a significant reduction of glutathione reductase activity in HHcy rat livers. Taken together, these results suggested that the redox equilibrium of GSH was shifted to oxidative phase during HHcy.

Table 4.6 Enzymatic Antioxidant in Livers

	Control	HHcy
Enzymatic		
SOD (U/mg)	200.27±18.10	148.20±21.54*
Catalase(U/mg)	447.08±13.19	351.20±10.46*
Glutathione Peroxidase (U/g)	309.47±14.80	316.15±35.37

Rats were fed with following diets for 4 weeks: a regular diet (Control) or a high methionine diet (HHcy). Superoxide dismutase (SOD), catalase, and glutathione peroxidase activities were determined in livers; results were expressed international unit per mg or g of protein. Results were expressed as mean ± SEM (n = 12). *P < 0.05 compared with control values.

(From Masella *et al.*, Journal of Nutritional Biochemistry 16: 577-586, 2005)

Figure 4.6 Glutathione metabolic pathway

Glutathione (GSH) exerts its antioxidant activity by direct scavenging free radicals or being a substrate of glutathione peroxidase (GPx) and glutathione S-transferase (GST). During detoxification, GSH can attack toxic compounds with the assistance of GST (Reaction A). GSH-adducts is then excreted out of cell. During the antioxidant reaction of GPx, GSH is oxidized to GSSG (oxidized form glutathione) (Reaction B). GSSG can be converted back to GSH through the action of glutathione reductase (GRed) (Reaction C) (Masella *et al.*, 2005).

Table 4.7 Glutathione Level and Glutathione Reductase Activity in Livers

	Control	HHcy
Glutathione		
GSH (μmol/g wet wt)	8.06.±0.21	8.41±0.16
GSSG (nmol/g wet wt)	21.29±2.23	98.62±30.06*
GSSG:GSH(×100)	0.273±0.025	0.857±0.358*
GSH metabolic enzyme		
Glutathione reductase (U/mg)	42.78±1.68	37.76±1.88*

Rats were fed with following diets for 4 weeks: a regular diet (Control) or a high methionine diet (HHcy). The hepatic levels of reduced (GSH) and oxidized (GSSG) forms of glutathione were measured and expressed as per g of wet weight of liver. Glutathione reductase activity was determined in livers; results were expressed international unit per mg of protein. Results were expressed as mean ± SEM (n = 12). *P < 0.05 compared with control values.

The transsulfuration pathway in Hcy metabolism produces cysteine, and contributes to the production of glutathione (Figure 1.2 and Figure 4.6). It has been suggested that liver injury in CBS-deficient HHcy would be due to the depletion of GSH caused by decreased CBS activity (Robert *et al.*, 2005). As shown in Figure 4.7, hepatic CBS activity was not changed in the livers of diet-induced HHcy rat.

4.2.3 Role of Oxidative Stress in HHcy-induced Liver Injury

The results from previous sections had shown that superoxide anion content was increased in HHcy rat livers. Such an increase was due to an elevation of superoxide anion production via the up-regulation of NADPH oxidase and a decrease in enzymatic scavenging mechanism. It remained unknown if the increased oxidative stress could lead to liver injury during HHcy. To investigate the role of oxidative stress in liver injury during HHcy, a series of experiments were performed using an inhibitor of NADPH oxidase.

To further elucidate the role of oxidative stress in HHcy-induced liver injury, a group of HHcy rats were treated with apocynin, an inhibitor for NADPH oxidase (van der Goes *et al.*, 1998) for 3 days prior to euthanasia. As shown in Table 4.8, administration of apocynin completely blocked HHcy-induced NADPH oxidase activity and the elevation of superoxide anion levels in the liver. Apocynin treatment also completely blocked HHcy-induced nitrotyrosine formation and lipid peroxidation in the liver as well (Table 4.8 and Figure 4.8). These results suggested that superoxide anion was indeed the main free radical initiating peroxynitrite formation and lipid peroxidation in HHcy rat livers.

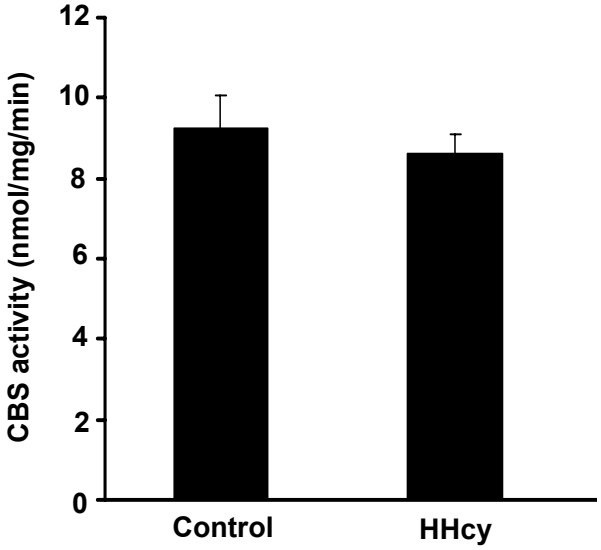

Figure 4.7 Cystathionine β-Synthase Activity in Livers

Rats were fed with following diets for 4 weeks: a regular diet (Control) or a high methionine diet (HHcy). Cystathionine β-synthase (CBS) activity was measure in livers. Results were expressed as mean ± SEM (n = 6).

Table 4.8 Effect of Apocynin on Hepatic Oxidative Stress and Liver Injury

	Control	HHcy	HHcy + Apocynin
Liver			
O_2^- content (% of control)	100.00±4.78	131.61±14.93*	84.92±14.59#
NADPH oxidase (μmol/mg/min)	303.83±23.09	398.87±30.09*	351.10±36.95
Lipid peroxides/MDA (nmol/g)	298.94±33.53	403.42±33.89*	344.61±29.47#
Serum			
Hcy (μM)	3.52±0.34	25.48±3.01*	28.01±5.84*
AST (IU/L)	26.62±3.82	42.89±7.60*	28.56±2.08#
ALT (IU/L)	36.28±6.06	60.62±9.54*	46.11±4.68

Rats were fed with following diets for 4 weeks: a regular diet (Control), a high methionine diet (HHcy). One group of high-methionine fed rats was given IP injection of apocynin (4 mg/kg, daily) for 3 days prior to euthanasia (HHcy+Apocynin). Hcy was measured in serum as well as AST and ALT activities. Superoxide anion content and NADPH oxidase activity were determined in livers. Lipid peroxides in livers was determined by measuring the amount of MDA in liver tissue. Results were expressed as mean ± SEM (n = 12). *P < 0.05 compared with control values. #P < 0.05 compared with values of high-methionine treated group (HHcy).

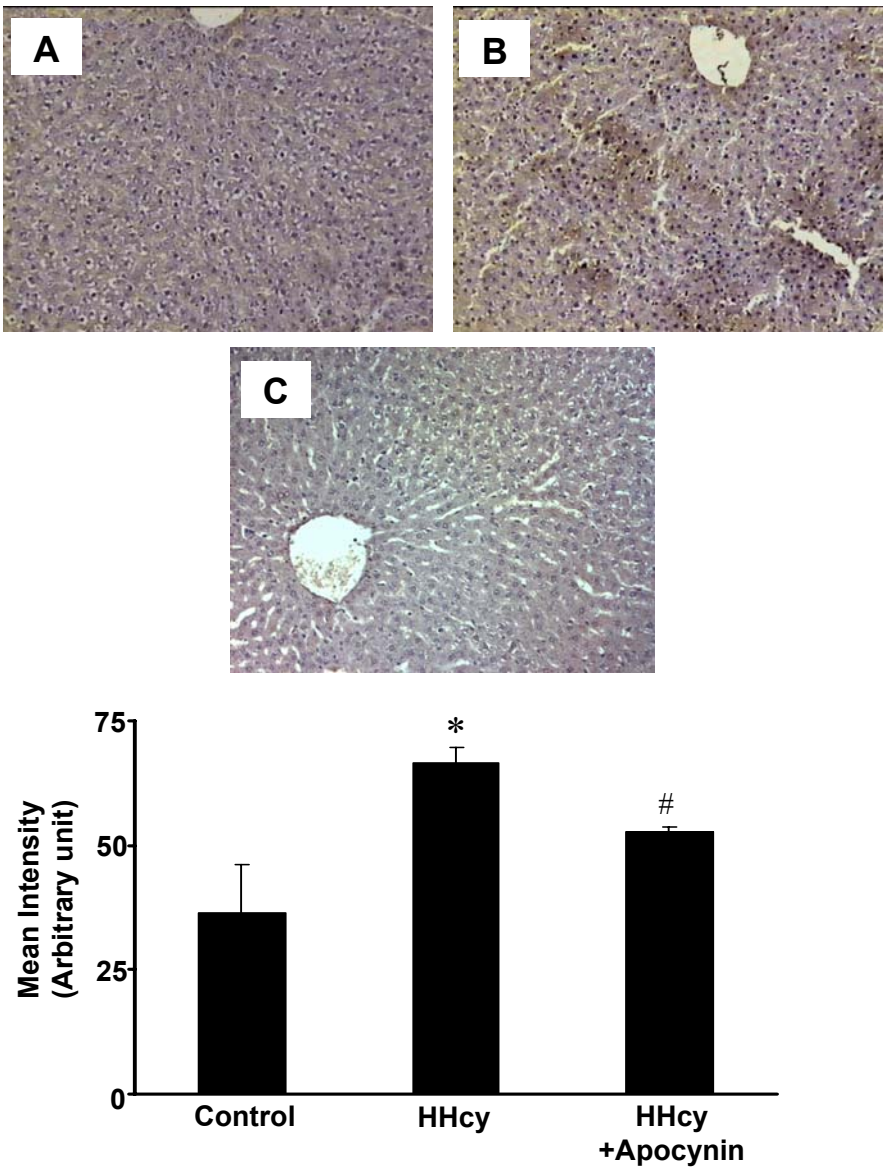

Figure 4.8 Effect of Apocynin on Nitrotyrosine Adduct Protein in Liver

Livers were fixed in 10% neutral-buffered formalin overnight and then embedded in paraffin. Immunohistochemical staining for nitrotyrosine protein adducts was performed with anti-nitrotyrosine antibodies. After counterstaining with Harris hematoxylin, nitrotyrosine was identified under light microscope with a magnification of 200×. Representative photos were obtained from rats fed (A) a regular diet, (B) a high-methionine diet (HHcy) and (C) a high-methionine plus IP injection of apocynin (4 mg/kg, daily) for 3 days prior to euthanasia (HHcy+Apocynin). Staining analyses were performed in livers isolated from 8 rats per treatment group, and 4 sections were prepared for each liver. Representative images were shown. *$P < 0.05$ compared with control values. #$P < 0.05$ compared with values of high-methionine treated group (HHcy).

Futhermore, apocynin treatment ameliorated liver injury in HHcy rats as demonstrated by a reduction of both AST and ALT activities (Table 4.8). These results suggested that HHcy-induced liver injury might be mediated via increased NADPH oxidase-dependent superoxide anion production.

4.2.4 Increase in Hepatic Oxidative Burden

Oxidative stress can lead to direct tissue damage as well as stimulate inflammatory reactions that in turn contribute to tissue injury (Garcia-Tevijano *et al.*, 2001; Robert *et al.*, 2005). Oxidative stress is thought to be one of the important mechanisms for Hcy-induced cardiovascular dysfunction (Au-Yeung *et al.*, 2004; Dayal *et al.*, 2006). In the first part of the present study, elevation of both alanine aminotransferase and aspartate aminosferase activites (common markers for liver injury) was observed in the serum of HHcy rats. Several lines of evidence from the present study suggested that HHcy-induced liver injury was mediated via oxidative stress. First, there was a significant increase in peroxynitrite formation in the liver of HHcy rat. An increase in the level of peroxynitrite could be due to an elevation of superoxide anion and/or NO levels. Our results clearly demonstrated that activation of NADPH oxidase during HHcy caused an increase in superoxide anion production in the liver. Conversely, NOS activity and NO concentration were not altered in the liver during HHcy. These results suggested that peroxynitrite formation in HHcy rat livers was mainly due to Hcy-induced superoxide anion production. Second, peroxynitrite is a potent oxidant that can damage cells by modifying lipids, proteins and DNA. There was a significant increase in the levels of lipid peroxides and nitrotyrosine protein adducts in the livers of HHcy rats, suggesting oxidative damage occurred. Third, the involvement of NADPH oxidase in hepatic oxidative stress was furthered confirmed by the experiments using a known NADPH oxidase inhibitor, apocynin (Stolk *et al.*, 1994). NADPH oxidase activity, superoxide anion level,

peroxynitrite formation as well as lipid peroxidation were reduced to the basal levels in HHcy rats treated with apocynin. The elevated serum aminotransferase activities in these rats were also ameliorated by the administration of apocynin. Taken together, these results indicate that NADPH oxidase-dependent superoxide anion generation plays a major role in oxidative stress-mediated liver injury during HHcy.

NADPH oxidase is most abundantly expressed in phagocytic cells and plays a major role in immune defense against microorganism invasion. The expression of NAPDH oxidase in non-phagocytic cells has been reported in past decades. The ROS generated by non-phagocytic NAPDH oxidase has been shown to involve cell signaling, proliferation, apoptosis and cellular senescence (Finkel, 1999). The phagocytic NADPH oxidase consists of a cystolic subunit ($p47^{phox}$, $p67^{phox}$ and rac) and a membrane-bound subunit ($p22^{phox}$ and $gp91^{phox}$) (Czaja, 2005; Zalba *et al.*, 2001). In non-phagocytic cells, several homologues of $gp91^{phox}$ subunit have been identified including Nox and Duox (Czaja, 2005). Nox and Duox mRNA have been found in rat hepatocytes (Reinehr *et al.*, 2005a). Several studies suggest that Kupffer cells (liver residing macrophage)- derived ROS exacerbates liver injury (Teufelhofer *et al.*, 2005; Wheeler *et al.*, 2001a). A recent study has found that hydrophobic bile acids can activate NADPH oxidase in hepatocytes leading to oxidative stress-mediated apoptosis (Reinehr *et al.*, 2005b). In the present study, we demonstrated that Hcy increased NADPH oxidase activity, and inhibition of NADPH oxidase was able to ameliorate Hcy-induced liver injury. A previous study showed that a rapid increase in superoxide anion production upon angiotensin II stimulation in human microvascular endothelial cells (after 5 to 10 minutes incubation) was due to the direct activation of NAPDH oxidase via phosphorylation (Li & Shah,

2003). Our results showed that liver homogenate pre-incubated with Hcy for 15 minutes showed a significant increase in NADPH oxidase activity compared with that of the homogenate alone (129.73% ± 2.11% of non-treated homogenate). Since the activation of NADPH oxidase occurred within such a short period of time, it is reasonable to speculate that Hcy can directly activate the enzyme through direct activation of NAPDH oxidase. However, the underlying mechanism by which Hcy induces the oxidase activity and the type(s) of cells in the liver that contribute to the increased superoxide anion during HHcy remains to be investigated.

4.2.5 Decrease in Enzymatic Antioxidant Defence

Several studies have demonstrated a reduction in antioxidant enzymes in acute and chronic liver injuries (Chen *et al.*, 1995; Misra *et al.*, 1992). In the present study, the activities of hepatic antioxidant enzymes, namely superoxide dismutase and catalase were decreased in HHcy rats while gluathionine peroxidase remained unchanged in HHcy rat livers. These results suggested another mechanism for the increased superoxide anion and lipid peroxidation in HHcy livers. In fact, a study showed an increase in circulating extracellular superoxide dismutase expression in inherited HHcy patients (Wilcken *et al.*, 2000). It was suggested that an auto-protective mechanism was elicited to prevent an increase in oxidative stress during HHcy (Wilcken *et al.*, 2000). Another study, however, demonstrated a decrease in glutathione peroxidase activity and gene expression in endothelial cells treated with Hcy (Upchurch *et al.*, 1997). Taken together, our results suggested that Hcy-induced oxidative stress might be distinct in different tissues via unique mechanisms.

4.2.6 Role of Glutathione in Oxidative Stress

Several studies have suggested that glutathione depletion is the underlying mechanism of increased oxidative stress in the liver during HHcy (Robert *et al.*, 2005). Such hypothesis is based on the CBS-deficient HHcy model. A decrease or an absence of CBS activity in this model yields a decrease in the level of cystathionine which can be converted to cysteine and eventually glutathione (Figure 1.2 and Figure 4.6). It was suggested that glutathione depletion in the liver would be due to the decreased synthesis of cysteine from cystathionine (Robert *et al.*, 2005). However, in the diet-induced HHcy model used in the present study, hepatic CBS activity was the same as that of the control group. Total glutathione level in HHcy rat livers was also similar to that of the control and only oxidized form of glutathione (GSSG) level was increased. Glutathione reductase is the enzyme reducing GSSG to GSH (reduced form of glutathione). It was interesting to note that the hepatic glutathione reductase was decreased in HHcy rats, which provided an explanation for the accumulation of GSSG in HHcy rat livers. These results suggested that Hcy-induced oxidative stress in the liver was mainly due to the elevation of NADPH oxidase activity as well as a decrease in superoxide dismutase and catalase activities.

Several models of HHcy including CBS-deficient or methylenetretrahydrofolate reductase-deficient mice demonstrate signs of oxidative stress in the livers (Huang *et al.*, 2001; Robert *et al.*, 2005). Due to the different phenotypes of these genetically modified models, various mechanisms have been proposed to explain the cause(s) of oxidative stress. The results of the present study demonstrate that, in the absence of other risk factors, liver injury occurs in the diet-induced HHcy rat. The presence of oxidative stress

indicated by an elevation of superoxide anion, lipid peroxidation and peroxynitrite levels has been observed in HHcy rat livers. Such oxidative stress is mediated via elevated NADPH oxidase activity and decreased enzymatic antioxidant defence in the livers. Inhibition of Hcy-increased NADPH oxidase activity can ameliorate oxidative stress and liver injury during HHcy. Taken together, our results suggest that liver injury of the diet-induced HHcy rats is mediated by Hcy-induced oxidative stress.

4.3 Increase in Cholesterol Biosynthesis in Hyperhomocysteinemia

Objective

Several *in vivo* studies have shown abnormal lipid metabolism during HHcy (Namekata *et al.*, 2004; Werstuck *et al.*, 2001; Woo *et al.*, 2005). In section 4.1, the results showed lipid accumulation in diet-induced HHcy rat liver, and the quantitative analysis demonstrated an increase in cholesterol content in the liver. Our laboratory previously also demonstrated that Hcy activated HMG-CoA reductase, the enzyme catalyzing the rate limiting step of cholesterol biosynthesis in human hepatocyte (O *et al.*, 1998). Hcy-induced HMG-CoA reductase activation led to an elevation of cholesterol production in hepatocytes (O *et al.*, 1998). This *in vitro* study showed that Hcy-induced HMG-CoA reductase activation was not due to direct interaction of Hcy with the enzyme (O *et al.*, 1998). An extensive period of time (24 to 48 hours) was required to observe Hcy-increased HMG-CoA reductase activity and cholesterol production in hepatocytes (O *et al.*, 1998). It was suggested that Hcy-induced HMG-CoA reductase activation was mediated at the translation or transcription level (O *et al.*, 1998). The **third objective** of my study was to investigate the underlying mechanism of HHcy-induced cholesterol biosynthesis in the liver. The transcriptional regulation of HMG-CoA reductase would be the focus of this part of the study. The molecular mechanim was investigated in both *in vivo* and *in vitro* studies.

Results

4.3.1 Increase in Hepatic HMG-CoA Reductase Expression in Liver

In section 4.1, hepatic steatosis was observed in HHcy rat liver (Figure 4.1). The quantitative analysis revealed that the lipids accumulated in HHcy rat livers were mainly

cholesterol esters (Table 4.3). Approximately half of total cholesterol in the body is synthesized *de novo* in the liver. HMG-CoA reductase is the rate limiting enzyme controlling cholesterol biosynthesis. The expression of HMG-CoA reductase in HHcy rat liver was examined.

4.3.1.1 Increased HMG-CoA Reductase Activity

To investigate whether an elevation of cholesterol content in the liver and serum of HHcy rats was due to activation of HMG-CoA reductase, hepatic HMG-CoA reductase activity was measured using a radiochemical method. There was a significant increase in HMG-CoA reductase activity in HHcy rat livers compared to controls (Figure 4.9).

4.3.1.2 Elevated HMG-CoA Reductase Protein Level and mRNA Expression

In the previous *in vitro* study, it was shown that Hcy did not directly interact with HMG-CoA reductase (O *et al.*, 1998). To examine whether Hcy-induced HMG-CoA reductase activity was via translation or transcription regulation, the enzyme protein levels and mRNA expressions were examined in livers. There was a significant increase in HMG-CoA reductase protein level in livers isolated from HHcy rats (Figure 4.10). Next, hepatic HMG-CoA reductase mRNA expression was also determined. As shown in Figure 4.11, the expression of HMG-CoA reductase mRNA was significantly elevated in HHcy rat livers. These results suggested that Hcy-induced HMG-CoA reductase activity was due to increased expression of the enzyme.

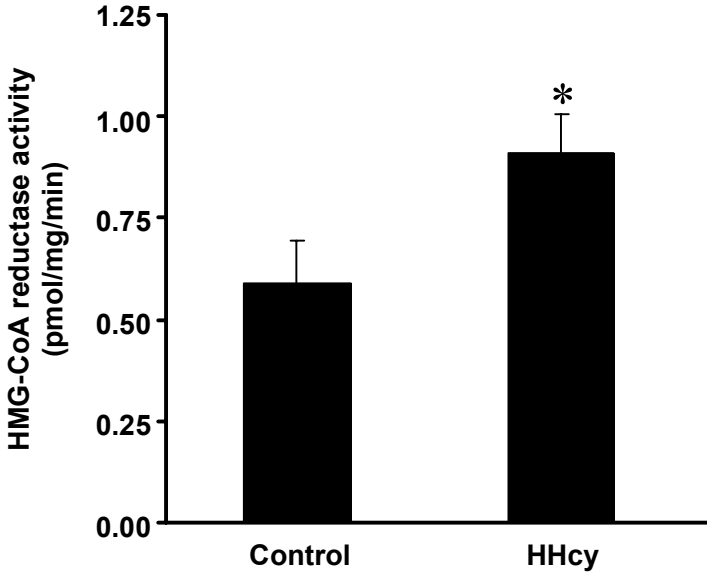

Figure 4.9 Enzymatic Activity of HMG-CoA reductase in Livers

HMG-CoA reductase activity was determined using a radiochemical method in livers isolated from rats fed with control, or high-methione diet (HHcy). Results (n = 9) are expressed as means ± SEM. *P < 0.05 compared with control values

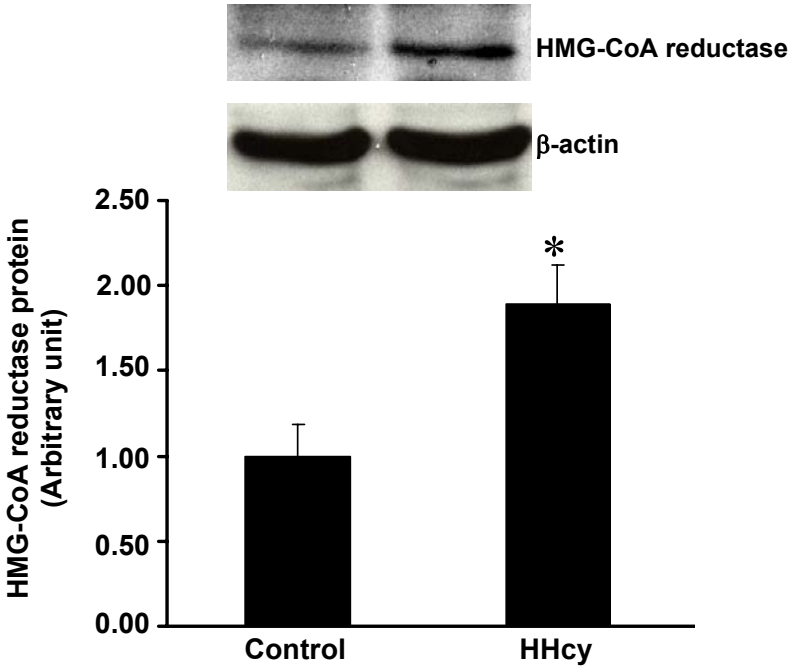

Figure 4.10 Protein Level of HMG-CoA Reductase in Livers

HMG-CoA reductase protein levels were determined by Western immunoblot analysis in livers isolated from rats fed with control or high-methionine (HHcy). Results (n = 12) are expressed as means ± SEM. *P < 0.05 compared with control values (expressed as arbitrary unit).

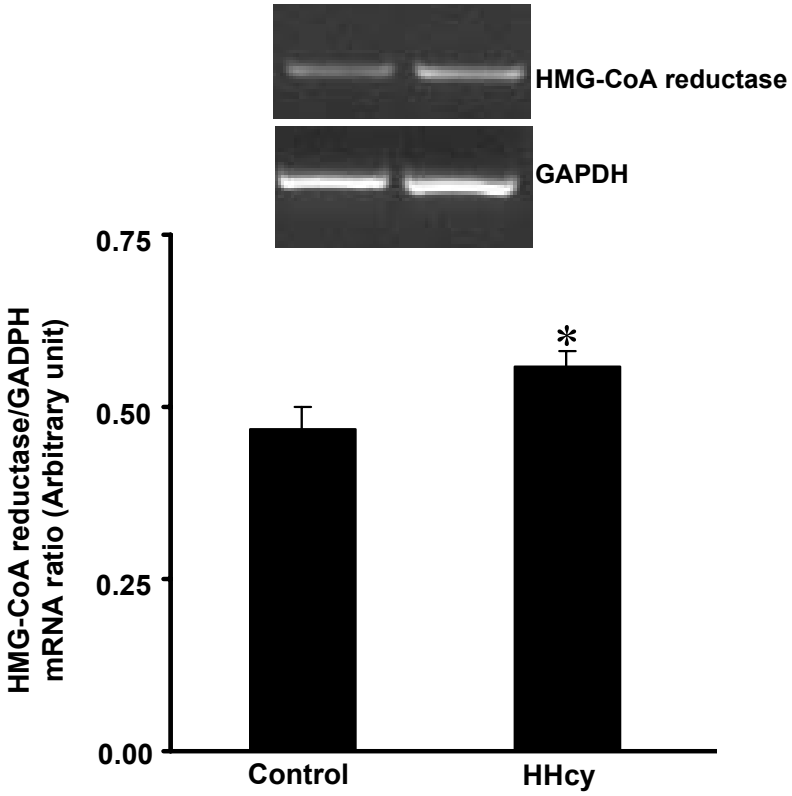

Figure 4.11 Messenger RNA Expression of HMG-CoA Reductase in Livers

HMG-CoA reductase mRNA expression was examined in livers isolated from rats fed with control or high-methionine diet (HHcy) using RT-PCR with GAPDH mRNA as internal control. Results (n = 12) are expressed as means ± SEM. *P < 0.05 compared with control values (expressed as arbitrary unit).

4.3.2 Mechanism of HHcy-induced Transcription of HMG-CoA Reductase in Hepatocytes

In HHcy rat livers, HMG-CoA reductase protein and mRNA expressions were up-regulated. To investigate the mechanism by which HMG-CoA reductase expression was increased in HHcy livers, experiments were performed in rat hepatocytes.

4.3.2.1 Increased HMG-CoA Reductase Expression and Cholesterol Biosynthesis

First, HMG-CoA reductase mRNA expression and cholesterol concentration were determined in Hcy-treated rat hepatocytes. There was 1.7-fold elevation of the intracellular Hcy concentrations in hepatocytes incubated with Hcy (1 mM) for 15 minutes (2.17 ± 0.02 vs. 1.26 ± 0.35 nmol/mg cellular protein in control cells). After 60 minutes incubation, the intracellular Hcy level was increased 2-fold in hepatocytes (2.59 ± 0.04 vs. 1.26 ± 0.35 nmol/mg cellular protein in control cells). As shown in Figure 4.12, an increase in HMG-CoA reductase mRNA expression was observed in cells incubated with Hcy at concentrations of 0.5 mM and 1.0 mM. Addition of Hcy (up to 2 mM) into the culture medium did not affect the viability of hepatocytes. It was noted that a 10-times higher concentration of Hcy was required to elicit the effect in hepatocytes (1 mM), compared to other cell types such as endothelial cells and vascular smooth muscle cells (0.1mM) (Sung *et al.*, 2001; Wang *et al.*, 2000). Hepatocytes might be relatively resistant to the stimulation of extracellular Hcy because of the higher basal intracellular

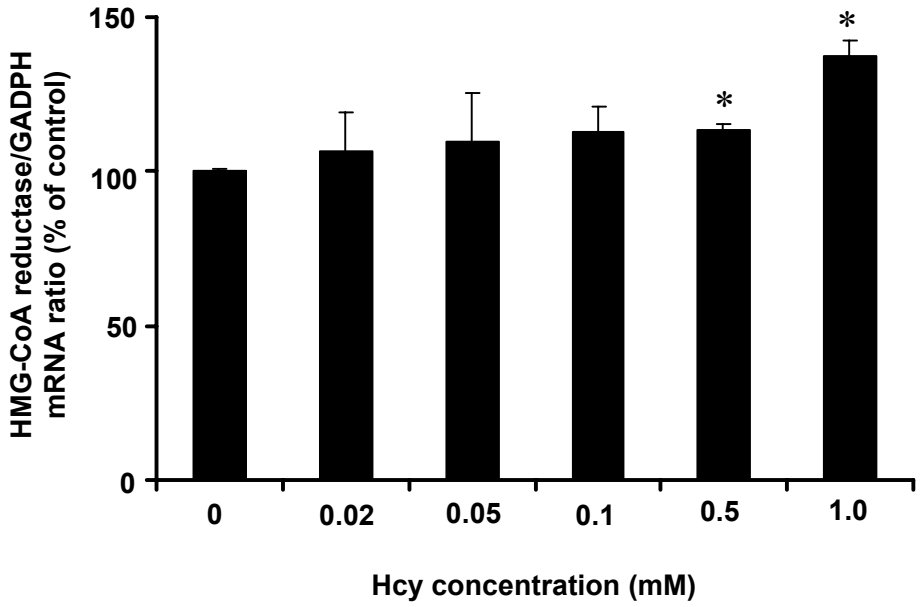

Figure 4.12 HMG-CoA Reductase mRNA Expression in Hepatocytes

Cells were incubated with Hcy at various concentrations for 4 hours. HMG-CoA reductase mRNA and GAPDH mRNA were determined by RT-PCR. Results are expressed as ratio of HMG-CoA reductase to GAPDH mRNA and depicted as means ± SEM. *$P < 0.05$ compared with control values (expressed as 100%).

Hcy level. When hepatocytes were incubated with 1 mM Hcy for various time periods, a significant increase in HMG-CoA reductase mRNA expression was observed in cells incubated for 2 to 8 hours (Figure 4.13). In addition, cholesterol concentrations in hepatocytes and medium were determined. The intracellular cholesterol concentration was significantly increased in hepatocytes after incubation with Hcy for 6 hours (Figure 4.14). The amount of cholesterol secreted by hepatocytes into the culture medium was also significantly elevated upon Hcy treatment (Figure 4.14). Taken together, Hcy was able to increase HMG-CoA reductase expression leading to elevated cholesterol production in hepatocytes. The responses of the isolated hepatocytes to Hcy treatment *in vitro* were similar to the results obtained in HHcy rat liver. In the next sections, the mechanism by which Hcy increased the expression of HMG-CoA reductase was explored.

4.3.2.2 Specificity of Hcy to Increase HMG-CoA Reductase mRNA Expression

In the *in vivo* study, a high-methionine diet was used to induce HHcy. Methionine is a sulfur-containing amino acid. It has been suggested that methionine itself can elicit toxicity (Troen *et al.*, 2003). To investigate whether methionine was able to affect HMG-CoA reductase expression, hepatocytes were incubated with methionine (1mM). Addition of methionine in the culture medium was unable to stimulate the HMG-CoA reductase mRNA expression (Figure 4.15). On the other hand, Hcy is a sulfhydryl group (-SH) containing amino acid. It has been suggested some pathophysiological effect of Hcy may be mediated by the sulfhydryl group (Lentz & Sadler, 1991; Lentz & Sadler, 1993). In order to find out whether the effect of Hcy on HMG-CoA reductase was due to the presence of sulfhydryl group, another sulfhydryl group-containing amino acid, cysteine was included in the experiments. As shown in Figure 4.15, cysteine treatment

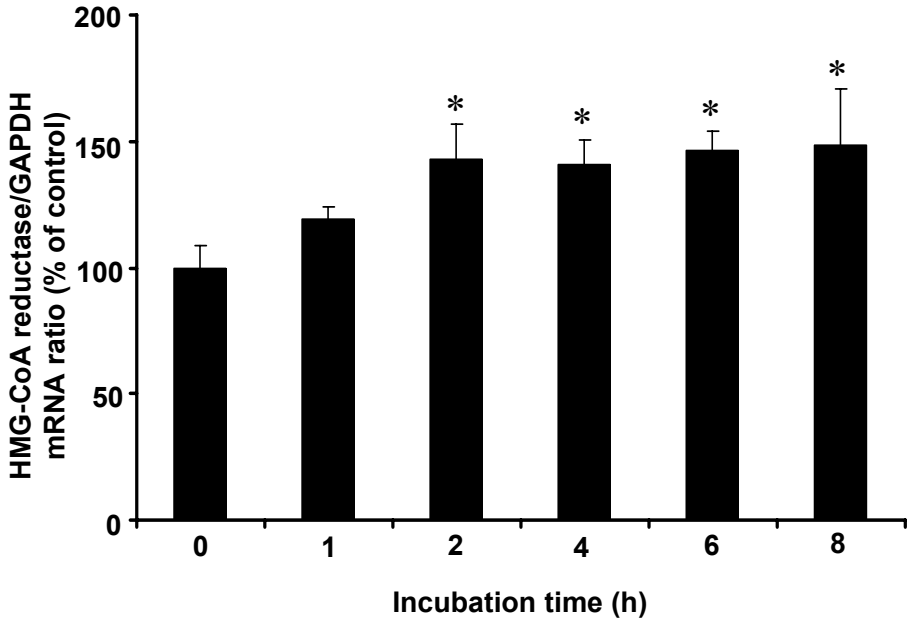

Figure 4.13 HMG-CoA Reductase mRNA Expression in Hepatocytes

Cells were incubated with Hcy (1 mM) for various time periods. HMG-CoA reductase and GAPDH mRNA were determined by RT-PCR. Results are expressed as ratio of HMG-CoA reductase to GAPDH mRNA and depicted as means ± SEM. *P < 0.05 compared with the corresponding control values (expressed as 100%).

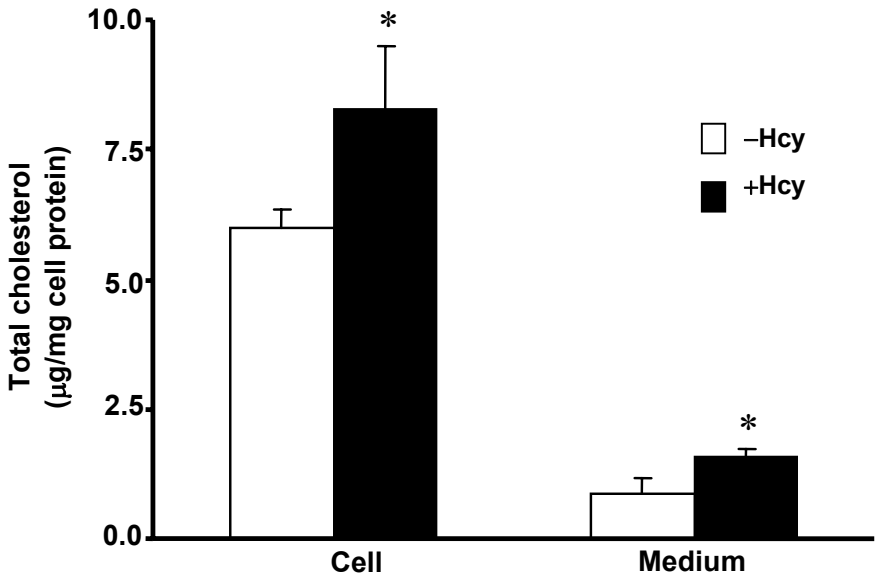

Figure 4.14 Cholesterol Concentrations in Hepatocytes and in Culture Medium

Hepatocytes were isolated from rats fed a regular diet. Cells were incubated in the absence or presence of Hcy (1 mM) for 6 hour. Cholesterol concentrations in cells and in culture medium were determined. Results are expressed as means ±SEM. *P <0.05 compared with control values.

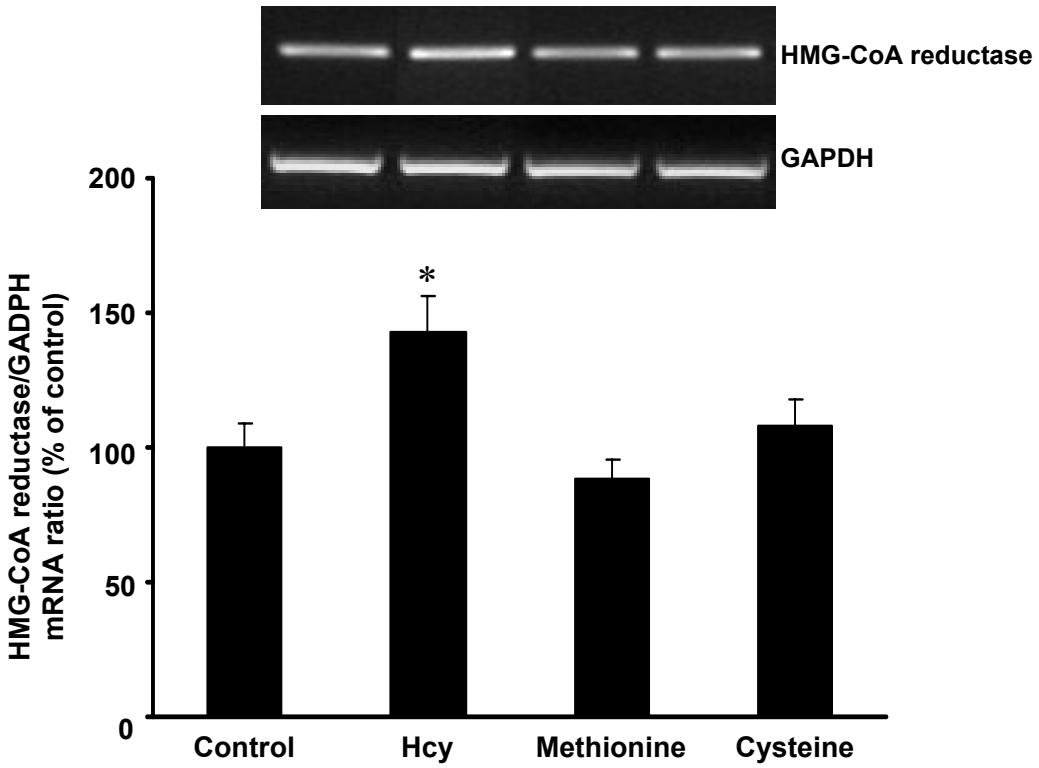

Figure 4.15 Effects of Sulfur-containing Amino Acids on HMG-CoA Reductase mRNA

Hepatocytes were incubated with incubated with Hcy, methionine or cysteine at concentration of 1 mM for 4 hours. HMG-CoA reductase and GAPDH mRNA were determined by RT-PCR. Results are expressed as ratio of HMG-CoA reductase to GAPDH mRNA and depicted as means ± SEM. *P < 0.05 compared with control values (expressed as 100%).

did not stimulate the expression of HMG-CoA reductase mRNA in hepatocytes. These results suggested that the stimulatory effect on HMG-CoA reductase was specifically elicited by Hcy.

4.3.2.3 Increased Stability of HMG-CoA Reductase mRNA

As shown in Figure 4.10 and Figure 4.11, the degree of increase in HMG-CoA reductase protein level was higher than the change in the mRNA level in HHcy rat livers. It was speculated that an increase in the stability of the enzyme mRNA might contribute to elevated protein production. A previous study showed that Hcy was able to increase HMG-CoA reductase mRNA stability in endothelial cells (Li *et al.*, 2002). In the present study, hepatocytes were isolated from rat liver and treated with actinomycin D in the presence or absence of Hcy. Actinomycin D can inhibit transcription by interfering the elongation of transcribed RNA chains by RNA polymerase (Sobell, 1985). Once the transcription of DNA to RNA is terminated by actinomycin D, the degradation rate of the existing RNA can be determined. The half-life of mRNA could be estimated by observing the decay of mRNA or protein synthesis after transcription being stopped by actinomycin D. As shown in Figure 4.16, Hcy increased the stability of HMG-CoA reductase mRNA in rat hepatocytes. The half-life of HMG-CoA mRNA in rat hepatocytes was increased from 9.5 hours (basal) to 13.4 hours upon the treatment of Hcy. These results suggested that protein synthesis of HMG-CoA reductase might be prolonged by the treatment with Hcy. This finding supports the observation of a greater increase in hepatic HMG-CoA reductase protein than in mRNA during HHcy (Figure 4.10 and Figure 4.11).

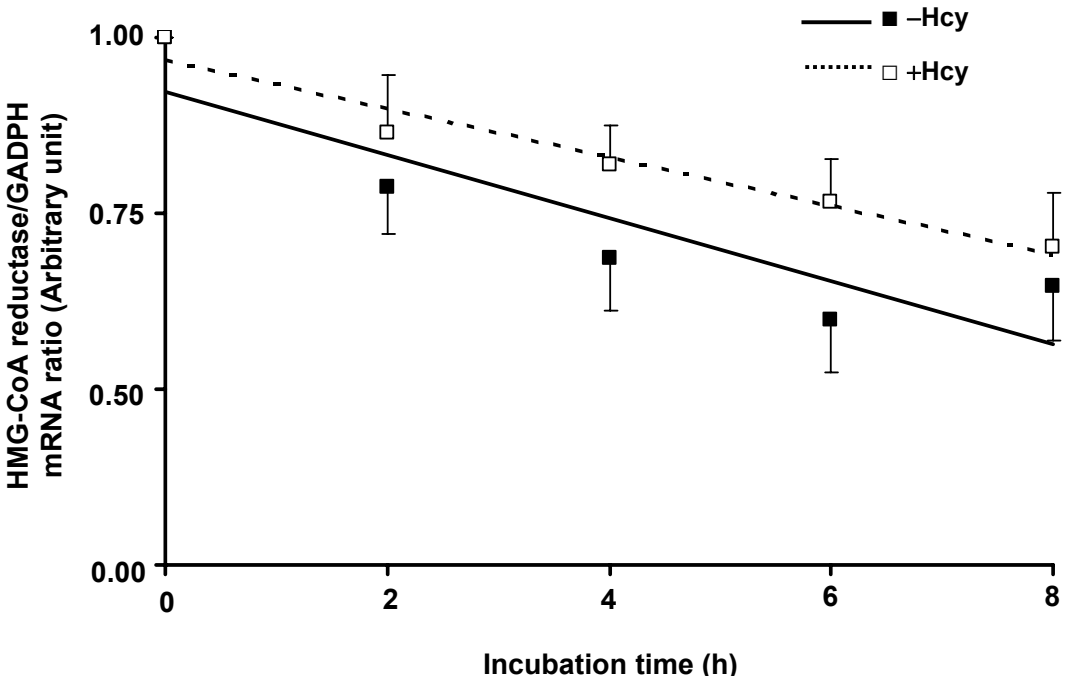

Figure 4.16 Stability of HMG-CoA reductase mRNA

Rat hepatocytes were treated with actinomycin D (5 μg/mL) in the presence or absence of Hcy for various incubation periods. HMG-CoA reductase mRNA expression was examined in hepatocytes using RT-PCR with GAPDH mRNA as internal control. Results are expressed as means ± SEM.

4.3.2.4 Activation of Transcription Factors

The expression of HMG-CoA reductase mRNA was increased in both Hcy-treated hepatocytes and HHcy rat livers (Figure 4.11 and Figure 4.12). Activation of transcription factors might be one of the mechanisms for the up-regulation of HMG-CoA reductase expression by Hcy. Several transcription factors for HMG-CoA reductase have been identified including SREBP-2, CREB and NF-Y (Figure 4.17) (Bennett & Osborne, 2000; Ngo *et al.*, 2002; Vallett *et al.*, 1996). SREBP-2 is a weak transcription factor which requires the presence of co-activators, NF-Y and CREB to yield the maximal stimulation of HMG-CoA reductase transcription. Figure 4.17 shows the schematic illustration of the binding sites for these three transcription factors in the promoter region of HMG-CoA reductase (Ngo *et al.*, 2002). The activation of the transcription factors for HMG-CoA reductase was examined in Hcy-treated hepatocytes. Cells were incubated with Hcy for various time periods, and nuclear proteins were prepared to determine the activation of transcription factors.

The precursor form of SREBP-2 (125kDa) is a protein embedding in the endoplasmic reticulum membrane. When the cell is deprived of sterol or is stimulated, SREBP-2 is transported to the Golgi apparatus and cleaved by proteases into a truncated form (68kDa). The truncated SREBP-2 is released to the cytosol and then enters the nucleus. The nuclear SREBP-2 binds to the promoter region of target genes. Unlike other common transcription factors, no strict sterol regulatory element (SRE) consensus sequence for SREBPs has been identified (Liscum, 2002). The activation of SREBP-2 was determined by detecting the expression of the truncated SREBP-2 (68kDa, referred as n-SREBP-2) in the nuclear content of hepatocytes using Western immunoblot analysis.

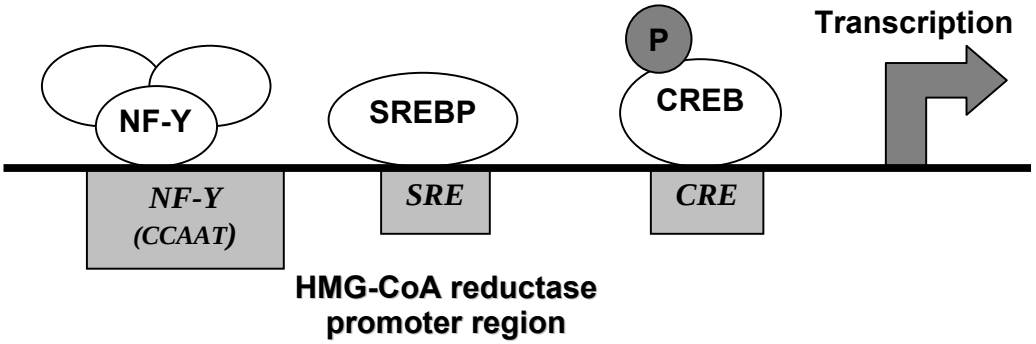

(Based on ideas from Ngo *et al*., Journal of Biological Chemistry, 277: 33901-33905, 2002.)

Figure 4.17 Promoter Region of HMG-CoA Reductase.

The promoter region of HMG-CoA reductase contains binding sites for nuclear factor-Y (NF-Y), sterol-regulatory element binding protein (SREBP) and cAMP responsive element binding protein (CREB). Abbreviation: SRE, sterol-regulatory element; CRE, cAMP responsive element.

The activation of SREBP-2 became evident after cells were incubated with Hcy for 15 minutes (Figure 4.18).

CREB is a transcription factor present in the nucleus prior to activation of transcription. It is activated via phosphorylation at the Ser-133 site (Servillo *et al.*, 2002). Several kinases are able to phosphorylate CREB, including cAMP-dependent kinase (PKA), p38 mitogen-activating protein kinase (p38 MPAK) and extracellular signal-regulated kinase-1/2 (ERK-1/2). The phosphorylated CREB binds to the cAMP response element on the promoter region of target gene to initiate transcription. The binding activity of CREB to DNA was determined by the EMSA assay. After hepatocytes were incubated with Hcy for only 5 minutes, there was a significant elevation of CREB/DNA binding in the nuclear fraction (Figure 4.19). The binding activity declined rapidly and no elevation of the CREB/DNA binding was observed after 30 minutes of incubation (Figure 4.19).

NF-Y is a transcription factor consisting of three subunits, NF-YA, NF-YB and NF-YC. All of the subunits are required for DNA binding (Liang & Maity, 1998). The three subunits interact and form a heterotrimer. The heterodimer binds to the CCAAT sequence on the promoter region of DNA to form NF-Y/DNA complex (Figure 1.10) (Liang & Maity, 1998; Mantovani, 1999). After hepatocytes were incubated with Hcy for 15 minutes, the NF-Y/DNA binding activity was markedly enhanced as assayed by EMSA (Figure 4.20). Hcy induced-binding activity of NF-Y to DNA persisted longer than the other two transcription factors, SREBP-2 and CREB.

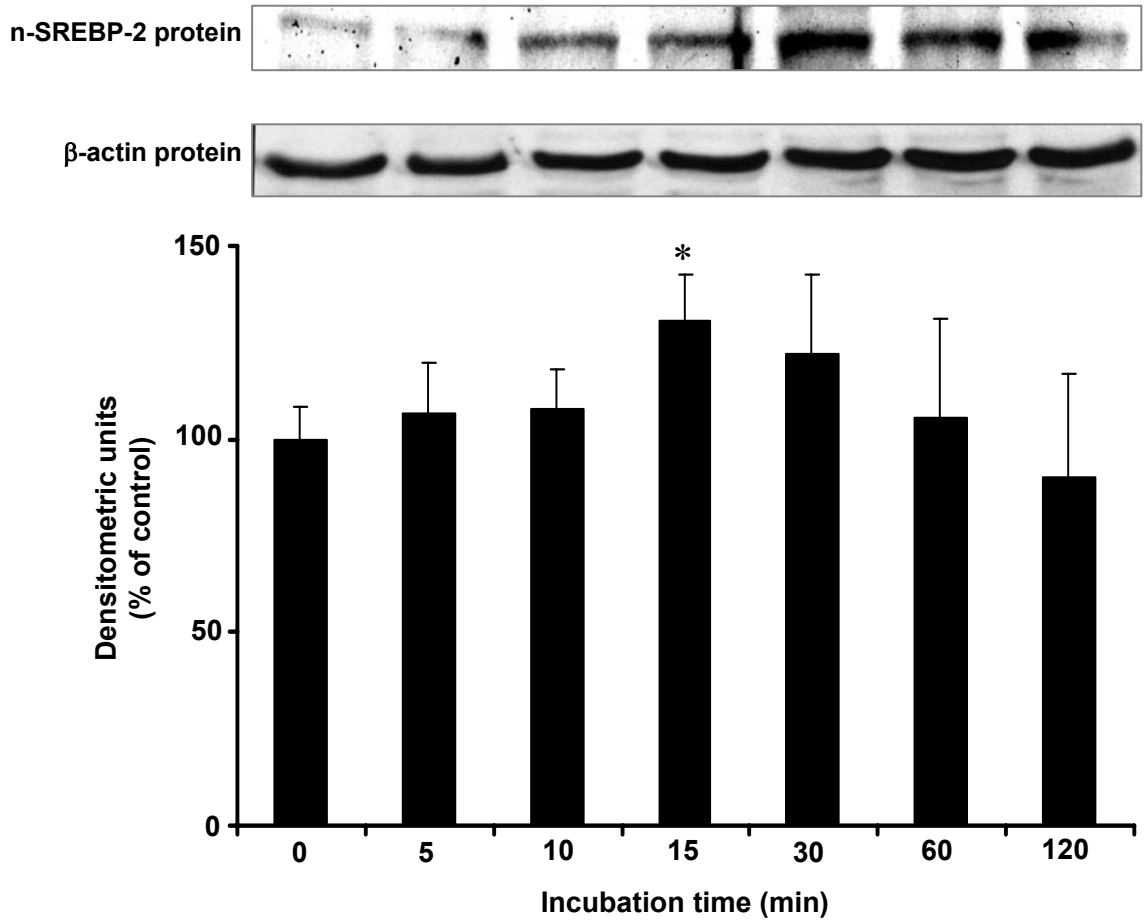

Figure 4.18 SREBP Activation in Hepatocytes

Hepatocytes were isolated from rats fed a regular diet and cells were incubated in the absence or presence of Hcy (1 mM) for various time periods. Nuclear proteins were isolated, and the level of SREBP-2 in the nucleus (nSREBP-2) was determined by Western immunoblot analysis. Results are expressed as mean ± SEM (n = 5) *$P < 0.05$ compared with control values (expressed as 100%).

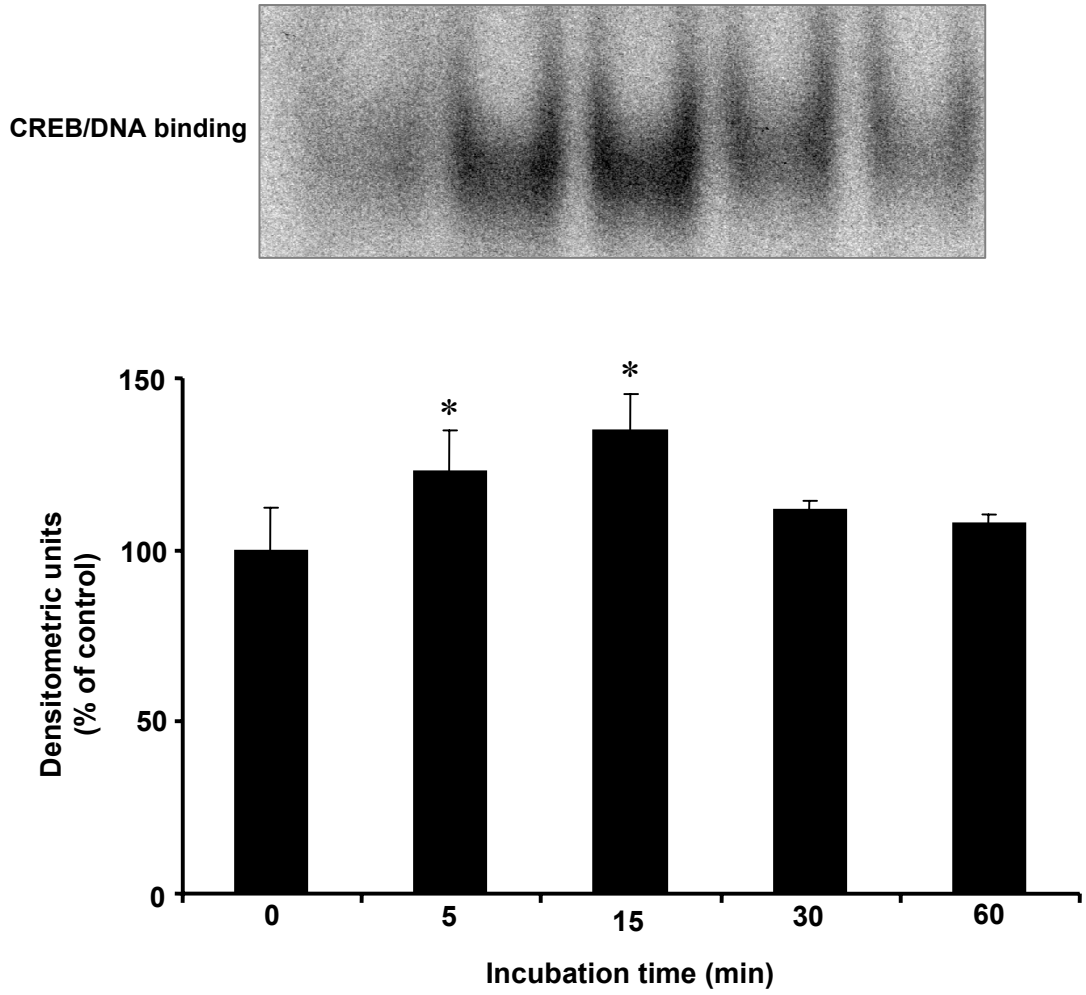

Figure 4.19 CREB/DNA Binding in Hepatocytes.

Hepatocytes were isolated from rats fed a regular diet and cells were incubated in the absence or presence of Hcy (1 mM) for various time periods. Nuclear proteins were isolated, and the CREB/DNA binding was determined by EMSA. Results are expressed as mean ± SEM (n = 5). **P* < 0.05 compared with control values (expressed as 100%).

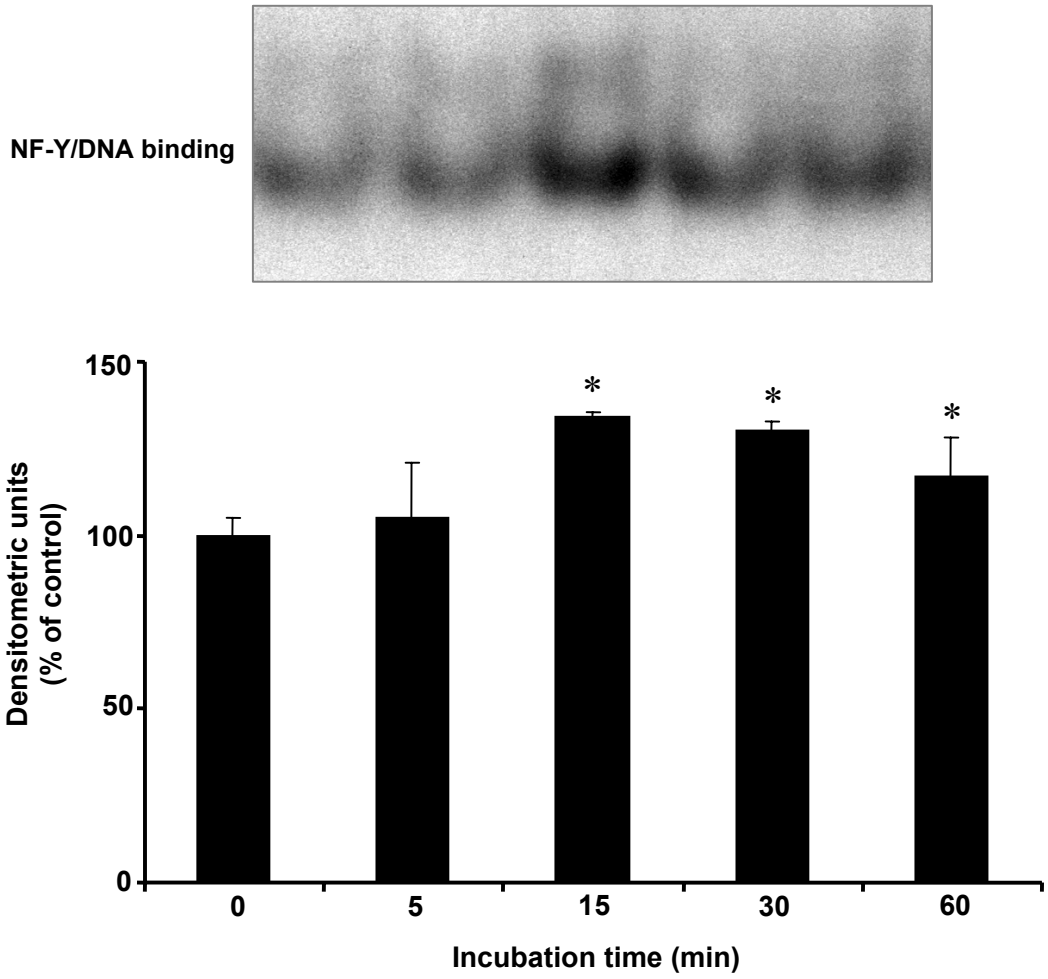

Figure 4.20 NF-Y/DNA Binding in Hepatocytes

Hepatocytes were isolated from rats fed a regular diet and cells were incubated in the absence or presence of Hcy (1 mM) for various time periods. Nuclear proteins were isolated, and the NF-Y/DNA binding was determined by EMSA. Results are expressed as mean ± SEM (n = 5). **P* < 0.05 compared with control values (expressed as 100%).

To further examine the localization of the three transcription factors in hepatocytes, the immunofluorescent staining was performed using the antibodies against SREBP-2, phosphorylated CREB (pCREB), and NF-YA after 15 minutes treatment of Hcy. The secondary antibodies for the individual primary antibodies were conjugated with different fluors in order to differentiate the detection of different transcription factors. The fluors used in the study were FITC (green fluorescence) for SREBP-2, Cy3 (red fluorescence) for pCREB and Alex Fluor 405 (blue fluorescence) for NF-YA. As shown in Figure 4.21, the immunofluorescence imaging analysis revealed a marked increase in the nuclear staining intensity for SREBP-2 (in green) and pCREB (in red) in hepatocytes treated with Hcy. The green fluorescence observed in hepatocytes was more intense in the nuclear area when cells were treated with Hcy (Figure 4.21). These results indicated that the more activated (truncated) form of SREBP-2 was present in Hcy-treated cells. The antibody against pCREB was used to detect the activated CREB. The red fluorescence in the hepatocyte nuclei was stronger after Hcy treatment (Figure 4.21). The activation of NF-Y relies on the interaction of the three subunits which are constitutively present in the nucleus. The binding of NF-YA onto the NF-YB/NF-YC complex determines the specificity and affinity of the DNA binding (Mantovani, 1999). The antibody used for detecting NF-YA (blue fluorescene) was unable to specifically detect the activated form of NF-YA. It was noted that the blue fluorescent signal located only in the nucleus. However, there was no significant difference in the blue fluorescence signal between the Hcy-treated and non-treated hepatocyte (Figure 4.21). The activation of NF-Y was detected using EMSA assay as shown in Figure 4.20 in the previous section.

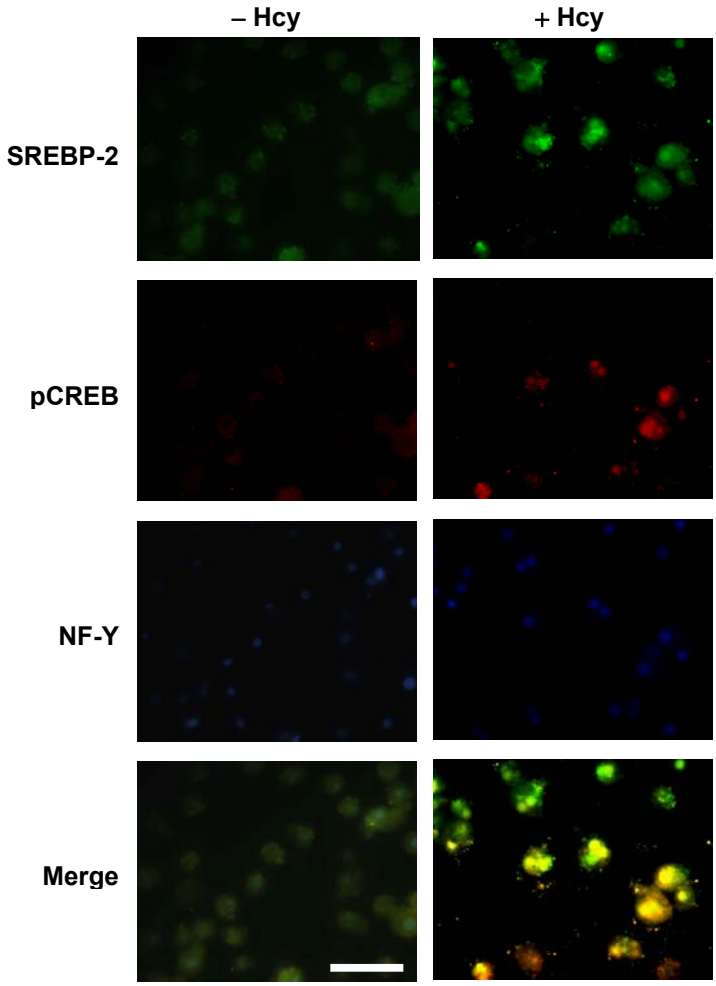

Figure 4.21 Immunofluorescence Staining of Transcription Factors in Hepatocytes

Hepatocytes were isolated from rats fed a regular diet. Cells were incubated in the absence (–Hcy) or presence of Hcy (+Hcy) for 15 min. Immunofluorescence staining was performed. Specific antibodies were used to identify SREBP-2 (green fluorescence), phosphorylated-CREB (pCREB, red fluorescence) or NF-Y (blue fluorescence). Representative photos were obtained from 5 separate experiments. Bar, 20μm.

4.3.2.5 Transcription Factor Inhibitors Decreased Hcy-induced HMG-CoA Reductase Expression

Activation of the transcription factors for HMG-CoA reductase was observed in Hcy-treated hepatocytes as shown in previous sections. To further investigate whether Hcy-induced HMG-CoA reductase expression was mediated via the activation of these three transcription factors (SREBP-2, CREB, and NF-Y), individual inhibitors for these transcription factors were included in the experiments. First, a serine protease inhibitor, AEBSF was added to cultured hepatocytes to inhibit the activation of SREBP-2. This inhibitor was shown to inhibit the production of the mature form of SREBP-2 in HeLa cells (Okada *et al.*, 2003). AEBSF inhibits the proteases that cleave the precursor form of SREBP-2 (125 kDa) to prevent its activation. Hepatocytes were pretreated with 300 μM AEBSF for 30 minutes followed by incubation with 1 mM Hcy for another 15 minutes. Nuclear proteins were isolated and the truncated from of SREBP-2 (68 kDa, n-SREBP-2) was detected by Western immunoblot analysis. As shown in Figure 4.22, addition of AEBSF to the culture medium prevented Hcy-induced SREBP-2 activation. Pretreatment of AEBSF also abolished Hcy-stimulated HMG-CoA reductase mRNA expression in hepatocytes (Figure 4.23).

Next, the involvement of CREB in Hcy-induced HMG-CoA reductase expression was examined by adding cAMP-dependent protein kinase (PKA) inhibitor, H89 to cultured hepatocytes. It has been shown that phosphorylation of CREB by PKA can lead to an activation of this transcription factor (Servillo *et al.*, 2002). H89 can selectively inhibit the activity of PKA by competing the kinase binding to adenosine triphosphate (ATP)

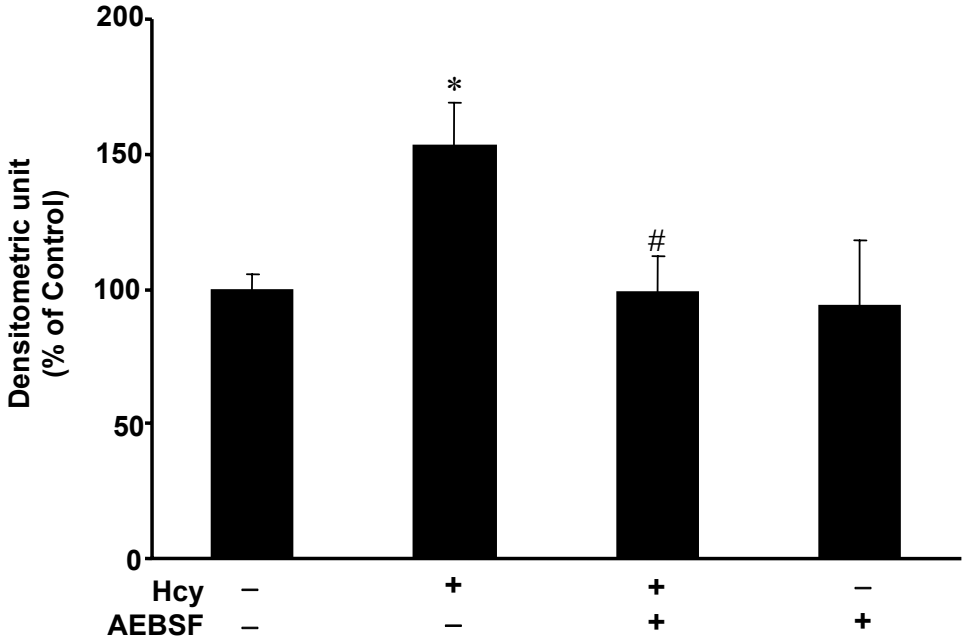

Figure 4.22 Effect of AEBSF on SREBP-2 Activation in Hepatocytes

Hepatocytes were isolated from rats fed a regular diet. Cells were incubated with Hcy (1 mM) in the absence or presence of SREBP-2 inhibitor (AEBSF, 300μM). Nuclear proteins were isolated from cells after 15 minutes of incubation. The level of SREBP-2 in the nucleus (nSREBP-2) was determined by Western immunoblot analysis. Results were quantified on the basis of the densitometric unit and are expressed as means ± SEM. *$P < 0.05$ compared with control values (expressed as 100%). #$P < 0.05$ compared with values obtained from Hcy-treated cells.

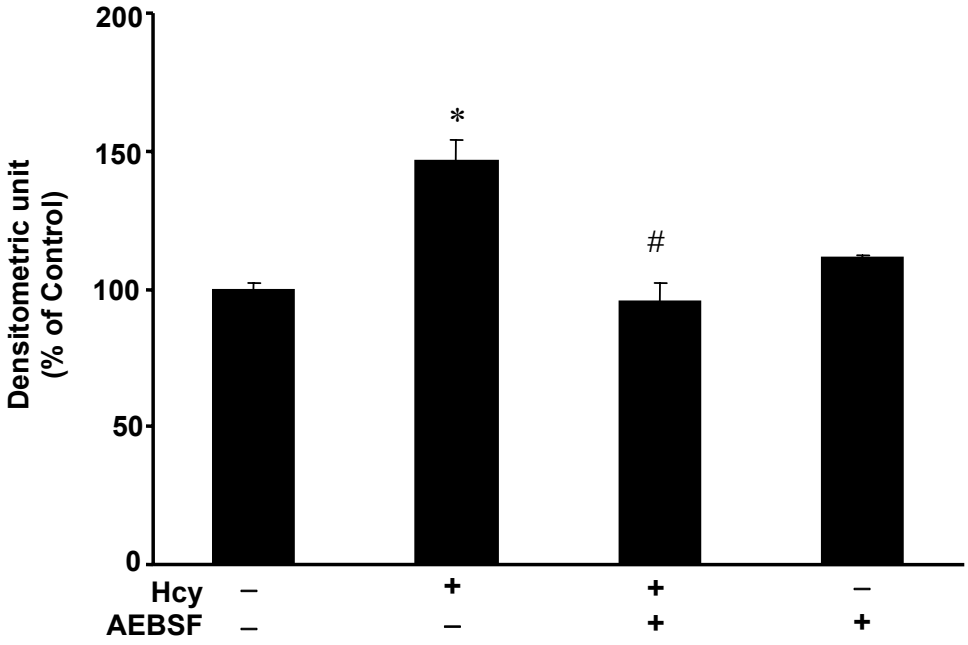

Figure 4.23 Effect of AEBSF on HMG-CoA reductase mRNA Expression in Hepatocytes

Hepatocytes were isolated from rats fed a regular diet. Cells were incubated with Hcy (1 mM) in the absence or presence of SREBP-2 inhibitor (AEBSF, 300μM). Total RNA was prepared from cells after 4 hours of incubation. Expression of HMG-CoA reductase mRNA, which was normalized to GAPDH mRNA, was determined by RT-PCR analysis. Results were expressed as the ratio of HMG-CoA reductase to GAPDH mRNA and are depicted as means ± SEM. *$P < 0.05$ compared with control values (expressed as 100%). #$P < 0.05$ compared with values obtained from Hcy-treated cells.

and subsequently inhibit the phosphorylation of CREB (Engh *et al.*, 1996; Reinehr *et al.*, 2002). Pretreatment of hepatocytes with H89 for 30 minutes was shown to block the Hcy-induced CREB/DNA binding (Figure 4.24). H89 treatment also prevented Hcy-induced HMG-CoA reductase mRNA expression in hepatocytes (Figure 4.25).

Finally, the role of NF-Y in Hcy-induced HMG-CoA reductase mRNA expression was examined by using N-ethylmaleimide (NEM) as an inhibitor. NEM alkylates cysteine residues resulting in the inhibition of NF-Y complex binding to DNA (Nakshatri *et al.*, 1996). Hepatocytes were preteated with 1 mM NEM for 30 minutes prior to incubation with Hcy for 15 minutes. The treatment with NEM was shown to prevent Hcy-induced NF-Y activation (Figure 4.26) as well as HMG-CoA reductase expression (Figure 4.27).

The treatment of the individual inhibitors alone did not significantly alter the basal level of HMG-CoA redutase mRNA expression in hepatocytes (Figure 4.22 to Figure 4.27). Taken togther, these results indicated that Hcy-induced HMG-CoA reductase expression in hepatocytes was likely to be mediated via transcriptional regulation by SREBP-2, CREB, and NF-Y. It was shown that inhibition of any one of these transcription factors for HMG-CoA reductase was able to inhibit Hcy-induced HMG-CoA reductase mRNA expression. These results suggested that the concurrent activations of all three transcription factors were essential to Hcy-induced HMG-CoA reductase expression.

SREBP-2 is the essential transcription factor of HMG-CoA reductase mRNA expression. It is recruited to the promoter region of HMG-CoA reductase gene when the cell is depleted of sterol. Studies have shown that both CREB and NF-Y are bound to the promoter region of HMG-CoA reductase gene in sterol-depleted cells (Bennett & Osborne, 2000; Ngo *et al.*, 2002). However, it is not clear how these three transcription

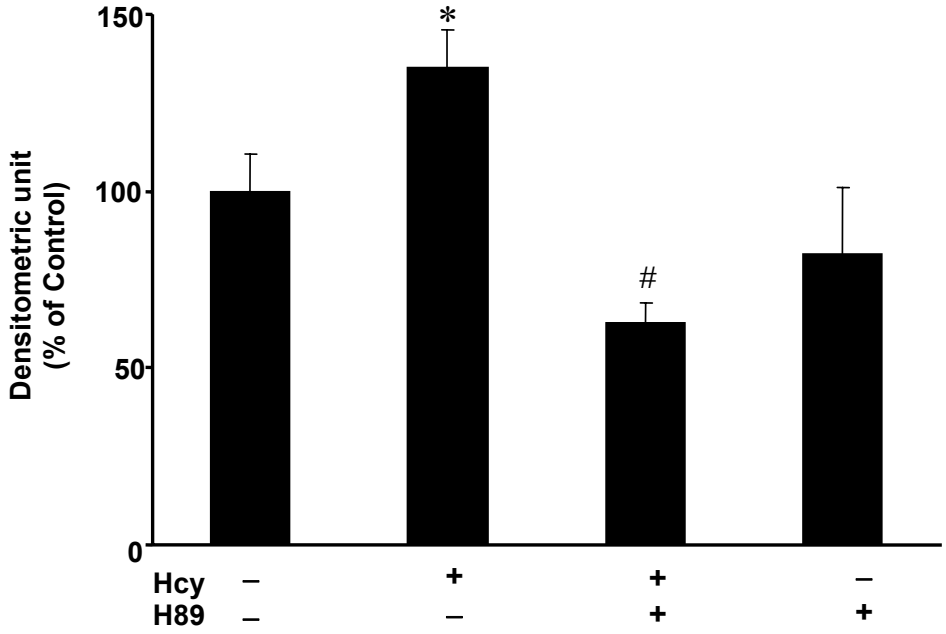

Figure 4.24 Effect of H89 on CREB Activation in Hepatocytes

Hepatocytes were isolated from rats fed a regular diet. Cells were incubated with Hcy (1 mM) in the absence or presence of CREB inhibitor (H89, 5 μM). Nuclear proteins were isolated from cells after 15 minutes of incubation. CREB/DNA binding activity was determined by EMSA and quantified on the basis of the densitometric unit. Results are expressed as means ± SEM (n = 5) *P < 0.05 compared with control values (expressed as 100%). #P < 0.05 compared with values obtained from Hcy-treated cells.

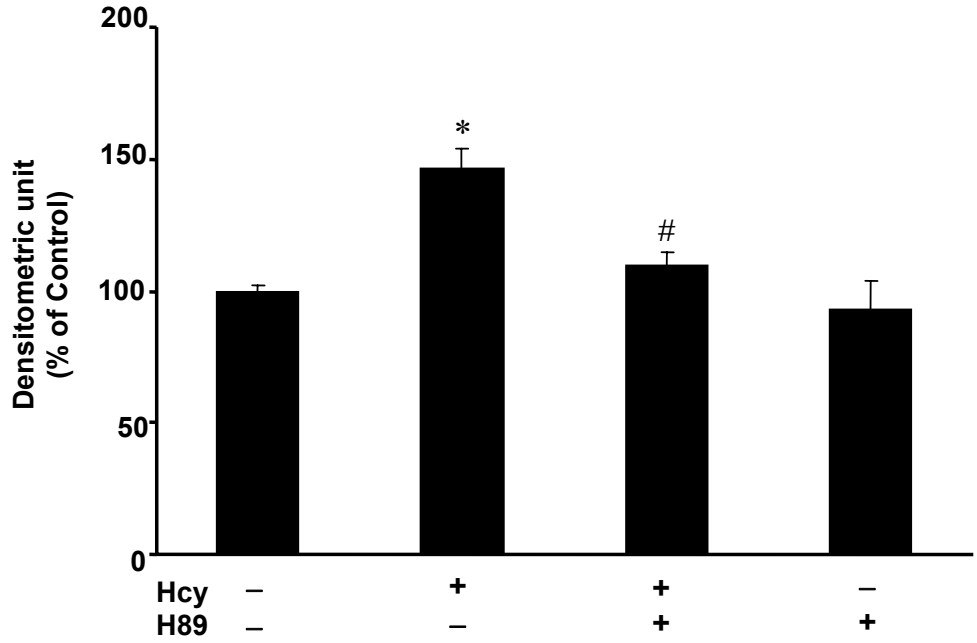

Figure 4.25 Effect of H89 on HMG-CoA Reductase mRNA Expression in Hepatocytes

Hepatocytes were isolated from rats fed a regular diet. Cells were incubated with Hcy (1 mM) in the absence or presence of CREB inhibitor (H89, 5 μM). Total RNA was prepared from cells after 4 hours of incubation. Expression of HMG-CoA reductase mRNA, which was normalized to GAPDH mRNA, was determined by RT-PCR analysis. Results were expressed as the ratio of HMG-CoA reductase to GAPDH mRNA and are depicted as means ± SEM (n = 5). *$P < 0.05$ compared with control values (expressed as 100%). #$P < 0.05$ compared with values obtained from Hcy-treated cells.

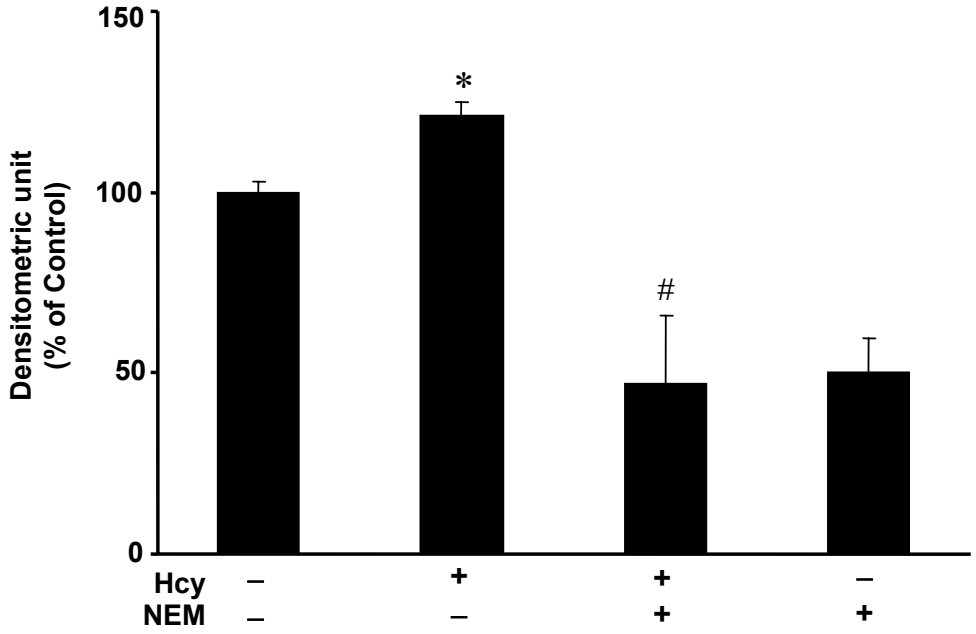

Figure 4.26 Effect of NEM on NF-Y Activation in Hepatocytes

Hepatocytes were isolated from rats fed a regular diet. Cells were incubated with Hcy (1 mM) in the absence or presence of NF-Y inhibitor, N-ethylmaleimide (NEM, 1 mM). Nuclear proteins were isolated from cells after 15 minutes of incubation. NF-Y/DNA binding activity was determined by EMSA and quantified on the basis of the densitometric unit and are expressed as means ± SEM (n = 5). *P < 0.05 compared with control values (expressed as 100%). #P < 0.05 compared with values obtained from Hcy-treated cells.

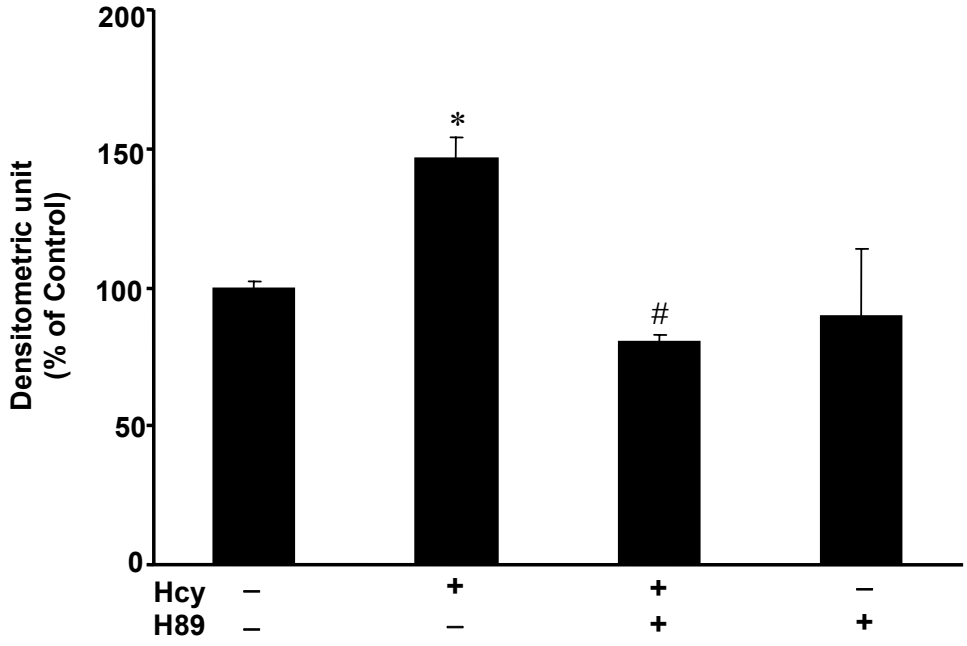

Figure 4.27 Effect of NEM on HMG-CoA Reductase mRNA Expression in Hepatocytes

Hepatocytes were isolated from rats fed a regular diet. Cells were incubated with Hcy (1 mM) in the absence or presence of NF-Y inhibitor, N-ethylmaleimide (NEM, 1 mM). Total RNA was prepared from cells after 4 hours of incubation. Expression of HMG-CoA reductase mRNA, which was normalized to GAPDH mRNA, was determined by RT-PCR analysis. Results were expressed as the ratio of HMG-CoA reductase to GAPDH mRNA and are depicted as means ± SEM (n = 5). *P < 0.05 compared with control values (expressed as 100%). #P < 0.05 compared with values obtained from Hcy-treated cells.

factors interact with each other in order to promote the transcription of HMG-CoA reductase.

4.3.3 Activation of Transcription Factors *in vivo*

In the previous sections, it was shown that Hcy could activate the transcription factors, SREBP-2, CREB and NF-Y in isolated rat hepatocytes. Hcy-induced activation of these transcription factors contributed to increased HMG-CoA reductase expression in hepatocytes. In the following sections, the activation of transcription factors in the liver of HHcy rat was investigated.

HHcy was induced in Sprague-Dawley rats by feeding a high-methionine diet for 4 weeks. Livers were collected from HHcy rats and control rats. Nuclear proteins were isolated from liver samples. The truncated form of SREBP-2 (n-SREBP-2, 68 kDa) was detected by Western immunoblot analysis. It was shown that the level of n-SREBP-2 was significantly elevated in HHcy rat livers (Figure 4.28). Next, the same nuclear protein samples were subjected to EMSA analysis to examine the DNA binding activities of CREB and NF-Y. The CREB/DNA and NF-Y/DNA binding activity were significantly higher in HHcy rat livers than that of the control (Figure 4.28). These results were congruent with the observation in Hcy-treated rat hepatocytes, and further supported the hypothesis that Hcy-induced HMG-CoA reductase mRNA expression via the activation of transcription factors.

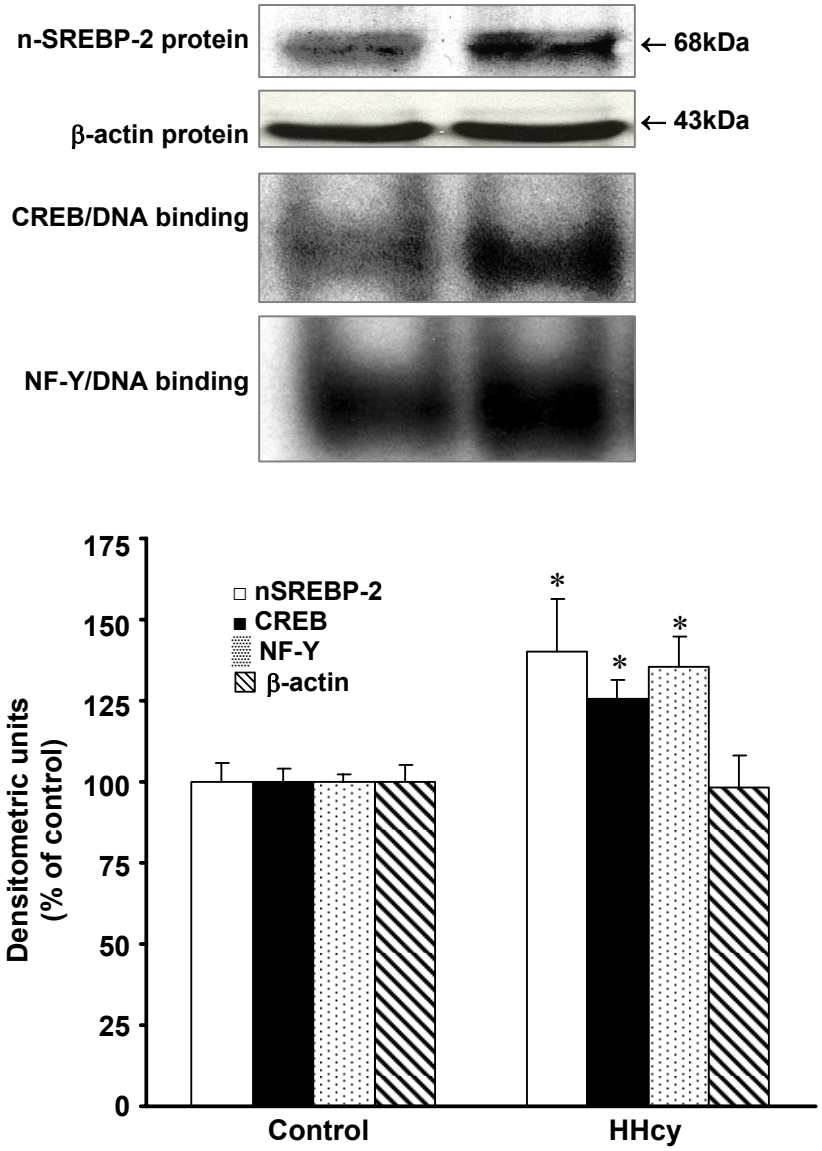

Figure 4.28 Activation of Transcription Factors in Livers

Nuclear proteins were isolated from livers of rats fed control, or high-methionine diet (HHcy). Nuclear sterol regulatory element-binding protein-2 (n-SREBP-2) was determined by Western immunblot analysis. β-Actin was used to confirm equal loading amount of proteins from each sample. CREB/DNA or NF-Y/DNA binding activity was determined by EMSA. The levels of n-SREBP-2, β-actin, and CREB/DNA or NF-Y/DNA binding activity were quantified on the basis of the densitometric unit and are expressed as means ± SEM (n = 12). *P < 0.05 compared with control values (expressed as 100%).

4.3.4 Hepatic Cholesterol Accumulation

Congruent with the finding of hepatic steatosis in HHcy patients and in experimental animals (Carson *et al.*, 1965; McCully, 1969; Watanabe *et al.*, 1995; Werstuck *et al.*, 2001), the present study revealed that small lipid droplets were accumulated in the liver of HHcy rat. Lipid accumulation in the liver was induced by the upregulation of HMG-CoA reductase mRNA expression. The upregulated reductase expression resulted in enhanced hepatic cholesterol biosynthesis leading to an elevation of cholesterol concentration in the serum of HHcy rat. Although a 22% increase in HMG-CoA reductase mRNA level was found in the liver of HHcy rat, the reductase protein level was 200% and the activity was 150% of the control values (Figure 4.9 and Figure 4.10). The half-life of mRNA determines how fast the protein synthesis is terminated after transcription has ceased. The half-life of HMG-CoA reductase mRNA in rat hepatocytes was extended 4 hours longer upon treatment of Hcy. These results suggested that the protein synthesis of HMG-CoA reductase might be prolonged by the treatment of Hcy. The observation of a larger increase in hepatic HMG-CoA reductase protein than mRNA in HHcy rat might be due to the extended time for protein synthesis.

4.3.5 Mechanism of Hcy-induced HMG-CoA Reductase Expression

Within the last decade, several transcription factors that regulate HMG-CoA reductase gene expression have been identified (Bennett & Osborne, 2000; Datta *et al.*, 2006; Ngo *et al.*, 2002; Vallett *et al.*, 1996). A sterol sensitive transcription factor, sterol regulatory element binding protein-2 (SREBP-2) is thought to play a critical role in cholesterol

biosynthesis (Horton *et al.*, 2002; Horton *et al.*, 1998; Vallett *et al.*, 1996). Upon stimulation, the full-length SREBP-2 (125 kDa) in rough endoplasmic reticulum membrane is cleaved in Golgi apparatus to a truncated form (68 kDa), which enters the nucleus and activates transcription of target genes such as HMG-CoA reductase. In the present study, the level of SREBP-2 in the nucleus was found to be significantly elevated in the liver of HHcy rats as well as in Hcy-treated hepatocytes. To efficiently activate HMG-CoA reductase transcription, the concurrent activation of other transcriptional factors (co-regulators) along with SREBP-2 are essential. The two known co-regulators for HMG-CoA reductase are cAMP response element binding protein (CREB) and nuclear factor-Y (NF-Y) (Bennett & Osborne, 2000; Ngo *et al.*, 2002). A study suggested that a direct protein interaction of SREBP-2 with CREB and NF-Y might lead to the activation of HMG-CoA reductase transcription (Bennett & Osborne, 2000). In the present study, both CREB/DNA and NF-Y/DNA binding activities were significantly elevated in the liver of HHcy rat as well as in Hcy-treated hepatocytes. These results suggested that activation of SREBP-2 and its co-regulators (CREB and NF-Y) by Hcy played an important role in hepatic expression of HMG-CoA reductase in HHcy rat.

It was reported that insulin, a known activator of HMG-CoA reductase, could enhance CREB transcriptional activity in HepG2 cells through the induction of CREB phosphorylation (Klemm *et al.*, 1998). The binding of phosphorylated CREB to CREB-binding protein (CBP) is crucial in CREB-mediated transcription activation (Kwok *et al.*, 1994). It has been suggested that a direct interation of SREBP with CBP in cells occurs during sterol depletion (Ericsson & Edwards, 1998). However, others have showed that a physical interation may occur between SREBP and CREB (Dooley *et al.*, 1999). The

binding mechanism of CREB in SREBP-mediated transcriptional activation during HHcy remains to be investigated. Conversely, the binding of NF-Y onto the CCAAT element on the promoter region increased the affinity of SREBP bound to DNA (Ericsson *et al.*, 1996). Another study showed a direct protein-protein interaction of NF-Y and SREBP (Dooley *et al.*, 1998). The NF-Y and DNA binding activity was increased in hepatocytes upon Hcy treatment as well as in HHcy rat livers. Further studies are required to explore the mechanism by which NF-Y acts synergistically with SREBP-2 to activate transcription of HMG-CoA reductase during HHcy.

In the present study, treatment of cultured hepatocytes with individual inhibitors for SREBP-2, CREB, or NF-Y not only blocked Hcy-mediated activation of corresponding transcription factors but also prevented Hcy-induced HMG-CoA reductase mRNA expression. These results suggest that the simultaneous activation of these three transcription factors is essential for Hcy-induced HMG-CoA reductase expression. The possibility that Hcy may enhance the interaction of these three transcription factors and the binding mechanism are appealing for further investigations.

Abnormal cholesterol metabolism can cause serious complications of many diseases, including metabolic syndrome, atherosclerosis and hepatic steatosis. Hepatic steatosis can progress to fibrosis and cirrhosis upon inflammatory tiggers (Durrington, 2003; Harrison & Di Bisceglie, 2003). Cirrhosis causes loss of liver function and eventually leads to liver failure. The ability of Hcy to promote cholesterol biosynthesis in hepatocytes would provide one of the plausible mechanisms of HHcy-associated liver pathology. However, it should be noted that pathological changes in the liver caused by short-term HHcy

induced by dietary manipulation might be different from that caused by long-standing HHcy due to a congenital enzyme defect in patients including inherited cystathionine-β-synthase deficiency.

4.4 Regulation of CREB Activation in Hyperhomocysteinemia

Objective

The results from the previous section showed that CREB was activated in HHcy rat livers as well as in hepatocytes. CREB is a ubiquitous protein which plays an important role in regulating the transcription of many genes participating in lipid and glucose metabolism (Montminy *et al.*, 2004; Xing & Quinn, 1993). The ability of Hcy to activate CREB implies a possible effect of Hcy on metabolic syndrome and its complications. The mechanism of CREB activation involves phosphorylation at the site of serine-133 (Ser-133) (Gonzalez & Montminy, 1989). The structure of CREB includes an activation domain and a DNA binding domain (Servillo *et al.*, 2002). The site of Ser-133 is located at the P-box (kinase inducible domain, KID) within the activation domain (Servillo *et al.*, 2002). Several kinases are able to phosphorylate Ser-133 of CREB, including cAMP-dependent kinase (protein kinase A, PKA), p38 mitogen-activating protein kinase (p38 MAPK), extracellular signal-regulated kinase-1/2 (ERK-1/2) and calmodulin kinases (CaMK) (Shaywitz & Greenberg, 1999) (Figure 4.29). The **fourth objective** of the present study was to investigate the mechanism by which Hcy induced CREB phosphorylation and activation *in vitro* and *in vivo*.

Results

4.4.1 CREB activation in Liver

The activation of transcription by CREB requires the phosphorylation of CREB at Ser133 (Servillo *et al.*, 2002). CREB-binding protein (CBP) specifically binds to phosphorylated CREB. The interaction between phosphorylated CREB and CBP allows the binding

(From Servillo *et al.*, Experimental Cell Research, 275: 143-154, 2002)

Figure 4.29 Pathways of Phosphorylation of CREB

CREB can be phosphorylated by several kinases including cAMP-dependent kinase (protein kinase A, PKA), p38 mitogen-activating protein kinase (p38 MAPK), calmodulin kinase (CaMK) and extracellular signal-regulated kinase (ERK). Different stimuli can activate different kinases to phosphorylate CREB. For example, hormones can activate G-coupling protein resulting in elevation of cAMP levels by stimulation of adenylyl cyclase. The elevated cAMP levels can activate PKA to phosphorylate CREB.

of CBP to the general transcription factor IIB (TFIIB) and RNA polymerase (Servillo *et al.*, 2002). In section 4.3.2, we observed increased CREB/DNA binding activity in HHcy rat livers (Figure 4.28). The phosphorylation of CREB and its role in CREB activation in HHcy rat livers were examined.

4.4.1.1 Increased Phosphorylation of CREB without Altering Total CREB Protein Level

To determine the level of phosphorylated CREB protein in the liver during HHcy, Western immunoblot analysis was performed using specific antibodies that recognized phospho-CREB at Ser-133. There was a significant increase in the level of phosphorylated CREB in the livers isolated from HHcy rats (Figure 4.30). To investigate whether there was an increase in CREB expression, the level of total CREB protein was measured by Western immunoblot analysis. No difference was observed in the liver samples between the control and HHcy rats (Figure 4.30).

4.4.1.2 Necessity of Phosphorylation in CREB/DNA Binding Activity

To confirm that it was the phosphorylated CREB that bound to DNA, electrophoretic mobility shift assay (EMSA) was performed. There was a significant increase in the binding activity of CREB to DNA in HHcy rat livers (Figure 4.31). Addition of anti-phospho-CREB antibodies resulted in a supershift of the CREB/DNA complex (Figure 4.31). The attachment of anti-phospho-CREB antibodies to the CREB/DNA complex delayed its migration within the gel, which was displayed as a shift of the band. A stronger shift was observed when more anti-phospho-CREB antibodies were added to the

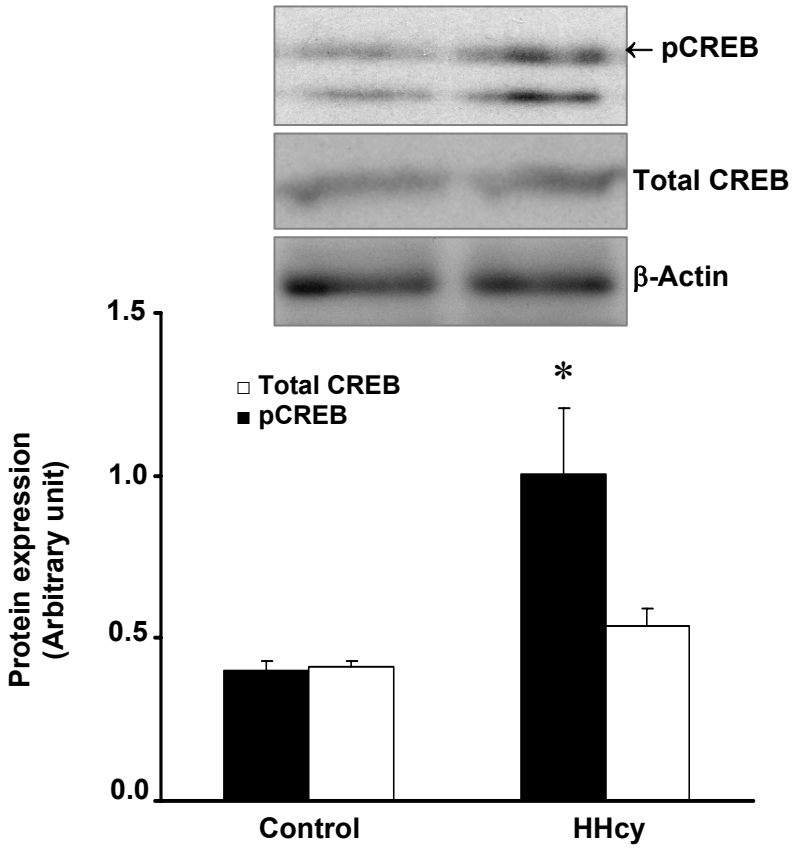

Figure 4.30 Phosphorylated CREB Expression in Livers

Livers were isolated from rats fed a regular diet (control) or a high-methionine diet (HHcy) for 4 weeks. Western immunoblotting analysis was performed to detect phosphorylated CREB (pCREB) and total CREB proteins. Results were expressed as mean ± SEM (n = 12). *P<0.05 when compared with the value obtained from the control group.

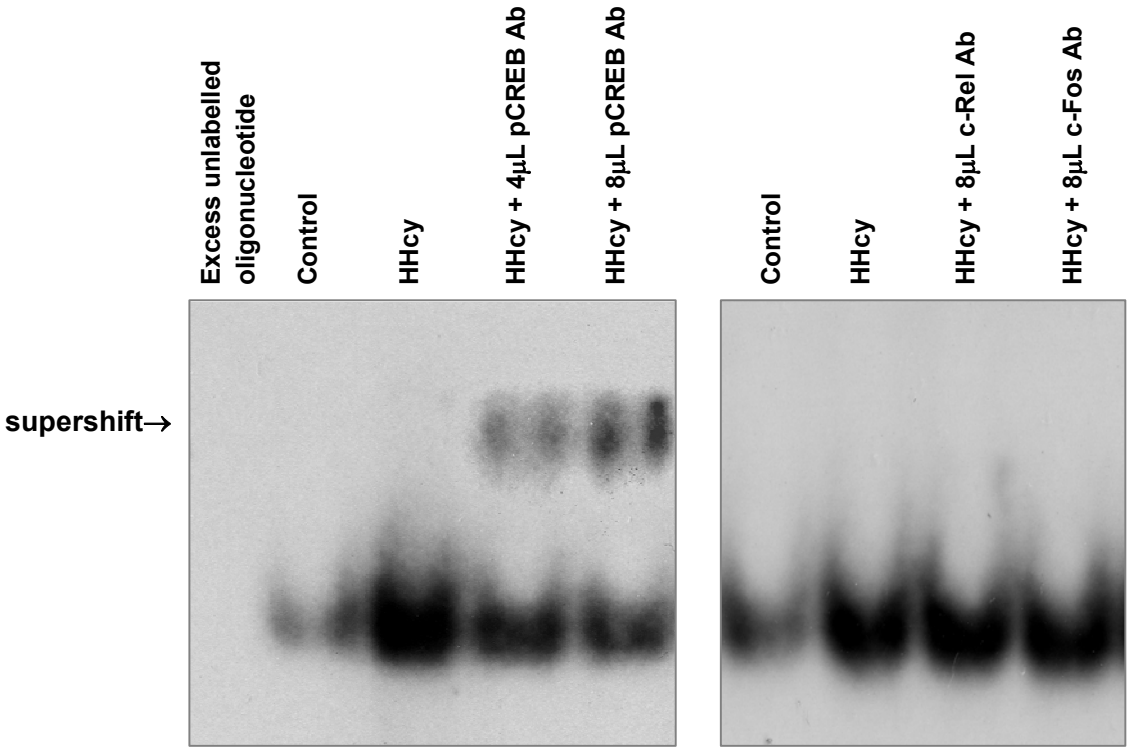

Figure 4.31 Phosphorylated CREB in DNA binding activity in Livers

Livers were isolated from rats fed a regular diet (control) or a high-methionine diet (HHcy) for 4 weeks. EMSA was performed to determine the CREB/DNA binding activity in livers. Supershift assays were performed in the presence of antibodies against pCREB (Ser133), c-Rel (NF-κB subunit), or c-Fos (AP-1 subunit).

nuclear content (8 μL vs. 4 μL) (Figure 4.31). To further characterize the nuclear protein/DNA complex in the EMSA, antibodies specific against other nuclear proteins were added. Incubation of nuclear proteins with anti- c-Rel antibody or anti- c-Fos antibody did not induce a shift of nuclear protein/DNA complex in the gel (Figure 4.31). The absence of signal in autoradiography was observed in the sample pre-treated with 100-fold excessive unlabeled CREB consensus oligonucleotides (Figure 4.31). This result indicated the specific radioactive signal of CREB consensus sequence binding. Taken together, these results indicated that it was the phosphorylated form of CREB binding to the CREB consensus sequence.

4.4.1.3 Increase in PKA Activity and cAMP Concentrations

Several kinases are able to phosphorylate CREB including cAMP-dependent kinase (PKA), p38 MAP kinase, and calmodulin kinases (Figure 4.29) (Mayr & Montminy, 2001; Servillo *et al.*, 2002). A study suggests that PKA not only phosphorylates CREB but also affects a downstream event such as the phosphorylation of CREB binding protein, leading to CREB activation (Cardinaux *et al.*, 2000). To investigate whether cAMP/PKA was involved in CREB activation during HHcy, PKA activity and cAMP concentration in HHcy rat livers were measured by a radiochemical assay and a commercial kit, respectively. There was 46% increase in PKA activity in the livers of HHcy rats as compared with the control group (Figure 4.32). The hepatic levels of cAMP in HHcy rats were markedly elevated (105.72 ± 24.64 pmol/mg protein versus 39.23 ± 8.31 pmol/mg protein in control rats).

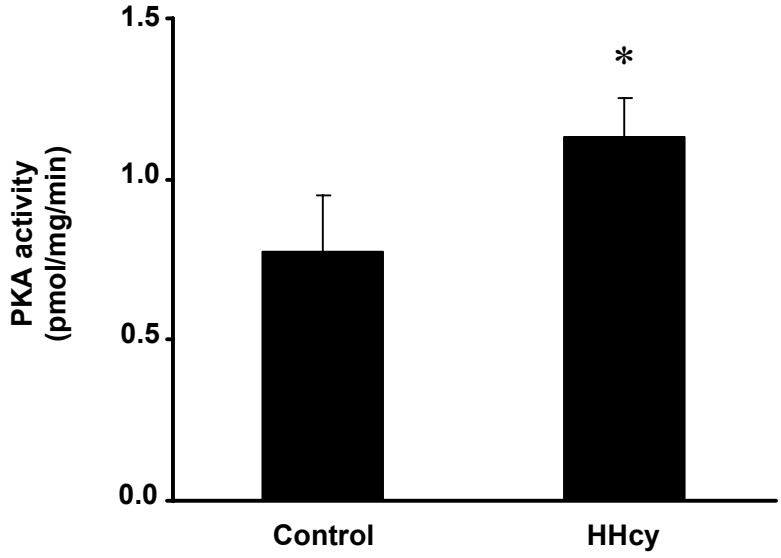

Figure 4.32 PKA activity in Livers

Livers were isolated from rats fed a regular diet (control) or a high-methionine diet (HHcy) for 4 weeks. PKA activity was determined using radiochemical assay. Results were expressed as mean ± SEM (n = 12). *P<0.05 when compared with the value obtained from the control group.

4.4.2 Mechanism of CREB Activation in HepG2 Cells

In section 4.3, an increase in CREB/DNA binding activity in rat hepatocytes treated with Hcy was observed. This result was consistent with the finding in HHcy rat livers. To examine whether such activation would take place in human cells, the experiments were carried out in human hepatocyte, HepG2 cells.

4.4.2.1 Increase in Phosphorylated CREB

HepG2 cells were treated with Hcy (20 - 100 μM) for 60 minutes. The phosphorylated CREB and total CREB expression was determined by Western immunoblot analysis. Hcy treatment induced CREB phosphorylation in a concentration-dependent manner (Figure 4.33). However, such a treatment did not cause a significant change in total CREB protein levels (Figure 4.33). These results were similar to the *in vivo* findings in HHcy rat livers. The induction of CREB phosphorylation was also observed in cells incubated with Hcy for 15 to 120 minutes (Figure 4.34).

4.4.2.2 Elevated CREB and DNA Binding Activity

Upon phosphorylation, there was a significant increase in CREB/DNA binding activity in Hcy-treated cells (Figure 4.35). These results suggested that Hcy was able to induce phosphorylation and subsequently activation of CREB in human hepatocytes. Hcy is a sulfhydryl (-SH) group-containing amino acid. To investigate whether the activation of CREB was mediated via the presence of the –SH group, another –SH group containing amino acid, cysteine was included in the experiments. Interestingly, cysteine treatment did not alter the total CREB protein levels but caused a significant increase in the phosphorylated CREB protein level in HepG2 cells (Figure 4.36). These results were

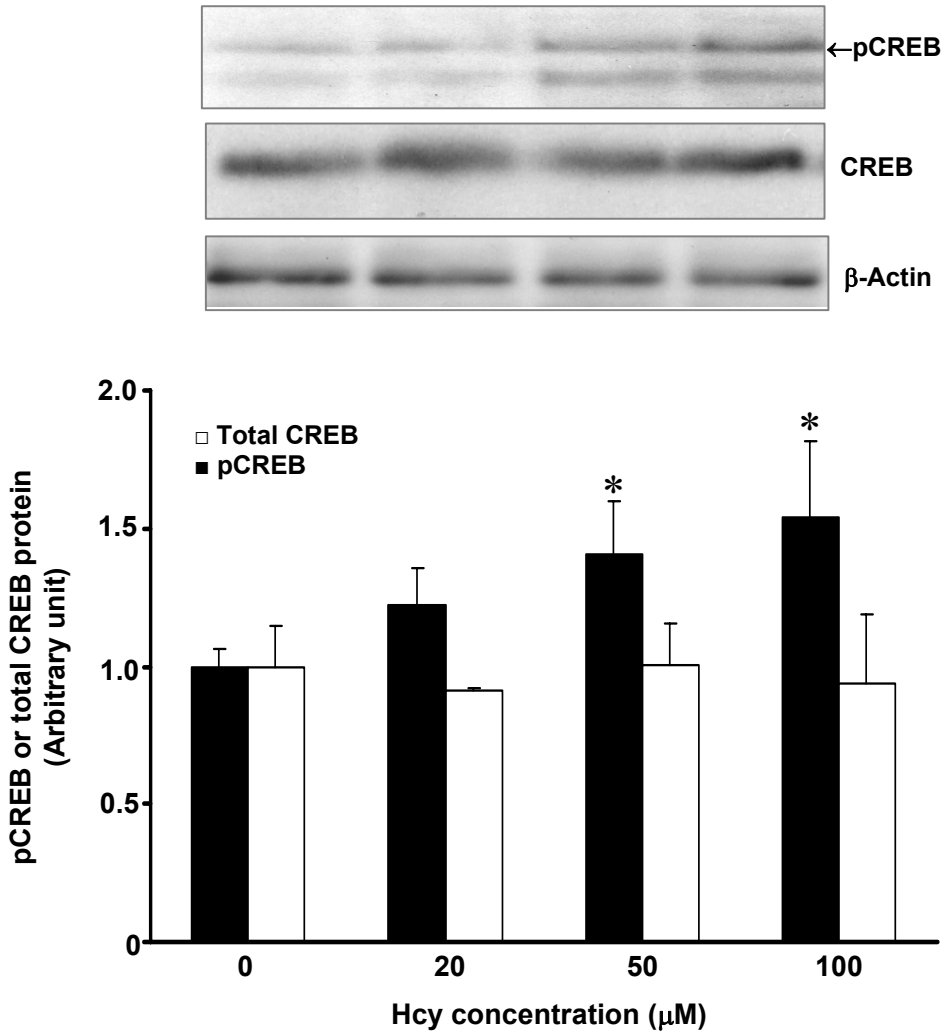

Figure 4.33 Phospho-CREB and Total CREB Protein Levels in HepG2 Cells

Cells were incubated with Hcy at various concentrations for 60 minutes. Western immunoblot analysis was performed to determine the cellular levels of phosphorylated CREB (pCREB) and total CREB proteins Results are expressed as mean ± SD (n=5, each performed in duplicate). *P<0.05 when compared with the value obtained from cells cultured in the absence of Hcy.

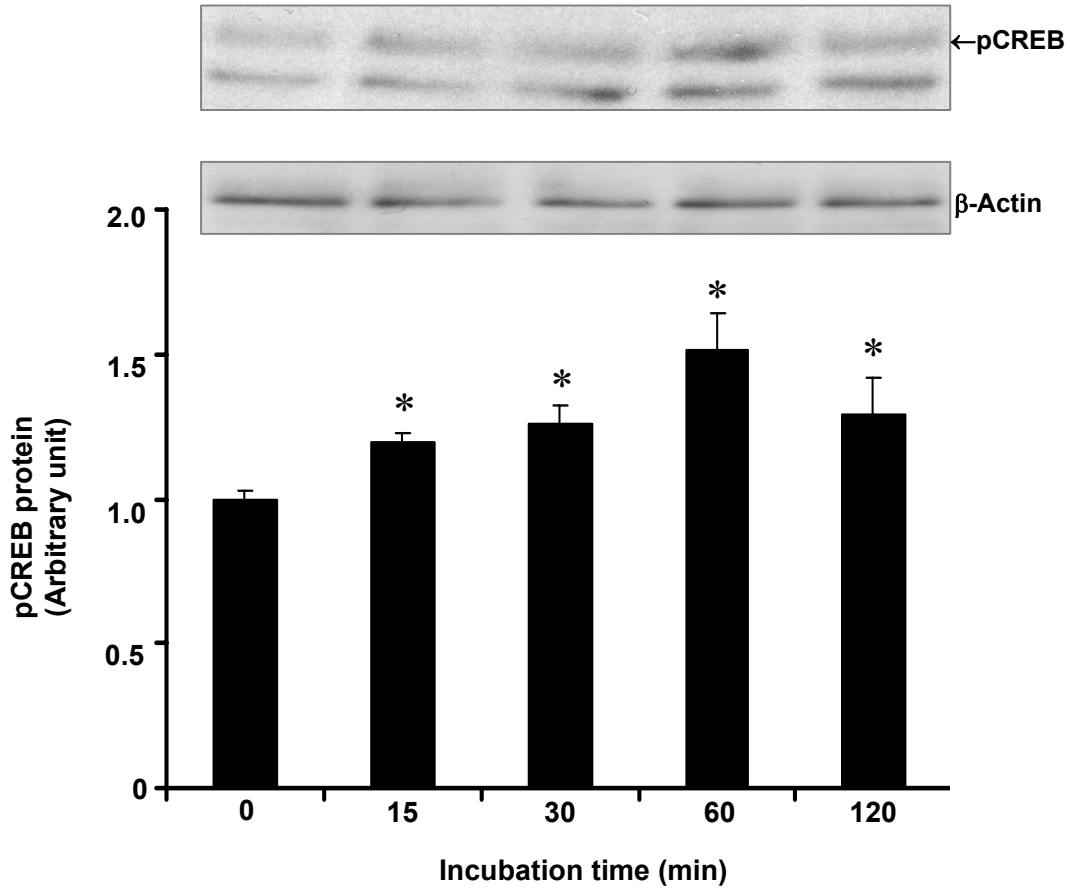

Figure 4.34 Phosphorylation of CREB in HepG2 Cells

Cells were incubated with Hcy (100 μM) for various time periods. Western immunoblot analysis was performed to measure the cellular levels of phosphorylated CREB. Results are expressed as mean ± SD (n = 5, each performed in duplicate). *P<0.05 when compared with the corresponding control values.

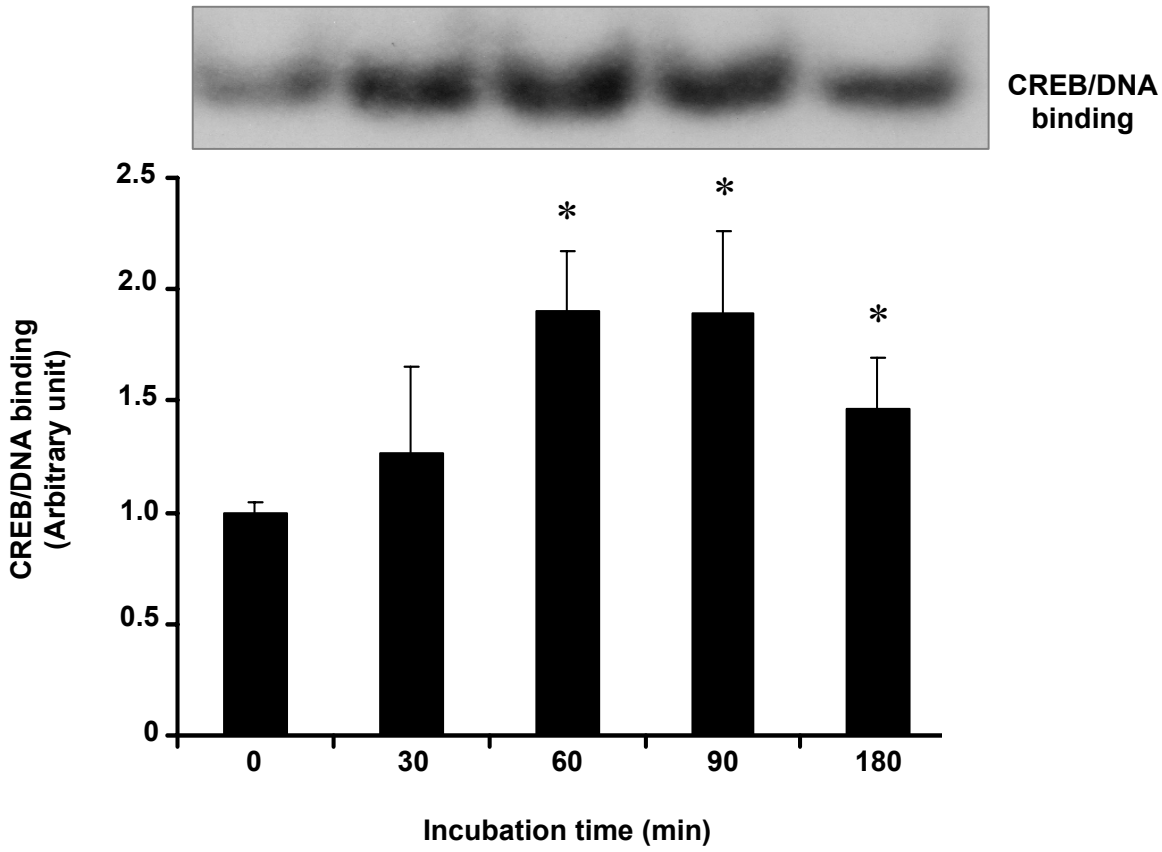

Figure 4.35 Activation of CREB in HepG2 Cells

Cells were incubated with Hcy (100 μM) for various time periods. EMSA was performed to determine the CREB/DNA binding activity. Results are expressed as mean ± SD. (n = 5, each performed in duplicate). *P<0.05 when compared with the corresponding control values.

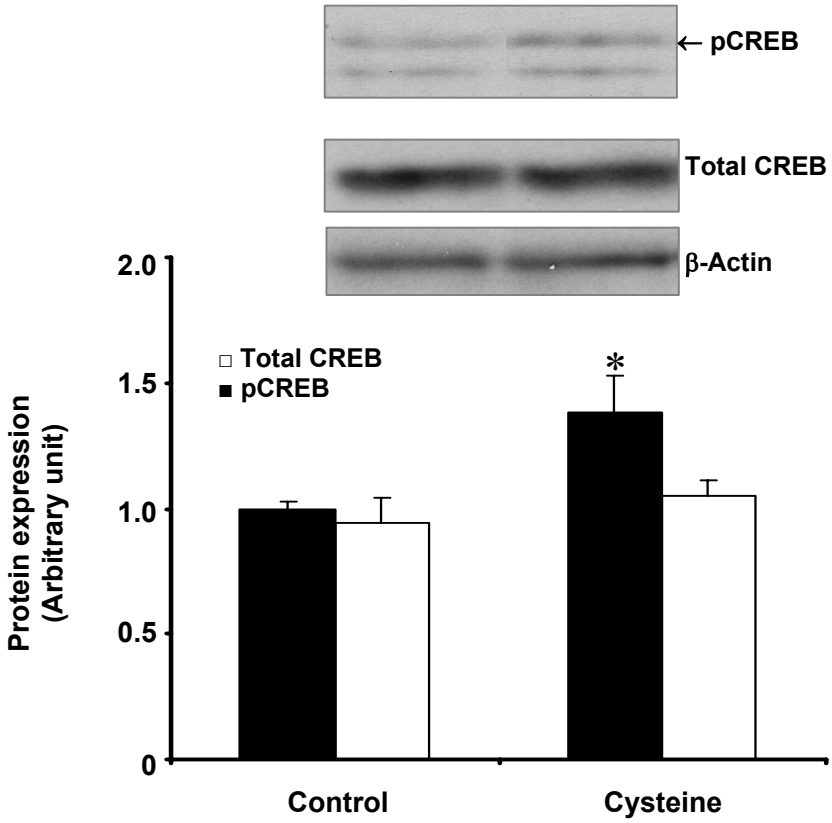

Figure 4.36 Effect of Cysteine on Phospho-CREB and Total CREB in HepG2 Cells

pCREB and total CREB proteins were determined in cells incubated with cysteine (100 μM) for 30 minutes and 60 minutes, respectively. Results are expressed as mean ± SD (n = 5, each performed in duplicate). *P<0.05 when compared with with the value obtained from cells cultured in the absence of cysteine.

similar to that observed in Hcy-treated HepG2 cells. However, cysteine treatment was unable to activate CREB binding to DNA (Figure 4.37). These results suggested that in addition to phosphorylation of CREB, another mechanism might be required to activate CREB.

4.4.2.3 A Role of PKA in Hcy-induced CREB Activation

To investigate whether the PKA signaling pathway was responsible for Hcy-induced CREB activation, a PKA inhibitor, H89 was added to cultured cells. Pretreatment of cells with H89 completely inhibited Hcy-induced CREB activation (Figure 4.38), indicating that PKA signaling pathway might mediate Hcy-induced CREB activation. Next, to investigate whether other protein kinases might also be involved in CREB activation, cells were pretreated with PD98059, an inhibitor for ERK-1/2 or SB203580, an inhibitor for p38 MAP kinase before incubation with Hcy. Pretreatment of cells with PD98059 or SB203580 could not prevent Hcy-induced CREB activation in these cells (Figure 4.38). These results suggested that ERK and p38 MAP kinase signaling pathways might not be involved in Hcy-induced CREB activation in hepatocytes.

4.4.2.4 Increased PKA Activity and cAMP Concentration

To further investigate the mechanism by which the PKA signaling pathway was involved in Hcy-induced CREB activation, the activity of PKA and cAMP levels were measured. There was a significant increase in PKA activity in cells incubated with Hcy (100 μM) for 30 minutes (Figure 4.39). Preincubation of cells with H89 completely abolished Hcy stimulated PKA activity (Figure 4.39). Cysteine treatment did not affect the PKA activity in HepG2 cells (Figure 4.39). PKA is cAMP-dependent protein kinase and its activation

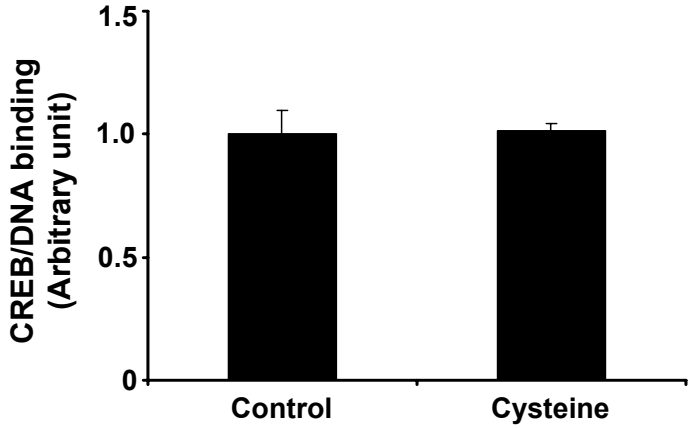

Figure 4.37 Effect of Cysteine on Activation of CREB in HepG2 Cells

CREB/DNA binding were determined in cells incubated with cysteine (100 μM) for 30 minutes and 60 minutes, respectively. Results are expressed as mean ± SD (n = 5, each performed in duplicate).

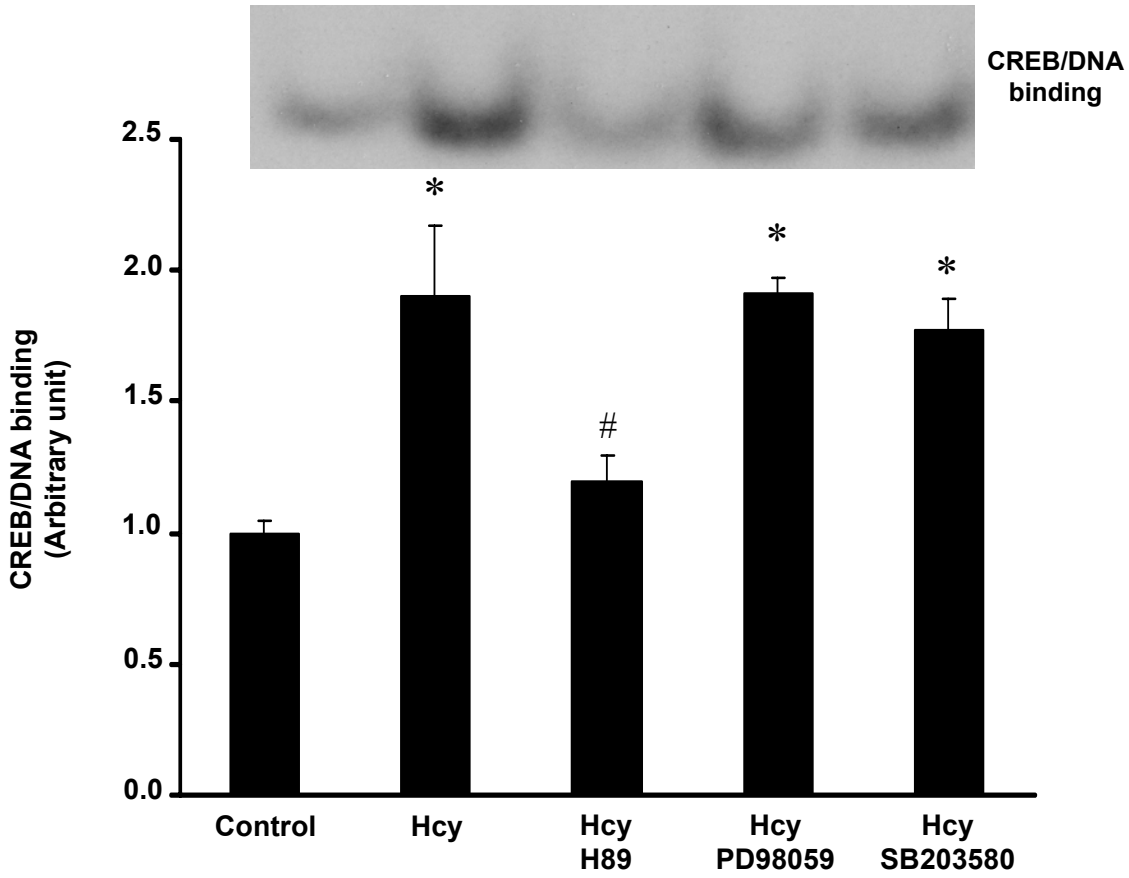

Figure 4.38 Effects of Kinase Inhibitors on CREB Activation in HepG2 Cells

Cells were pre-incubated with H89 (5 μM), PD98059 (10 μM) or SB203580 (10 μM) for 30 minutes followed by incubation with Hcy (100 μM) for another 60 minutes to determine the CREB/DNA binding activity. Cells cultured in the absence of inhibitors or Hcy were used as the control. Results are expressed as mean ± SD (n = 5, each performed in duplicate). *P<0.05 when compared with control values and #P<0.05 when compared with the value obtained from cells incubated with Hcy (100 μM) alone.

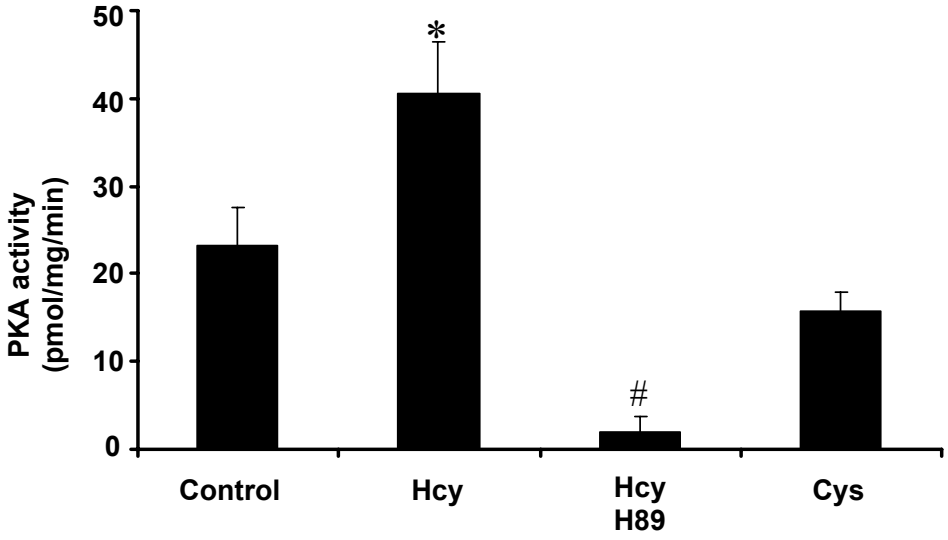

Figure 4.39 PKA Activity in HepG2 Cells

Cells were pre-incubated with H89 (5 μM) for 30 minutes followed by incubation in the absence (control) or presence of Hcy (100 μM) or with cysteine (100 μM) for another 60 minutes. At the end of incubation period, PKA activity was determined. Results were expressed as mean ± SD (n = 5, each performed in duplicate). *P<0.05 when compared with the control value.

depends on the elevation of intracellular cAMP levels. The levels of cAMP were measured in cells before and after Hcy treatment. The cellular levels of cAMP were markedly elevated after incubation with Hcy for 10 to 15 minutes (Figure 4.40).

4.4.2.5 Adenylyl Cyclase Inhibitor abolished Hcy-induced CREB Activation

The classical mechanism to elevate intracellular cAMP concentrations is mediated via the activation of adenylyl cyclase (Sutherland *et al.*, 1962). To further demonstrate the involvement of the cAMP/PKA signaling pathway in Hcy-induced CREB activation in hepatocytes, cells were preincubated with adenylyl cyclase toxin (ACT) (Calbiochem, San Diego, CA, USA), a specific inhibitor for adenylyl cyclase. Inhibition of adenylyl cyclase effectively reduced the cellular cAMP content to the basal levels (1343.05 ± 336.32 pmol/mg vs. 651.34 ± 265.59 pmol/mg) as well as inhibited Hcy-induced PKA activation (Figure 4.41 and Figure 4.42). Furthermore, inhibition of cAMP production by ACT completely abolished Hcy-induced phosphorylation of CREB in these cells (Figure 4.43). Taken together, these results suggested that Hcy-stimulated CREB activation was mediated via activation of adenylyl cyclase/PKA signaling pathway.

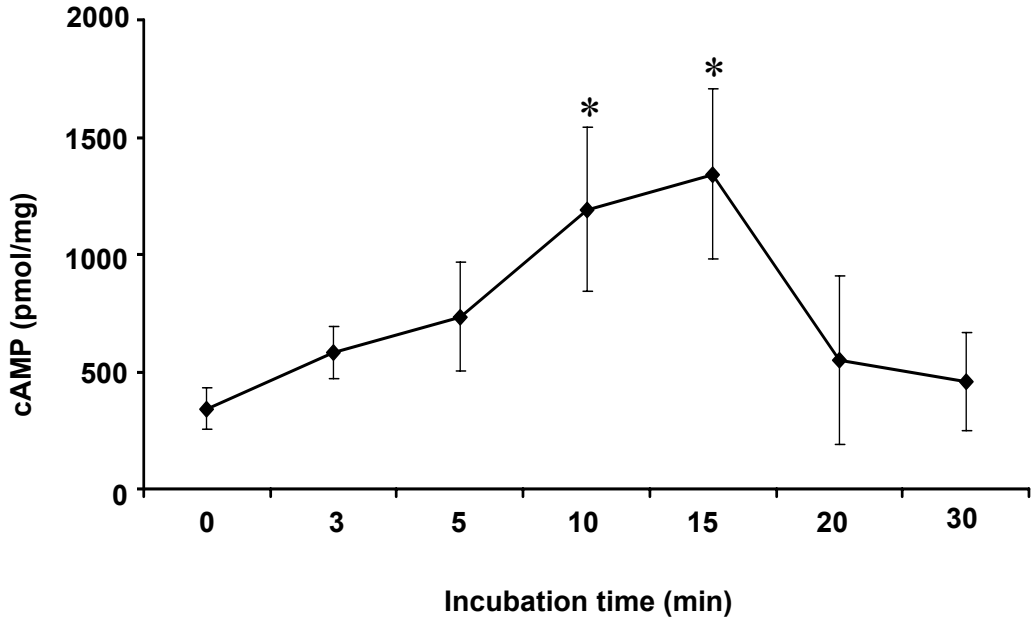

Figure 4.40 cAMP Content in HepG2 Cells

Cells were incubated with Hcy (100 μM) for various time periods. The levels of intracellular cAMP were measured. Results were expressed as mean ± SD (n = 5, each performed in duplicate). *P<0.05 when compared with the control value.

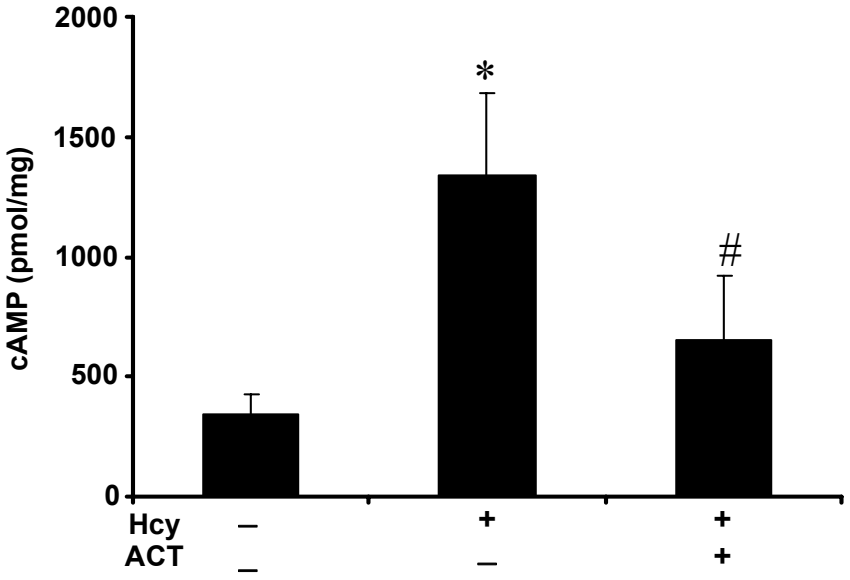

Figure 4.41 Effect of Adenylyl Cyclase Inhibitor on Hcy-increased cAMP levels

Cells were pre-incubated with adenylyl cyclase toxin (100 μM, ACT) for 30 minutes followed by incubation with Hcy (100 μM). After 15 minutes of incubation with Hcy, the intracellular cAMP level was measured. Results were expressed as mean ± SD (n = 5, each performed in duplicate). *P<0.05 when compared with the control value and #P<0.05 compared with the value obtained from Hcy-treated (100 μM) group.

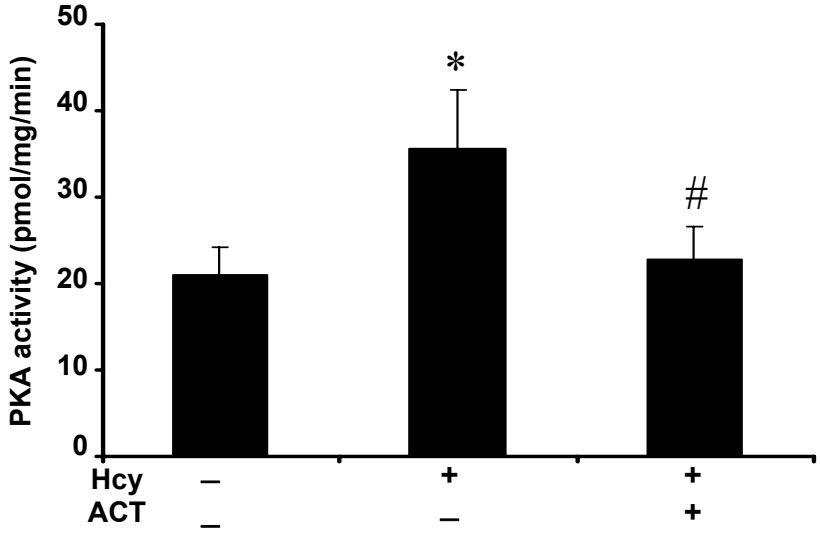

Figure 4.42 Effect of Adenylyl Cyclase Inhibitor on Hcy-induced PKA Activity

Cells were pre-incubated with adenylyl cyclase toxin (100 μM, ACT) for 30 minutes followed by incubation with Hcy (100 μM). PKA activity was determined after 30 minutes incubation of Hcy. Results were expressed as mean ± SD (n = 5, each performed in duplicate). *P<0.05 when compared with the control value and #P<0.05 compared with the value obtained from Hcy-treated (100 μM) group.

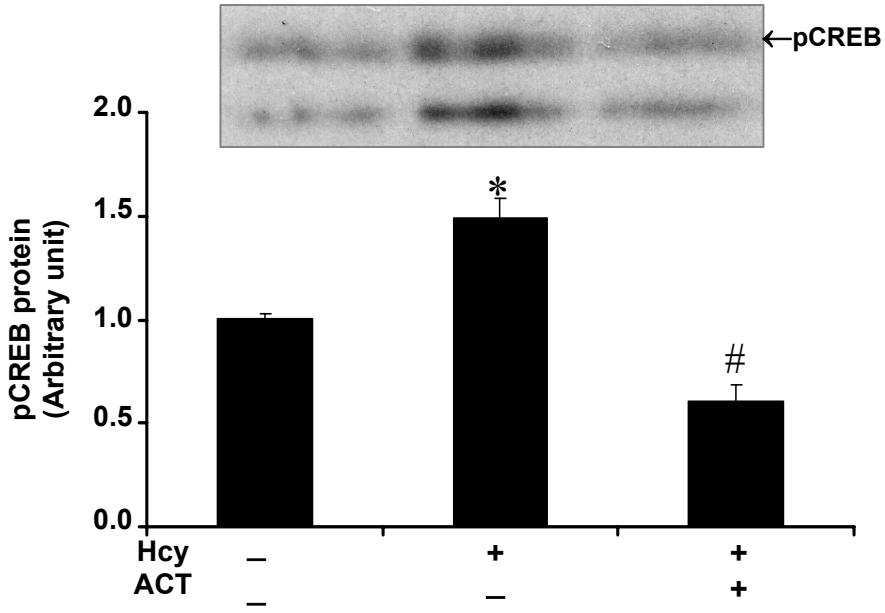

Figure 4.43 Effect of Adenylyl Cyclase Inhibitor on Hcy-induced pCREB Expression

Cells were pre-incubated with adenylyl cyclase toxin (100 μM, ACT) for 30 minutes followed by incubation with Hcy (100 μM). After 60 minutes of incubation, the levels of phosphorylated CREB were measured using Western immunoblot analysis. Cells cultured in the absence of inhibitor and Hcy were used as a control group. Results were expressed as mean ± SD (n = 5, each performed in duplicate). *P<0.05 when compared with the control value and #P<0.05 compared with the value obtained from Hcy-treated (100 μM) group.

4.4.3 Role of cAMP/PKA Pathway in HMG-CoA Reductase Expression

The results from previous section showed that Hcy was able to activate CREB via adenylyl cyclase/PKA pathway in human hepatocytes. In the section 4.3.2, it was shown that Hcy increased CREB activation leading to HMG-CoA reductase mRNA expression in rat hepatocytes. In the following section, the role of CREB activation in HMG-CoA reductase expression in human hepatocytes was examined.

4.4.3.1 Activation of cAMP/PKA Pathway in HMG-CoA Reductase Expression

CREB is one of the important transcriptional factors for lipid metabolism (Dooley *et al.*, 1999; Klemm *et al.*, 1998; Ngo *et al.*, 2002; Woo *et al.*, 2005). The activity of HMG-CoA reductase was increased in Hcy-treated HepG2 cells (Figure 4.44). Inhibition of adenylyl cyclase activity by ACT or inhibition of PKA activation by H89 completely abolished Hcy-induced HMG-CoA reductase activation (Figure 4.44) and reduced the reductase protein expression to the control level (Figure 4.45). These results suggested the importance of cAMP/PKA pathway in cholesterol biosynthesis.

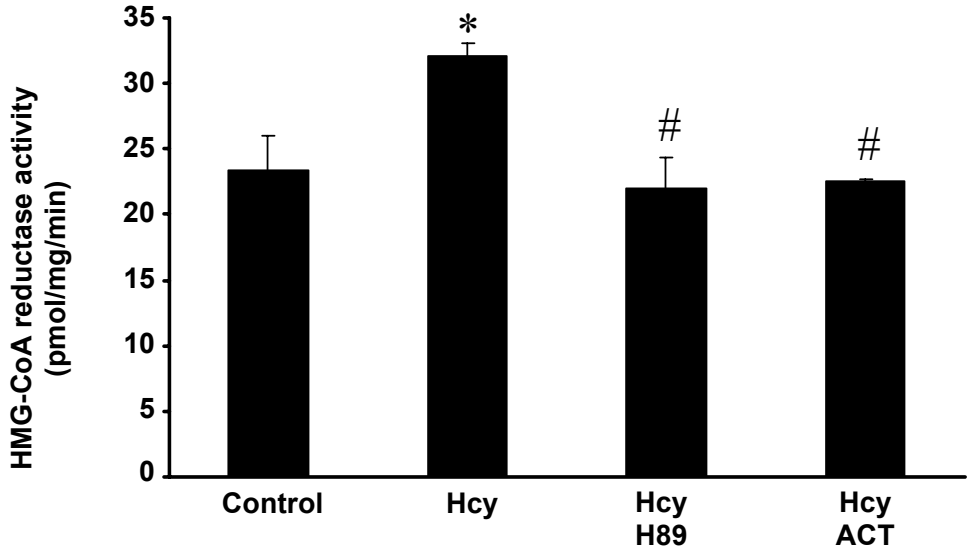

Figure 4.44 HMG-CoA Reductase Activity in HepG2 Cells

HepG2 cells were pre-incubated with or without H89 (5 μM) or ACT (100 μM) for 30 minutes followed by incubation with Hcy (100 μM) for 4 hours. HMG-CoA reductase activity was determined. Results were expressed as mean ± SD (n = 5, each performed in duplicate). *P<0.05 when compared with the control value and #P<0.05 compared with the value obtained from Hcy (100 μM) treated cells.

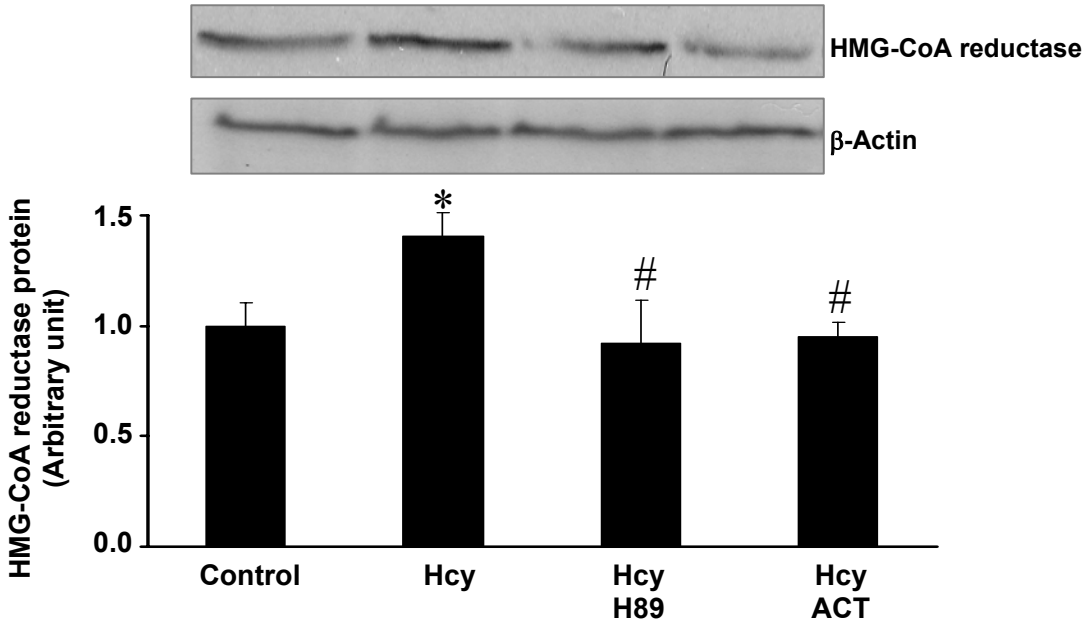

Figure 4.45 HMG-CoA Reductase Protein in HepG2 Cells

HepG2 cells were pre-incubated with or without H89 (5 μM) or ACT (100 μM) for 30 minutes followed by incubation with Hcy (100 μM) for 4 hours. HMG-CoA reductase protein levels were determined. Results were expressed as mean ± SD (n = 5, each performed in duplicate). *P<0.05 when compared with the control value and #P<0.05 compared with the value obtained from Hcy (100 μM) treated cells.

4.4.4 Activation of Protein kinase A in the Liver during HHcy

CREB plays an important role in regulating transcription of many genes that are involved in cell proliferation, neuronal sypnastic plasticity and hepatic lipid metabolism (Dalle *et al.*, 2004; Dooley *et al.*, 1999; Klemm *et al.*, 1998; Montminy *et al.*, 2004; Ngo *et al.*, 2002; Rosenberg *et al.*, 2002). In the present study, activation of CREB along with other transcription factors in hepatocytes was found to contribute to increased gene expression of HMG-CoA reductase and cholesterol biosynthesis in the liver of HHcy rat (Woo *et al.*, 2005). The present results showed that the activation of CREB was involved in Hcy-induced HMG-CoA reductase expression in human hepatocytes, HepG2. These results suggest that CREB plays an important role in cholesterol biosynthesis during HHcy.

CREB requires phosphorylation at its Ser-133 to enhance the transcription of target genes that contain cAMP response element (CRE) in the promoter region (Mayr & Montminy, 2001; Shaywitz & Greenberg, 1999). Several protein kinases are known to phosphorylate CREB such as PKA, ERK-1/2, and p38 MAP kinase (Shaywitz & Greenberg, 1999). The type of protein kinases that phosphorylate as well as activate CREB depends on the type of stimuli and the type of cells (Johannessen *et al.*, 2004). For example, glutamate can phosphorylate CREB in cultured neuron via activation of calmodulin kinases (Mabuchi *et al.*, 2001). Phenylepherine stimulates phosphorylation and activation of CREB via several kinases including PKA, p38 MAP kinase and ERK-1/2 (Markou *et al.*, 2004).

The PKA signaling pathway is thought to play a major role in CREB activation in many types of cells. Activation of PKA is regulated by changes in the intracellular cAMP levels

(Gonzalez & Montminy, 1989; Walsh *et al.*, 1968). An elevation of intracellular cAMP levels can be caused by increased activity of adenylyl cyclase and/or decreased activity of phosphodiesterases (Francis & Kono, 1982; Sutherland *et al.*, 1962). In the present study, several lines of evidence support the notion that the activation of adenylyl cyclase and cAMP/PKA signaling pathway play a major role in Hcy-induced activation of CREB in hepatocytes. First, Hcy treatment caused a significant elevation in the intracellular cAMP levels, which proceeded to the activation of PKA. Second, treatment of cells with an adenylyl cyclase inhibitor completely prevented Hcy-induced elevation of cellular cAMP levels and PKA activation. Inhibition of the cAMP/PKA signaling pathway also abolished Hcy-induced CREB phosphorylation. Third, inhibition of other protein kinase activities such as ERK or p38 MAP kinase could not block Hcy-induced CREB activation. Furthermore, a significant increase in hepatic cAMP levels, PKA activity and CREB activation were found in rats during HHcy. Taken together, these results suggested that Hcy-induced elevation of cellular cAMP levels activated PKA that, in turn, phosphorylated and subsequently activated CREB. Hcy is a sulfhydryl-containing amino acid and some of its pathological effects may be mediated via a sulfhydryl-dependent mechanism (Lentz & Sadler, 1991; Lentz & Sadler, 1993). In the present study, treatment of HepG2 cells with another sulfhydryl containing amino acid (cysteine) failed to activate PKA as well as CREB. These results suggested that Hcy-induced CREB activation via PKA signaling pathway may be mediated through a sulfhydryl-independent process.

4.4.5 Involvement of cAMP in Hcy-induced HMG-CoA Reductase Expression

Cyclic AMP (cAMP) is an important second messenger that involves a wide range of cellular processes and gene regulations. Studies have shown a consistently elevated basal cAMP level in the liver during diabetes (Jefferson *et al.*, 1968; Pilkis *et al.*, 1974). The cAMP/CREB signaling pathway regulates the expression of key genes in glucose metabolism as well as in lipid metabolism (Dooley *et al.*, 1999; Klemm *et al.*, 1998; Ngo *et al.*, 2002; Pilkis *et al.*, 1974). The present study demonstrated that the levels of cAMP were significantly elevated in the livers of HHcy rats as well as in Hcy-treated HepG2. Alterations in hepatic lipid metabolism have been observed to be associated with HHcy in several studies (Namekata *et al.*, 2004; Werstuck *et al.*, 2001). It is plausible that an alteration of intracellular cAMP levels may serve as one of the important mechanisms by which Hcy impairs lipid metabolism in the liver. The results from the present study showed that HMG-CoA reductase activity was elevated in the livers of HHcy rats as well as in Hcy-treated HepG2 cells. Inhibition of adenylyl cyclase or PKA activity completely abolished Hcy-induced HMG-CoA reductase activation. These results suggest a direct link between Hcy-induced cAMP/PKA signaling and lipid metabolism via the stimulation of HMG-CoA reductase expression. cAMP is a second messenger not only involved in lipid metabolism but also in diverse physiological processes. The ability of Hcy to affect cAMP levels may have implications for other Hcy-associated diseases.

CREB is a transcription factor that is involved in lipid and glucose metabolism. A study suggested that activation of CREB might contribute to insulin resistance in individuals susceptible to diabetes (Herzig *et al.*, 2003). An elevation of basal hepatic cAMP levels was observed in diabetic individuals (Jefferson *et al.*, 1968; Pilkis *et al.*, 1974). The observation that Hcy can induce hepatic CREB activation may provide evidence for a possible role of Hcy in glucose metabolism. It is tempting to speculate that Hcy may play a role in metabolic syndrome. However, extensive studies are required to test such a hypothesis.

4.5 Protective Effect of Folic Acid in Hyperhomocysteinemia

Objective

Folic acid supplementation has been shown to successfully decrease serum or plasma Hcy levels in individuals with HHcy (Doshi *et al.*, 2001; Woo *et al.*, 1999). It has been shown that folic acid exerts the beneficial effects on cardiovascular diseases both dependent and independent of Hcy-reduction (Doshi *et al.*, 2001; Doshi *et al.*, 2002). Other studies have shown that folate depletion contributes to alcoholic liver injury (Esfandiari *et al.*, 2005; Halsted *et al.*, 2002). However, limited studies have been done to examine the protective effect of folic acid supplementation in liver diseases. To investigate whether folic acid was able to reverse the effect of Hcy on hepatic abnormalities, a group of rats fed a high-methionine and folic acid enriched diet was included in the present study (see Method section 3.2). The **fifth objective** of the present study was to investigate the protective role of folic acid supplementation in Hcy-induced oxidative stress and liver injury.

Results

4.5.1 Protective Effect of Folic Acid against HHcy-induced Liver Injury

As shown in Table 4.9, supplementation of folic acid (0.025% w/w) in the diet did not affect the body weight of the HHcy rats. Addition of folic acid in the diet significantly decreased the serum and liver Hcy levels in HHcy rats. However, the Hcy levels were still significantly higher than that of the control (Table 4.9). HHcy rats fed with 0.025% folic acid demonstrated a 3 fold increase in serum folate levels compared to the control

Table 4.9 Folic Acid and Hcy Levels in Serum and Livers

	Control	HHcy	HHcy+Folic acid
Body weight (g)	458.46±7.09	433.26±8.62	443.33±11.22
Serum			
Hcy (μM)	3.52±0.34	25.48±3.01*	18.66±1.39*#
Folate (ng/mL)	89.43±7.13	89.70±7.58	255.94±24.94*#
Liver			
Hcy (μM)	3.74±0.21	12.23±0.97*	7.69±0.94*#

Rats were fed with following diets for 4 weeks: a regular diet (Control), a high methionine diet (HHcy), or a high methionine plus folic acid diet (HHcy+Folic acid). Folate levels were measured in the serum and Hcy levels were measured in serum and livers. Results were expressed as mean ± SEM (n = 12). *P < 0.05 compared with control values. #P < 0.05 compared with values of high-methionine treated group.

group and the HHcy group (Table 4.9). In section 4.2, the results demonstrated that HHcy caused liver injury by inducing oxidative stress. Hcy-induced oxidative stress was due to both an elevation of reactive oxygen species and an impairment of enzymatic antioxidant defences in the HHcy rat liver. To investigate whether folic acid was able to protect the HHcy rat against liver injury, the serum activities of AST and ALT were measured. As shown in Table 4.10, the serum AST and ALT activities in the HHcy plus folic acid group were lower than that of the HHcy rats. However, HHcy-induced lipid peroxidation was prevented by the administration of folic acid (Table 4.10). These results indicated that folic acid supplementation was able to ameliorate HHcy-induced oxidative stress and liver injury.

4.5.2.1 Folic acid Decreased Oxidative Burden

The effect of folic acid on Hcy-induced oxidative burden was examined. The superoxide anion content and NADPH oxidase activity in the livers were elevated in HHcy rats (Table 4.10). As shown in Table 4.10, addition of folic acid to the diet decreased the hepatic superoxide anion content in HHcy rats. Folic acid supplementation significantly prevented HHcy-increased NAPDH oxidase activity in the livers. The staining of nitrotyrosine protein adducts in the livers of HHcy plus folic acid group was much less intense than that of the HHcy group (Figure 4.46). Although the hepatic nitric oxide concentration and nitric oxide synthase in the HHcy plus folic acid group was slightly lower than that of the control, the difference was not statistically significant (Table 4.10). These results suggested that folic acid was able to prevent the increased oxidative burden in the livers of HHcy rats mainly through an inhibition of NADPH oxidase-mediated superoxide anion production.

Table 4.10 Parameters of Liver Injury and Oxidative Stress in Livers

	Control	HHcy	HHcy +Folic acid
Serum			
AST (IU/L)	26.62±3.82	42.89±7.60*	34.07±4.47
ALT (IU/L)	36.28±6.06	60.62±9.54*	38.19±5.84#
Liver			
Lipid peroxides/MDA (nmol/g)	298.94±33.53	403.42±33.89*	307.68±42.26#
O_2^- content (% of control)	100.00±4.78	131.61±14.93*	111.03±18.13
NADPH oxidase (μmol/mg/min)	303.83±23.09	398.87±30.09*	279.59±21.20#
NO metabolites (nmol/g)	393.88±29.18	381.79±22.18	372.66±31.37
NOS activity (pmol/mg/min)	4.44±0.66	4.71±0.66	4.04±0.46

Rats were fed with following diets for 4 weeks: a regular diet (Control), a high methionine diet, or a high methionine plus folic acid diet. Hcy and folate levels were measured in serum as well as AST and ALT activities. Lipid peroxides (TBARS) in livers was determined by measuring the amount of MDA. Superoxide anion content, NADPH oxidase activity, nitric oxide metabolites and nitric oxide synthase activity were determined in livers as well Results were expressed as mean ± SEM (n = 12). *$P < 0.05$ compared with control values. #$P < 0.05$ compared with values of high-methionine treated group.

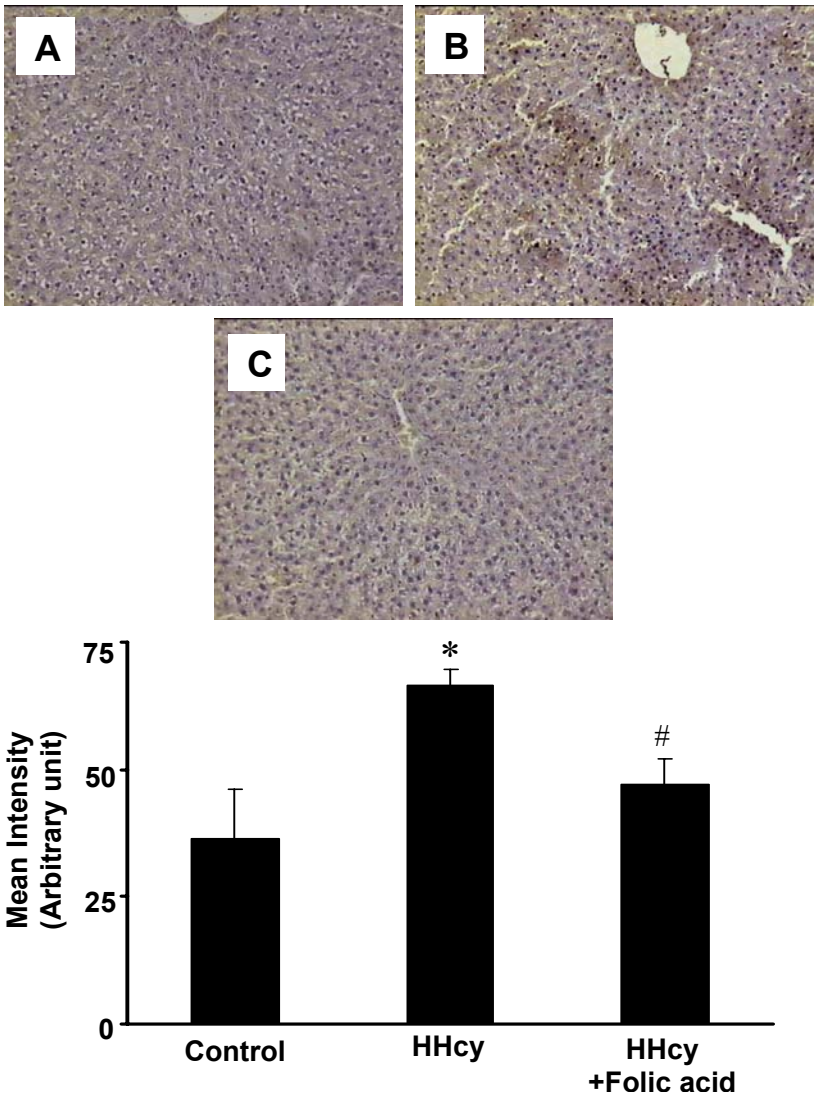

Figure 4.46 Immunohistochemical Staining of Nitrotyrosine in Livers

Livers were fixed in 10% neutral-buffered formalin overnight and then embedded in paraffin. Immunohistochemical staining for nitrotyrosine protein adducts was performed with anti-nitrotyrosine antibodies. After counterstaining with Harris hematoxylin, nitrotyrosine was identified under light microscope with a magnification of 200×. Representative photos were obtained from rats fed (A) a regular diet, (B) high-methionine diet (HHcy), (C) high-methionine plus folic acid diet. Staining analyses were performed in livers isolated from 8 rats per treatment group, and 4 sections were prepared fro each liver. Representative images are shown. *$P < 0.05$ compared with control values, where #$P < 0.05$ compared with values of high-methionine treated group (HHcy).

4.5.2.2 Effect of Folic acid on Hepatic Antioxidant Defence Mechanisms

To investigate whether folic acid could also strengthen the antioxidant defence in HHcy rat livers, the activities of antioxidant enzymes were measured. As shown in Table 4.11, folic acid was able to partially restore the catalase activity in HHcy rat livers. Hepatic superoxide dismutase (SOD) was significantly decreased in HHcy rat livers whereas no change was observed in glutathione peroxidase (Table 4.11). Folic acid supplementation did not affect hepatic activities of SOD and glutathione peroxidase in HHcy rats (Table 4.11).

Glutathione is the most important non-enzymatic antioxidant in the liver. The reduced glutathione (GSH) content in HHcy rat livers remained unchanged whereas the oxidized glutathione (GSSG) content was significantly elevated (Table 4.12). Folic acid supplementation could prevent the elevation of GSSG concentrations in HHcy rat livers (Table 4.12). However, this treatment did not affect total GSH concentration and glutathione reductase activity in HHcy rat livers (Table 4.12). The decreased hepatic GSSG concentration might be due to an overall lower oxidative burden in HHcy rats supplemented with folic acid (Table 4.10). Taken together, these results suggested that folic acid exerts a protective effect on certain antioxidant enzymes such as catalase.

Table 4.11 Effect of Folic Acid on Enzymatic Antioxidants in Livers

	Control	HHcy	HHcy +Folic acid
SOD (U/mg)	200.27±18.10	148.20±21.54*	139.41±17.36*
Catalase(U/mg)	447.08±13.19	351.20±10.46*	395.69±21.41*#
Glutathione Peroxidase(U/g)	309.47±14.80	316.15±35.37	273.63±34.73

Rats were fed the following diets for 4 weeks: a regular diet (Control), a high methionine diet (HHcy), or a high methionine plus folic acid diet (HHcy+Folic acid). Superoxide dismutase (SOD), catalase, and glutathione peroxidase activities were determined in the livers; results were expressed as per mg or g of protein. Results were expressed as mean ± SEM (n = 12). *P < 0.05 compared with control values. #P < 0.05 compared with values of high-methionine treated group (HHcy).

Table 4.12 Effect of Folic Acid on Non-Enzymatic Antioxidants in Livers

	Control	HHcy	HHcy +Folic acid
GSH (μmol/g wet wt)	8.06±0.21	8.41±0.16	8.27±0.16
GSSG (nmol/g wet wt)	21.29±2.23	98.62±30.06*	18.10±7.39#
GSSG:GSH(×100)	0.273±0.025	0.857±0.358*	0.214±0.080
Glutathione reductase (U/mg)	42.78±1.68	37.76±1.88*	35.24±3.36*

Rats were fed with following diets for 4 weeks: a regular diet (Control), a high methionine diet (HHcy), or a high methionine plus folic acid diet (HHcy+Folic acid). The hepatic levels of reduced (GSH) and oxidized forms (GSSG) of glutathione were measured and expressed as per g of wet weight of liver. Results were expressed as mean ± SEM. (n = 12). *P < 0.05 compared with control values. #P < 0.05 compared with values of high-methionine treated group.

4.4.5.3 Threshold Effect of Hcy on Hepatic Oxidative Stress

In the previous sections, the results showed that folic acid supplementation was able to decrease hepatic oxidative stress induced by HHcy. However, the serum and liver Hcy concentrations of HHcy plus folic acid group were significantly higher than that of the control. The addition of folic acid in the diet decreased the serum Hcy concentration to 18.66 μM in HHcy rats (Table 4.9). It was speculated that decreasing serum or liver Hcy concentration to a threshold level might prevent the adverse effects caused by HHcy.

In order to test such a hypothesis, the correlation of serum Hcy levels and oxidative stress in livers was examined. There was a significant correlation between the serum Hcy levels and the hepatic superoxide anion levels (Figure 4.47). The correlation coefficient was higher in samples with serum Hcy concentrations higher than 19 μM, which indicated a better prediction of hepatic superoxide anion content from serum Hcy levels above 19 μM (Figure 4.48). When the samples with serum Hcy concentrations less than 19 μM were subjected to the same analysis, no significant correlation was observed (Figure 4.49). These results suggested that decreasing the serum Hcy level below 19 μM might be sufficient to prevent the Hcy-induced oxidative stress in liver.

Different degrees of HHcy were induced in rats by adding different amounts of methionine (0.8% and 1.7% methionine) to the diet. In rats fed a 1.7% methionine diet, the serum Hcy level was increased to 25.48 μM (Figure 4.50). A significant elevation in serum Hcy levels was also achieved in rats fed a 0.8% methionine diet (7.47 μM vs. 3.52 μM in the control group) (Figure 4.50). The level of lipid peroxidation in the liver of rats

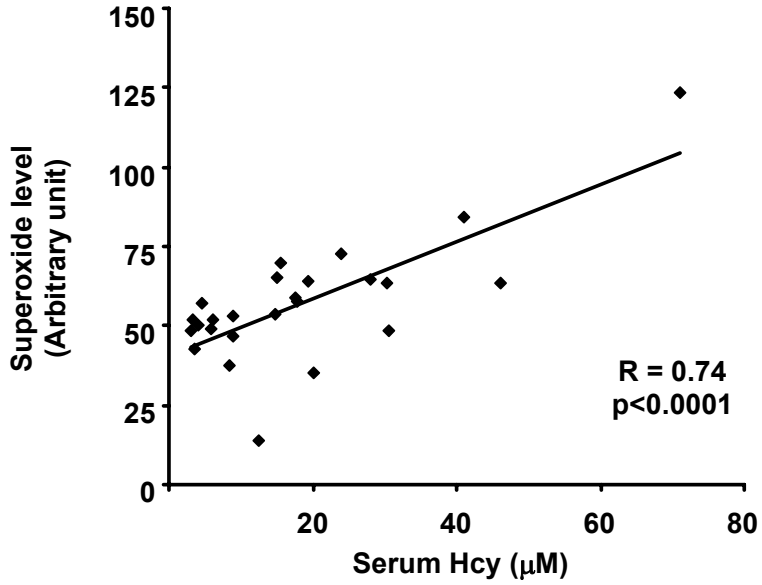

Figure 4.47 Correlation of Hcy Levels and Superoxide Anion Content

Pearson's correlation between serum Hcy levels and hepatic superoxide anion content in all experimental rats were analyzed. R values and p values were calculated.

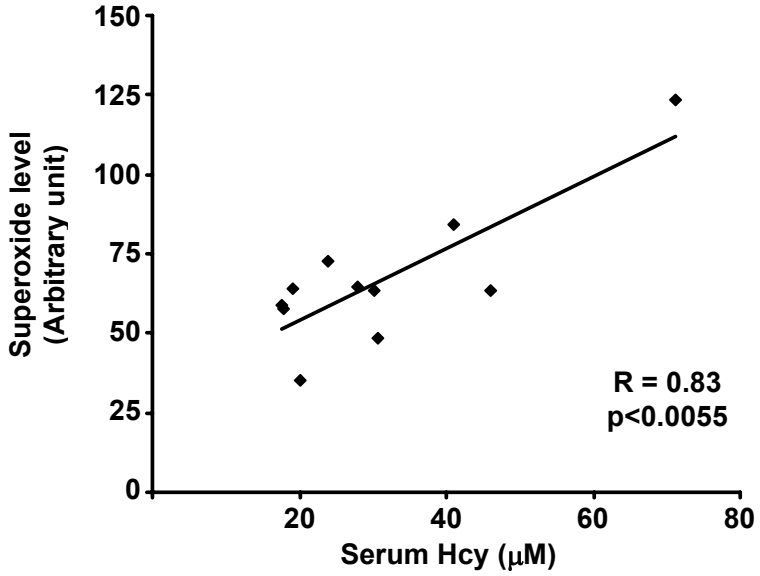

Figure 4.48 Correlation of Hcy Levels Above 19 μM and Superoxide Anion Content

Pearson's correlation between serum Hcy levels and hepatic superoxide anion content in rats with serum Hcy above 19 μM were analyzed. R values and p values were calculated.

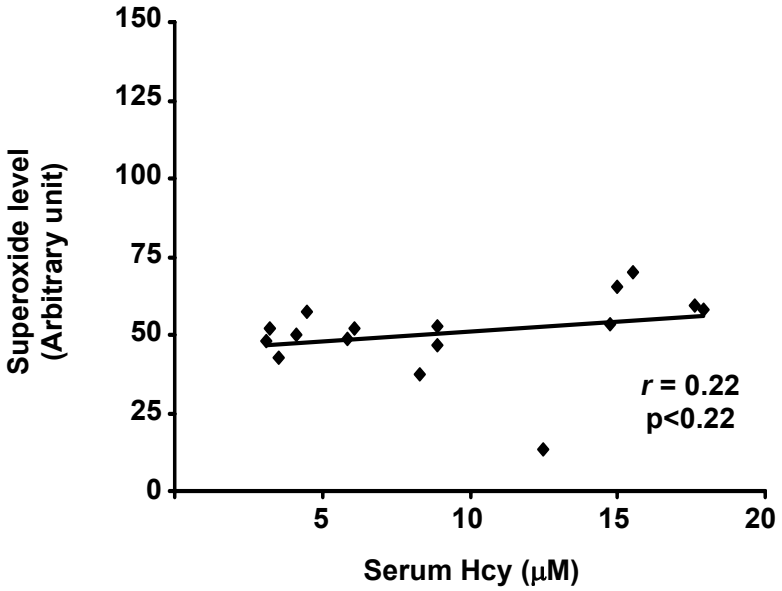

Figure 4.49 Correlation of Hcy Levels Below 19 μM and Superoxide Anion Content

Pearson's correlation between serum Hcy levels and hepatic superoxide anion content in rats with serum Hcy below 19 μM were analyzed. R values and p values were calculated.

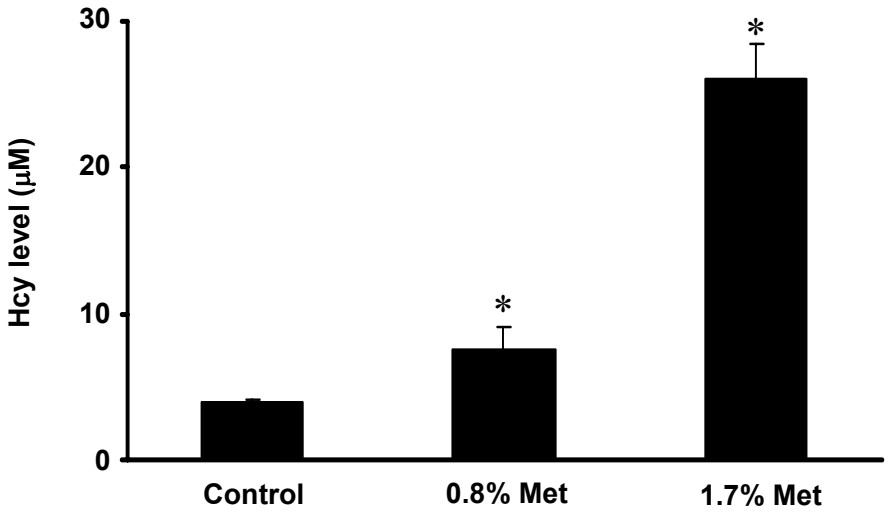

Figure 4.50 Serum Levels of Hcy in Rats Fed Different Amounts of Methionine

Rats were fed with following diets for 4 weeks: a regular diet (Control), a 0.8% methionine diet (0.8% Met), and a 1.7% methionine diet (1.7% Met) (n = 4 for each group). Serum Hcy levels were determined. Results were expressed as mean ± SEM. *P < 0.05 compared with control values.

with different degrees of HHcy was examined. As shown in Figure 4.51, there was a significant elevation of lipid peroxidation in 1.7% methionine diet group. However, the lipid peroxidation in the livers of 0.8% methionine-fed rats was similar to that found in the control group (Figure 4.51). These results suggested that mild HHcy was unable to induce oxidative stress in livers.

4.5.3 Folic Acid Supplementation Prevents Hepatic Cholesterol Accumulation

In section 4.3, the results demonstrated that cholesterol content was elevated in the liver of HHcy rats. In HHcy rats supplemented with high folic acid, the serum and liver Hcy levels were significantly decreased compared to that of the HHcy rats. The lipid content in the livers was extracted and measured for cholesterol and triacylglycerol. The total cholesterol levels in the liver of HHcy plus folic acid group were significantly lower than that of the HHcy rats (Table 4.13). There was a significant decrease in hepatic triacylglycerol levels in the HHcy plus folic acid group as well (Table 4.13). These results suggested that the increased cholesterol content in the liver of HHcy rats was correctable by folic acid supplementation. Folic acid supplementation protected the liver from excess lipid accumulation during HHcy.

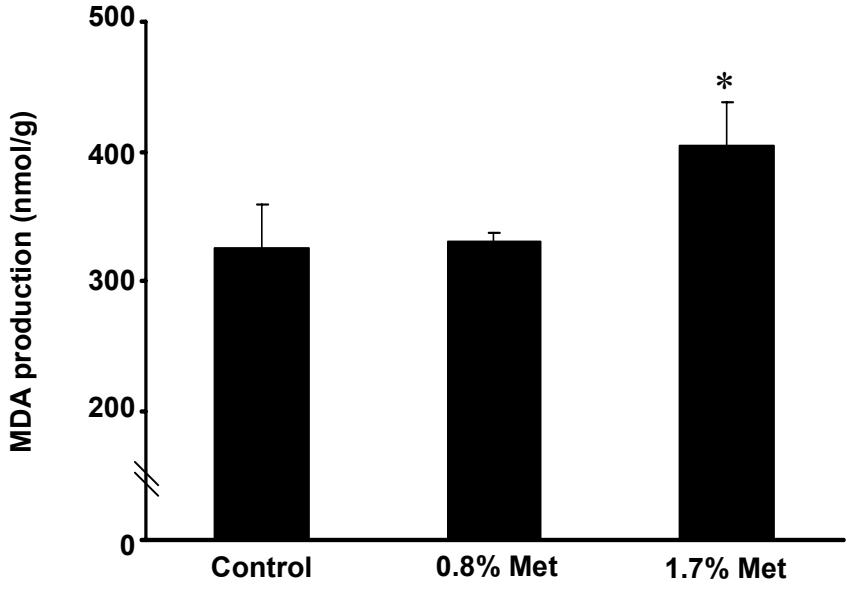

Figure 4.51 Lipid Peroxidation in Livers

Rats were fed with following diets for 4 weeks: a regular diet (Control), a 0.8% methionine diet (0.8% Met), and a 1.7% methionine diet (1.7% Met) (n = 4 for each group). Lipid peroxides (TBARS) in livers were determined by measuring the amount of MDA in the liver tissue. Results were expressed as mean ± SEM. *P < 0.05 compared with control values.

Table 4.13 Lipid parameters in Livers

	Control	HHcy	HHcy +Folic acid
Liver (per g of wet weight)			
Total cholesterol (mg/g)	1.75±0.06	2.29±0.15*	1.69±0.18#
Free cholesterol (mg/g)	1.62±0.09	2.04±0.16*	1.39±0.12#
Cholesteryl ester (mg/g)	0.17±0.13	0.27±0.06*	0.22±0.05
Triacylglycerol (mg/g)	8.13±0.61	8.85±1.00	7.06±0.63#

Values are means ± SEM. Rats were divided into 3 groups (n = 12 for each group) fed with different diet: regular, high-methionine (HHcy) or high-methionine plus folic acid (HHcy+Folic acid). *$P < 0.05$ compared with control values and #$P < 0.05$ compared with the high-methionine group.

4.5.4 Protective Effect of Folic Acid against Liver Injury

Folic acid supplementation is viewed as a promising treatment for patients with cardiovascular disease associated with HHcy. Oral folic acid supplementation has been shown to improve endothelium-dependent vascular function in patients with mild HHcy (Doshi *et al.*, 2001; Doshi *et al.*, 2002; Woo *et al.*, 1999). The underlying mechanisms of such an effect are not fully understood. It has been proposed that the beneficial effect of folic acid on cardiovascular disease is attributed to Hcy reduction as well as its ability to antagonize oxidative stress (Doshi *et al.*, 2001; Doshi *et al.*, 2002; Woo *et al.*, 1999). In the present study, folic acid supplementation to HHcy rats resulted in a 2.9-fold increase in serum folate concentrations as compared with that of the control group. Such a treatment led to a significant reduction in the serum Hcy level (from 25.48 μM to 18.66 μM). Although the serum Hcy level in HHcy plus folic acid group was still significantly higher than that found in the control group (18.66 μM versus 3.52 μM), folic acid supplementation completely abolished HHcy-induced superoxide anion generation, peroxynitrite formation, and lipid peroxidation in the liver. Furthermore, folic acid supplementation could alleviate liver injury in HHcy rats. It is tempting to speculate that the protective effect of folic acid supplementation in the liver may be mediated, in part, via its direct effect on oxdative stress. On the contrary, it is also possible that reduction of serum Hcy levels by folic acid supplementation below a certain threshold may be able to abolish HHcy-induced oxidative stress and liver injury. It was shown that no positive correlation of hepatic superoxide anion content with serum Hcy levels was found in

HHcy rats with serum Hcy levels lower than 19 μM. In addition, in rats fed with 0.8% methionine diet, the serum Hcy level was 2-fold higher than that of the control but there was no elevation in lipid peroxidation in the liver. A mild HHcy (yielded by 0.8% methionine diet) was unable to elicit oxidative stress as observed in a moderate HHcy (yielded by 1.7% methionine diet). These results suggested that decreasing Hcy to a certain level may be sufficient to prevent hepatic oxidative stress. However, the present study does not rule out the possibility of a direct effect of folic acid against oxidative stress. It was noted that folic acid supplementation restored some antioxidant enzyme activity (catalase) in the liver of HHcy rat. The activities of antioxidant enzymes remained at a level lower than the control levels, which might be due to the elevated Hcy levels in the HHcy plus folic acid group. It is possible that the antioxidant enzymes may be more sensitive to the presence of Hcy. The solitary effect of folic acid on antioxidant enzyme activities requires further investigation.

An increase in cholesterol synthesis and content in the liver was also observed in HHcy rats. The addition of folic acid to the diet of HHcy rats was able to reduce cholesterol levels in the liver. These results suggest that folic acid can prevent lipid accumulation in the liver during HHcy, which may imply a possible protective role of folic acid in non-alcoholic hepatic steatosis.

Several studies have suggested that the beneficial effect of folic acid is mediated by its effect on endothelial function. Oral folic acid supplementation (5 mg) can restore the impaired endothelium-dependent vasodilation in familial hypercholesterolemia patients (Verhaar *et al.*, 1999). It has been suggested that folic acid can restore the enzymatic

coupling of endothelial nitric oxide synthase (eNOS) (Antoniades *et al.*, 2006). Such a restoration results in amelioration of nitric oxide-mediated endothelial function by preventing superoxide anion production from the uncoupling eNOS (Antoniades *et al.*, 2006). These studies suggest that the protective effect of folic acid on endothelial function is independent of its Hcy-lowering effect (Antoniades *et al.*, 2006; Doshi *et al.*, 2002). Although several studies have shown the beneficial effect of folic acid on cardiovascular risk (Antoniades *et al.*, 2006; Doshi *et al.*, 2001; Doshi *et al.*, 2002), a recent study has contested this (Lange *et al.*, 2004). The study included 636 patients who had undergone successful coronary stenting, and they were supplemented with a low dose (1 mg to1.2 mg) of folic acid along with 48 mg vitamin B6 and 60 μg vitamin B12 or a placebo daily for 6 months (Lange *et al.*, 2004). Patients with folate therapy had an increased risk of in-stent restenosis and the need for target-vessel revascularization (Lange *et al.*, 2004). Interestingly, the study also showed that folate therapy lowered the risk of restenosis in patients with markedly elevated Hcy levels in the circulation (15 μM or higher) (Lange *et al.*, 2004). The result suggested that the beneficial effect of folic acid was dependent upon its Hcy-lowering ability. It has also been suggested that the role of folic acid in thymidine synthesis and DNA methylation may promote cell proliferation or alter cell phenotype, possibly resulting in an exacerbation of atherosclerotic plaque formation (Loscalzo, 2006). The beneficial effect of folic acid on cardiovascular disease needs to be re-addressed with further studies on the molecular mechanisms by which folic acid affects biological pathways (Loscalzo, 2006). It would be valuable to explore the effects of folic acid supplementation, both beneficial and detrimental, in disease states with and without the presence of HHcy.

V Summary and Conclusion

Summary

The present study demonstrates that (1) Hcy can cause oxidative stress and liver injury via increased superoxide anion generation and decreased enzymatic antioxidant defence; (2) Hcy stimulates cholesterol biosynthesis by activating the transcription factors for HMG-CoA reductase gene expression in hepatocytes; (3) Hcy can activate the cAMP/PKA signaling pathway in hepatocytes leading to CREB phosphorylation and subsequent activation; and (4) folic acid supplementation offers a hepatoprotective effect by preventing the oxidative stress-mediated liver injury and hepatic cholesterol accumulation during HHcy.

5.1 Hcy-induced Oxidative Stress and Liver Injury

In the present study, there is an elevation of serum aspartate aminotransferase (AST) and alanine aminotransferase (ALT) activities in HHcy rat, indicating the occurrence of liver injury. An increase in lipid peroxidation was also observed, denoting oxidative stress in HHcy liver. Our results have clearly demonstrated that Hcy can cause oxidative stress and liver injury via increased superoxide anion generation and decreased enzymatic antioxidant activities. Elevation of superoxide anion leading to the formation of peroxynitrite contributes to the oxidative stress in HHcy rat liver. Such an increase in the superoxide anion content in the liver is caused by an elevation of NADPH oxidase activity and a decrease in the activities of antioxidant enzymes including superoxide dismutase and catalase. Inhibition of Hcy-induced NADPH oxidase activation ameliorates liver injury. These results suggest that superoxide anion-mediated oxidative stress leads to liver injury in HHcy rats. Oxidative stress is considered to be a major

contributor to different types of liver injuries (Choi & Ou, 2006; Chowdhury *et al.*, 2006; Wheeler *et al.*, 2001a). It is suggested that oxidative stress can cause direct tissue damage by modifying proteins, lipids and DNA as well as stimulating inflammatory responses. Several studies have proposed that increased oxidative stress in the liver during CBS-deficient HHcy may be due to glutathione depletion caused by disruption of the transsulfuration pathway (Figure 1.2) (Robert *et al.*, 2005; Vitvitsky *et al.*, 2004). The present study, for the first time, shows that in the absence of other risk factors, Hcy can induce oxidative stress in the liver by interfering with enzymatic redox homeostasis. Oxidative stress is shown to trigger the transition of non-fatal hepatic steatosis to steatohepatitis with progressive fibrosis (Starkel *et al.*, 2003). Several studies have shown that Hcy can induce fibrotic factors in hepatic cells (Garcia-Tevijano *et al.*, 2001; Torres *et al.*, 1999). It is tempting to speculate that a longer exposure to HHcy may lead to the development of liver fibrosis. Such a hypothesis remains to be investigated in future studies.

5.2 Hcy-induced Cholesterol Biosynthesis via Transcriptional Regulation

Early studies revealed hepatic steatosis in patients with HHcy (Carson *et al.*, 1965; McCully, 1969). Several recent studies demonstrated hepatic lipid accumulation in genetically modified HHcy animal model as well as in combination with dietary modification (Namekata *et al.*, 2004; Robert *et al.*, 2005; Werstuck *et al.*, 2001). Steatosis can accelerate fibrosis and liver damage in chronic hepatitis C patients (Adinolfi *et al.*, 2001). It has been suggested that Hcy can promote the development of fibrosis in chronic liver disease by inducing steatosis (Adinolfi *et al.*, 2005). In the present study, hepatic

steatosis is observed in HHcy rats. The result shows that cholesteryl ester is the major lipid accumulated in HHcy rat liver. Our results have demonstrated that Hcy induces cholesterol biosynthesis in the liver and the cultured hepatocytes (Woo *et al.*, 2005). Hcy-induced cholesterol biosynthesis is mediated via the activation of HMG-CoA reductase. Hcy activated the transcription factors for the HMG-CoA reductase gene, namely, sterol-regulatory element binding protein-2 (SREBP-2), cAMP-response element binding protein (CREB) and nuclear factor-Y (NF-Y) (Woo *et al.*, 2005). Inhibition of one of these three transcription factors can abolish Hcy-induced HMG-CoA reductase expression. These results suggest that the concurrent activations of all three transcription factors are crucial in Hcy-induced activation of HMG-CoA reductase expression. The ability of Hcy to activate these transcription factors may imply a disruption of other pathways in lipid metabolism. It is possible that Hcy-induced cholesterol biosynthesis in the liver may contribute to the aggravation or other complications of liver diseases or metabolic disorders.

5.3 Hcy-induced CREB activation

The present study shows that Hcy can activate CREB leading to up-regulation of HMG-CoA reductase. Such an activation of CREB is due to Hcy-activated cAMP/protein kinase A (PKA) pathway (Woo *et al.*, 2006b). Hcy can increase intracellular cAMP levels via activation of adenylyl cyclase. Increased intracellular cAMP levels results in elevated PKA activity. PKA, in turn, activates CREB in hepatocytes via phosphorylation of this transcription factor (Woo *et al.*, 2006b). CREB is an important transcription factor for the expression of genes that regulate lipid and glucose metabolism. Other studies have shown the involvement of cAMP and CREB in diabetes (Dalle *et al.*, 2004; Herzig *et al.*,

2003). Many studies including the present one demonstrate the alteration of genes involved in the lipid metabolism in HHcy livers (Hamelet *et al.*, 2007; Liao *et al.*, 2006; Woo *et al.*, 2005). It is not known whether the long term exposure to mild HHcy alone would exacerbate or initiate the onset of metabolic syndrome. Extensive studies are required to investigate the possible involvement of HHcy during metabolic syndrome.

5.4 Protective Effect of Folic Acid Supplementation

Folic acid supplementation can lower the blood Hcy levels in HHcy and is found beneficial for individuals at risk for cardiovascular disease. In the present study, addition of folic acid in the diet lowers the serum Hcy levels in HHcy rats. Folic acid supplementation successfully inhibits Hcy-induced oxidative stress and prevents oxidative stress-mediated liver injury (Woo *et al.*, 2006a). It can also prevent cholesterol accumulation in the liver of HHcy rats. Although the serum Hcy levels of HHcy rats with folic acid supplementation are significantly higher than that of the control, the correlation analysis indicates that lowering the serum Hcy to a certain level is sufficient to ameliorate HHcy-induced oxidative stress. The results of the present study suggest a protective role of folic acid in restoring liver function during HHcy. To examine whether folic acid can exert beneficial effects independent of lowering Hcy levels, additional studies should be performed in alternative experimental models of hepatic steatosis or oxidative stress mediated-liver injury induced by other stimuli.

Conclusion

In conclusion, the present study demonstrates that Hcy induces oxidative stress and cholesterol biosynthesis in the liver during HHcy, resulting in liver injury. Folic acid

supplementation can protect the liver from oxidative stress-mediated liver injury and lipid accumulation during HHcy. The liver is an important organ controlling lipid metabolism and detoxification in the body. Hcy-induced oxidative stress and cholesterol biosynthesis may represent an important mechanism for liver injury. Understanding the molecular mechanisms of liver abnormalities in HHcy may suggest a new perspective for the role of Hcy in liver pathophysiology as well as other related disorders.

VI. Future Perspectives

1. ***Long-term effect of HHcy on liver pathophysiological changes.*** In the present study, oxidative liver injury and hepatic steatosis are observed in HHcy liver. Oxidative stress has been suggested as a trigger for the transit of non-fatal hepatosteatosis to steatohepatitis or fibrosis/cirrhosis leading to liver failure (Starkel *et al.*, 2003). The HHcy rat model used in this study was exposed to 4-weeks high-methionine diet, which can be considered as a relatively short-term HHcy. The possible development of steatohepatitis or fibrosis in long-term exposure to HHcy remains to be investigated.
2. ***Effect of HHcy on inflammatory response in the liver.*** Lipid peroxidation can initiate propagation of inflammatory responses. Many pro-inflammatory factors including cytokines and acute phase response protein are synthesized in the liver. Several studies have demonstrated an increased production of pro-inflammatory factors in the liver upon injury (Dzikaite *et al.*, 2006; Haukeland *et al.*, 2006; Kanno *et al.*, 2005). Lipid peroxides have been shown to elicit an inflammatory response in the liver (Jayatilleke & Shaw, 1998; Mottaran *et al.*, 2002). It has been suggested that hepatic inflammation may contribute to low-grade systemic inflammation (Haukeland *et al.*, 2006; Kerner *et al.*, 2005). Our results demonstrate an increase in lipid peroxidation in HHcy rat liver. Increased hepatic lipid peroxidation and liver injury associated with HHcy may stimulate hepatic inflammation or further systemic inflammation. The effect of HHcy on the inflammatory response in the liver remains to be investigated in future studies.

3. ***Involvement of other transcription factors and signal transduction in lipid metabolism during HHcy.*** A recent study has found that liver receptor homologue-1 (LRH-1) binding site is present at the promoter region of HMG-CoA reductase gene (Datta *et al.*, 2006). LRH-1 is a nuclear receptor controlling the transcription of several enzymes for bile acid and cholesterol metabolism (Francis *et al.*, 2003). In spite of the presence of a ligand binding domain on LRH-1, the activation of transcription can be achieved without any ligand bound to it (Fayard *et al.*, 2004). Small heterodimer protein-1 (SHP-1) is a repressor ligand of LRH-1 (Goodwin *et al.*, 2000). The binding of SHP-1 to the ligand binding domain on LRH-1 represses LRH-1-mediated transcription (Datta *et al.*, 2006). The trancription of HMG-CoA reductase is activated by LRH-1 but repressed by SHP-1 (Datta et al., 2006). SHP-1 suppresses LRH-1-mediated promoter activation but it does not affect SREBP-2-mediated transcription activation (Datta et al., 2006). The present study demonstrates that Hcy can increase HMG-CoA reductase expression via activating the transcription factors including SREBP-2, CREB and NF-Y. It remains to be investigated whether Hcy affects the SHP-1/LRH-1 pathway in the up-regulation of HMG-CoA reductase expression.
4. ***Pathophysiology of chronic diseases in the presence of HHcy.*** Since the discovery or suggestion of the links of Hcy and atherosclerosis in early studies, a lot of controversies have been generated among research groups (2006; Kaul *et al.*, 2006). The main reasons for such debate are the unknown mechanisms and the mild pathophysiological differences observed in HHcy individuals in a clinical setting. In the present studies and other studies, Hcy has been shown to affect the upstream

signalling (e.g. transcription factor) or biological pathways which results in diverse physiological responses (Hamelet *et al.*, 2007; Wang *et al.*, 2000; Woo *et al.*, 2006b). Such diverse downstream pathways may weaken the pathophysiological responses aroused by Hcy due to the complexity of human physiology. Hcy may aggravate the dysfunction of certain biological systems of individuals who have or are prone to have long-term diseases such as hypertension, metabolic syndrome or cancer. Other than studying HHcy alone, the future research on HHcy combined with other long-term diseases such as hypertension and diabetes may help to design a more effective therapy as the maintainence of good health in the body.

VII. References

(1984). The Lipid Research Clinics Coronary Primary Prevention Trial results. II. The relationship of reduction in incidence of coronary heart disease to cholesterol lowering. *Jama* **251:** 365-74.

(1994). National Cholesterol Education Program. Second Report of the Expert Panel on Detection, Evaluation, and Treatment of High Blood Cholesterol in Adults (Adult Treatment Panel II). *Circulation* **89:** 1333-445.

(1998). Lowering blood homocysteine with folic acid based supplements: meta-analysis of randomised trials. Homocysteine Lowering Trialists' Collaboration. *Bmj* **316:** 894-8.

(2006). Homocysteine-lowering trials for prevention of cardiovascular events: a review of the design and power of the large randomized trials. *Am Heart J* **151:** 282-7.

Adinolfi L. E., Gambardella M., Andreana A., Tripodi M. F., Utili R., and Ruggiero G. (2001). Steatosis accelerates the progression of liver damage of chronic hepatitis C patients and correlates with specific HCV genotype and visceral obesity. *Hepatology* **33:** 1358-64.

Adinolfi L. E., Ingrosso D., Cesaro G., Cimmino A., D'Anto M., Capasso R., Zappia V., and Ruggiero G. (2005). Hyperhomocysteinemia and the MTHFR C677T polymorphism promote steatosis and fibrosis in chronic hepatitis C patients. *Hepatology* **41:** 995-1003.

Aebi H. (1984). Catalase in vitro. *Methods Enzymol* **105:** 121-6.

Albano E., Mottaran E., Vidali M., Reale E., Saksena S., Occhino G., Burt A. D., and Day C. P. (2005). Immune response towards lipid peroxidation products as a predictor of progression of non-alcoholic fatty liver disease to advanced fibrosis. *Gut* **54:** 987-93.

Anderson M. E. (1985). Determination of glutathione and glutathione disulfide in biological samples. *Methods Enzymol* **113:** 548-55.

Antoniades C., Shirodaria C., Warrick N., Cai S., de Bono J., Lee J., Leeson P., Neubauer S., Ratnatunga C., Pillai R., Refsum H., and Channon K. M. (2006). 5-methyltetrahydrofolate rapidly improves endothelial function and decreases superoxide production in human vessels: effects on vascular tetrahydrobiopterin availability and endothelial nitric oxide synthase coupling. *Circulation* **114:** 1193-201.

Au-Yeung K. K., Woo C. W., Sung F. L., Yip J. C., Siow Y. L., and O K. (2004). Hyperhomocysteinemia activates nuclear factor-kappaB in endothelial cells via oxidative stress. *Circ Res* **94:** 28-36.

Bailey S. M., Patel V. B., Young T. A., Asayama K., and Cunningham C. C. (2001). Chronic ethanol consumption alters the glutathione/glutathione peroxidase-1 system and protein oxidation status in rat liver. *Alcohol Clin Exp Res* **25:** 726-33.

Baraona E., Zeballos G. A., Shoichet L., Mak K. M., and Lieber C. S. (2002). Ethanol consumption increases nitric oxide production in rats, and its peroxynitrite-mediated toxicity is attenuated by polyenylphosphatidylcholine. *Alcohol Clin Exp Res* **26:** 883-9.

Bazzano L. A., Reynolds K., Holder K. N., and He J. (2006). Effect of folic acid supplementation on risk of cardiovascular diseases: a meta-analysis of randomized controlled trials. *Jama* **296:** 2720-6.

Beg Z. H., Stonik J. A., and Brewer H. B., Jr. (1979). Characterization and regulation of reductase kinase, a protein kinase that modulates the enzymic activity of 3-hydroxy-3-methylglutaryl-coenzyme A reductase. *Proc Natl Acad Sci U S A* **76:** 4375-9.

Beg Z. H., Stonik J. A., and Brewer H. B., Jr. (1985). Phosphorylation of hepatic 3-hydroxy-3-methylglutaryl coenzyme A reductase and modulation of its enzymic activity by calcium-activated and phospholipid-dependent protein kinase. *J Biol Chem* **260:** 1682-7.

Bellavite P. (1988). The superoxide-forming enzymatic system of phagocytes. *Free Radic Biol Med* **4:** 225-61.

Bennett M. K., and Osborne T. F. (2000). Nutrient regulation of gene expression by the sterol regulatory element binding proteins: increased recruitment of gene-specific coregulatory factors and selective hyperacetylation of histone H3 in vivo. *Proc Natl Acad Sci U S A* **97:** 6340-4.

Bi W., Wu L., Coustry F., de Crombrugghe B., and Maity S. N. (1997). DNA binding specificity of the CCAAT-binding factor CBF/NF-Y. *J Biol Chem* **272:** 26562-72.

Bjorkegren J., Beigneux A., Bergo M. O., Maher J. J., and Young S. G. (2002). Blocking the secretion of hepatic very low density lipoproteins renders the liver more susceptible to toxin-induced injury. *J Biol Chem* **277:** 5476-83.

Bonaa K. H., Njolstad I., Ueland P. M., Schirmer H., Tverdal A., Steigen T., Wang H., Nordrehaug J. E., Arnesen E., and Rasmussen K. (2006). Homocysteine lowering and cardiovascular events after acute myocardial infarction. *N Engl J Med* **354:** 1578-88.

Bostom A. G., Jacques P. F., Nadeau M. R., Williams R. R., Ellison R. C., and Selhub J. (1995). Post-methionine load hyperhomocysteinemia in persons with normal fasting total plasma homocysteine: initial results from the NHLBI Family Heart Study. *Atherosclerosis* **116:** 147-51.

Botolin D., and Jump D. B. (2003). Selective proteolytic processing of rat hepatic sterol regulatory element binding protein-1 (SREBP-1) and SREBP-2 during postnatal development. *J Biol Chem* **278:** 6959-62.

Boushey C. J., Beresford S. A., Omenn G. S., and Motulsky A. G. (1995). A quantitative assessment of plasma homocysteine as a risk factor for vascular disease. Probable benefits of increasing folic acid intakes. *Jama* **274:** 1049-57.

Brown M. S., and Goldstein J. L. (1976). Familial hypercholesterolemia: A genetic defect in the low-density lipoprotein receptor. *N Engl J Med* **294:** 1386-90.

Brown M. S., and Goldstein J. L. (1986). A receptor-mediated pathway for cholesterol homeostasis. *Science* **232:** 34-47.

Brown M. S., and Goldstein J. L. (1997). The SREBP pathway: regulation of cholesterol metabolism by proteolysis of a membrane-bound transcription factor. *Cell* **89:** 331-40.

Brown M. S., Goldstein J. L., and Dietschy J. M. (1979). Active and inactive forms of 3-hydroxy-3-methylglutaryl coenzyme A reductase in the liver of the rat. Comparison with the rate of cholesterol synthesis in different physiological states. *J Biol Chem* **254:** 5144-9.

Browning J. D., and Horton J. D. (2004). Molecular mediators of hepatic steatosis and liver injury. *J Clin Invest* **114:** 147-52.

Buetler T. M., Krauskopf A., and Ruegg U. T. (2004). Role of superoxide as a signaling molecule. *News Physiol Sci* **19:** 120-3.

Cardinaux J. R., Notis J. C., Zhang Q., Vo N., Craig J. C., Fass D. M., Brennan R. G., and Goodman R. H. (2000). Recruitment of CREB binding protein is sufficient for CREB-mediated gene activation. *Mol Cell Biol* **20:** 1546-52.

Carson N. A., Dent C. E., Field C. M., and Gaull G. E. (1965). Homocystinuria: Clinical and Pathological Review of Ten Cases. *J Pediatr* **66:** 565-83.

Chambers C. M., and Ness G. C. (1997). Translational regulation of hepatic HMG-CoA reductase by dietary cholesterol. *Biochem Biophys Res Commun* **232:** 278-81.

Chen L. H., Xi S., and Cohen D. A. (1995). Liver antioxidant defenses in mice fed ethanol and the AIN-76A diet. *Alcohol* **12:** 453-7.

Choi J., and Ou J. H. (2006). Mechanisms of liver injury. III. Oxidative stress in the pathogenesis of hepatitis C virus. *Am J Physiol Gastrointest Liver Physiol* **290:** G847-51.

Chowdhury A., Santra A., Bhattacharjee K., Ghatak S., Saha D. R., and Dhali G. K. (2006). Mitochondrial oxidative stress and permeability transition in isoniazid and rifampicin induced liver injury in mice. *J Hepatol* **45:** 117-26.

Chrivia J. C., Kwok R. P., Lamb N., Hagiwara M., Montminy M. R., and Goodman R. H. (1993). Phosphorylated CREB binds specifically to the nuclear protein CBP. *Nature* **365:** 855-9.

Clarke P. R., and Hardie D. G. (1990). Regulation of HMG-CoA reductase: identification of the site phosphorylated by the AMP-activated protein kinase in vitro and in intact rat liver. *Embo J* **9:** 2439-46.

Clarke R., Daly L., Robinson K., Naughten E., Cahalane S., Fowler B., and Graham I. (1991). Hyperhomocysteinemia: an independent risk factor for vascular disease. *N Engl J Med* **324:** 1149-55.

Collinsova M., Strakova J., Jiracek J., and Garrow T. A. (2006). Inhibition of betaine-homocysteine S-methyltransferase causes hyperhomocysteinemia in mice. *J Nutr* **136:** 1493-7.

Coman D. R. (1954). Cellular adhesiveness in relation to the invasiveness of cancer; electron microscopy of liver perfused with a chelating agent. *Cancer Res* **14:** 519-21.

Crapo J. D., McCord J. M., and Fridovich I. (1978). Preparation and assay of superoxide dismutases. *Methods Enzymol* **53:** 382-93.

Czaja M. J. (2005). Another way for NADPH oxidase to send a signal for liver injury. *Gastroenterology* **129:** 2110-3.

Dalery K., Lussier-Cacan S., Selhub J., Davignon J., Latour Y., and Genest J., Jr. (1995). Homocysteine and coronary artery disease in French Canadian subjects: relation with vitamins B12, B6, pyridoxal phosphate, and folate. *Am J Cardiol* **75:** 1107-11.

Dalle S., Longuet C., Costes S., Broca C., Faruque O., Fontes G., Hani el H., and Bataille D. (2004). Glucagon promotes cAMP-response element-binding protein phosphorylation via activation of ERK1/2 in MIN6 cell line and isolated islets of Langerhans. *J Biol Chem* **279:** 20345-55.

Datta S., Wang L., Moore D. D., and Osborne T. F. (2006). Regulation of 3-hydroxy-3-methylglutaryl coenzyme A reductase promoter by nuclear receptors liver receptor homologue-1 and small heterodimer partner: a mechanism for

differential regulation of cholesterol synthesis and uptake. *J Biol Chem* **281:** 807-12.

Dayal S., Wilson K. M., Leo L., Arning E., Bottiglieri T., and Lentz S. R. (2006). Enhanced susceptibility to arterial thrombosis in a murine model of hyperhomocysteinemia. *Blood* **108:** 2237-43.

Dignam J. D., Lebovitz R. M., and Roeder R. G. (1983). Accurate transcription initiation by RNA polymerase II in a soluble extract from isolated mammalian nuclei. *Nucleic Acids Res* **11:** 1475-89.

Dooley K. A., Bennett M. K., and Osborne T. F. (1999). A critical role for cAMP response element-binding protein (CREB) as a Co-activator in sterol-regulated transcription of 3-hydroxy-3-methylglutaryl coenzyme A synthase promoter. *J Biol Chem* **274:** 5285-91.

Dooley K. A., Millinder S., and Osborne T. F. (1998). Sterol regulation of 3-hydroxy-3-methylglutaryl-coenzyme A synthase gene through a direct interaction between sterol regulatory element binding protein and the trimeric CCAAT-binding factor/nuclear factor Y. *J Biol Chem* **273:** 1349-56.

Doshi S. N., McDowell I. F., Moat S. J., Lang D., Newcombe R. G., Kredan M. B., Lewis M. J., and Goodfellow J. (2001). Folate improves endothelial function in coronary artery disease: an effect mediated by reduction of intracellular superoxide? *Arterioscler Thromb Vasc Biol* **21:** 1196-202.

Doshi S. N., McDowell I. F., Moat S. J., Payne N., Durrant H. J., Lewis M. J., and Goodfellow J. (2002). Folic acid improves endothelial function in coronary artery disease via mechanisms largely independent of homocysteine lowering. *Circulation* **105:** 22-6.

Duerre J. A., and Miller C. H. (1966). Preparation of L-homocysteine from L-homocysteine thiolactone. *Anal Biochem* **17:** 310-5.

Durrington P. (2003). Dyslipidaemia. *Lancet* **362:** 717-31.

Dzikaite V., Holmstrom P., Stal P., Eckes K., Hagen K., Eggertsen G., Gafvels M., Melefors O., and Hultcrantz R. (2006). Regulatory effects of tumor necrosis factor-alpha and interleukin-6 on HAMP expression in iron loaded rat hepatocytes. *J Hepatol* **44:** 544-51.

Endemann D. H., and Schiffrin E. L. (2004). Endothelial dysfunction. *J Am Soc Nephrol* **15:** 1983-92.

Engh R. A., Girod A., Kinzel V., Huber R., and Bossemeyer D. (1996). Crystal structures of catalytic subunit of cAMP-dependent protein kinase in complex with isoquinolinesulfonyl protein kinase inhibitors H7, H8, and H89. Structural implications for selectivity. *J Biol Chem* **271:** 26157-64.

Ericsson J., and Edwards P. A. (1998). CBP is required for sterol-regulated and sterol regulatory element-binding protein-regulated transcription. *J Biol Chem* **273:** 17865-70.

Ericsson J., Jackson S. M., and Edwards P. A. (1996). Synergistic binding of sterol regulatory element-binding protein and NF-Y to the farnesyl diphosphate synthase promoter is critical for sterol-regulated expression of the gene. *J Biol Chem* **271:** 24359-64.

Esfandiari F., Villanueva J. A., Wong D. H., French S. W., and Halsted C. H. (2005). Chronic ethanol feeding and folate deficiency activate hepatic endoplasmic reticulum stress pathway in micropigs. *Am J Physiol Gastrointest Liver Physiol* **289:** G54-63.

Estevez A. G., and Jordan J. (2002). Nitric oxide and superoxide, a deadly cocktail. *Ann N Y Acad Sci* **962:** 207-11.

Everson C. A., Laatsch C. D., and Hogg N. (2005). Antioxidant defense responses to sleep loss and sleep recovery. *Am J Physiol Regul Integr Comp Physiol* **288:** R374-83.

Farrell G. C., and Larter C. Z. (2006). Nonalcoholic fatty liver disease: from steatosis to cirrhosis. *Hepatology* **43:** S99-S112.

Faurschou M., Nielsen O. J., Jensen M. K., and Hasselbalch H. C. (2000). High prevalence of hyperhomocysteinemia due to marginal deficiency of cobalamin or folate in chronic myeloproliferative disorders. *Am J Hematol* **65:** 136-40.

Fayard E., Auwerx J., and Schoonjans K. (2004). LRH-1: an orphan nuclear receptor involved in development, metabolism and steroidogenesis. *Trends Cell Biol* **14:** 250-60.

Feron O., Dessy C., Desager J. P., and Balligand J. L. (2001). Hydroxy-methylglutaryl-coenzyme A reductase inhibition promotes endothelial nitric oxide synthase activation through a decrease in caveolin abundance. *Circulation* **103:** 113-8.

Finkel T. (1999). Signal transduction by reactive oxygen species in non-phagocytic cells. *J Leukoc Biol* **65:** 337-40.

Folch J., Lees M., and Sloane Stanley G. H. (1957). A simple method for the isolation and purification of total lipides from animal tissues. *J Biol Chem* **226:** 497-509.

Francis G. A., Fayard E., Picard F., and Auwerx J. (2003). Nuclear receptors and the control of metabolism. *Annu Rev Physiol* **65:** 261-311.

Francis S. H., and Kono T. (1982). Hormone-sensitive cAMP phosphodiesterase in liver and fat cells. *Mol Cell Biochem* **42:** 109-16.

Garcia-Tevijano E. R., Berasain C., Rodriguez J. A., Corrales F. J., Arias R., Martin-Duce A., Caballeria J., Mato J. M., and Avila M. A. (2001). Hyperhomocysteinemia in liver cirrhosis: mechanisms and role in vascular and hepatic fibrosis. *Hypertension* **38:** 1217-21.

Gaull G., Sturman J. A., and Schaffner F. (1974). Homocystinuria due to cystathionine synthase deficiency: enzymatic and ultrastructural studies. *J Pediatr* **84:** 381-90.

Gibbons G. F. (1994). A comparison of in-vitro models to study hepatic lipid and lipoprotein metabolism. *Curr Opin Lipidol* **5:** 191-9.

Girotti A. W. (1998). Lipid hydroperoxide generation, turnover, and effector action in biological systems. *J Lipid Res* **39:** 1529-42.

Glass C. K., and Witztum J. L. (2001). Atherosclerosis. the road ahead. *Cell* **104:** 503-16.

Goldstein J. L., and Brown M. S. (1973). Familial hypercholesterolemia: identification of a defect in the regulation of 3-hydroxy-3-methylglutaryl coenzyme A reductase activity associated with overproduction of cholesterol. *Proc Natl Acad Sci U S A* **70:** 2804-8.

Goldstein J. L., and Brown M. S. (1984). Progress in understanding the LDL receptor and HMG-CoA reductase, two membrane proteins that regulate the plasma cholesterol. *J Lipid Res* **25:** 1450-61.

Goldstein J. L., and Brown M. S. (1989). Chapter 48: Familial Hypercholesterolemia. *In* "The Metabolic Basis of Inherited Disease - I" (C. R. Scriver, A. L. Beaudet, W. S. Sly, and D. Valle, Eds.), pp. 1215-1250, McGraw-Hill Inc., New York.

Goldstein J. L., Schrott H. G., Hazzard W. R., Bierman E. L., and Motulsky A. G. (1973). Hyperlipidemia in coronary heart disease. II. Genetic analysis of lipid levels in 176 families and delineation of a new inherited disorder, combined hyperlipidemia. *J Clin Invest* **52:** 1544-68.

Gonzalez G. A., and Montminy M. R. (1989). Cyclic AMP stimulates somatostatin gene transcription by phosphorylation of CREB at serine 133. *Cell* **59:** 675-80.

Goodwin B., Jones S. A., Price R. R., Watson M. A., McKee D. D., Moore L. B., Galardi C., Wilson J. G., Lewis M. C., Roth M. E., Maloney P. R., Willson T. M., and Kliewer S. A. (2000). A regulatory cascade of the nuclear receptors FXR, SHP-1, and LRH-1 represses bile acid biosynthesis. *Mol Cell* **6:** 517-26.

Gotto A. M., Jr. (1992). Hypertriglyceridemia: risks and perspectives. *Am J Cardiol* **70:** 19H-25H.

Gulsen M., Yesilova Z., Bagci S., Uygun A., Ozcan A., Ercin C. N., Erdil A., Sanisoglu S. Y., Cakir E., Ates Y., Erbil M. K., Karaeren N., and Dagalp K. (2005). Elevated plasma homocysteine concentrations as a predictor of steatohepatitis in

patients with non-alcoholic fatty liver disease. *J Gastroenterol Hepatol* **20:** 1448-55.

Guttormsen A. B., Schneede J., Fiskerstrand T., Ueland P. M., and Refsum H. M. (1994). Plasma concentrations of homocysteine and other aminothiol compounds are related to food intake in healthy human subjects. *J Nutr* **124:** 1934-41.

Halsted C. H., Villanueva J. A., Devlin A. M., Niemela O., Parkkila S., Garrow T. A., Wallock L. M., Shigenaga M. K., Melnyk S., and James S. J. (2002). Folate deficiency disturbs hepatic methionine metabolism and promotes liver injury in the ethanol-fed micropig. *Proc Natl Acad Sci U S A* **99:** 10072-7.

Hamelet J., Demuth K., Paul J. L., Delabar J. M., and Janel N. (2007). Hyperhomocysteinemia due to cystathionine beta synthase deficiency induces dysregulation of genes involved in hepatic lipid homeostasis in mice. *J Hepatol* **46:** 151-9.

Hardie D. G. (1992). Regulation of fatty acid and cholesterol metabolism by the AMP-activated protein kinase. *Biochim Biophys Acta* **1123:** 231-8.

Harker L. A., Ross R., Slichter S. J., and Scott C. R. (1976). Homocystine-induced arteriosclerosis. The role of endothelial cell injury and platelet response in its genesis. *J Clin Invest* **58:** 731-41.

Harrison S. A., and Di Bisceglie A. M. (2003). Advances in the understanding and treatment of nonalcoholic fatty liver disease. *Drugs* **63:** 2379-94.

Hatch F. T., Larrabee A. R., Cathou R. E., and Buchanan J. M. (1961). Enzymatic synthesis of the methyl group of methionine. I. Identification of the enzymes and cofactors involved in the system isolated from Escherichia coli. *J Biol Chem* **236:** 1095-101.

Haukeland J. W., Damas J. K., Konopski Z., Loberg E. M., Haaland T., Goverud I., Torjesen P. A., Birkeland K., Bjoro K., and Aukrust P. (2006). Systemic inflammation in nonalcoholic fatty liver disease is characterized by elevated levels of CCL2. *J Hepatol* **44:** 1167-74.

Havel R. J., Goldstein J. L., and Brown M. S. (1980). Lipoproteins and lipid transport. *In* "Metabolic control of disease " (P. K. Bondy, and L. E. Rosenberg, Eds.), pp. 393-494, Sauders, Philadelphia.

Herzig S., Hedrick S., Morantte I., Koo S. H., Galimi F., and Montminy M. (2003). CREB controls hepatic lipid metabolism through nuclear hormone receptor PPAR-gamma. *Nature* **426:** 190-3.

Hillman R. S. (2001). Hematopoietic agents, Growth factors, minerals and vitamins. *In* "Goodman & Gillman's The Pharmacological basis of Therapeutics" (J. G. Hardman, and L. E. Limbird, Eds.), pp. 1487-1517, McGraw-Hill, New York.

Hofmann M. A., Lalla E., Lu Y., Gleason M. R., Wolf B. M., Tanji N., Ferran L. J., Jr., Kohl B., Rao V., Kisiel W., Stern D. M., and Schmidt A. M. (2001). Hyperhomocysteinemia enhances vascular inflammation and accelerates atherosclerosis in a murine model. *J Clin Invest* **107:** 675-83.

Horton J. D., Goldstein J. L., and Brown M. S. (2002). SREBPs: activators of the complete program of cholesterol and fatty acid synthesis in the liver. *J Clin Invest* **109:** 1125-31.

Horton J. D., Shimomura I., Brown M. S., Hammer R. E., Goldstein J. L., and Shimano H. (1998). Activation of cholesterol synthesis in preference to fatty acid synthesis in liver and adipose tissue of transgenic mice overproducing sterol regulatory element-binding protein-2. *J Clin Invest* **101:** 2331-9.

Huang R. F., Hsu Y. C., Lin H. L., and Yang F. L. (2001). Folate depletion and elevated plasma homocysteine promote oxidative stress in rat livers. *J Nutr* **131:** 33-8.

Hyndman M. E., Verma S., Rosenfeld R. J., Anderson T. J., and Parsons H. G. (2002). Interaction of 5-methyltetrahydrofolate and tetrahydrobiopterin on endothelial function. *Am J Physiol Heart Circ Physiol* **282:** H2167-72.

Ischiropoulos H., Zhu L., Chen J., Tsai M., Martin J. C., Smith C. D., and Beckman J. S. (1992). Peroxynitrite-mediated tyrosine nitration catalyzed by superoxide dismutase. *Arch Biochem Biophys* **298:** 431-7.

Ito Y., Abril E. R., Bethea N. W., and McCuskey R. S. (2004). Role of nitric oxide in hepatic microvascular injury elicited by acetaminophen in mice. *Am J Physiol Gastrointest Liver Physiol* **286:** G60-7.

Jackson R. L., Morrisett J. D., and Gotto A. M., Jr. (1976). Lipoprotein structure and metabolism. *Physiol Rev* **56:** 259-316.

Jackson S. M., Ericsson J., Mantovani R., and Edwards P. A. (1998). Synergistic activation of transcription by nuclear factor Y and sterol regulatory element binding protein. *J Lipid Res* **39:** 767-76.

Jacobsen D. W. (2000). Biochemistry and Metabolism. *In* "Homocysteine and Vascular Disease" (K. Robinson, Ed.), pp. 15-40, Kluwer Academic Publishers, Dordrecht.

Jaeschke H., Knight T. R., and Bajt M. L. (2003). The role of oxidant stress and reactive nitrogen species in acetaminophen hepatotoxicity. *Toxicol Lett* **144:** 279-88.

James L. P., Mayeux P. R., and Hinson J. A. (2003). Acetaminophen-induced hepatotoxicity. *Drug Metab Dispos* **31:** 1499-506.

Javitt N. B. (1990). Hep G2 cells as a resource for metabolic studies: lipoprotein, cholesterol, and bile acids. *Faseb J* **4:** 161-8.

Jayatilleke A., and Shaw S. (1998). Stimulation of monocyte interleukin-8 by lipid peroxidation products: a mechanism for alcohol-induced liver injury. *Alcohol* **16:** 119-23.

Jefferson L. S., Exton J. H., Butcher R. W., Sutherland E. W., and Park C. R. (1968). Role of adenosine 3',5'-monophosphate in the effects of insulin and anti-insulin serum on liver metabolism. *J Biol Chem* **243:** 1031-8.

Ji C., and Kaplowitz N. (2003). Betaine decreases hyperhomocysteinemia, endoplasmic reticulum stress, and liver injury in alcohol-fed mice. *Gastroenterology* **124:** 1488-99.

Johannessen M., Delghandi M. P., and Moens U. (2004). What turns CREB on? *Cell Signal* **16:** 1211-27.

Jourd'heuil D., Jourd'heuil F. L., Kutchukian P. S., Musah R. A., Wink D. A., and Grisham M. B. (2001). Reaction of superoxide and nitric oxide with peroxynitrite. Implications for peroxynitrite-mediated oxidation reactions in vivo. *J Biol Chem* **276:** 28799-805.

Kang S. S., Zhou J., Wong P. W., Kowalisyn J., and Strokosch G. (1988). Intermediate homocysteinemia: a thermolabile variant of methylenetetrahydrofolate reductase. *Am J Hum Genet* **43:** 414-21.

Kanno K., Tazuma S., Nishioka T., Hyogo H., and Chayama K. (2005). Angiotensin II participates in hepatic inflammation and fibrosis through MCP-1 expression. *Dig Dis Sci* **50:** 942-8.

Kaplowitz N., and Tsukamoto H. (1996). Oxidative stress and liver disease. *Prog Liver Dis* **14:** 131-59.

Kashiwagi A., Shinozaki K., Nishio Y., Maegawa H., Maeno Y., Kanazawa A., Kojima H., Haneda M., Hidaka H., Yasuda H., and Kikkawa R. (1999). Endothelium-specific activation of NAD(P)H oxidase in aortas of exogenously hyperinsulinemic rats. *Am J Physiol* **277:** E976-83.

Kaul S., Zadeh A. A., and Shah P. K. (2006). Homocysteine hypothesis for atherothrombotic cardiovascular disease: not validated. *J Am Coll Cardiol* **48:** 914-23.

Kerner A., Avizohar O., Sella R., Bartha P., Zinder O., Markiewicz W., Levy Y., Brook G. J., and Aronson D. (2005). Association between elevated liver enzymes and C-reactive protein: possible hepatic contribution to systemic inflammation in the metabolic syndrome. *Arterioscler Thromb Vasc Biol* **25:** 193-7.

Kim C. G., and Sheffery M. (1990). Physical characterization of the purified CCAAT transcription factor, alpha-CP1. *J Biol Chem* **265:** 13362-9.

Kim D. J., Koh J. M., Lee O., Kim N. J., Lee Y. S., Kim Y. S., Park J. Y., Lee K. U., and Kim G. S. (2006). Homocysteine enhances apoptosis in human bone marrow stromal cells. *Bone* **39:** 582-90.

Klaunig J. E., and Kamendulis L. M. (2004). The role of oxidative stress in carcinogenesis. *Annu Rev Pharmacol Toxicol* **44:** 239-67.

Klemm D. J., Roesler W. J., Boras T., Colton L. A., Felder K., and Reusch J. E. (1998). Insulin stimulates cAMP-response element binding protein activity in HepG2 and 3T3-L1 cell lines. *J Biol Chem* **273:** 917-23.

Koch O. R., De Leo M. E., Borrello S., Palombini G., and Galeotti T. (1994). Ethanol treatment up-regulates the expression of mitochondrial manganese superoxide dismutase in rat liver. *Biochem Biophys Res Commun* **201:** 1356-65.

Koh J. M., Lee Y. S., Kim Y. S., Kim D. J., Kim H. H., Park J. Y., Lee K. U., and Kim G. S. (2006). Homocysteine enhances bone resorption by stimulation of osteoclast formation and activity through increased intracellular ROS generation. *J Bone Miner Res* **21:** 1003-11.

Kono H., Rusyn I., Uesugi T., Yamashina S., Connor H. D., Dikalova A., Mason R. P., and Thurman R. G. (2001). Diphenyleneiodonium sulfate, an NADPH oxidase inhibitor, prevents early alcohol-induced liver injury in the rat. *Am J Physiol Gastrointest Liver Physiol* **280:** G1005-12.

Kono H., Rusyn I., Yin M., Gabele E., Yamashina S., Dikalova A., Kadiiska M. B., Connor H. D., Mason R. P., Segal B. H., Bradford B. U., Holland S. M., and Thurman R. G. (2000). NADPH oxidase-derived free radicals are key oxidants in alcohol-induced liver disease. *J Clin Invest* **106:** 867-72.

Kwiterovich P. O., Jr. (2000). The metabolic pathways of high-density lipoprotein, low-density lipoprotein, and triglycerides: a current review. *Am J Cardiol* **86:** 5L-10L.

Kwok R. P., Lundblad J. R., Chrivia J. C., Richards J. P., Bachinger H. P., Brennan R. G., Roberts S. G., Green M. R., and Goodman R. H. (1994). Nuclear protein CBP is a coactivator for the transcription factor CREB. *Nature* **370:** 223-6.

Laemmli U. K. (1970). Cleavage of structural proteins during the assembly of the head of bacteriophage T4. *Nature* **227:** 680-5.

Lange H., Suryapranata H., De Luca G., Borner C., Dille J., Kallmayer K., Pasalary M. N., Scherer E., and Dambrink J. H. (2004). Folate therapy and in-stent restenosis after coronary stenting. *N Engl J Med* **350:** 2673-81.

Lawrence de Koning A. B., Werstuck G. H., Zhou J., and Austin R. C. (2003). Hyperhomocysteinemia and its role in the development of atherosclerosis. *Clin Biochem* **36:** 431-41.

Leffler C. W., Balabanova L., and Williams K. K. (1999). cAMP production by piglet cerebral vascular smooth muscle cells: pH(o), pH(i), and permissive action of PGI(2). *Am J Physiol* **277:** H1878-83.

Lehr H. A., van der Loos C. M., Teeling P., and Gown A. M. (1999). Complete chromogen separation and analysis in double immunohistochemical stains using Photoshop-based image analysis. *J Histochem Cytochem* **47:** 119-26.

Lentz S. R., Erger R. A., Dayal S., Maeda N., Malinow M. R., Heistad D. D., and Faraci F. M. (2000). Folate dependence of hyperhomocysteinemia and vascular dysfunction in cystathionine beta-synthase-deficient mice. *Am J Physiol Heart Circ Physiol* **279:** H970-5.

Lentz S. R., and Sadler J. E. (1991). Inhibition of thrombomodulin surface expression and protein C activation by the thrombogenic agent homocysteine. *J Clin Invest* **88:** 1906-14.

Lentz S. R., and Sadler J. E. (1993). Homocysteine inhibits von Willebrand factor processing and secretion by preventing transport from the endoplasmic reticulum. *Blood* **81:** 683-9.

Li H., Lewis A., Brodsky S., Rieger R., Iden C., and Goligorsky M. S. (2002). Homocysteine induces 3-hydroxy-3-methylglutaryl coenzyme a reductase in vascular endothelial cells: a mechanism for development of atherosclerosis? *Circulation* **105:** 1037-43.

Li J. M., and Shah A. M. (2003). Mechanism of endothelial cell NADPH oxidase activation by angiotensin II. Role of the p47phox subunit. *J Biol Chem* **278:** 12094-100.

Li Y., Zhu H., Kuppusamy P., Roubaud V., Zweier J. L., and Trush M. A. (1998). Validation of lucigenin (bis-N-methylacridinium) as a chemilumigenic probe for detecting superoxide anion radical production by enzymatic and cellular systems. *J Biol Chem* **273:** 2015-23.

Liang S. G., and Maity S. N. (1998). Pathway of complex formation between DNA and three subunits of CBF/NF-Y. Photocross-linking analysis of DNA-protein interaction and characterization of equilibrium steps of subunit interaction and dna binding. *J Biol Chem* **273:** 31590-8.

Liao D., Tan H., Hui R., Li Z., Jiang X., Gaubatz J., Yang F., Durante W., Chan L., Schafer A. I., Pownall H. J., Yang X., and Wang H. (2006). Hyperhomocysteinemia decreases circulating high-density lipoprotein by inhibiting apolipoprotein A-I Protein synthesis and enhancing HDL cholesterol clearance. *Circ Res* **99:** 598-606.

Liscum L. (2002). Chapter 15: Cholesterol Biosynthesis. *In* "Biochemsitry of Lipids, Lipoproteins and Membranes" (D. E. Vance, and J. E. Vance, Eds.), pp. 409-430, Elsevier, Amsterdam.

Loscalzo J. (2006). Homocysteine trials--clear outcomes for complex reasons. *N Engl J Med* **354:** 1629-32.

Lu S. C. (1999). Regulation of hepatic glutathione synthesis: current concepts and controversies. *Faseb J* **13:** 1169-83.

Lucock M. (2000). Folic acid: nutritional biochemistry, molecular biology, and role in disease processes. *Mol Genet Metab* **71:** 121-38.

Mabuchi T., Kitagawa K., Kuwabara K., Takasawa K., Ohtsuki T., Xia Z., Storm D., Yanagihara T., Hori M., and Matsumoto M. (2001). Phosphorylation of cAMP response element-binding protein in hippocampal neurons as a protective response after exposure to glutamate in vitro and ischemia in vivo. *J Neurosci* **21:** 9204-13.

Manninen V., Elo M. O., Frick M. H., Haapa K., Heinonen O. P., Heinsalmi P., Helo P., Huttunen J. K., Kaitaniemi P., Koskinen P., and et al. (1988). Lipid alterations and decline in the incidence of coronary heart disease in the Helsinki Heart Study. *Jama* **260:** 641-51.

Mantovani R. (1999). The molecular biology of the CCAAT-binding factor NF-Y. *Gene* **239:** 15-27.

Markou T., Hadzopoulou-Cladaras M., and Lazou A. (2004). Phenylephrine induces activation of CREB in adult rat cardiac myocytes through MSK1 and PKA signaling pathways. *J Mol Cell Cardiol* **37:** 1001-11.

Marnett L. J. (2002). Oxy radicals, lipid peroxidation and DNA damage. *Toxicology* **181-182:** 219-22.

Masella R., Di Benedetto R., Vari R., Filesi C., and Giovannini C. (2005). Novel mechanisms of natural antioxidant compounds in biological systems: involvement of glutathione and glutathione-related enzymes. *J Nutr Biochem* **16:** 577-86.

Mayr B., and Montminy M. (2001). Transcriptional regulation by the phosphorylation-dependent factor CREB. *Nat Rev Mol Cell Biol* **2:** 599-609.

McCully K. S. (1969). Vascular pathology of homocysteinemia: implications for the pathogenesis of arteriosclerosis. *Am J Pathol* **56:** 111-28.

McLean R. R., Jacques P. F., Selhub J., Tucker K. L., Samelson E. J., Broe K. E., Hannan M. T., Cupples L. A., and Kiel D. P. (2004). Homocysteine as a predictive factor for hip fracture in older persons. *N Engl J Med* **350:** 2042-9.

Mikael L. G., Genest J., Jr., and Rozen R. (2006). Elevated homocysteine reduces apolipoprotein A-I expression in hyperhomocysteinemic mice and in males with coronary artery disease. *Circ Res* **98:** 564-71.

Misra U. K., Bradford B. U., Handler J. A., and Thurman R. G. (1992). Chronic ethanol treatment induces H2O2 production selectively in pericentral regions of the liver lobule. *Alcohol Clin Exp Res* **16:** 839-42.

Mizukami Y., Matsubara F., Matsukawa S., and Izumi R. (1983). Cytochemical localization of glutaraldehyde-resistant NAD(P)H-oxidase in rat hepatocytes. *Histochemistry* **79:** 259-67.

Montminy M., Koo S. H., and Zhang X. (2004). The CREB family: key regulators of hepatic metabolism. *Ann Endocrinol (Paris)* **65:** 73-5.

Morabia A., and Costanza M. C. (2005). The obesity epidemic as harbinger of a metabolic disorder epidemic: trends in overweight, hypercholesterolemia, and diabetes treatment in Geneva, Switzerland, 1993-2003. *Am J Public Health* **95:** 632-5.

Mottaran E., Stewart S. F., Rolla R., Vay D., Cipriani V., Moretti M., Vidali M., Sartori M., Rigamonti C., Day C. P., and Albano E. (2002). Lipid peroxidation contributes to immune reactions associated with alcoholic liver disease. *Free Radic Biol Med* **32:** 38-45.

Mudd S. H., Levy H. L., and Skovby F. (1995). Disorders of Transsulfuration. *In* "The Metabolic and Molecular Basis of Inherited Disease" (C. R. Scriver, A. L. Beaudet, W. S. Sly, and D. Valle, Eds.), pp. 1279-1321, McGraw-Hill Inc., New York.

Muntjewerff J. W., Kahn R. S., Blom H. J., and den Heijer M. (2006). Homocysteine, methylenetetrahydrofolate reductase and risk of schizophrenia: a meta-analysis. *Mol Psychiatry* **11:** 143-9.

Nakshatri H., Bhat-Nakshatri P., and Currie R. A. (1996). Subunit association and DNA binding activity of the heterotrimeric transcription factor NF-Y is regulated by cellular redox. *J Biol Chem* **271:** 28784-91.

Namekata K., Enokido Y., Ishii I., Nagai Y., Harada T., and Kimura H. (2004). Abnormal lipid metabolism in cystathionine beta-synthase-deficient mice, an animal model for hyperhomocysteinemia. *J Biol Chem* **279:** 52961-9.

Navasumrit P., Ward T. H., Dodd N. J., and O'Connor P. J. (2000). Ethanol-induced free radicals and hepatic DNA strand breaks are prevented in vivo by antioxidants: effects of acute and chronic ethanol exposure. *Carcinogenesis* **21:** 93-9.

Nekrassova A. A. (1963). Activity of Serum and Cardiac Enzymes in Clinical and Experimental Atherosclerosis and Coronary Insufficiency. *Enzymol Biol Clin (Basel)* **74:** 209-18.

Ness G. C., Wiggins L., and Zhao Z. (1994). Insulin increases hepatic 3-hydroxy-methylglutaryl coenzyme A reductase mRNA and immunoreactive protein levels in diabetic rats. *Arch Biochem Biophys* **309:** 193-4.

Ngo T. T., Bennett M. K., Bourgeois A. L., Toth J. I., and Osborne T. F. (2002). A role for cyclic AMP response element-binding protein (CREB) but not the highly similar ATF-2 protein in sterol regulation of the promoter for 3-hydroxy-3-methylglutaryl coenzyme A reductase. *J Biol Chem* **277:** 33901-5.

Nygard O., Vollset S. E., Refsum H., Stensvold I., Tverdal A., Nordrehaug J. E., Ueland M., and Kvale G. (1995). Total plasma homocysteine and cardiovascular risk profile. The Hordaland Homocysteine Study. *Jama* **274:** 1526-33.

O K., Lynn E. G., Chung Y. H., Siow Y. L., Man R. Y., and Choy P. C. (1998). Homocysteine stimulates the production and secretion of cholesterol in hepatic cells. *Biochim Biophys Acta* **1393:** 317-24.

Ohkawa H., Ohishi N., and Yagi K. (1979). Assay for lipid peroxides in animal tissues by thiobarbituric acid reaction. *Anal Biochem* **95:** 351-8.

Okada T., Haze K., Nadanaka S., Yoshida H., Seidah N. G., Hirano Y., Sato R., Negishi M., and Mori K. (2003). A serine protease inhibitor prevents endoplasmic reticulum stress-induced cleavage but not transport of the membrane-bound transcription factor ATF6. *J Biol Chem* **278:** 31024-32.

Pacheco-Quinto J., Rodriguez de Turco E. B., DeRosa S., Howard A., Cruz-Sanchez F., Sambamurti K., Refolo L., Petanceska S., and Pappolla M. A. (2006). Hyperhomocysteinemic Alzheimer's mouse model of amyloidosis shows increased brain amyloid beta peptide levels. *Neurobiol Dis* **22:** 651-6.

Page D. T., and Garvey J. S. (1979). Isolation and characterization of hepatocytes and Kupffer cells. *J Immunol Methods* **27:** 159-73.

Pilkis S. J., Exton J. H., Johnson R. A., and Park C. R. (1974). Effects of glucagon on cyclic AMP and carbohydrate metabolism in livers from diabetic rats. *Biochim Biophys Acta* **343:** 250-67.

Pullin C. H., Ashfield-Watt P. A., Burr M. L., Clark Z. E., Lewis M. J., Moat S. J., Newcombe R. G., Powers H. J., Whiting J. M., and McDowell I. F. (2001). Optimization of dietary folate or low-dose folic acid supplements lower homocysteine but do not enhance endothelial function in healthy adults, irrespective of the methylenetetrahydrofolate reductase (C677T) genotype. *J Am Coll Cardiol* **38:** 1799-805.

Qureshi N., Dugan R. E., Cleland W. W., and Porter J. W. (1976). Kinetic analysis of the individual reductive steps catalyzed by beta-hydroxy-beta-methylglutaryl-coenzyme A reductase obtained from yeast. *Biochemistry* **15:** 4191-07.

Rader D. J. (2002). High-density lipoproteins and atherosclerosis. *Am J Cardiol* **90:** 62i-70i.

Rader D. J. (2006). Molecular regulation of HDL metabolism and function: implications for novel therapies. *J Clin Invest* **116:** 3090-100.

Reardon M. F., Sakai H., and Steiner G. (1982). Roles of lipoprotein lipase and hepatic triglyceride lipase in the catabolism in vivo of triglyceride-rich lipoproteins. *Arteriosclerosis* **2:** 396-402.

Reinehr R., Becker S., Eberle A., Grether-Beck S., and Haussinger D. (2005a). Involvement of NADPH oxidase isoforms and Src family kinases in CD95-dependent hepatocyte apoptosis. *J Biol Chem* **280:** 27179-94.

Reinehr R., Becker S., Keitel V., Eberle A., Grether-Beck S., and Haussinger D. (2005b). Bile salt-induced apoptosis involves NADPH oxidase isoform activation. *Gastroenterology* **129:** 2009-31.

Reinehr R., Fischer R., and Haussinger D. (2002). Regulation of endothelin-A receptor sensitivity by cyclic adenosine monophosphate in rat hepatic stellate cells. *Hepatology* **36:** 861-73.

Richards H. H., Chiang P. K., and Cantoni G. L. (1978). Adenosylhomocysteine hydrolase. Crystallization of the purified enzyme and its properties. *J Biol Chem* **253:** 4476-80.

Robert K., Nehme J., Bourdon E., Pivert G., Friguet B., Delcayre C., Delabar J. M., and Janel N. (2005). Cystathionine beta synthase deficiency promotes oxidative stress, fibrosis, and steatosis in mice liver. *Gastroenterology* **128:** 1405-15.

Romier C., Cocchiarella F., Mantovani R., and Moras D. (2003). The NF-YB/NF-YC structure gives insight into DNA binding and transcription regulation by CCAAT factor NF-Y. *J Biol Chem* **278:** 1336-45.

Roncales M., Achon M., Manzarbeitia F., Maestro de las Casas C., Ramirez C., Varela-Moreiras G., and Perez-Miguelsanz J. (2004). Folic acid supplementation for 4 weeks affects liver morphology in aged rats. *J Nutr* **134:** 1130-3.

Rosenberg D., Groussin L., Jullian E., Perlemoine K., Bertagna X., and Bertherat J. (2002). Role of the PKA-regulated transcription factor CREB in development and tumorigenesis of endocrine tissues. *Ann N Y Acad Sci* **968:** 65-74.

Sacks F. M., Pfeffer M. A., Moye L. A., Rouleau J. L., Rutherford J. D., Cole T. G., Brown L., Warnica J. W., Arnold J. M., Wun C. C., Davis B. R., and Braunwald

E. (1996). The effect of pravastatin on coronary events after myocardial infarction in patients with average cholesterol levels. Cholesterol and Recurrent Events Trial investigators. *N Engl J Med* **335:** 1001-9.

Sadrzadeh S. M., Nanji A. A., and Meydani M. (1994). Effect of chronic ethanol feeding on plasma and liver alpha- and gamma-tocopherol levels in normal and vitamin E-deficient rats. Relationship to lipid peroxidation. *Biochem Pharmacol* **47:** 2005-10.

Schmidt H., and Kelm M. (1996). Determination of Nitrite and Nitrate by the Griess reaction. *In* "Methods in nitric oxide research" (M. Feelisch, and J. S. Stamler, Eds.), pp. 491-497, John Wiley & Sons Ltd., New York

Schneede J., Refsum H., and Ueland P. M. (2000). Biological and environmental determinants of plasma homocysteine. *Semin Thromb Hemost* **26:** 263-79.

Schnyder G., Roffi M., Flammer Y., Pin R., and Hess O. M. (2002). Effect of homocysteine-lowering therapy with folic acid, vitamin B12, and vitamin B6 on clinical outcome after percutaneous coronary intervention: the Swiss Heart study: a randomized controlled trial. *Jama* **288:** 973-9.

Schwab U., Torronen A., Toppinen L., Alfthan G., Saarinen M., Aro A., and Uusitupa M. (2002). Betaine supplementation decreases plasma homocysteine concentrations but does not affect body weight, body composition, or resting energy expenditure in human subjects. *Am J Clin Nutr* **76:** 961-7.

Selhub J. (1999). Homocysteine metabolism. *Annu Rev Nutr* **19:** 217-46.

Selhub J., Jacques P. F., Wilson P. W., Rush D., and Rosenberg I. H. (1993). Vitamin status and intake as primary determinants of homocysteinemia in an elderly population. *Jama* **270:** 2693-8.

Sengupta S., Wehbe C., Majors A. K., Ketterer M. E., DiBello P. M., and Jacobsen D. W. (2001). Relative roles of albumin and ceruloplasmin in the formation of homocystine, homocysteine-cysteine-mixed disulfide, and cystine in circulation. *J Biol Chem* **276:** 46896-904.

Servillo G., Della Fazia M. A., and Sassone-Corsi P. (2002). Coupling cAMP signaling to transcription in the liver: pivotal role of CREB and CREM. *Exp Cell Res* **275:** 143-54.

Seshadri S., Beiser A., Selhub J., Jacques P. F., Rosenberg I. H., D'Agostino R. B., Wilson P. W., and Wolf P. A. (2002). Plasma homocysteine as a risk factor for dementia and Alzheimer's disease. *N Engl J Med* **346:** 476-83.

Shah V., Toruner M., Haddad F., Cadelina G., Papapetropoulos A., Choo K., Sessa W. C., and Groszmann R. J. (1999). Impaired endothelial nitric oxide synthase activity

associated with enhanced caveolin binding in experimental cirrhosis in the rat. *Gastroenterology* **117:** 1222-8.

Shaywitz A. J., and Greenberg M. E. (1999). CREB: a stimulus-induced transcription factor activated by a diverse array of extracellular signals. *Annu Rev Biochem* **68:** 821-61.

Simonet W. S., and Ness G. C. (1988). Transcriptional and posttranscriptional regulation of rat hepatic 3-hydroxy-3-methylglutaryl-coenzyme A reductase by thyroid hormones. *J Biol Chem* **263:** 12448-53.

Sinha S., Maity S. N., Lu J., and de Crombrugghe B. (1995). Recombinant rat CBF-C, the third subunit of CBF/NFY, allows formation of a protein-DNA complex with CBF-A and CBF-B and with yeast HAP2 and HAP3. *Proc Natl Acad Sci U S A* **92:** 1624-8.

Siow Y. L., Chilcote T. J., Benfenati F., Greengard P., and Thiel G. (1992). Synapsin IIa: expression in insect cells, purification, and characterization. *Biochemistry* **31:** 4268-75.

Sitrin R. G., Pan P. M., Srikanth S., and Todd R. F., 3rd (1998). Fibrinogen activates NF-kappa B transcription factors in mononuclear phagocytes. *J Immunol* **161:** 1462-70.

Smith L. C., Pownall H. J., and Gotto A. M., Jr. (1978). The plasma lipoproteins: structure and metabolism. *Annu Rev Biochem* **47:** 751-7.

Smithells R. W., Sheppard S., Schorah C. J., Seller M. J., Nevin N. C., Harris R., Read A. P., and Fielding D. W. (1980). Possible prevention of neural-tube defects by periconceptional vitamin supplementation. *Lancet* **1:** 339-40.

Sobell H. M. (1985). Actinomycin and DNA transcription. *Proc Natl Acad Sci U S A* **82:** 5328-31.

Starkel P., Sempoux C., Leclercq I., Herin M., Deby C., Desager J. P., and Horsmans Y. (2003). Oxidative stress, KLF6 and transforming growth factor-beta up-regulation differentiate non-alcoholic steatohepatitis progressing to fibrosis from uncomplicated steatosis in rats. *J Hepatol* **39:** 538-46.

Steinberg S. E. (1984). Mechanisms of folate homeostasis. *Am J Physiol* **246:** G319-24.

Stolk J., Hiltermann T. J., Dijkman J. H., and Verhoeven A. J. (1994). Characteristics of the inhibition of NADPH oxidase activation in neutrophils by apocynin, a methoxy-substituted catechol. *Am J Respir Cell Mol Biol* **11:** 95-102.

Stott D. J., MacIntosh G., Lowe G. D., Rumley A., McMahon A. D., Langhorne P., Tait R. C., O'Reilly D. S., Spilg E. G., MacDonald J. B., MacFarlane P. W., and Westendorp R. G. (2005). Randomized controlled trial of homocysteine-lowering

vitamin treatment in elderly patients with vascular disease. *Am J Clin Nutr* **82:** 1320-6.

Straka M. S., and Panini S. R. (1995). Post-transcriptional regulation of 3-hydroxy-3-methylglutaryl coenzyme A reductase by mevalonate. *Arch Biochem Biophys* **317:** 235-43.

Stroes E. S., van Faassen E. E., Yo M., Martasek P., Boer P., Govers R., and Rabelink T. J. (2000). Folic acid reverts dysfunction of endothelial nitric oxide synthase. *Circ Res* **86:** 1129-34.

Sultatos L. G. (1988). Effects of acute ethanol administration on the hepatic xanthine dehydrogenase/oxidase system in the rat. *J Pharmacol Exp Ther* **246:** 946-9.

Sung F. L., Slow Y. L., Wang G., Lynn E. G., and O K. (2001). Homocysteine stimulates the expression of monocyte chemoattractant protein-1 in endothelial cells leading to enhanced monocyte chemotaxis. *Mol Cell Biochem* **216:** 121-8.

Sutherland E. W., Rall T. W., and Menon T. (1962). Adenyl cylase. I. Distribution, preparation, and properties. *J Biol Chem* **237:** 1220-7.

Symons J. D., Mullick A. E., Ensunsa J. L., Ma A. A., and Rutledge J. C. (2002). Hyperhomocysteinemia evoked by folate depletion: effects on coronary and carotid arterial function. *Arterioscler Thromb Vasc Biol* **22:** 772-80.

Takahashi K. (2000). Glutathione peroxidase: coupled enzyme assay. *In* "Experimental protocols for reactive oxygen and nitrogen species" (N. Taniguchi, and J. M. C. Gutteridge, Eds.), pp. 79-80, Oxford university press, New York.

Taoka S., Ohja S., Shan X., Kruger W. D., and Banerjee R. (1998). Evidence for heme-mediated redox regulation of human cystathionine beta-synthase activity. *J Biol Chem* **273:** 25179-84.

Tershakovec A. M., Jawad A. F., Stouffer N. O., Elkasabany A., Srinivasan S. R., and Berenson G. S. (2002). Persistent hypercholesterolemia is associated with the development of obesity among girls: the Bogalusa Heart Study. *Am J Clin Nutr* **76:** 730-5.

Teufelhofer O., Parzefall W., Kainzbauer E., Ferk F., Freiler C., Knasmuller S., Elbling L., Thurman R., and Schulte-Hermann R. (2005). Superoxide generation from Kupffer cells contributes to hepatocarcinogenesis: studies on NADPH oxidase knockout mice. *Carcinogenesis* **26:** 319-29.

Torres L., Garcia-Trevijano E. R., Rodriguez J. A., Carretero M. V., Bustos M., Fernandez E., Eguinoa E., Mato J. M., and Avila M. A. (1999). Induction of TIMP-1 expression in rat hepatic stellate cells and hepatocytes: a new role for homocysteine in liver fibrosis. *Biochim Biophys Acta* **1455:** 12-22.

Tribble D. L., Aw T. Y., and Jones D. P. (1987). The pathophysiological significance of lipid peroxidation in oxidative cell injury. *Hepatology* **7:** 377-86.

Troen A. M., Lutgens E., Smith D. E., Rosenberg I. H., and Selhub J. (2003). The atherogenic effect of excess methionine intake. *Proc Natl Acad Sci U S A* **100:** 15089-94.

Tsai J. C., Wang H., Perrella M. A., Yoshizumi M., Sibinga N. E., Tan L. C., Haber E., Chang T. H., Schlegel R., and Lee M. E. (1996). Induction of cyclin A gene expression by homocysteine in vascular smooth muscle cells. *J Clin Invest* **97:** 146-53.

Ueland P. M., Helland S., Broch O. J., and Schanche J. S. (1984). Homocysteine in tissues of the mouse and rat. *J Biol Chem* **259:** 2360-4.

Upchurch G. R., Jr., Welch G. N., Fabian A. J., Freedman J. E., Johnson J. L., Keaney J. F., Jr., and Loscalzo J. (1997). Homocyst(e)ine decreases bioavailable nitric oxide by a mechanism involving glutathione peroxidase. *J Biol Chem* **272:** 17012-7.

Vallett S. M., Sanchez H. B., Rosenfeld J. M., and Osborne T. F. (1996). A direct role for sterol regulatory element binding protein in activation of 3-hydroxy-3-methylglutaryl coenzyme A reductase gene. *J Biol Chem* **271:** 12247-53.

van der Goes A., Brouwer J., Hoekstra K., Roos D., van den Berg T. K., and Dijkstra C. D. (1998). Reactive oxygen species are required for the phagocytosis of myelin by macrophages. *J Neuroimmunol* **92:** 67-75.

van Meurs J. B., Dhonukshe-Rutten R. A., Pluijm S. M., van der Klift M., de Jonge R., Lindemans J., de Groot L. C., Hofman A., Witteman J. C., van Leeuwen J. P., Breteler M. M., Lips P., Pols H. A., and Uitterlinden A. G. (2004). Homocysteine levels and the risk of osteoporotic fracture. *N Engl J Med* **350:** 2033-41.

Venn B. J., Green T. J., Moser R., and Mann J. I. (2003). Comparison of the effect of low-dose supplementation with L-5-methyltetrahydrofolate or folic acid on plasma homocysteine: a randomized placebo-controlled study. *Am J Clin Nutr* **77:** 658-62.

Verhaar M. C., Wever R. M., Kastelein J. J., van Loon D., Milstien S., Koomans H. A., and Rabelink T. J. (1999). Effects of oral folic acid supplementation on endothelial function in familial hypercholesterolemia. A randomized placebo-controlled trial. *Circulation* **100:** 335-8.

Vitvitsky V., Dayal S., Stabler S., Zhou Y., Wang H., Lentz S. R., and Banerjee R. (2004). Perturbations in homocysteine-linked redox homeostasis in a murine model for hyperhomocysteinemia. *Am J Physiol Regul Integr Comp Physiol* **287:** R39-46.

Wald D. S., Law M., and Morris J. K. (2002). Homocysteine and cardiovascular disease: evidence on causality from a meta-analysis. *Bmj* **325:** 1202.

Walsh D. A., Perkins J. P., and Krebs E. G. (1968). An adenosine 3',5'-monophosphate-dependant protein kinase from rabbit skeletal muscle. *J Biol Chem* **243:** 3763-5.

Wang G., and O K. (2001). Homocysteine stimulates the expression of monocyte chemoattractant protein-1 receptor (CCR2) in human monocytes: possible involvement of oxygen free radicals. *Biochem J* **357:** 233-40.

Wang G., Siow Y. L., and O K. (2000). Homocysteine stimulates nuclear factor kappaB activity and monocyte chemoattractant protein-1 expression in vascular smooth-muscle cells: a possible role for protein kinase C. *Biochem J* **352 Pt 3:** 817-26.

Wang G., Siow Y. L., and O K. (2001). Homocysteine induces monocyte chemoattractant protein-1 expression by activating NF-kappaB in THP-1 macrophages. *Am J Physiol Heart Circ Physiol* **280:** H2840-7.

Wang G., Woo C. W., Sung F. L., Siow Y. L., and O K. (2002). Increased monocyte adhesion to aortic endothelium in rats with hyperhomocysteinemia: role of chemokine and adhesion molecules. *Arterioscler Thromb Vasc Biol* **22:** 1777-83.

Wang H., Jiang X., Yang F., Gaubatz J. W., Ma L., Magera M. J., Yang X., Berger P. B., Durante W., Pownall H. J., and Schafer A. I. (2003). Hyperhomocysteinemia accelerates atherosclerosis in cystathionine beta-synthase and apolipoprotein E double knock-out mice with and without dietary perturbation. *Blood* **101:** 3901-7.

Wang J. F., Komarov P., Sies H., and de Groot H. (1992). Inhibition of superoxide and nitric oxide release and protection from reoxygenation injury by Ebselen in rat Kupffer cells. *Hepatology* **15:** 1112-6.

Watanabe M., Osada J., Aratani Y., Kluckman K., Reddick R., Malinow M. R., and Maeda N. (1995). Mice deficient in cystathionine beta-synthase: animal models for mild and severe homocyst(e)inemia. *Proc Natl Acad Sci U S A* **92:** 1585-9.

Weiss N., Heydrick S. J., Postea O., Keller C., Keaney J. F., Jr., and Loscalzo J. (2003). Influence of hyperhomocysteinemia on the cellular redox state--impact on homocysteine-induced endothelial dysfunction. *Clin Chem Lab Med* **41:** 1455-61.

Welch G. N., and Loscalzo J. (1998). Homocysteine and atherothrombosis. *N Engl J Med* **338:** 1042-50.

Werstuck G. H., Lentz S. R., Dayal S., Hossain G. S., Sood S. K., Shi Y. Y., Zhou J., Maeda N., Krisans S. K., Malinow M. R., and Austin R. C. (2001). Homocysteine-induced endoplasmic reticulum stress causes dysregulation of the cholesterol and triglyceride biosynthetic pathways. *J Clin Invest* **107:** 1263-73.

Wheeler M. D., Kono H., Yin M., Nakagami M., Uesugi T., Arteel G. E., Gabele E., Rusyn I., Yamashina S., Froh M., Adachi Y., Iimuro Y., Bradford B. U., Smutney O. M., Connor H. D., Mason R. P., Goyert S. M., Peters J. M., Gonzalez F. J., Samulski R. J., and Thurman R. G. (2001a). The role of Kupffer cell oxidant production in early ethanol-induced liver disease. *Free Radic Biol Med* **31:** 1544-9.

Wheeler M. D., Nakagami M., Bradford B. U., Uesugi T., Mason R. P., Connor H. D., Dikalova A., Kadiiska M., and Thurman R. G. (2001b). Overexpression of manganese superoxide dismutase prevents alcohol-induced liver injury in the rat. *J Biol Chem* **276:** 36664-72.

White A. R., Huang X., Jobling M. F., Barrow C. J., Beyreuther K., Masters C. L., Bush A. I., and Cappai R. (2001). Homocysteine potentiates copper- and amyloid beta peptide-mediated toxicity in primary neuronal cultures: possible risk factors in the Alzheimer's-type neurodegenerative pathways. *J Neurochem* **76:** 1509-20.

Wilce P. A., and Kroon P. A. (1992). Assay of 3-hydroxy-3-methylglutaryl coenzyme A (HMG-CoA) reductase. *In* "Lipoprotein Analysis, A Practical Approach" (C. A. Converse, and E. R. Skinner, Eds.), pp. 207-214, IRL Press, Oxford.

Wilcken D. E., Wang X. L., Adachi T., Hara H., Duarte N., Green K., and Wilcken B. (2000). Relationship between homocysteine and superoxide dismutase in homocystinuria: possible relevance to cardiovascular risk. *Arterioscler Thromb Vasc Biol* **20:** 1199-202.

Willems F. F., Aengevaeren W. R., Boers G. H., Blom H. J., and Verheugt F. W. (2002). Coronary endothelial function in hyperhomocysteinemia: improvement after treatment with folic acid and cobalamin in patients with coronary artery disease. *J Am Coll Cardiol* **40:** 766-72.

Woo C. W., Cheung F., Chan V. W., Siow Y. L., and O K. (2003). Homocysteine stimulates inducible nitric oxide synthase expression in macrophages: antagonizing effect of ginkgolides and bilobalide. *Mol Cell Biochem* **243:** 37-47.

Woo C. W., Prathapasinghe G. A., Siow Y. L., and O K. (2006a). Hyperhomocysteinemia induces liver injury in rat: Protective effect of folic acid supplementation. *Biochim Biophys Acta* **1762:** 656-65.

Woo C. W., Siow Y. L., and O K. (2006b). Homocysteine activates cAMP-response element binding protein in HepG2 through cAMP/PKA signaling pathway. *Arterioscler Thromb Vasc Biol* **26:** 1043-50.

Woo C. W., Siow Y. L., Pierce G. N., Choy P. C., Minuk G. Y., Mymin D., and O K. (2005). Hyperhomocysteinemia induces hepatic cholesterol biosynthesis and lipid accumulation via activation of transcription factors. *Am J Physiol Endocrinol Metab* **288:** E1002-10.

Woo K. S., Chook P., Lolin Y. I., Sanderson J. E., Metreweli C., and Celermajer D. S. (1999). Folic acid improves arterial endothelial function in adults with hyperhomocystinemia. *J Am Coll Cardiol* **34:** 2002-6.

Wu L. L., Wu J., Hunt S. C., James B. C., Vincent G. M., Williams R. R., and Hopkins P. N. (1994). Plasma homocyst(e)ine as a risk factor for early familial coronary artery disease. *Clin Chem* **40:** 552-61.

Xing L., and Quinn P. G. (1993). Involvement of 3',5'-cyclic adenosine monophosphate regulatory element binding protein (CREB) in both basal and hormone-mediated expression of the phosphoenolpyruvate carboxykinase (PEPCK) gene. *Mol Endocrinol* **7:** 1484-94.

Yamada J., Tomiyama H., Yambe M., Koji Y., Motobe K., Shiina K., Yamamoto Y., and Yamashina A. (2006). Elevated serum levels of alanine aminotransferase and gamma glutamyltransferase are markers of inflammation and oxidative stress independent of the metabolic syndrome. *Atherosclerosis* **189:** 198-205.

Zalba G., San Jose G., Moreno M. U., Fortuno M. A., Fortuno A., Beaumont F. J., and Diez J. (2001). Oxidative stress in arterial hypertension: role of NAD(P)H oxidase. *Hypertension* **38:** 1395-9.

Zou A. P., Li N., and Cowley A. W., Jr. (2001). Production and actions of superoxide in the renal medulla. *Hypertension* **37:** 547-53.

Appendix I

Reagents/Chemicals	*Companies*
Acrylamide/bis 30% solution 37.5:1 (2.6% C)	Bio-Rad
Actinomycin	Sigma-Aldrich
Adenosine triphosphate, ATP	Cell Signaling
Adenosine triphosphate-[^{32}P], [^{32}P]-ATP	PerkinElmer
Adenylyl cyclase toxin	Calbiochem
AEBSF	Calbiochem
Agarose	Invitrogen
ALT kit	Wako Japan
Ammonium Persulfate	Sigma-Aldrich
Anti-CREB antibody	Cell Signaling
Anti-CREB antibody (for supershift assay)	Upstate
Anti-HMG-CoA reductase antibody	Upstate
Anti-NF-YA/CBF-B antibody	Santa Cruz
Anti-phospho-CREB antibody	Cell Signaling
Anti-pCREB antibody	Santa Cruz
Anti-Rabbit IgG, HRP-link antibody	Zymed
Anti-SREBP-2 antibody	Santa Cruz
Aprotonin	Sigma-Aldrich
Arginine-L-[^{3}H]	PerkinElmer
AST kit	Wako Japan
Bis-benzimide	Sigma-Aldrich
Boric acid	Fisher
Bovine serum albumin, BSA	EMD
Bromophenol blue	Sigma-Aldrich
Calcium chloride ($CaCl_2$-$2H_2O$)	Fisher
cAMP Defia kit	Perkin Elmer
Chloroform ($CHCl_3$)	Fisher

Collagnease from Clostridium histolyticum	Sigma-Aldrich
CREB consensus oligonucleotide	Promega
Cysteine, L-	Sigma-Aldrich
D-Glucose (Dextrose)	Fisher
Diethyl pyrocarbonate, DEPC	Sigma-Aldrich
Disodium hydrogen orthophosphate (Na_2HPO_4)	Sigma-Aldrich
Disodium pyrophosphate	Sigma-Aldrich
Dithiothreitol, DTT	Sigma-Aldrich
DMEM	Hyclone
DMSO	Fisher
dNTPs set	Invitrogen
Ethidium bromide, EtBr	Sigma-Aldrich
Ethylene glycol tetraacetic acid, EGTA	Sigma-Aldrich
Ethylenediaminetetraacetic acid, EDTA	Sigma-Aldrich
Fetal Bovine Serum	Gibco
First Strand buffer 5x	Invitrogen
Folate Defia kit	Perkin Elmer
Folic acid	Sigma-Aldrich
Formaldehyde	Sigma-Aldrich
Free Cholesterol kit	Wako USA
Glucose-6-phosphate dehydrogenase	Sigma-Aldrich
Glutathione Reductase	Sigma-Aldrich
Glutathione, oxidized form, GSSG	Sigma-Aldrich
Glutathione, reduced form, GSH	Sigma-Aldrich
Glycerol	Fisher
Glycerol-2-phosphate disodium salt hydrate	Sigma-Aldrich
Glycine	Invitrogen
GOT (ALT) kit	Wako Japan
GPT (AST) kit	Wako Japan
H89	Calbiochem
Hanks balanced salt solution, HBSS	Hyclone

Hematoxylin, Harris	Sigma-Aldrich
HEPES, 4-(2-hydroxyethyl)-1-piperazineethanesulfonic acid	Fisher
HMG-CoA	Sigma-Aldrich
HMG-CoA-[^{14}C]	PerkinElmer
Homocysteine thiolactone, L-	Sigma-Aldrich
Homocysteine, DL	Sigma-Aldrich
Hydrochloric acid	Fisher
Hydrogen peroxide 30%	Fisher
Isopropanol	Fisher
Leupeptin	Sigma-Aldrich
Lipid calibrator	Wako USA
Magnesium chloride hexahydrate	Fisher
Magnesium sulfate heptahydrate	EM-Science
Mercaptoethanol-β	Sigma-Aldrich
Methanol	VWR
Methionine, DL-	Sigma-Aldrich
Mevalonic acid lactone, DL- (Mevalonolactone)	Sigma-Aldrich
M-MLV-Reverse transcriptase 200U/mL	Invitrogen
N-(1-naphtyl)-ethylenediamine	Sigma-Aldrich
NADPH, nicotinamide adenine dinucleotide phosphate (reduced)	Sigma-Aldrich
N-ethylmalemide, NEM	Sigma-Aldrich
NF-Y (CBF) consensus oligonucleotide	Santa Cruz
Nonidet-P	Sigma-Aldrich
Oil Red O	Sigma-Aldrich
Oligo(dT)$_{12-18}$ primer, 0.5μg/μL	Invitrogen
Omnifluor	New England Nuclear
PCR buffer 10x	New England Biolab
PD 98059	Cell Signaling
Pentobarbital	Sigma-Aldrich
Pepstatin A	Sigma-Aldrich

Perchloric acid	Sigma-Aldrich
Phenylmethanesulfonyl fluoride, PMSF	Sigma-Aldrich
Phosphoric acid, H_3PO_4	Fisher
Potassium Chloride	Sigma-Aldrich
Potassium Phosphate dibasic	Sigma-Aldrich
Potassium Phosphate monobasic	Sigma-Aldrich
Propyl gallate	Sigma-Aldrich
Propylene glycol	Fisher
Protein A agarose	Calbiochem
Protein assay	Bio-Rad
RNase inhibitor 40/mL	Promega
Serine-L	Fisher
Serine-L-[^{14}C]	PerkinElmer
Sodium Azide	Fisher
Sodium bicarbonate	Sigma-Aldrich
Sodium Chloride	VWR
Sodium dodecyl sulfate	Fisher
Sodium Fluoride	Fisher
Sodium orthovandate	Sigma-Aldrich
Sodium phosphate dibasic	Sigma-Aldrich
Sodium phosphate monobasic	Sigma-Aldrich
Sulfanilamide	Sigma-Aldrich
Superoxide dismutase	Sigma-Aldrich
T4 Polynucleotide kinase	Promega
T4 Polynucleotide kinase 10x buffer	Promega
Taq polymerase 5000U/mL	New England Biolab
t-butyl-hydroperoxide	Sigma-Aldrich
TE (Tris-EDTA) buffer, 50×	USB
TEMED	EMD
Toluene	Sigma-Aldrich
Total cholesterol kit	Wako USA

Triacylglycerol TG kit	Wako USA
Trichloroacetic acid	EMD
Tris	Invitrogen
Triton X-100	Sigma-Aldrich
Trizol Reagent	Invitrogen
Trypan blue	Invitrogen
Trypsin-EDTA 10x	Gibco
Tween	Fisher
Vinyl-pyridine, 2-	Sigma
Western Reprobe reagent	Calbiochem
Xanthine	Sigma Aldrich
Xanthine oxidase	Sigma Aldrich
Xylene	EMD

Appendix II

Buffers	*Ingredients*
Buffer A	10mM HEPES, 10mM KCl, 0.1mM EDTA, 1mM EGTA, 0.5mM PMSF, 1mM DTT, pH 7.9
Buffer C	20mM HEPES, 0.4M NaCl, 1mM EDTA, 1mM EGTA, 1mM PMSF, 1mM DTT, pH 7.9
Lysis Buffer	20mM Tris, 150mM NaCl, 1mM EDTA, 1mM EGTA, 2.5mM Sodium pyrophosphate, 1mM β-glycerophosphate, 1mM Sodium orthovanadate, 2.1μM Leupeptin, 1mM PMSF, 1% Triton-X 100, pH 7.4
Reaction buffer	100mM Tris, 1M NaCl, 50mM DTT, 10mM EDTA, 40% Glycerol, 1mg/ml BSA, 50ng/ml double-stranded poly (dI.dC), pH 7.5
SDS sample buffer	250mM Tris-base, 25% Glycerol, 10% SDS, 0.02% Bromophenol Blue, 5% β-mercaptoethanol
Separating gel buffer	1.5M Tris, 0.4% SDS
Stacking gel buffer	0.5M Tris, 0.4% SDS
Stripping buffer	2% SDS, 95mM β-mercaptoethanol in 1x TBS
TBE buffer 10x	89mM Tris, 89mM Boric acid, 2mM EDTA, pH 8.4
Tris buffered saline (TBS)	0.02M Tris, 0.14M NaCl, pH 7.6
Running Buffer	25mM Tris, 0.19M Glycine, 0.1% SDS
Transfer Buffer	20mM Tris, 0.15M Glycine, 20% Methanol
Trypsin/EDTA Buffer	140mM NaCl, 2.7mM KCl, 1.67mM KH_2PO_4, 27mM Dextrose, 8.1mM Na_2HPO_4, 10% 0.5% Trypsin/5.3mM EDTA (Gibco)

Appendix III

Models	*Companies*
Centrifuge 5804R	Eppendorf
Forma Direct Heat CO_2 Incubator HEPA Class 100	ThermoForma
Gel Doc	Bio Rad
IMx	Abbot
LS 6500 Multi-purpose Scintillation counter	Beckman Instrument
Lumet LB9507	Berthold Technologies GmbH & Co. KG
Minispin	Eppendorf
MRX TC Revelation	Dynex
My Cycler	Bio Rad
Slab Gel Dryer 2000	ThermoSavant
Spectra Max Gemini	Molecular Devices
Spectrophotometer DU 800	Beckman Coulter